

State of California
California Natural Resources Agency
DEPARTMENT OF WATER RESOURCES

Methodology for Flow and Salinity Estimates in the Sacramento-San Joaquin Delta and Suisun Marsh



**38th Annual Progress Report to the
State Water Resources Control Board in
Accordance with Water Right Decisions 1485 and 1641**

June 2017

Edmund G. Brown Jr.

Governor

State of California

John Laird

Secretary for Natural Resources

California Natural Resources Agency

William A. Croyle

Acting Director

Department of Water Resources



State of California
Edmund G. Brown Jr., Governor

California Natural Resources Agency
John Laird, Secretary for Natural Resources

Department of Water Resources
William A. Croyle, Acting Director

Cindy Messer, Chief Deputy Director

Chief Counsel
Spencer Kenner

Public Affairs
Ed Wilson, Assistant Director

Legislative Affairs
Kasey Schimke,
Assistant Director

Policy Advisor
Waiman Yip

California Water Commission
Joseph Yun,
Executive Officer

Deputy Directors

Gary Bardini	Integrated Water Management
Vacant	California Energy Resources Scheduling
Katherine S. Kishaba	Business Operations
Taryn Ravazzini	Special Initiatives
Mark Andersen, Acting	State Water Project
Christy Jones, Acting	Statewide Emergency Preparedness and Security
Vacant	Internal Audit Office
Stephanie Varrelman	Office of Workforce Equality

Bay Delta Office
Francis Chung, Chief

Modeling Support Branch
Tara Smith, Chief

Delta Modeling Section
Vacant, Chief

Edited by
Min Yu, Bay-Delta Office
(See individual chapters for authors.)

Editorial review
William O'Daly, Supervisor of Technical Publications
Jeff Woled, Research Writer



Foreword

This is the 38th annual progress report of the California Department of Water Resources' San Francisco Bay-Delta Evaluation Program, which is carried out by the Delta Modeling Section. This report is submitted annually by the section to the State Water Resources Control Board pursuant to its Water Right Decision D-1485, Term 9, which is still active pursuant to its Water Right Decision D-1641, Term 8.

This report documents progress in the development and enhancement of computer models for the Delta Modeling Section of the Bay-Delta Office. It also reports the latest findings of studies conducted as part of the program. This report was compiled under the direction of Tara Smith, Program Manager for the Bay-Delta Evaluation Program.

Online versions of previous annual progress reports are available at:

<http://baydeltaoffice.water.ca.gov/modeling/deltamodeling/annualreports.cfm>.

For more information contact:

Nicky Sandhu, Chief
Delta Modeling Section
Bay-Delta Office
California Department of Water Resources

Prabhjot.Sandhu@water.ca.gov

(916) 657-5071



Contents

Preface	ix
1 Evaluation of the Recalibrated Martinez Boundary Salinity Generator with DSM2 Version 8.1	1-1
1.1 INTRODUCTION.....	1-1
1.2 EXISTING CONDITION SCENARIOS	1-1
1.3 INCREMENTAL DIFFERENCES OF PROPOSED ALTERNATIVES	1-9
1.4 SUMMARY.....	1-21
2 DSM2 Nutrients Modeling Sensitivity Analysis	2-1
2.1 INTRODUCTION.....	2-1
2.2 MODELING BASE AND SENSITIVITY ANALYSIS SCENARIOS	2-1
2.3 PRELIMINARY MODELING RESULTS AND FINDINGS	2-1
2.3.1 Algae_Growth_1.0	2-2
2.3.2 NH3_Decay_0.02	2-5
2.3.3 NH3_Decay_0.6	2-5
2.3.4 Org-P_Decay_0.05	2-9
2.3.5 Algae_Die_0.002	2-9
2.3.6 Additional Discussion of Results	2-9
2.4 NEXT STEPS AND POTENTIAL FUTURE EFFORTS TO IMPROVE MODEL CALIBRATION ..	2-12
2.5 REFERENCES CITED.....	2-48
3 Implementing DETAW in Modeling Hydrodynamics and Water Quality in the Sacramento-San Joaquin Delta	3-1
3.1 INTRODUCTION.....	3-1
3.2 BACKGROUND.....	3-1
3.2.1 Current DWR Models.....	3-2
3.2.2 DETAW v1.0	3-3
3.3 DETAW V2.0: IMPLEMENTING DETAW IN THE MODELING OF DELTA HYDRODYNAMICS AND WATER QUALITY	3-5
3.3.1 Rewriting DETAW v1.0	3-5
3.3.2 Updating Seepage Rate Assumptions	3-5
3.3.3 Updating Crop Coefficients for Field Crops and Native Vegetation	3-6
3.3.4 Calibrating Crop Stress Coefficients.....	3-6
3.3.5 Estimating Net Channel Depletion for DETAW v2.0	3-11
3.4 DATA INPUT FOR DETAW V2.0.....	3-12
3.4.1 Land Use.....	3-12
3.4.2 Precipitation.....	3-13
3.4.3 Air Temperature.....	3-14
3.5 DETAW V2.0 RESULTS AS COMPARED WITH DETAW V1.0, DICU, AND DAYFLOW	3-14
3.5.1 Delta Net Channel Depletion	3-14
3.5.2 Net Delta Outflow	3-15
3.5.3 Simulation of Delta Electrical Conductivity with DSM2	3-18
3.6 CONCLUSION.....	3-25
3.7 REFERENCES CITED.....	3-25

3.7.1	Personal Communications	3-26
4	Clifton Court Forebay Transit Time Modeling Analysis.....	4-1
4.1	INTRODUCTION.....	4-1
4.1.1	Site Characterization.....	4-1
4.2	MODEL DESCRIPTION.....	4-7
4.2.1	Hydrodynamics	4-7
4.2.2	Radial Gate Parameterization.....	4-8
4.2.2.1	<i>Evaporation</i>	4-8
4.2.3	Particle Tracking.....	4-8
4.2.4	Mesh and Time Discritization	4-9
4.3	INPUT DATA SOURCES	4-11
4.3.1	Banks Pumping Plant Flow.....	4-11
4.3.2	Radial Gate Operations.....	4-11
4.3.3	Bathymetry	4-12
4.4	CALIBRATION AND VALIDATION	4-13
4.5	TRANSIT TIME AND VELOCITY ANALYSIS	4-21
4.5.1	Dredge and Fill Alternatives.....	4-21
4.5.2	Methods.....	4-21
4.5.3	Key Results	4-24
4.5.3.1	<i>Patterns and Variations in Particle Trajectories</i>	4-24
4.5.4	Transit Time	4-27
4.6	DISCUSSION.....	4-30
4.7	REFERENCES CITED.....	4-33
4.7.1	Personal Communications	4-34

Acronyms and Abbreviations

µmhos/cm	micromhos per centimeter
µS/cm	microSiemens per centimeter
ADCP	Argonaut Acoustic Doppler Current Profiler
Banks Pumping Plant or Banks	Harvey O. Banks Pumping Plant
BBID	Byron Bethany Irrigation District
BDCP	Bay-Delta Conservation Plan
BDO	Bay-Delta Office
CBOD	carbonaceous biochemical oxygen demand
CDEC	California Data Exchange Center
cfs	cubic feet per second
CIMIS	California Irrigation Management Information System
cm	centimeters
CSB	Control Systems Branch
CU	Consumptive Use Model
CVP	Central Valley Project
DCU	Delta consumptive use
Delta	Sacramento-San Joaquin Delta
DETAW	Delta Evapotranspiration of Applied Water Model
DFD	Delta Field Division
DICU	Delta Island Consumptive Use Model
DIV	total diversion
DO	dissolved oxygen
DSM2	Delta Simulation Model version 2.0
DSM2-GTM	General Transport Model
DWR	California Department of Water Resources
EC	electrical conductivity
ET	evapotranspiration
ETc	crop evapotranspiration
ETo	reference evapotranspiration
Forebay	Clifton Court Forebay
ft	feet

ft/s	feet per second
GIS	geographic information system
HS	Hargreaves-Samani equation
I_A	applied water
I_D	excess irrigation water
IEP	Interagency Ecological Program
Kc	crop coefficient
Ks	stress coefficient
LW _A	leach water applied
LW _D	leach water drained
m	meter
mg/L	milligrams per liter
mph	miles per hour
NAA	No-Action Alternative
NAVD88	North American Vertical Datum of 1988
NCDC	National Climatic Data Center
NCRO	North Central Regional Office
NDO	Net Delta Outflow
NDOI	Net Delta Outflow Index
NG	New Generator
NGVD29	National Geodetic Vertical Datum of 1929
NH ₃	ammonia
NMFS	National Marine Fisheries Service
NO ₂	nitrite
NO ₃	nitrate
NOAA	National Oceanic and Atmospheric Administration
O ₂	soil saturation-reduced root-zone oxygen
O&M	DWR Division of Operations and Maintenance
Org-N	organic nitrogen
Org-P	organic phosphorus
PA	Proposed Action
PEST	Parameter Estimation Software
PM	Penman-Monteith equation

PO ₄	ortho-phosphate, assumed to represent dissolved phosphorus
PPT	precipitation
PST	Pacific Standard Time
RET	returned flow
RMA	Resource Management Associates
RO	surface runoff
S	seepage
SAP	Systems Applications and Products
SCHIM	Semi-implicit Cross-scale Hydroscience Integrated System Model
SDFPF	John E. Skinner Delta Fish Protective Facility
SEBAL	Surface Energy Balance Algorithm for Land
SM	soil moisture
sq ft	square feet
SWP	State Water Project
taf	thousand acre-feet
UC IPM	Statewide Integrated Pest Management Program at University of California
USGS	U.S. Geological Survey
WY	water year

Preface

Chapter 1. Evaluation of the Recalibrated Martinez Boundary Salinity Generator with DSM2 Version 8.1

The Martinez boundary EC (electrical conductivity) generator for planning studies or forecasting was first developed by the Delta Modeling Section in 2001 (Ateljevich 2001), which was based on the original antecedent flow-salinity relations model, generally referred to as G-Model (Denton and Sullivan 1993), and incorporated tidal variation effect. The Martinez EC generator was recently recalibrated by using PEST, which is mathematically based calibration software (Sandhu and Zhou 2015). This chapter documents the effects of this recalibrated Martinez EC generator on planning studies. The Bay Delta Conservation Plan (BDCP)/California WaterFix simulations using Delta Simulation Model 2 (DSM2), version 8.0.4, during a 16-year planning simulation, 1974–1991, were converted to DSM2 version 8.1 with North American Vertical Datum of 1988 (NAVD88). We (Liu, Zhou, and Sandhu) will refer to the original Martinez EC Generator (Ateljevich 2001) as the Old Generator and the recalibrated Martinez EC Generator as the New Generator (noted as NG in figures). The simulation results were compared with the original results computed for BDCP by using DSM2 version (v)8.0.4. Studying the incremental differences in results between the two versions of DSM2 may reveal whether those differences would significantly affect or change any analysis conclusions in the simulations previously computed for BDCP by using DSM2 v8.0.4.

Chapter 2. DSM2 Nutrients Modeling Sensitivity Analysis

The California Department of Water Resources' Delta Modeling Section is developing a new Delta Simulation Model 2 (DSM2) transport module, called the General Transport Model (DSM2-GTM). Progress on this effort was previously reported in Hsu et al. (2014). When the model development is completed, DSM2-GTM will include sediment, dissolved oxygen (DO), and mercury cycling modules to simulate non-conservative constituents.

Part of the DSM2-GTM development process is to calibrate the DO module that simulates the transport and reaction of water temperature and nine non-conservative constituents that are currently included in the DSM2-QUAL computation. These nine constituents are DO, nitrate (NO_3^-), nitrite (NO_2^-), ammonia (NH_3), organic nitrogen (Org-N), carbonaceous biochemical oxygen demand (CBOD), ortho-phosphate (PO_4^{3-}) assumed to represent dissolved phosphorus, organic phosphorus (Org-P), and algae.

In general, there are two types of model calibration approaches — automatic and manual. If the manual calibration approach is used to carry out the DSM2-GTM calibration, choosing which constituent reaction rates to more efficiently calibrate the model could be challenging. To have a better idea regarding which constituent reaction rates may possess more significant effects on the model results, a sensitivity analysis was performed to test how the model results respond when changing certain constituent reaction rates. This chapter summarizes the sensitivity analysis approach and preliminary findings to date. This sensitivity analysis is an initial investigation and is also an on-going exercise along with the DSM2-GTM development.

Chapter 3. Implementing DETAW in Modeling Hydrodynamics and Water Quality in the Sacramento-San Joaquin Delta

Numerical modeling of the hydrodynamics and water quality in the Sacramento-San Joaquin Delta channels requires accounting for in-Delta net channel depletion because of agricultural diversions,

including seasonal leaching, seepage from channels to Delta lowland islands, riparian and native vegetation evapotranspiration, and evaporation from free-water surfaces. The California Department of Water Resources has recently developed a new model, the Delta Evapotranspiration of Applied Water Model (DETAW v2.0), which is a significant improvement over current methods for estimating Delta consumptive use and net channel depletion. This report presents the key aspects of DETAW v2.0 and its implementation in the detailed modeling of Delta conditions.

Chapter 4. Clifton Court Forebay Transit Time Modeling Analysis

This chapter is excerpted from Shu and Ateljevich (2017) and summarizes 3D hydrodynamic modeling performed by the California Department of Water Resources' Bay-Delta Office (BDO) to assess flow patterns and transit time in the Clifton Court Forebay (Forebay). The motivation for this work comes from the National Marine Fisheries Service 2009 Biological Opinion, Action IV.4.2 (National Marine Fisheries Service 2011), which prescribes limits on pre-screen losses of salmonids and steelhead in the Forebay and obliges DWR to study methods to reduce this loss. This report focuses on model development that has been completed and a study based on this model of how transit time across the Forebay responds to various filling and dredging actions. The premise underlying this investigation is that fish will benefit from faster transit which reduces their exposure to predators.

Methodology for Flow and Salinity Estimates in the Sacramento-San Joaquin Delta and Suisun Marsh

**38th Annual Progress Report
June 2017**

Chapter 1

Evaluation of the Recalibrated Martinez Boundary Salinity Generator with DSM2 Version 8.1

Authors: Lianwu Liu, Yu Zhou, Prabhjot Sandhu
Delta Modeling Section
Bay-Delta Office
California Department of Water Resources



Contents

1	Evaluation of the Recalibrated Martinez Boundary Salinity Generator with DSM2 Version 8.1.....	1-1
1.1	INTRODUCTION	1-1
1.2	EXISTING CONDITION SCENARIOS	1-1
1.3	INCREMENTAL DIFFERENCES OF PROPOSED ALTERNATIVES	1-9
1.4	SUMMARY.....	1-21
1.5	REFERENCES CITED	1-21

Figures

Figure 1-1	Martinez Electrical Conductivity Generated by the Old and New Generator	1-2
Figure 1-2	Comparison Electrical Conductivity at Collinsville (RSAC081).....	1-3
Figure 1-3	Comparison of Electrical Conductivity at Emmaton (RSAC092)	1-4
Figure 1-4	Comparison of Electrical Conductivity at Jersey Point (RSAN018)	1-5
Figure 1-5	Comparison of Electrical Conductivity at Old River at Rock Slough (ROLD024)	1-6
Figure 1-6	Comparison of Electrical Conductivity at Clifton Court Forebay	1-7
Figure 1-7	Comparison of Electrical Conductivity with D-1641 Standard at Collinsville (RSAC081).....	1-8
Figure 1-8	Comparison of Electrical Conductivity with D-1641 Standard at Emmaton (RSAC092).....	1-8
Figure 1-9	Comparison of Electrical Conductivity with D-1641 Standard at Jersey Point (RSAN018).....	1-8
Figure 1-10	Comparison of Electrical Conductivity with D-1641 Standard at Old River at RockSlough (ROLD024)	1-9
Figure 1-11	Comparison of Electrical Conductivity with D-1641 Standard at Clifton Court Forebay	1-9
Figure 1-12	Comparison of Electrical Conductivity at Collinsville (RSAC081)	1-11
Figure 1-13	Comparison of Electrical Conductivity at Emmaton (RSAC092)	1-12
Figure 1-14	Comparison of Electrical Conductivity at Jersey Point (RSAN018)	1-13
Figure 1-15	Comparison of Electrical Conductivity at Old River at Rock Slough (ROLD024)	1-14
Figure 1-16	Comparison of Electrical Conductivity at Clifton Court Forebay.....	1-15



1 Evaluation of the Recalibrated Martinez Boundary Salinity Generator with DSM2 Version 8.1

1.1 Introduction

The Martinez boundary EC (electrical conductivity) generator for planning studies or forecasting was first developed by the Delta Modeling Section in 2001 (Ateljevich 2001), which was based on the original antecedent flow-salinity relations model, generally referred to as G-Model (Denton and Sullivan 1993), and incorporated tidal variation effect. The Martinez EC generator was recently recalibrated by using PEST, which is mathematically based calibration software (Sandhu and Zhou 2015). This chapter documents the effects of this recalibrated Martinez EC generator on planning studies. The Bay Delta Conservation Plan (BDCP)/California WaterFix simulations by using Delta Simulation Model 2 (DSM2), version 8.0.4, during a 16-year planning simulation, 1974–1991, were converted to DSM2 version 8.1 with North American Vertical Datum of 1988 (NAVD88). We (Liu, Zhou, and Sandhu) will refer to the original Martinez EC Generator (Ateljevich 2001) as the Old Generator and the recalibrated Martinez EC Generator as the New Generator (noted as NG in figures). The simulation results were compared with the original results computed for BDCP by using DSM2 version (v)8.0.4. The incremental differences in results between the two versions of DSM2 may reveal whether those differences would significantly affect or change any analysis conclusions in the simulations previously computed for BDCP by using DSM2 v8.0.4.

1.2 Existing Condition Scenarios

EC results were compared for the following scenarios.

- Existing condition by using DSM2 v8.0.4.
- Existing condition by using DSM2 v8.1.
- Existing condition by using DSM2 v8.1 with the new Martinez EC Generator.

As shown in Figure 1-1, Martinez EC generated by the New Generator is generally higher than those generated by the Old Generator, especially for the high-EC period (i.e., more than 25,000 micromhos per centimeter [$\mu\text{mhos}/\text{cm}$]).

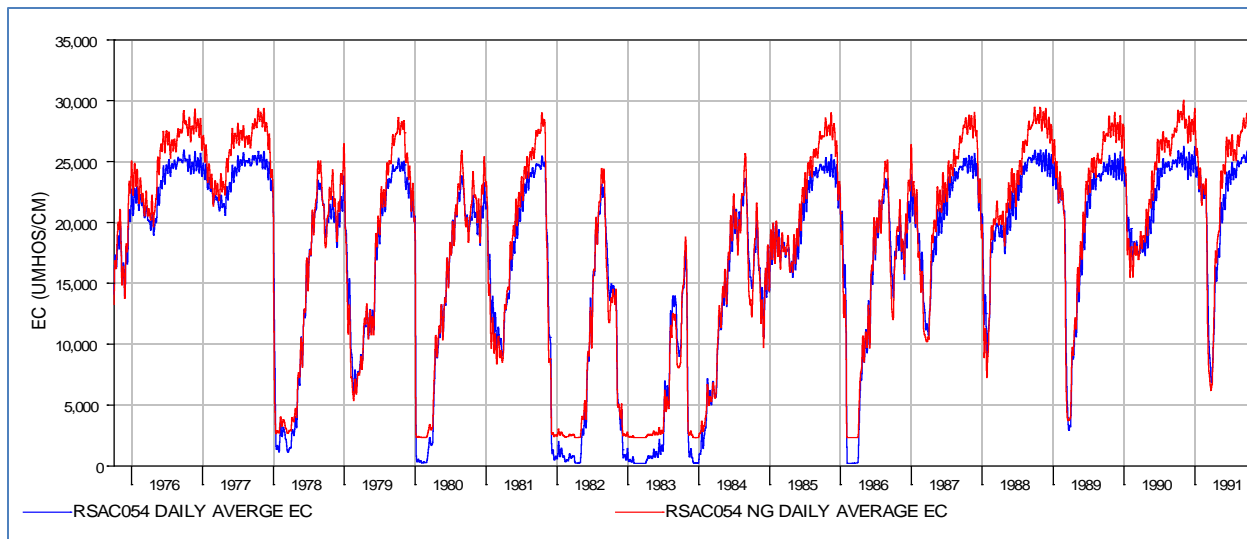


Figure 1-1 Martinez Electrical Conductivity Generated by the Old and New Generator

Notes: EC = electrical conductivity, $\mu\text{mhos}/\text{cm}$ = micromhos per centimeter

Monthly averaged EC results at key locations including Collinsville, Emmaton, Jersey Point, Rock Slough and Clifton Court, are plotted in Figures 1-2–1-6. The top graph in each figure shows the monthly averaged EC comparison for the three scenarios listed above. The bottom graph, also in each figure, shows averaged monthly EC for each month during the 16-year simulation period. The following are some observations.

1. When comparing DSM2 v8.1, only with the Old and New Generator, it is clear that the New Generator generally produces higher-EC values at every location and for most of the months (i.e., July–December, which are normally the high-EC periods). During the low-EC periods, January–June, the differences are negligible.
2. Comparing DSM2 v8.0.4 and DSM2 v8.1 with the New Generator, simulated EC values from DSM2 v8.1 with the New Generator are significantly higher than those from DSM2 v8.0.4 during October–December. Yet, the differences are insignificant during July–September.
3. Figures 1-7–1-11 show comparisons of the DSM2 results and the State Water Resources Control Board's Decision 1641 (D-1641) EC standard implemented in the CalSim model for two scenarios, which are DSM2 v8.0.4 and DSM2 v8.1 with the New Generator. According to the D-1641 requirements, monthly data are plotted at Collinsville (Figure 1-7) and Clifton Court (Figure 1-11), 14-day running average EC are plotted at Emmaton (Figure 1-8) and Jersey Point (Figure 1-9), and daily average data are plotted at Rock Slough (Figure 1-10). It is observed that larger differences during October–December (i.e., high-EC period) generally do not affect meeting the D-1641 standard of tighter restrictions that mainly apply to April–August. That's why this will not likely to have a significant effect on CalSim-computed results.

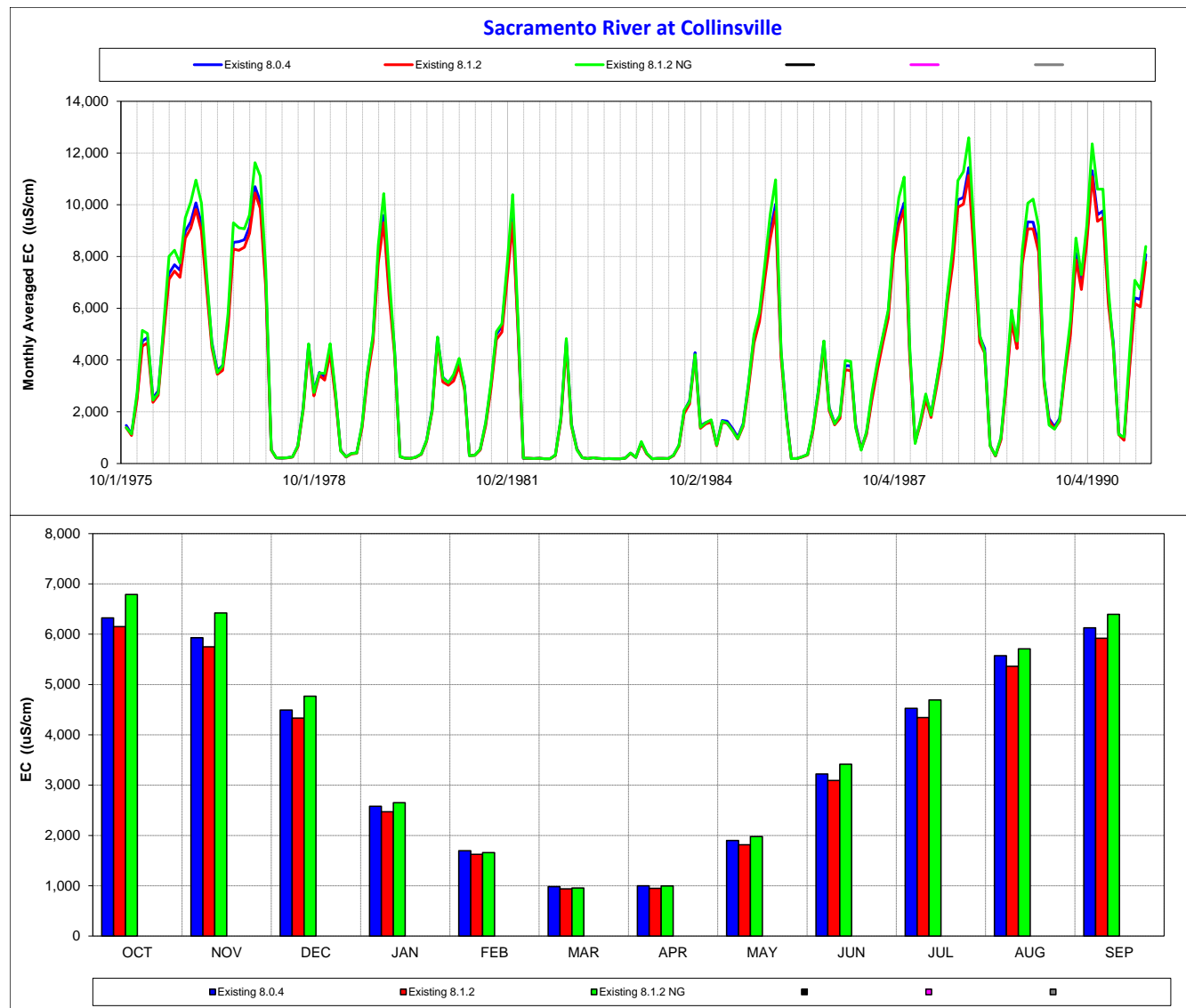
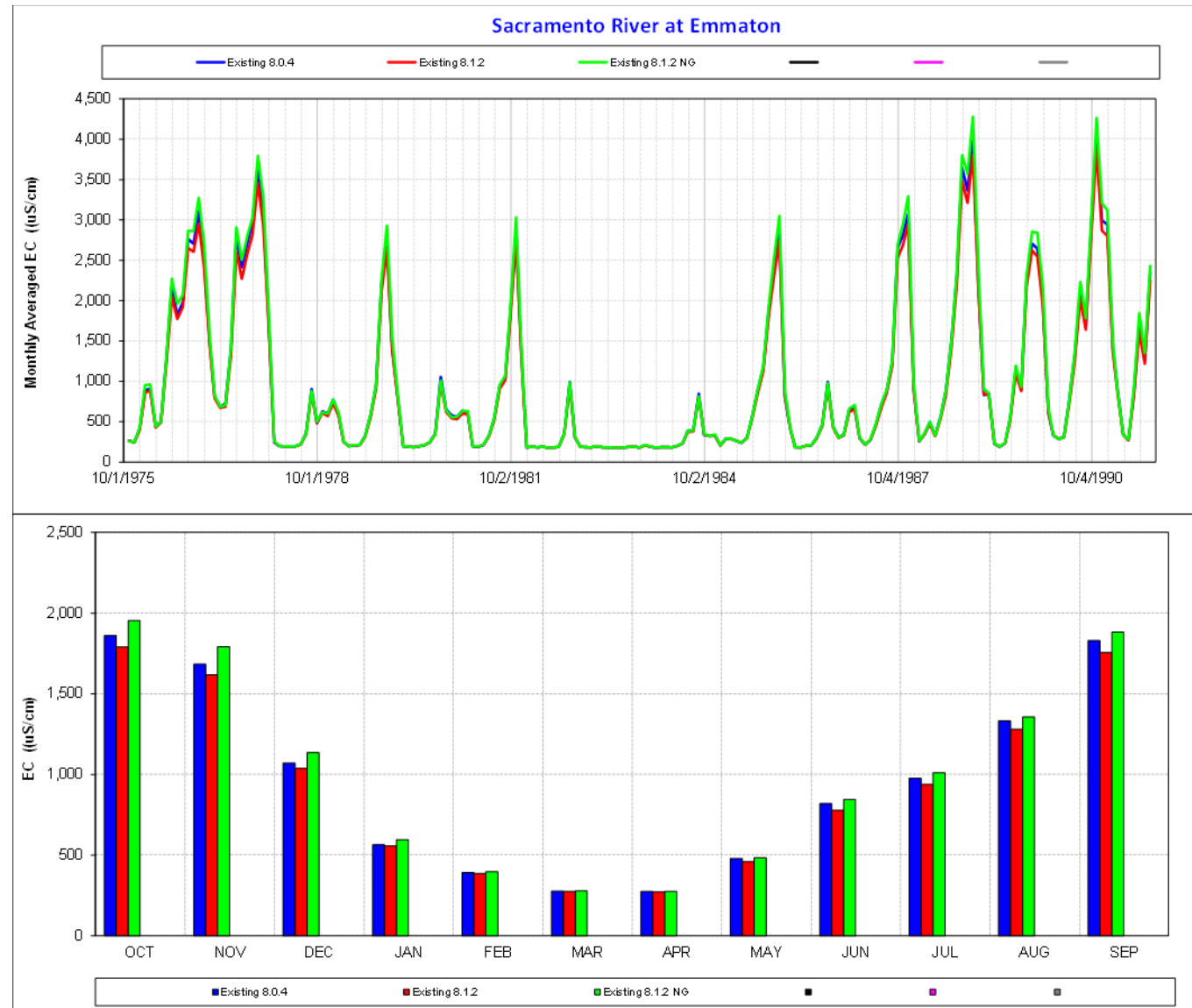
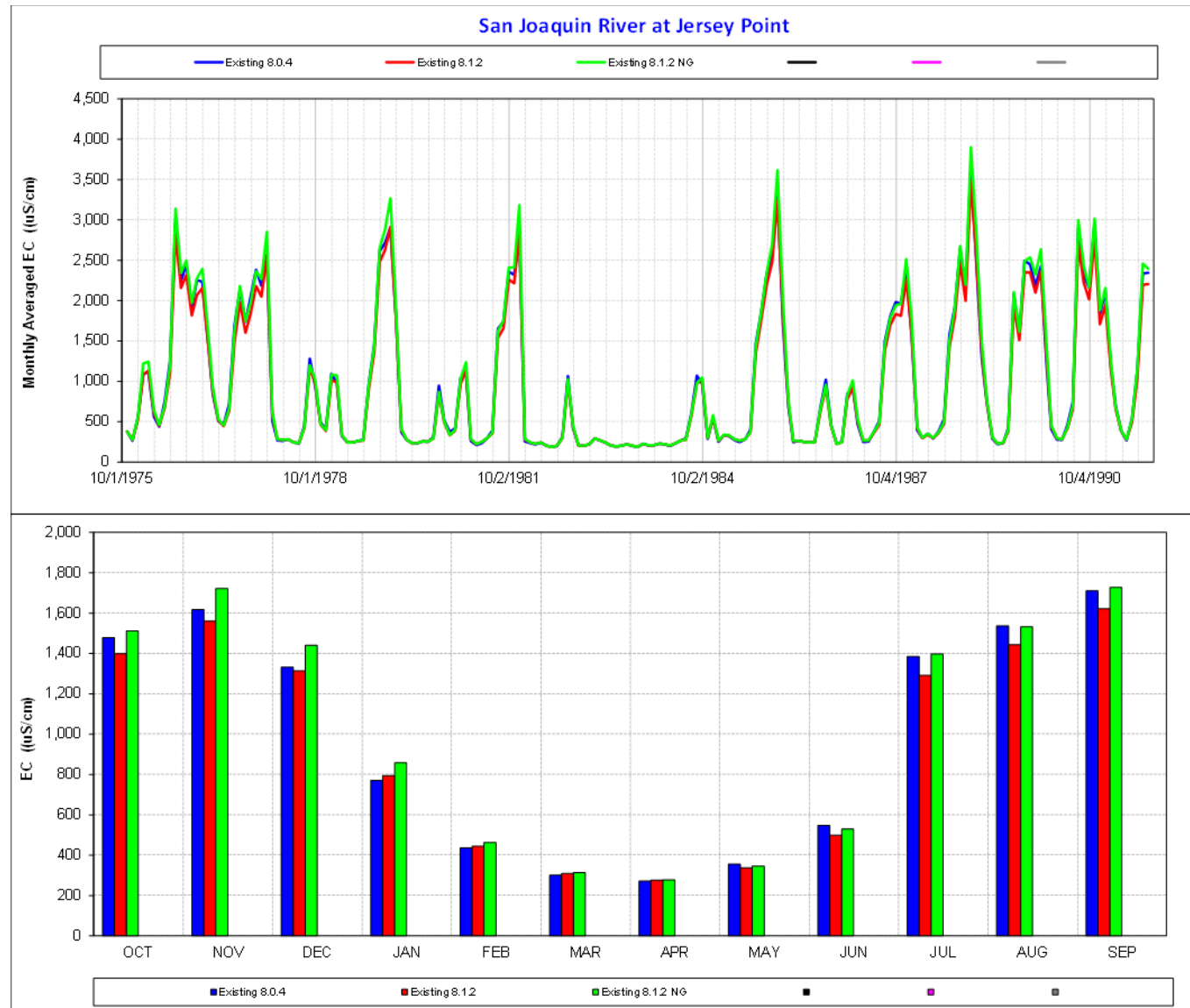
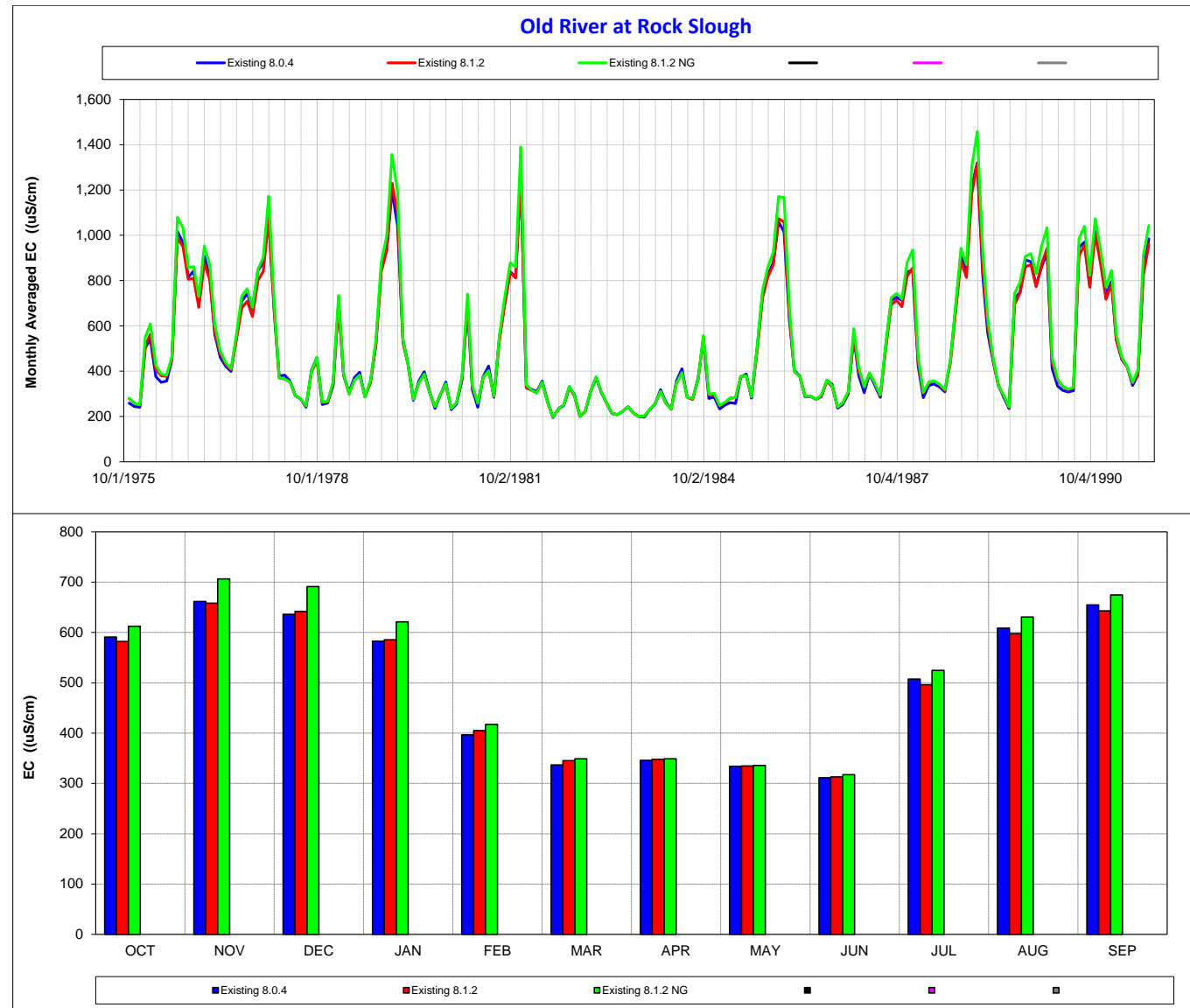


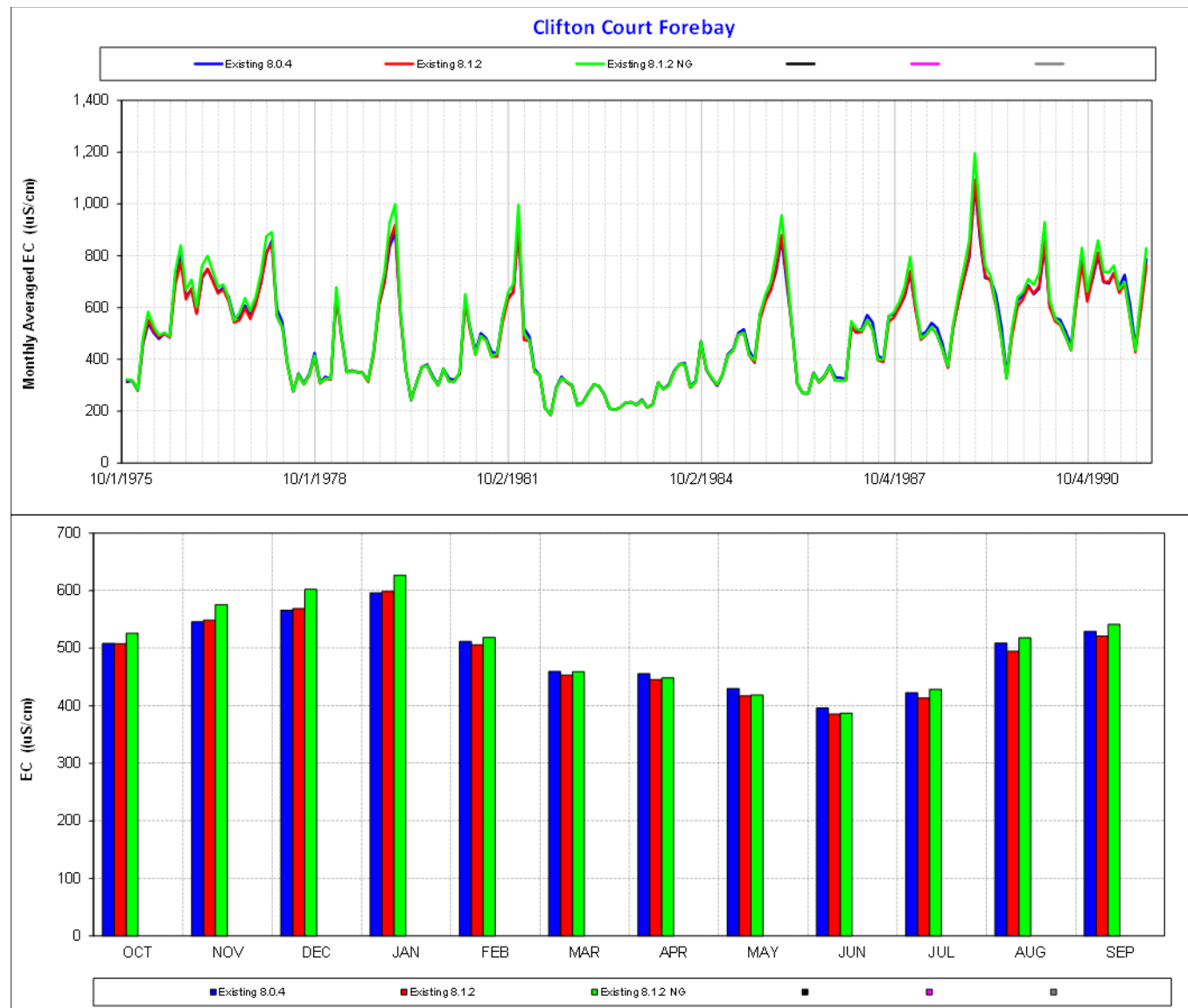
Figure 1-2 Comparison Electrical Conductivity at Collinsville (RSAC081)

Notes: EC = electrical conductivity, NG = New Generator, $\mu\text{S}/\text{cm}$ = microSiemens per centimeter

**Figure 1-3 Comparison of Electrical Conductivity at Emmaton (RSAC092)**Notes: EC = electrical conductivity, NG = New Generator, $\mu\text{S}/\text{cm}$ = microSiemens per centimeter

**Figure 1-4 Comparison of Electrical Conductivity at Jersey Point (RSAN018)**Notes: EC = electrical conductivity, NG = New Generator, $\mu\text{S}/\text{cm}$ = microSiemens per centimeter

**Figure 1-5 Comparison of Electrical Conductivity at Old River at Rock Slough (ROLD024)**Notes: EC = electrical conductivity, NG = New Generator, $\mu\text{S}/\text{cm}$ = microSiemens per centimeter

**Figure 1-6 Comparison of Electrical Conductivity at Clifton Court Forebay**Notes: EC = electrical conductivity, NG = New Generator, $\mu\text{S}/\text{cm}$ = microSiemens per centimeter

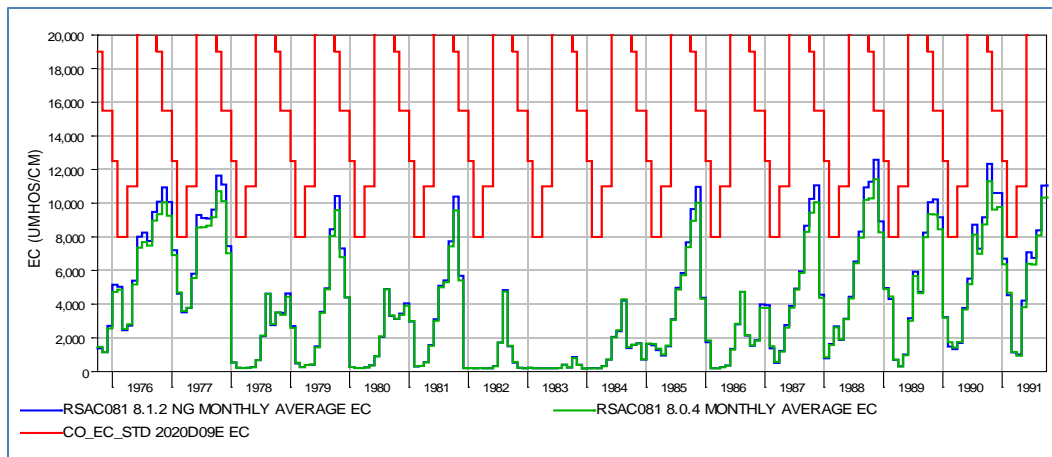


Figure 1-7 Comparison of Electrical Conductivity with D-1641 Standard at Collinsville (RSAC081)
Notes: EC = electrical conductivity, $\mu\text{mhos}/\text{cm}$ = micromhos per centimeter

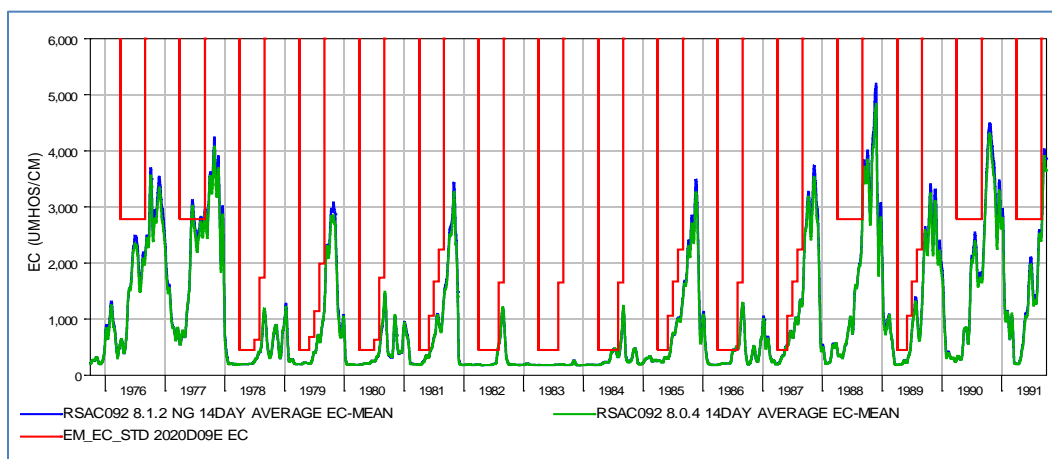


Figure 1-8 Comparison of Electrical Conductivity with D-1641 Standard at Emmaton (RSAC092)
Notes: EC = electrical conductivity, $\mu\text{mhos}/\text{cm}$ = micromhos per centimeter

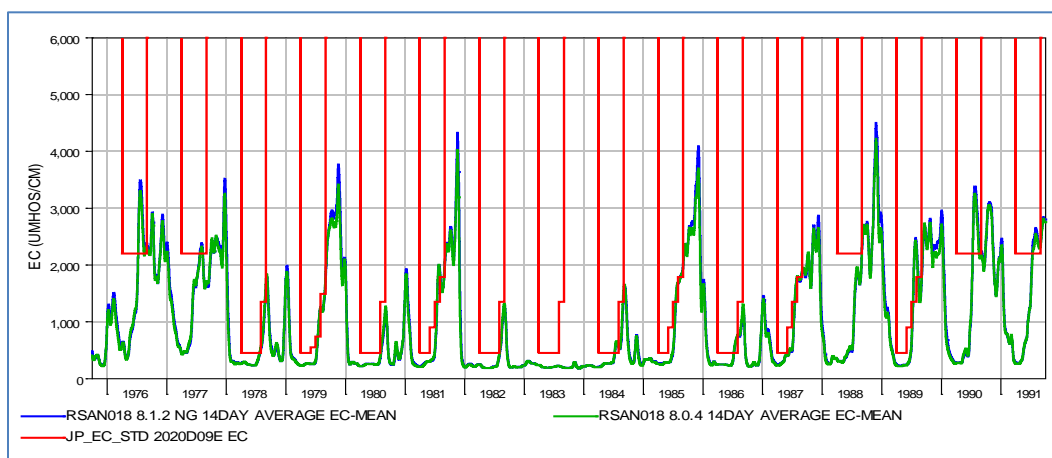


Figure 1-9 Comparison of Electrical Conductivity with D-1641 Standard at Jersey Point (RSAN018)
Notes: EC = electrical conductivity, $\mu\text{mhos}/\text{cm}$ = micromhos per centimeter

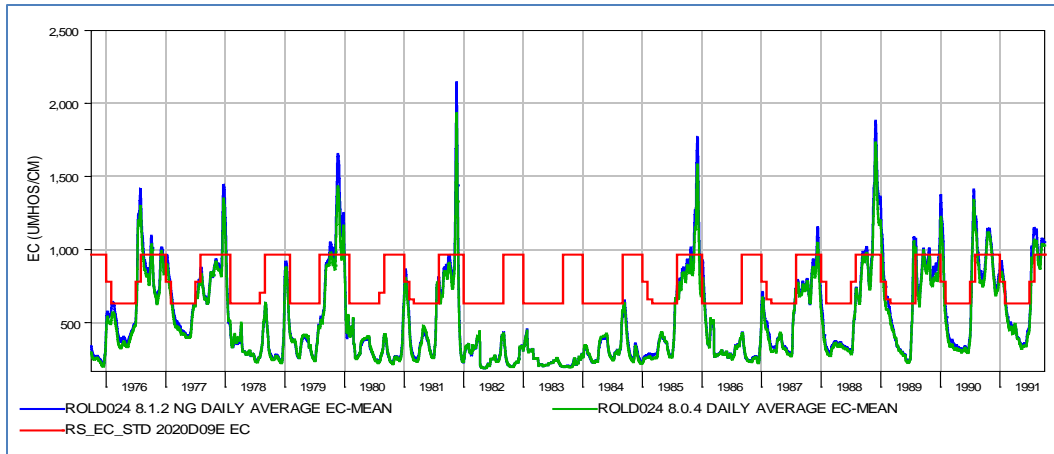


Figure 1-10 Comparison of Electrical Conductivity with D-1641 Standard at Old River at RockSlough (ROLD024)

Notes: EC = electrical conductivity, $\mu\text{mhos}/\text{cm}$ = micromhos per centimeter

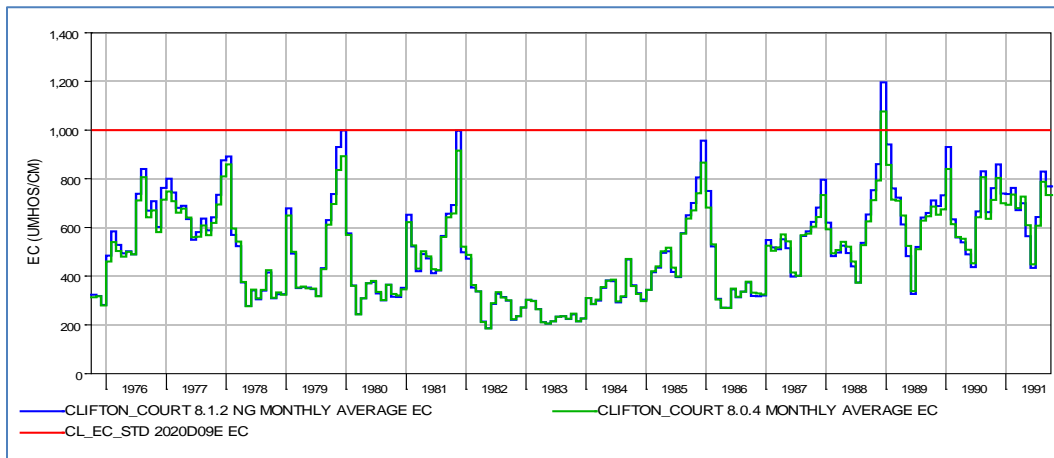


Figure 1-11 Comparison of Electrical Conductivity with D-1641 Standard at Clifton Court Forebay

Notes: EC = electrical conductivity, $\mu\text{mhos}/\text{cm}$ = micromhos per centimeter

1.3 Incremental Differences of Proposed Alternatives

EC results were compared for the following scenarios:

- Existing condition by using DSM2 v8.1.2.
- Existing condition by using DSM2 v8.1.2 with the New Generator.
- No Action Alternative (NAA) by using DSM2 v8.1.2.
- NAA by using DSM2 v8.1.2 with the New Generator.
- Proposed Action (PA) by using DSM2 v8.1.2.
- PA by using DSM2 v8.1.2 with the New Generator.

The detailed descriptions of modeling settings can be found in the Final BDCP/California WaterFix Environmental Impact Report/Environmental Impact Statement (California Department of Water Resources and U.S. Bureau of Reclamation 2016) and are briefly described below.

- Existing: Baseline with the current project conditions.
- NAA: Representation of the base Central Valley Project/State Water Project (CVP/SWP) operations and physical conditions (including climate, sea level rise and development, etc.) at approximately 2030.
- PA: In addition to continuing the CVP/SWP operations under the NAA, it includes several main components that will affect CVP/SWP operations and the hydrologic response of the system, which are the construction and operation of new north Delta intakes and associated conveyance and changes in the operation of the existing south Delta export facilities.

A sea level rise of 15 centimeters was assumed to occur at 2030 for the NAA and PA analyses. To reflect this effect, Martinez boundary EC is adjusted by using the equation

$$\text{EC_slr15} = 0.9954 * \text{EC} + 556.33.$$

Monthly averaged EC results at key locations — Collinsville, Emmaton, Jersey Point, Rock Slough, and Clifton Court — are plotted in Figures 1-12–1-16. The following conclusions can be made from the results:

1. When comparing results with Old and New Generators for each scenario (i.e., existing condition, NAA, and PA), it is clear that the New Generator presents higher EC at every location and for most of the months. During low-EC periods, January–May, the differences are negligible (Figures 1-12–1-16).
2. The incremental differences between the existing condition and PA are calculated and plotted in Figures 1-17–1-21. The incremental differences with the New Generator are very close to the results with the Old Generator. This helps justify the conclusion that the New Generator will not affect the results and conclusions made with previous version.

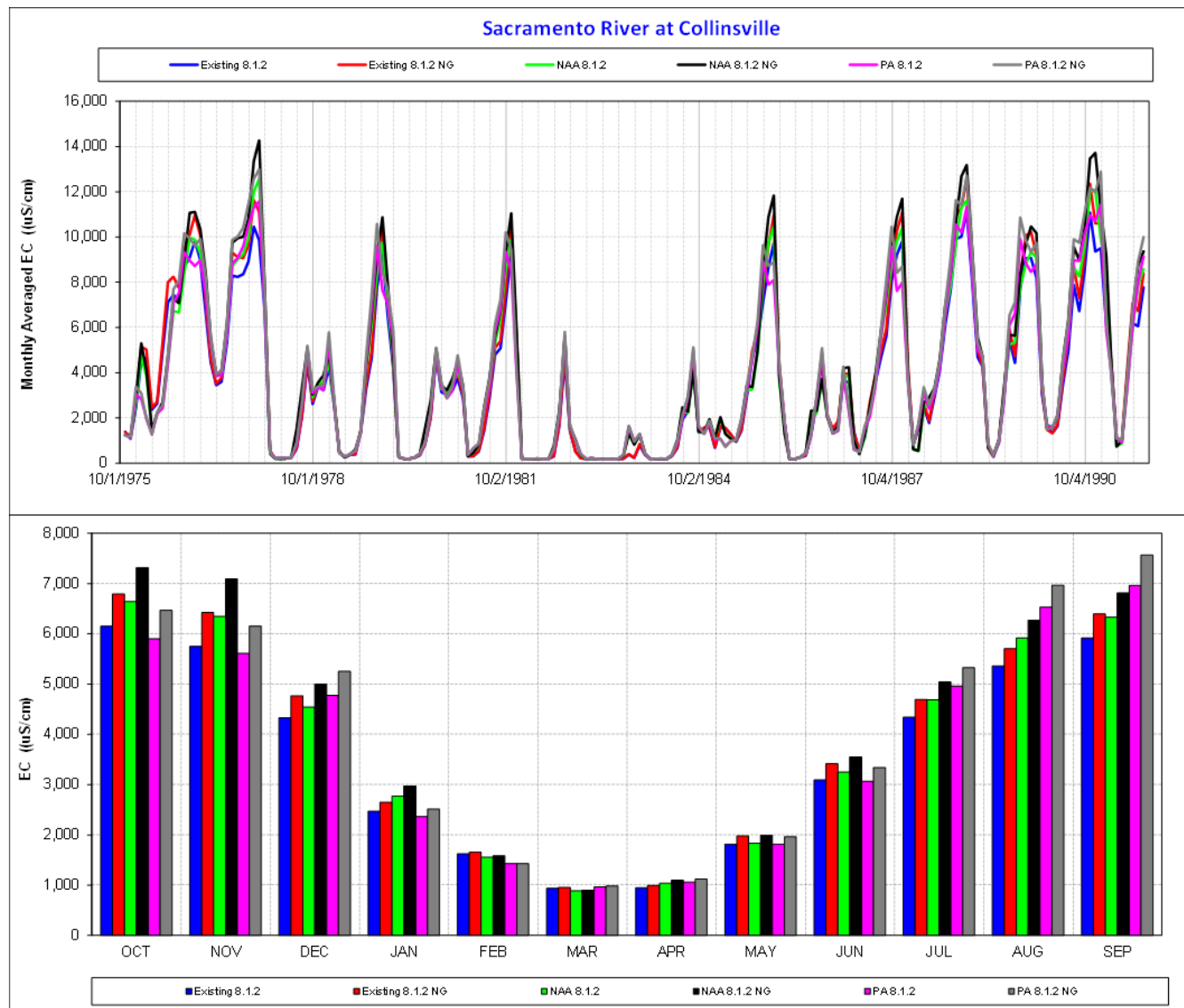


Figure 1-12 Comparison of Electrical Conductivity at Collinsville (RSAC081)

Notes: EC = electrical conductivity, NAA = no action alternative, NG = New Generator, PA = proposed action, $\mu\text{S}/\text{cm}$ = microSiemens per centimeter

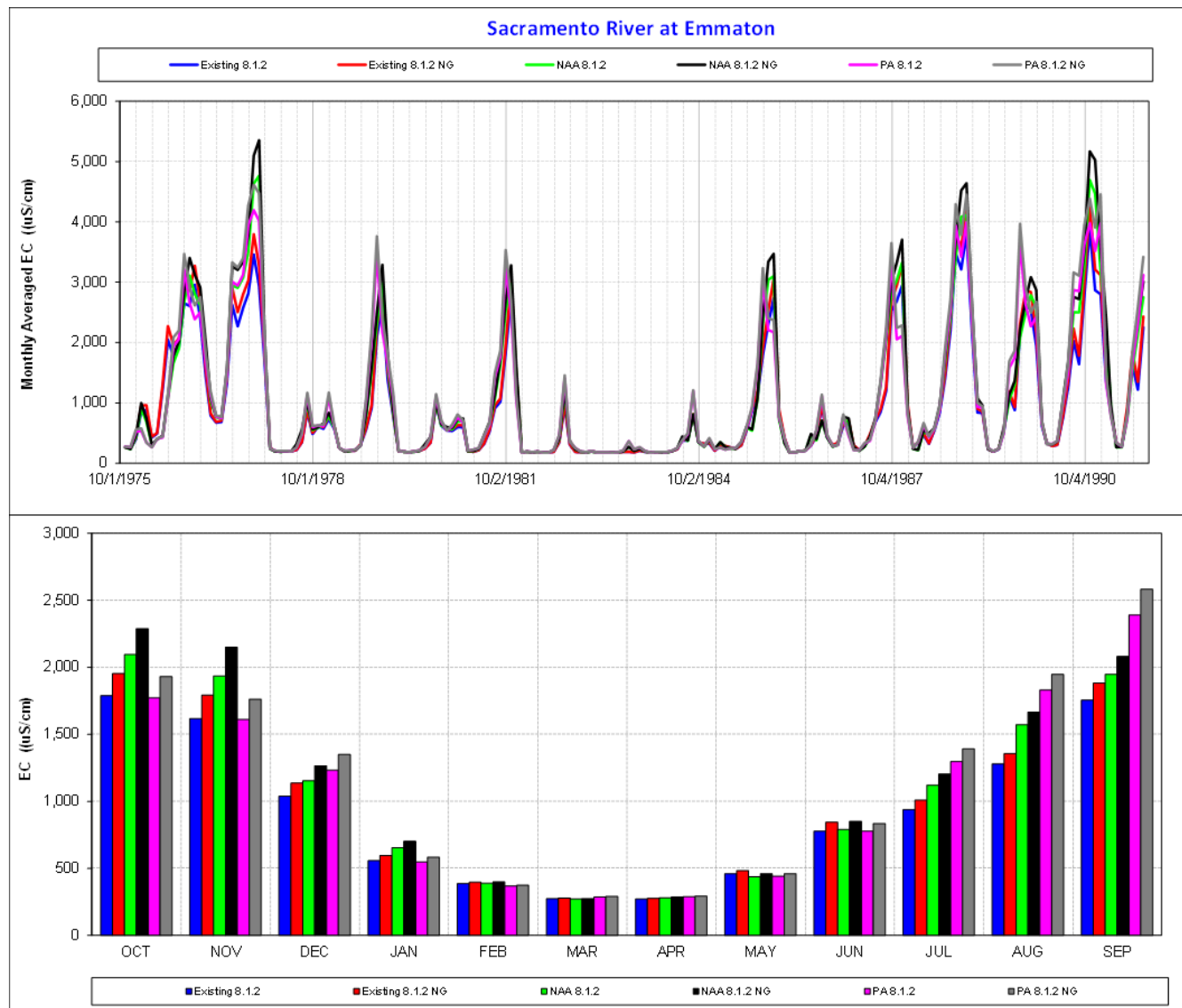
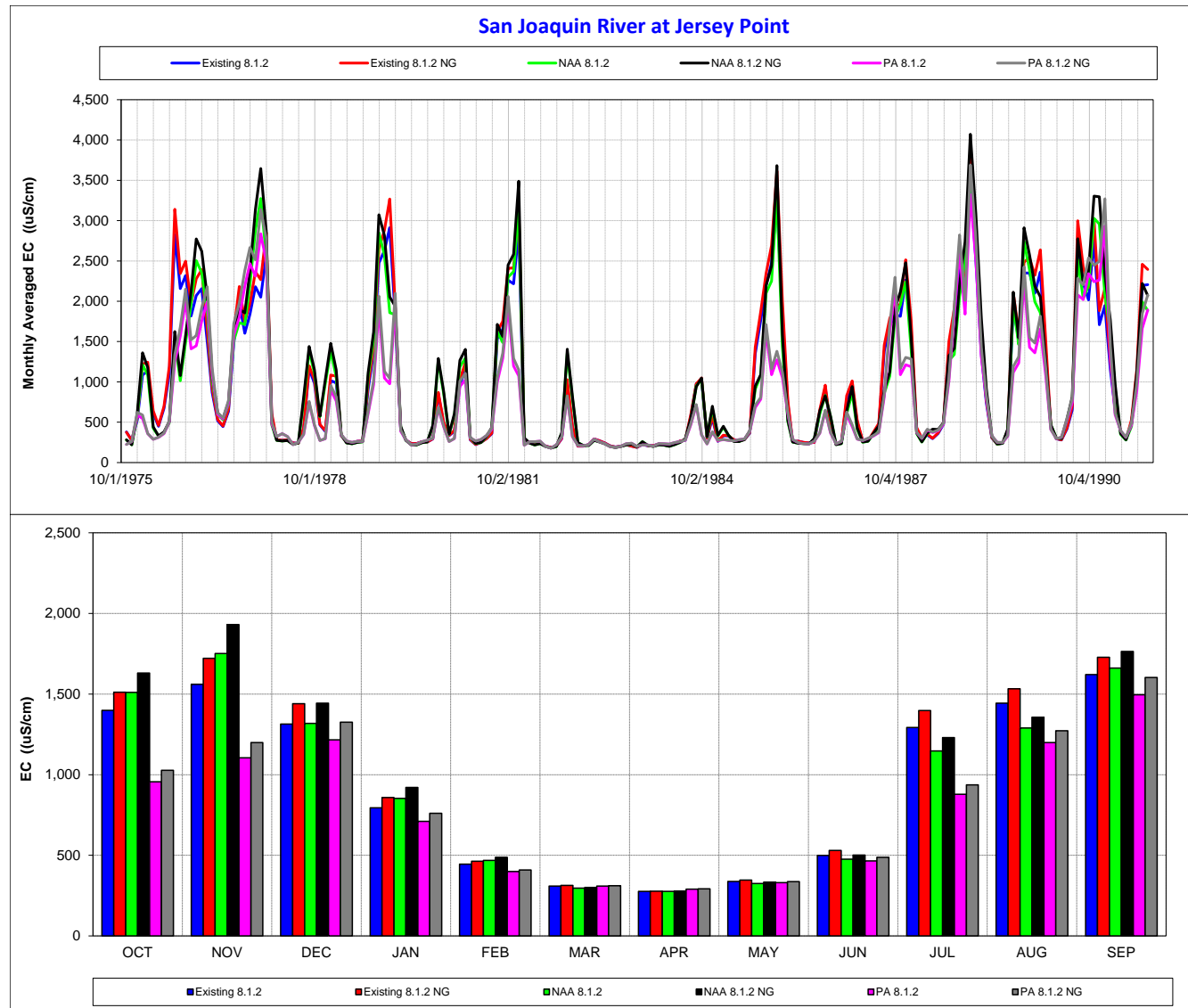


Figure 1-13 Comparison of Electrical Conductivity at Emmaton (RSAC092)

Notes: EC = electrical conductivity, NAA = no action alternative, NG = New Generator, PA = proposed action,
 $\mu\text{S}/\text{cm}$ = microSiemens per centimeter

**Figure 1-14 Comparison of Electrical Conductivity at Jersey Point (RSAN018)**

Notes: EC = electrical conductivity, NAA = no action alternative, NG = New Generator, PA = proposed action,
 $\mu\text{S}/\text{cm}$ = microSiemens per centimeter

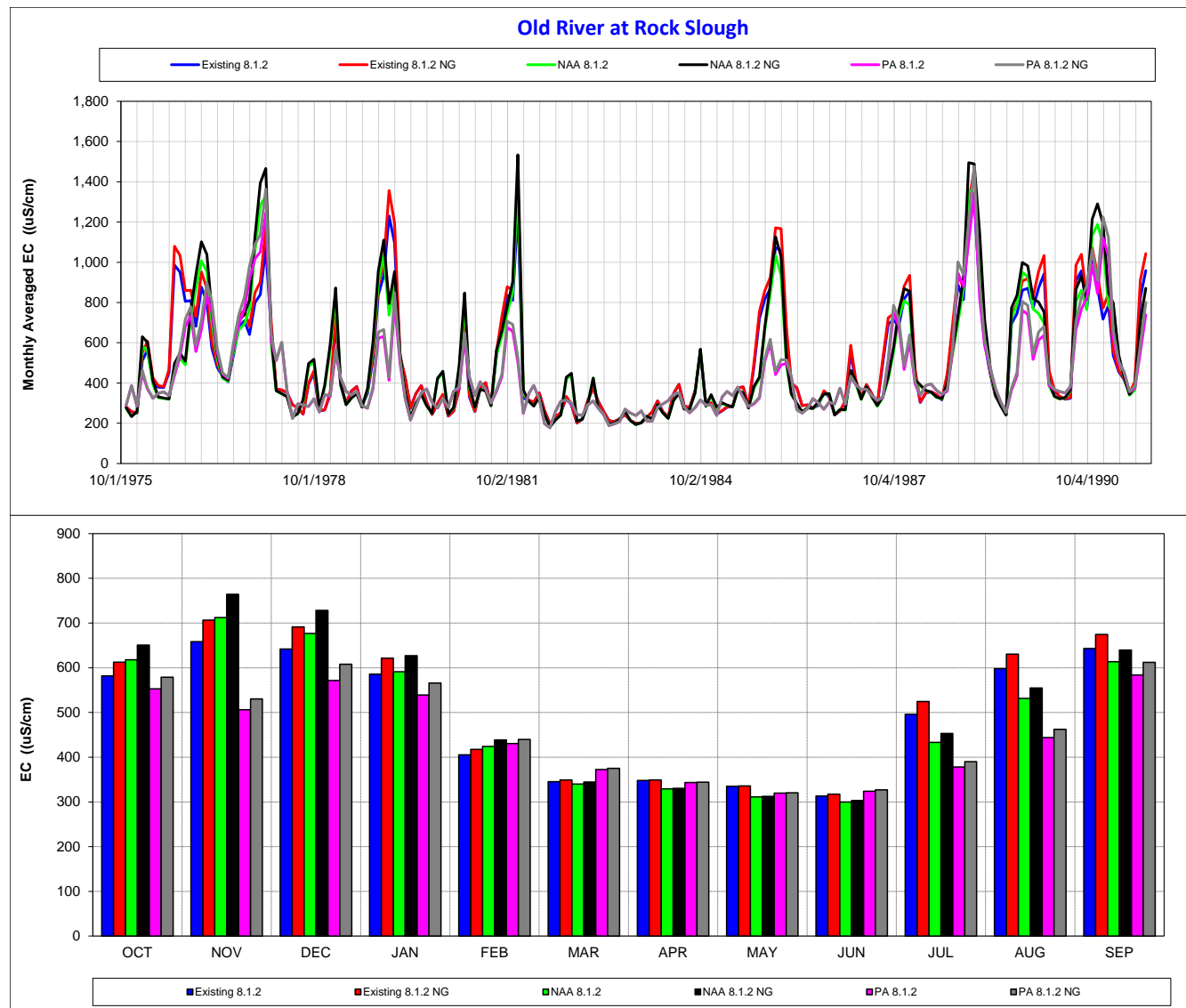
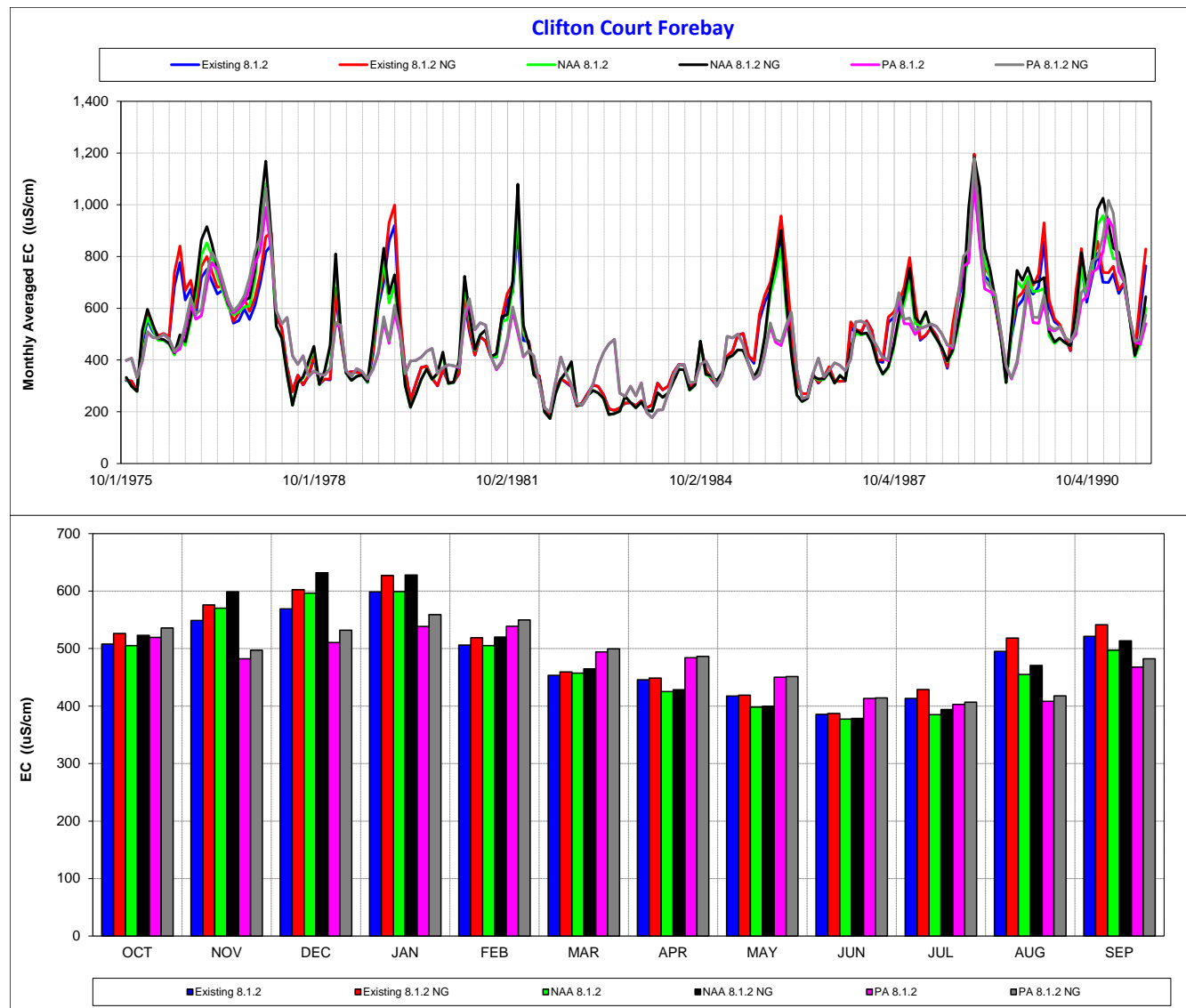
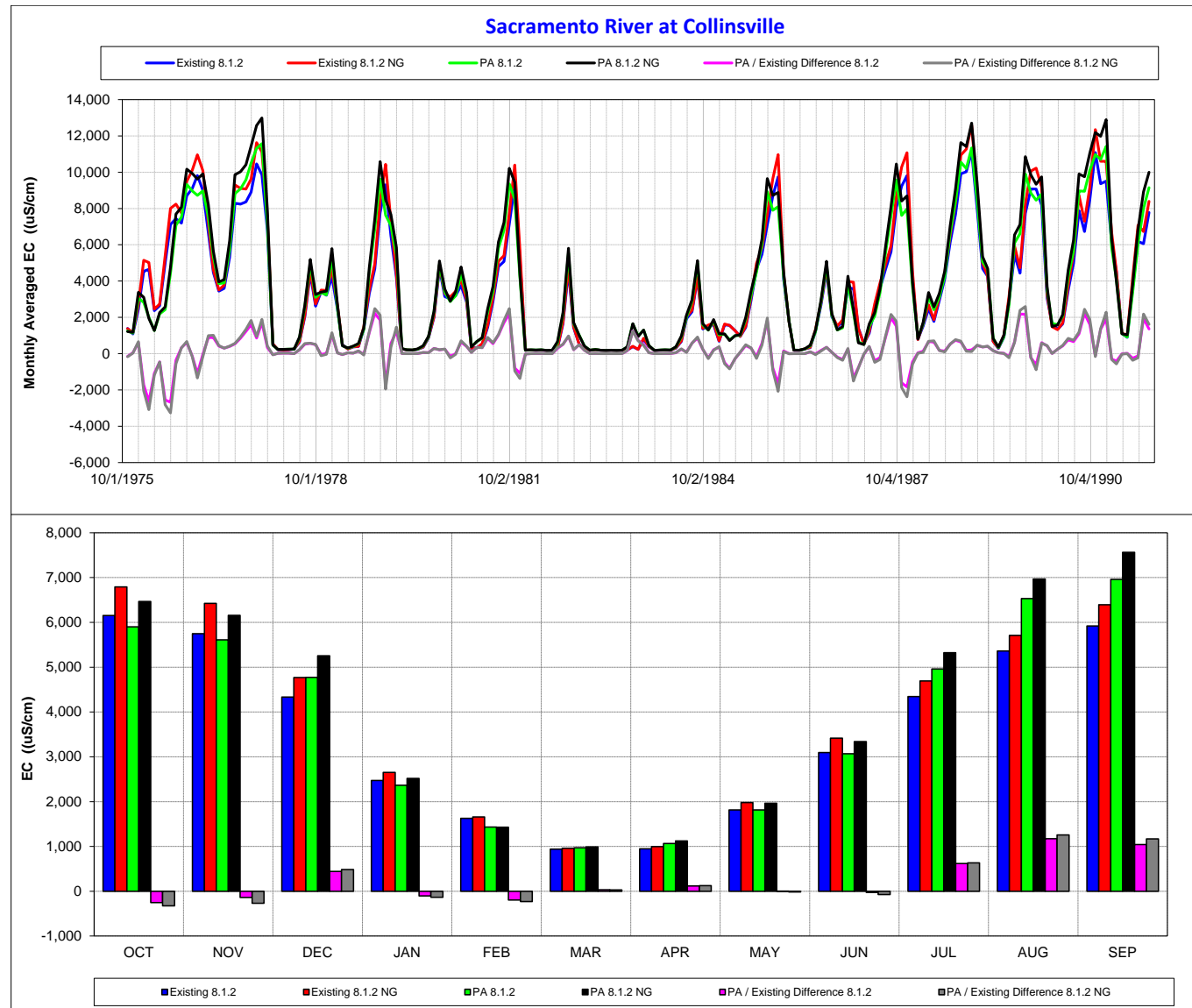


Figure 1-15 Comparison of Electrical Conductivity at Old River at Rock Slough (ROLD024)

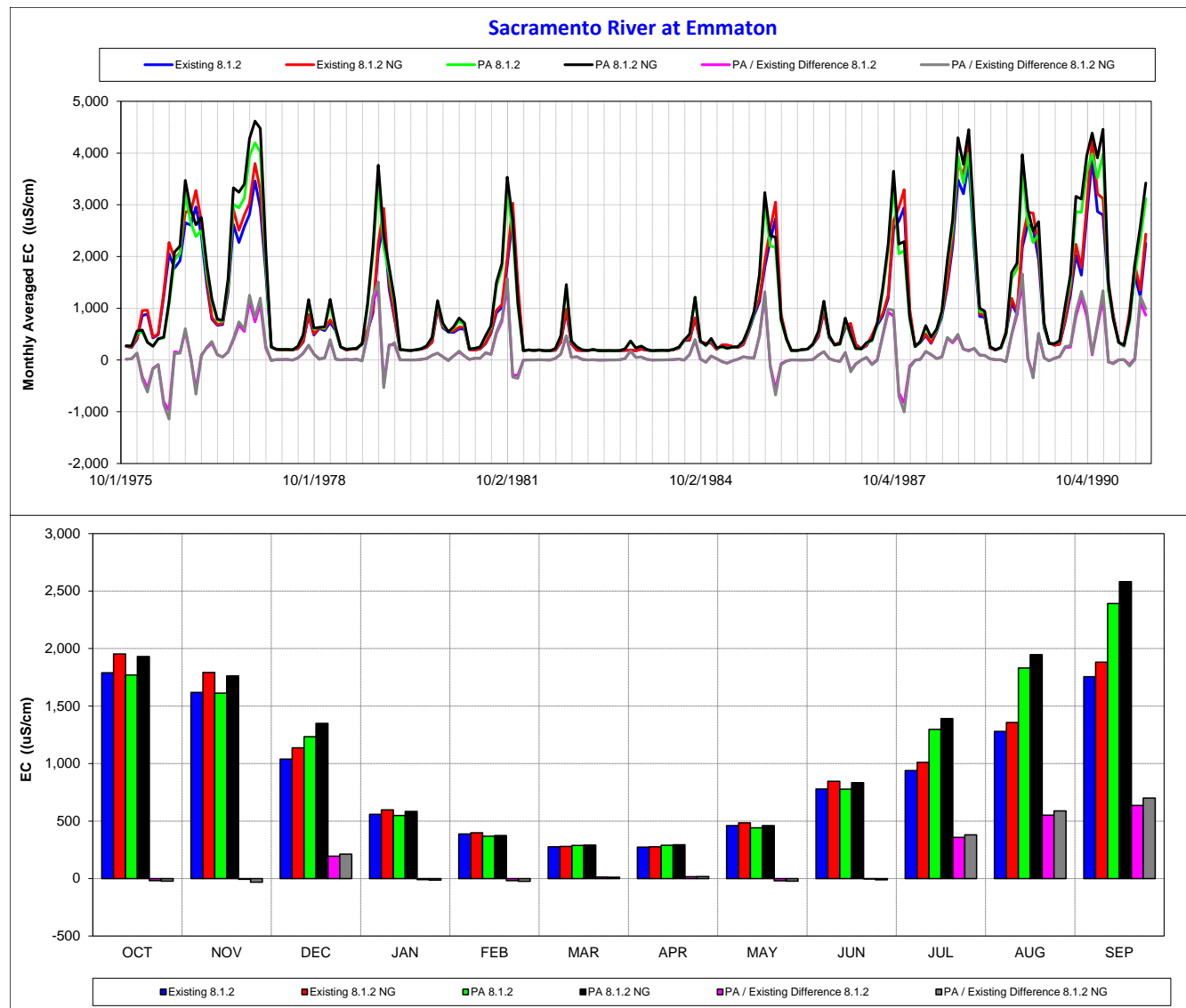
Notes: EC = electrical conductivity, NAA = no action alternative, NG = New Generator, PA = proposed action,
 $\mu\text{S}/\text{cm}$ = microSiemens per centimeter

**Figure 1-16 Comparison of Electrical Conductivity at Clifton Court Forebay**

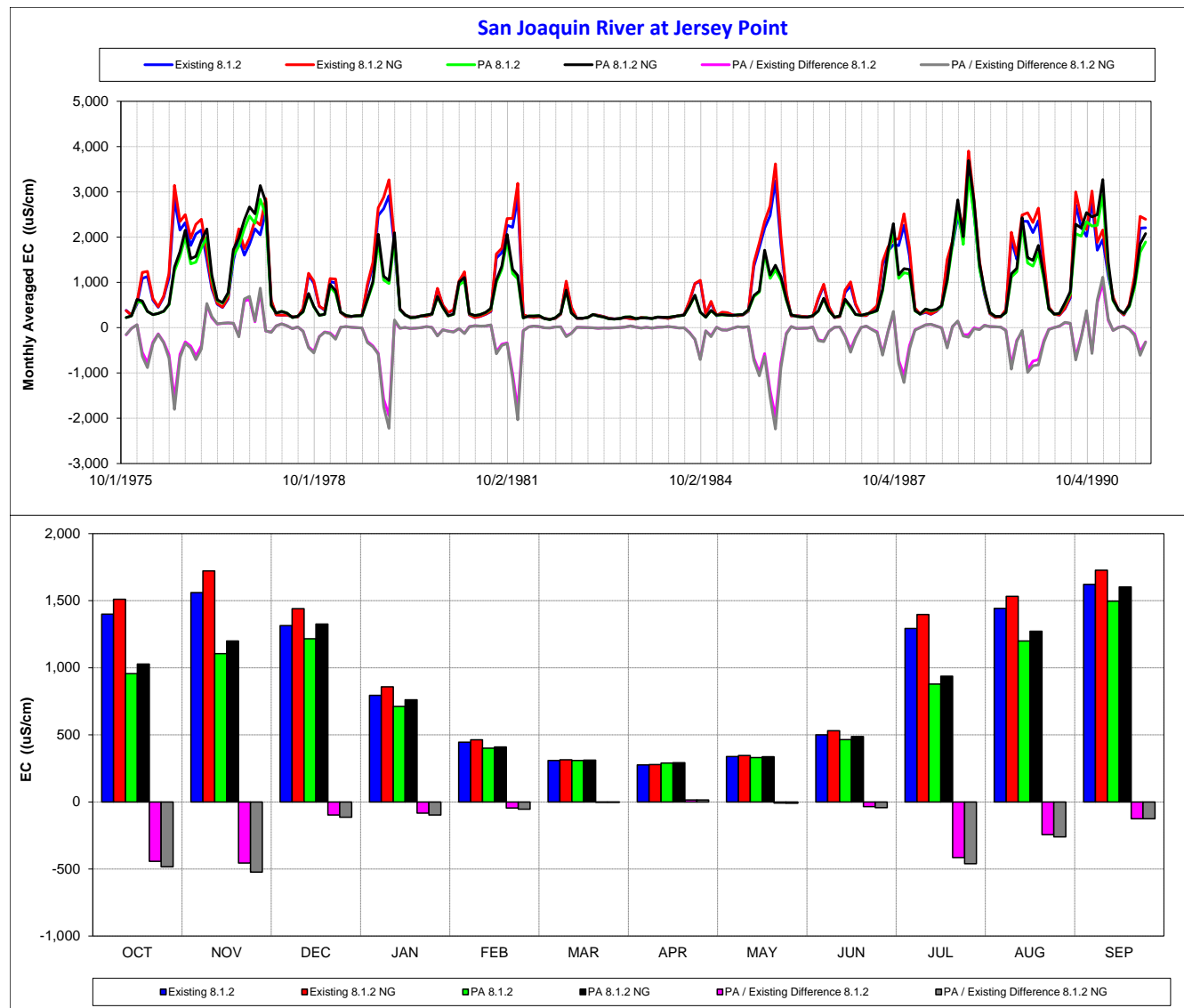
Notes: EC = electrical conductivity, NAA = no action alternative, NG = New Generator, PA = proposed action,
 $\mu\text{S}/\text{cm}$ = microSiemens per centimeter

**Figure 1-17 Comparison of Electrical Conductivity at Collinsville (RSAC081)**

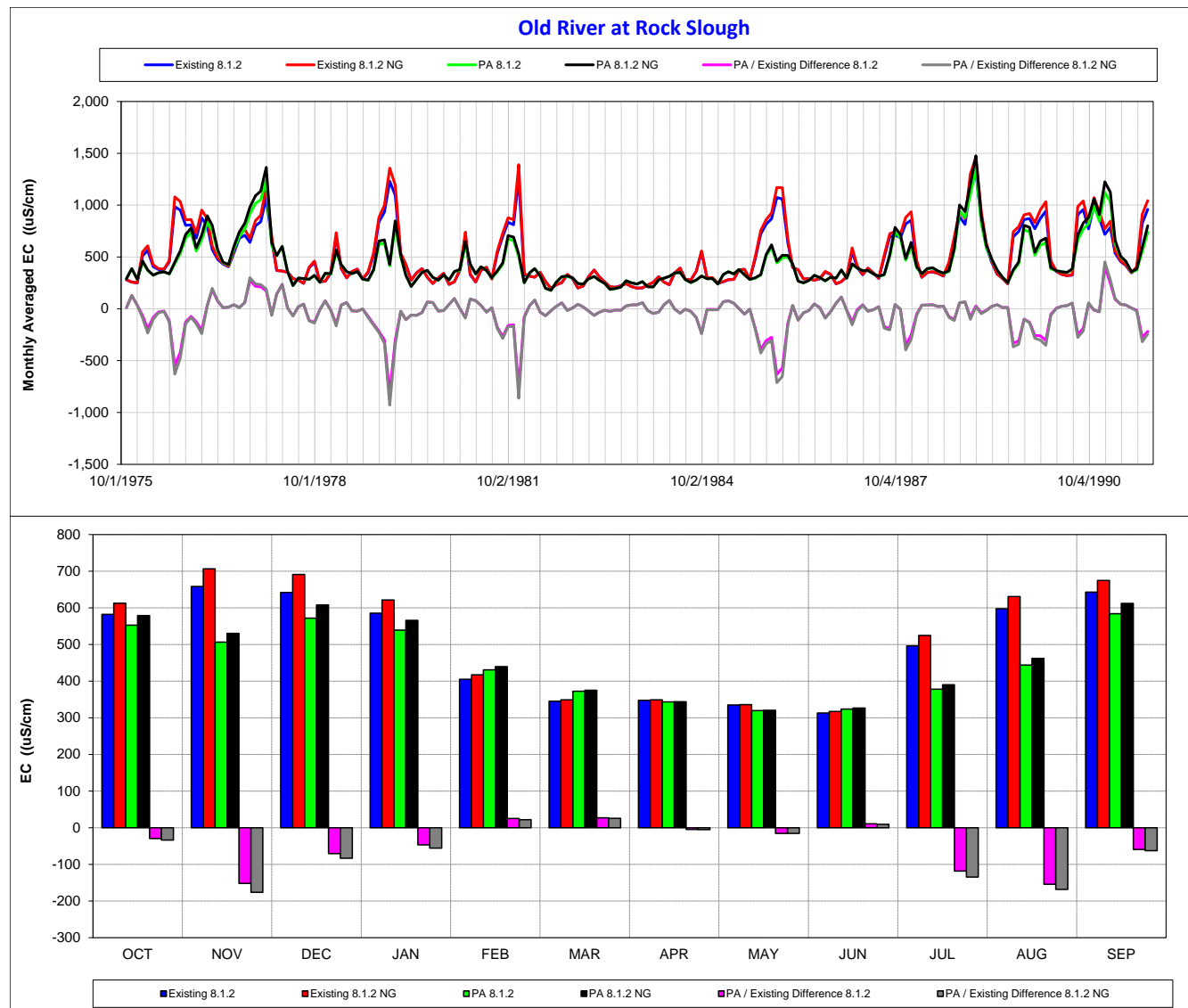
Notes: EC = electrical conductivity, NAA = no action alternative, NG = New Generator, PA = proposed action, $\mu\text{S}/\text{cm}$ = microSiemens per centimeter

**Figure 1-18 Comparison of Electrical Conductivity at Emmaton (RSAC092)**

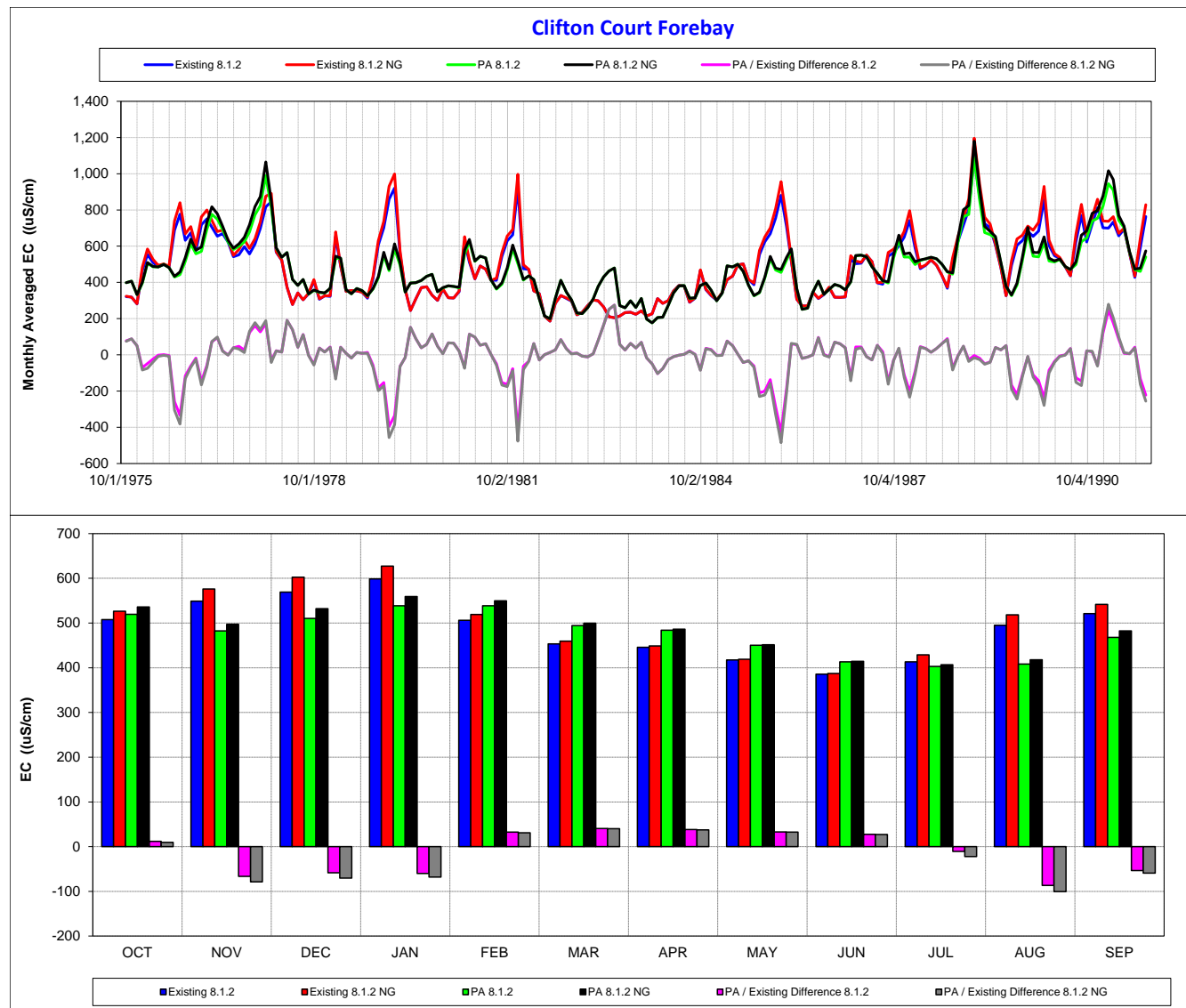
Notes: EC = electrical conductivity, NAA = no action alternative, NG = New Generator, PA = proposed action,
 $\mu\text{S}/\text{cm}$ = microSiemens per centimeter

**Figure 1-19 Comparison of Electrical Conductivity at Jersey Point (RSAN018)**

Notes: EC = electrical conductivity, NAA = no action alternative, NG = New Generator, PA = proposed action,
 $\mu\text{S}/\text{cm}$ = microSiemens per centimeter

**Figure 1-20 Comparison of Electrical Conductivity at Old River at Rock Slough (ROLD024)**

Notes: EC = electrical conductivity, NAA = no action alternative, NG = New Generator, PA = proposed action,
 $\mu\text{S}/\text{cm}$ = microSiemens per centimeter

**Figure 1-21 Comparison of Electrical Conductivity at Clifton Court Forebay**

Notes: EC = electrical conductivity, NAA = no action alternative, NG = New Generator, PA = proposed action,
 $\mu\text{S}/\text{cm}$ = microSiemens per centimeter

1.4 Summary

The new Martinez EC Generator was tested with different scenarios, including the existing condition, NAA, and PA. Although the simulated EC results produced by DSM2 v8.1, with the New Generator, are generally higher than the results produced by DSM2 v8.0.4, the differences would not have a significant impact on previous CalSim studies and conclusions based on results produced by DSM2 v8.0.4. The New Generator improved Martinez EC estimation, and accordingly the simulated EC results were also improved. It will be recommended that the Modeling Branch of the Bay-Delta Office adopt DSM2 v8.1, with the New Generator, for future planning studies.

1.5 References Cited

- Ateljevich E. 2001. "Improving Salinity Estimates at the Martinez Boundary." In: *Methodology for Flow and Salinity Estimates in the Sacramento-San Joaquin Delta and Suisun Marsh. 22nd Annual Progress Report*. Chapter 11. Sacramento (CA):) : Delta Modeling Section. Bay-Delta Office. California Department of Water Resources.
- Denton R. and Sullivan G. 1993. "Antecedent Flow-salinity Relations: Application to Delta Planning Model." In: *Methodology for Flow and Salinity Estimates in the Sacramento-San Joaquin Delta and Suisun Mars. 34th Annual Progress Report*. Sacramento (CA):) : Delta Modeling Section. Bay-Delta Office. California Department of Water Resources.
- Sandhu P. and Zhou Y. 2015. "Calibrating the Martinez Boundary Salinity Generator using PEST." In: *Methodology for Flow and Salinity Estimates in the Sacramento-San Joaquin Delta and Suisun Marsh. 36th Annual Progress Report*. Chapter 7.Sacramento (CA): Delta Modeling Section. Bay-Delta Office. California Department of Water Resources.
- California Department of Water Resources and U.S. Bureau of Reclamation. 2016. Volume I. In: *Bay Delta Conservation Plan/California WaterFix, Final Environmental Impact Report/Environmental Impact Statement* (December). Sacramento (CA): Viewed online at: http://baydeltaconservationplan.com/FinalEIREIS/FinalEIR-EIS_Volumel.aspx. Accessed: 2017.

Methodology for Flow and Salinity Estimates in the Sacramento-San Joaquin Delta and Suisun Marsh

**38th Annual Progress Report
June 2017**

Chapter 2

DSM2 Nutrients Modeling Sensitivity Analysis

Authors: Ming-Yen Tu and Hari Rajbhandari
Delta Modeling Section
Bay-Delta Office
California Department of Water Resources



Contents

Chapter 2 DSM2 Nutrients Modeling Sensitivity Analysis.....	2-i
2 DSM2 Nutrients Modeling Sensitivity Analysis.....	2-1
2.1 INTRODUCTION	2-1
2.2 MODELING BASE AND SENSITIVITY ANALYSIS SCENARIOS.....	2-1
2.3 PRELIMINARY MODELING RESULTS AND FINDINGS	2-1
2.3.1 <i>Algae_Growth_1.0</i>	2-2
2.3.2 <i>NH₃_Decay_0.02</i>	2-5
2.3.3 <i>NH₃_Decay_0.6</i>	2-5
2.3.4 <i>Org-P_Decay_0.05</i>	2-9
2.3.5 <i>Algae_Die_0.002</i>	2-9
2.3.6 <i>Additional Discussion of Results</i>	2-9
2.4 NEXT STEPS AND POTENTIAL FUTURE EFFORTS TO IMPROVE MODEL CALIBRATION.....	2-12
2.5 REFERENCES CITED	2-48

Figures

Figure 2-1 Nutrients Interactions	2-3
Figure 2-2 Example Locations in Delta for Showing the Model Results Sensitivity	2-4
Figure 2-3 Qualitative Assessments on Model Results of Algae_Growth_1.0 Scenario Compared with the Baseline Scenario	2-13
Figure 2-4 Time-Series Results of Baseline and Algae_Growth_1.0 Scenarios at San Joaquin River at Mossdale	2-14
Figure 2-5 Time-Series Results of Baseline and Algae_Growth_1.0 Scenarios at Rough and Ready Island.....	2-15
Figure 2-6 Time-Series Results of Baseline and Algae_Growth_1.0 Scenarios at San Joaquin River at Prisoners Point	2-16
Figure 2-7 Time-Series Results of Baseline and Algae_Growth_1.0 Scenarios at Old River at Tracy Road.....	2-17
Figure 2-8 Time-Series Results of Baseline and Algae_Growth_1.0 Scenarios at Middle River at Howard Road	2-18
Figure 2-9 Time-Series Results of Baseline and Algae_Growth_1.0 Scenarios at Clifton Court Forebay.....	2-19
Figure 2-10 Qualitative Assessments on Model Results of NH ₃ _Decay_0.02 Scenario Compared with the Baseline Scenario	2-20
Figure 2-11 Time-Series Results of Baseline and NH ₃ _Decay_0.02 Scenarios at San Joaquin River at Mossdale	2-21

Figure 2-12 Time-Series Results of Baseline and NH ₃ _Decay_0.02 Scenarios at Rough and Ready Island.....	2-22
Figure 2-13 Time-Series Results of Baseline and NH ₃ _Decay_0.02 Scenarios at San Joaquin River at Prisoners Point	2-23
Figure 2-14 Time-Series Results of Baseline and NH ₃ _Decay_0.02 Scenarios at Old River at Tracy Road	2-24
Figure 2-15 Time-Series Results of Baseline and NH ₃ _Decay_0.02 Scenarios at Middle River at Howard Road	2-25
Figure 2-16 Time-Series Results of Baseline and NH ₃ _Decay_0.02 Scenarios at Clifton Court Forebay.....	2-26
Figure 2-17 Qualitative Assessments on Model Results of NH ₃ _Decay_0.6 Scenario Compared with the Baseline Scenario	2-27
Figure 2-18 Time-Series Results of Baseline and NH ₃ _Decay_0.6 Scenarios at San Joaquin River at Mossdale	2-28
Figure 2-19 Time-Series Results of Baseline and NH ₃ _Decay_0.6 Scenarios at Rough and Ready Island	2-29
Figure 2-20 Time-Series Results of Baseline and NH ₃ _Decay_0.6 Scenarios at San Joaquin River at Prisoners Point	2-30
Figure 2-21 Time-Series Results of Baseline and NH ₃ _Decay_0.6 Scenarios at Old River at Tracy Road	2-31
Figure 2-22 Time-Series Results of Baseline and NH ₃ _Decay_0.6 Scenarios at Middle River at Howard Road	2-32
Figure 2-23 Time-Series Results of Baseline and NH ₃ _Decay_0.6 Scenarios at Clifton Court Forebay.....	2-33
Figure 2-24 Qualitative Assessments on Model Results of Org-P_Decay_0.05 Scenario Compared with the Baseline Scenario	2-34
Figure 2-25 Time-Series Results of Baseline and Org-P_Decay_0.05 Scenarios at San Joaquin River at Mossdale	2-35
Figure 2-26 Time-Series Results of Baseline and Org-P_Decay_0.05 Scenarios at Rough and Ready Island.....	2-36
Figure 2-27 Time-Series Results of Baseline and Org-P_Decay_0.05 Scenarios at San Joaquin River at Prisoners Point	2-37
Figure 2-28 Time-Series Results of Baseline and Org-P_Decay_0.05 Scenarios at Old River at Tracy Road.....	2-38
Figure 2-29 Time-Series Results of Baseline and Org-P_Decay_0.05 Scenarios at Middle River at Howard Road	2-39
Figure 2-30 Time-Series Results of Baseline and Org-P_Decay_0.05 Scenarios at Clifton Court Forebay.....	2-40
Figure 2-31 Qualitative Assessments on Model Results of Algae_Die_0.002 Scenario Compared with the Baseline Scenario	2-41
Figure 2-32 Time-Series Results of Baseline and Algae_Die_0.002 Scenarios at San Joaquin River at Mossdale	2-42

Figure 2-33 Time-Series Results of Baseline and Algae_Die_0.002 Scenarios at Rough and Ready Island.....	2-43
Figure 2-34 Time-Series Results of Baseline and Algae_Die_0.002 Scenarios at San Joaquin River at Prisoners Point	2-44
Figure 2-35 Time-Series Results of Baseline and Algae_Die_0.002 Scenarios at Old River at Tracy Road.....	2-45
Figure 2-36 Time-Series Results of Baseline and Algae_Die_0.002 Scenarios at Middle River at Howard Road	2-46
Figure 2-37 Time-Series Results of Baseline and Algae_Die_0.002 Scenarios at Clifton Court Forebay.....	2-47

Tables

Table 2-1 Summary of Nutrients Modeling Sensitivity Analysis Scenarios.....	2-2
Table 2-2 Baseline Constituents Reaction Rates	2-5
Table 2-3 Summary of Findings Comparing Algae_Growth_1.0 Scenario's Results with the Baseline	2-6
Table 2-4 Summary of Findings Comparing NH ₃ _Decay_0.02 Scenario's Results with the Baseline	2-7
Table 2-5 Summary of Findings Comparing NH ₃ _Decay_0.6 Scenario's Results with the Baseline	2-8
Table 2-6 Summary of Findings Comparing Org-P_Decay_0.05 Scenario's Results with the Baseline.....	2-10
Table 2-7 Summary of Findings Comparing Algae_Die_0.002 Scenario's Results with the Baseline	2-11



2 DSM2 Nutrients Modeling Sensitivity Analysis

2.1 Introduction

The California Department of Water Resources' Delta Modeling Section is developing a new Delta Simulation Model 2 (DSM2) transport module, called the General Transport Model (DSM2-GTM). Progress on this effort was previously reported in Hsu et al. (2014). When the model development is completed, DSM2-GTM will include sediment, dissolved oxygen (DO), and mercury cycling modules to simulate non-conservative constituents.

Part of the DSM2-GTM development process is to calibrate the DO module that simulates the transport and reaction of water temperature and nine non-conservative constituents that are currently included in the DSM2-QUAL computation. These nine constituents are DO, nitrate (NO_3^-), nitrite (NO_2^-), ammonia (NH_3), organic nitrogen (Org-N), carbonaceous biochemical oxygen demand (CBOD), ortho-phosphate (PO_4^{3-}) was assumed to represent dissolved phosphorus, organic phosphorus (Org-P), and algae.

In general, there are two types of model calibration approaches — automatic and manual. If the manual calibration approach is used to carry out the DSM2-GTM calibration, choosing which constituent reaction rates to more efficiently calibrate the model could be challenging. To have a better idea regarding which constituent reaction rates may possess more significant effects on the model results, a sensitivity analysis was performed to test how the model results respond when changing certain constituent reaction rates. This chapter summarizes the sensitivity analysis approach and preliminary findings to date. This sensitivity analysis is an initial investigation and is also an on-going exercise along with the DSM2-GTM development.

2.2 Modeling Base and Sensitivity Analysis Scenarios

Resource Management Associates (RMA) calibrated the DSM2-QUAL nutrients model in 2015. Calibration was in the context of utilizing model results by the San Francisco Estuary Institute as supplemental information to nutrient measurement data, with the goal of understanding better nutrient dynamics in the Sacramento-San Joaquin Delta (Delta). (See Guerin 2015 for more details about the approach, assumptions, data, and results of the model calibration.) For this sensitivity analysis, the RMA model was used as the model base (baseline) to test the sensitivity of model results. The simulation period is January 2000–March 2012, which includes various hydrology conditions (two wet years, three above-normal years, two below-normal years, four dry years, and one critical year).

The original constituent reaction rates in the RMA model varied, depending on the locations of channels in the Delta. For simplification purpose, this analysis investigated the sensitivity of model results by changing the nutrients rates from a range of numbers to a constant number that was applied to the entire Delta. To date, five sensitivity scenarios were tested. Table 2-1 summarizes the detailed information of these scenarios. Figure 2-1 shows the interactions between nutrients modeled in DSM2-QUAL and indicates certain nutrients that will be assessed under each sensitivity scenario.

2.3 Preliminary Modeling Results and Findings

An Excel spreadsheet tool was developed to compare the model results of the baseline scenario with original rates and the tested scenario with changed rates. The results of two different scenarios were shown in plots for easy understanding. The plots showed the daily average of desired nutrients and the differences of the two scenarios in terms of the percentages of the baseline results.

Scenarios	Descriptions of Changes			Types of Changes	Results Will Be Assessed
	Reaction Rates Changed	From	To		
Algae_Growth_1.0	Algae growth rate (per day)	1.5~3.0	1.0	Decrease	Algae, DO, Org-N, Org-P
NH ₃ _Decay_0.02	NH ₃ decay rate (per day)	0.04~0.6	0.02	Decrease	Algae, DO, NH ₃ , NO ₂
NH ₃ _Decay_0.6	NH ₃ decay rate (per day)	0.04~0.6	0.6	Increase or no change	Algae, DO, NH ₃ , NO ₂
Org-P_Decay_0.05	Org-P decay rate (per day)	0.005	0.05	Increase	Algae, DO, PO ₄ , Org-P
Algae_Die_0.002	Algae mortality rate (feet per day)	0.1~1.0	0.002	Decrease	Algae, DO, Org-N, Org-P

Notes: DO = dissolved oxygen, NH₃ = ammonia, NO₂ = nitrite, Org-N = organic nitrogen, Org-P = organic phosphorus, PO₄ = dissolved phosphorus

Table 2-1 Summary of Nutrients Modeling Sensitivity Analysis Scenarios

Six example locations (Figure 2-2) located in the central and south Delta were chosen to show the sensitivity of the model results. The baseline constituent reaction rates of these six locations are summarized in Table 2-2. Model results for other locations in the Delta are included in the spreadsheet tool and are available for review.

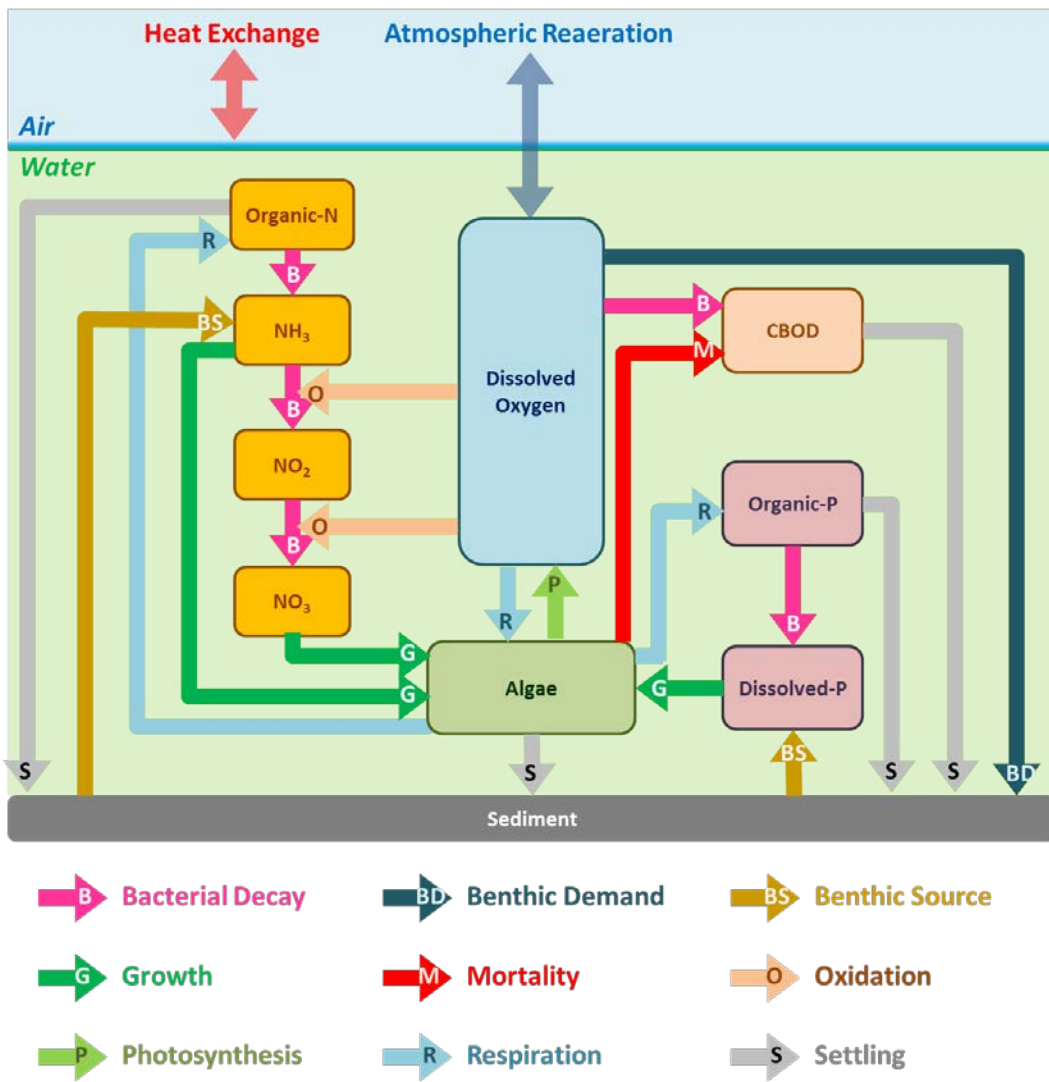
2.3.1 Algae_Growth_1.0

Figure 2-3 qualitatively summarizes the model results of the Algae_Growth_1.0 scenario compared with the baseline. Figures 2-4–2-9 show the detailed time-series results. Findings for each location are summarized in Table 2-3.

When the algae growth rate was reduced to 1.0, the algae results generally decreased compared with the baseline. For locations with greater algae growth rate reduction (i.e., San Joaquin River at Prisoners Point, Old River at Tracy Road, and Middle River at Howard Road), algae growth rates were reduced from 2.0 ~ 2.9 to 1.0, and the results showed greater algae reduction, as well. The results of the Clifton Court Forebay also showed greater algae reduction, even though the algae growth rate was reduced from 1.6 to 1.0. The results even showed that sometimes algae increased, although this result was rare. Compared with the four locations mentioned above, the changes of results of San Joaquin River at Mossdale and Rough and Ready Island were less. Although the rate reduction at Rough and Ready Island (from 1.3 to 1.0) was less than that at San Joaquin River at Mossdale (from 2.2 to 1.0), the results of former location generally showed greater changes than the latter location. This is likely because San Joaquin River at Mossdale, which is closer to the model boundary at Vernalis, was influenced more by conditions at the boundary than reaction-rate changes that are less sensitive.

When the algae growth rate was reduced, as expected, the Org-N and Org-P results at these six locations decreased accordingly to various degrees. The results also showed that the Org-P reduction results generally were greater than Org-N reduction results.

The interactions between algae and DO (e.g., algae produces oxygen via photosynthesis during daylight but consumes oxygen via respiration at night) create challenges to analyze DO, although the results generally showed that DO decreased when the algae growth rate was reduced. A more detailed analysis

**Figure 2-1 Nutrients Interactions**

Note: Adapted from Rajbhandari 2004

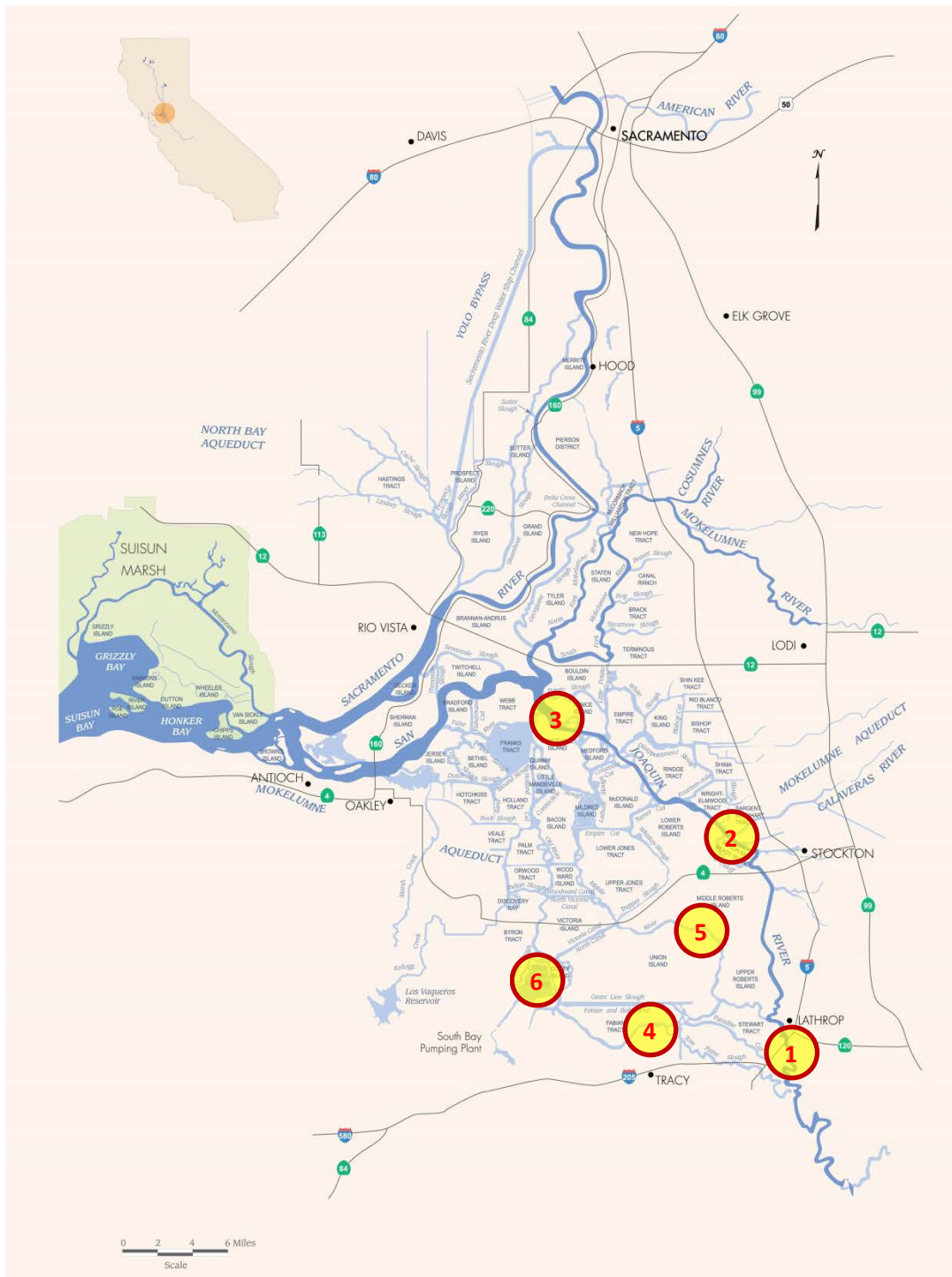


Figure 2-2 Example Locations in Delta for Showing the Model Results Sensitivity

Notes: 1 = San Joaquin River at Mossdale, 2 = Rough and Ready Island, 3 = San Joaquin River at Prisoners Point, 4 = Old River at Tracy Road, 5 = Middle River at Howard Road, 6 = Clifton Court Forebay

Locations	Algae Growth Rate	NH ₃ Decay Rate	Org-P Decay Rate	Algae Mortality Rate
San Joaquin River at Mossdale	2.2	0.4	0.005	0.1
Rough and Ready Island	1.3	0.6	0.005	0.2
San Joaquin River at Prisoners Point	2.9	0.2	0.005	0.3
Old River at Tracy Road	2.8	0.2	0.005	0.7
Middle River at Howard Road	2.0	0.2	0.005	1.0
Clifton Court Forebay	1.6	0.2	0.005	0.15

Notes: NH₃ = ammonia, Org-P = organic phosphorus

Table 2-2 Baseline Constituents Reaction Rates

that considers the day-night solar cycle will be needed to conduct a more comprehensive assessment. Also, it will be useful to include estimates of saturated DO levels for the simulation period.

2.3.2 NH₃_Decay_0.02

Figure 2-10 qualitatively summarizes the model results of the NH₃_Decay_0.02 scenario compared with the baseline. Figures 2-11–2-16 show the detailed time-series results. Findings for each location are summarized in Table 2-4.

As expected, compared with the baseline when the NH₃ decay rate was reduced to 0.02, NH₃ results generally increased at these six locations, except at San Joaquin River at Mossdale. The other five locations showed dramatic increases. DO results generally increased and NO₂ results generally decreased because less NH₃ decayed into NO₂ via oxidation with less oxygen. Note that the results of Old River at Tracy Road and of Clifton Court Forebay showed that NO₂ occasionally increased despite the general trend of reduction. This may be because the results are daily average values that did not reflect the real trend. A more detailed investigation on this phenomenon may be carried out in the future, if needed. The algae results generally showed no change.

2.3.3 NH₃_Decay_0.6

Figure 2-17 qualitatively summarizes the model results of the NH₃_Decay_0.6 scenario compared with the baseline. Figures 2-18–2-23 show the detailed time-series results. Findings for each location are summarized in Table 2-5.

When NH₃ decay rate was increased to 0.6, it was expected that the NH₃ results would decrease, and the results' trend of four locations (San Joaquin River at Mossdale, Old River at Tracy Road, Middle River at Howard Road, and Clifton Court Forebay) showed this. For Rough and Ready Island, the decay rate

Locations	Constituents Under Assessment			
	Algae	DO	Org-N	Org-P
San Joaquin River at Mossdale	Generally decreased with noticeable changes	Generally decreased with noticeable changes ^a	Generally decreased with minor changes	Generally decreased with minor changes
Rough and Ready Island	Generally decreased with noticeable changes	Sometimes increased and sometimes decreased with minor changes ^b	Generally decreased with minor changes	Generally decreased with noticeable changes
San Joaquin River at Prisoners Point	Generally decreased with noticeable changes	Generally decreased with minor changes	Generally decreased with minor changes	Generally decreased with noticeable changes
Old River at Tracy Road	Generally decreased with noticeable changes	Generally decreased with noticeable changes	Generally decreased with noticeable changes	Generally decreased with noticeable changes
Middle River at Howard Road	Generally decreased with noticeable changes	Generally decreased with minor changes	Generally decreased with minor changes	Generally decreased with noticeable changes
Clifton Court Forebay	Generally decreased with noticeable changes ^c	Generally decreased with minor changes	Generally decreased with minor changes ^d	Generally decreased with noticeable changes

Notes:

DO = dissolved oxygen, Org-N = organic nitrogen, Org-P= organic phosphorus

^aThe results occasionally increased with minor degrees in July 2009.

^bThe results occasionally increased with noticeable degrees in September 2002.

^cThe results occasionally increased with noticeable degrees in June 2001, June 2007, May ~ June 2008, and June 2009.

^dThe results occasionally increased with noticeable degrees in June 2001, June 2007, June 2008, and June 2009.

Table 2-3 Summary of Findings Comparing Algae_Growth_1.0 Scenario's Results with the Baseline

Locations	Constituents Under Assessment			
	Algae	DO	NH ₃	NO ₂
San Joaquin River at Mossdale	Generally no changes	Generally increased with minor changes	Generally increased with noticeable changes	Generally decreased with noticeable changes
Rough and Ready Island	Generally no changes ^a	Generally increased with noticeable changes	Generally increased with noticeable changes	Generally decreased with noticeable changes
San Joaquin River at Prisoners Point	Generally no changes	Generally increased with minor changes	Generally increased with noticeable changes	Generally decreased with noticeable changes
Old River at Tracy Road	Generally no changes	Generally increased with minor changes	Generally increased with noticeable changes	Generally decreased with noticeable changes ^b
Middle River at Howard Road	Generally no changes	Generally increased with minor changes	Generally increased with noticeable changes	Generally decreased with noticeable changes
Clifton Court Forebay	Generally no changes	Generally increased with minor changes	Generally increased with noticeable changes	Generally decreased with noticeable changes ^c

Notes: DO = dissolved oxygen, NH₃ = ammonia, NO₂ = nitrite

^aThe results occasionally decreased with noticeable degrees in September 2002.

^bThe results occasionally increased with noticeable degrees in November 2001, October ~ November 2002, October 2003, October 2004, October 2005, and October 2009.

^cThe results occasionally increased with noticeable degrees in September ~ November 2002, November 2008, and September 2009.

Table 2-4 Summary of Findings Comparing NH₃_Decay_0.02 Scenario's Results with the Baseline

was basically not changed, but the NH₃ results generally showed minor reduction. For San Joaquin River at Prisoners Point, NH₃ results generally deceased; sometimes the results showed unexpected increases, although this is rare. A more detailed investigation about these two phenomena may be carried out in the future, if needed.

When NH₃ oxidizes and decays with a greater rate, it would consume more oxygen, decay more, and then change NH₃ into NO₂. The DO results generally decreased and/or showed no change, except the DO increased during September 2002 at Rough and Ready Island. This may result from algal photosynthesis

Locations	Constituents Under Assessment			
	Algae	DO	NH ₃	NO ₂
San Joaquin River at Mossdale	Generally no changes	Generally no changes	Generally decreased with noticeable changes	Generally increased with minor changes
Rough and Ready Island	Generally no changes	Generally no changes ^a	Generally decreased with minor changes	Sometimes increased and sometimes decreased with minor changes
San Joaquin River at Prisoners Point	Generally no changes	Generally decreased with minor changes	Generally decreased with noticeable changes ^b	Generally increased with noticeable changes
Old River at Tracy Road	Generally no changes	Generally decreased with minor changes	Generally decreased with noticeable changes	Sometimes increased and sometimes decreased with noticeable changes
Middle River at Howard Road	Generally no changes	Generally decreased with minor changes	Generally decreased with noticeable changes	Generally increased with noticeable changes
Clifton Court Forebay	Generally no changes	Generally decreased with minor changes	Generally decreased with noticeable changes	Sometimes increased and sometimes decreased with noticeable changes

Notes: DO = dissolved oxygen, NH₃ = ammonia, NO₂ = nitrite
^aThe results occasionally increased with noticeable degrees in September 2002.
^bThe results occasionally increased with noticeable degrees in February ~ March 2000, January 2002, February 2004, January ~ March 2006, December 2010, January 2011, and March ~ April 2011.

Table 2-5 Summary of Findings Comparing NH₃_Decay_0.6 Scenario's Results with the Baseline

causing supersaturation during that time frame. Higher NH₃ decay, resulting in more NO₂ and NO₃, would likely raise algal biomass. In the next phase of this study, we (authors Ming-Yen Tu and Hari Rajbhandari) plan to estimate the saturated DO values to verify this phenomenon. We will also investigate for other possible reasons.

NO₂ results increased at San Joaquin River at Mossdale, San Joaquin River at Prisoners Point, and Middle River at Howard Road; however, for the other three locations, the NO₂ results sometimes increased and sometimes decreased with various degrees, especially the results of Clifton Court Forebay, which decreased most of the time. A more detailed investigation on this phenomenon may be carried out in the future, if needed. The algae results generally showed no change.

2.3.4 Org-P_Decay_0.05

Figure 2-24 qualitatively summarizes the model results of the Org-P_Decay_0.05 scenario compared with the baseline. Figures 2-25–2-30 show the detailed time-series results. Findings for each location are summarized in Table 2-6.

When the Org-P decay rate was increased to 0.05, the Org-P results generally decreased, as expected, and PO₄ generally increased at these six locations. The algae and DO results generally increased with various degrees and/or showed no changes. Decay of Org-P causes an increase in PO₄ that is used by algae during photosynthesis or growth. This will result in more algal biomass as well as more DO. Still, algae uses up oxygen during respiration and higher algal biomass results in a larger loss of DO. The process is more complex because of the limiting nutrient formulation used in the model. This approach, similar to Liebig's Law of the Minimum, assumes that nutrient in shortest supply controls algae growth. Accordingly, in situations when these mechanisms balance each other, the net DO change could be zero. In essence, depending upon whichever process dominates, that process will result in an increase, decrease, or no change in DO.

2.3.5 Algae_Die_0.002

Figure 2-31 qualitatively summarizes the model results of the Algae_Die_0.002 scenario compared with the baseline. Figures 2-32–2-37 show the detailed time-series results. Findings for each location are summarized in Table 2-7.

When the algae mortality rate was reduced to 0.002, as expected, the algae, Org-N and Org-P results generally increased, except at San Joaquin River at Mossdale. The other five locations even showed dramatic algae increases. Depending on locations, DO results would show no change, or sometimes increased and sometimes decreased with various degrees. This may be because the results are daily-average that did not capture the effects of the day-night solar cycle on oxygen.

2.3.6 Additional Discussion of Results

Some algae results that may seem inconsistent or counterintuitive may be likely because:

- Depending upon which nutrient is causing a limit, nitrogen or phosphorus may limit the growth of algae. Details on this concept are available in Rajbhandari (1998) or Chapra (1997).
- Change of reaction rate, in combination with benthic release rates of PO₄ or NH₃, may have triggered a different nutrient (from the one in the baseline), which would cause limiting the algae growth. This will require more detailed investigation to be definitive.

Locations	Constituents Under Assessment			
	Algae	DO	PO ₄	Org-P
San Joaquin River at Mossdale	Generally no changes ^a	Generally no changes ^b	Generally increased with minor changes ^c	Generally decreased with minor changes
Rough and Ready Island	Generally increased with noticeable changes	Generally no changes	Generally increased with noticeable changes	Generally decreased with noticeable changes
San Joaquin River at Prisoners Point	Generally increased with noticeable changes	Generally no changes	Generally increased with noticeable changes	Generally decreased with noticeable changes
Old River at Tracy Road	Generally increased with noticeable changes	Generally increased with minor changes	Generally increased with noticeable changes	Generally decreased with noticeable changes
Middle River at Howard Road	Generally increased with noticeable changes	Generally increased with minor changes	Generally increased with noticeable changes	Generally decreased with noticeable changes
Clifton Court Forebay	Generally increased with noticeable changes	Generally increased with minor changes	Generally increased with noticeable changes	Generally decreased with noticeable changes

Notes: DO = dissolved oxygen, Org-P = organic phosphorus, PO₄ = assumed to represent dissolved phosphorus,
^aThe results showed minor increases in July 2001, August 2002, July 2004, July ~ August 2007, June ~ August 2008, June ~ September 2009, and July ~ August 2010.
^bThe results showed minor increases in July 2001, July ~ August 2002, July 2004, July ~ August 2007, June ~ August 2008, and June ~ August 2009.
^cThe results increased with noticeable degrees in June ~ August 2001, July ~ August 2002, July 2004, July ~ August 2007, May ~ September 2008, and May ~ August 2009.

Table 2-6 Summary of Findings Comparing Org-P_Decay_0.05 Scenario's Results with the Baseline

Locations	Constituents Under Assessment			
	Algae	DO	Org-N	Org-P
San Joaquin River at Mossdale	Generally increased with minor-to-noticeable changes	Generally showed no changes ^a	Generally increased with minor changes	Generally increased with minor changes
Rough and Ready Island	Generally increased with noticeable changes	Generally decreased with noticeable changes	Generally increased with noticeable changes	Generally increased with noticeable changes
San Joaquin River at Prisoners Point	Generally increased with noticeable changes	Generally decreased with minor changes	Generally increased with noticeable changes	Generally increased with noticeable changes
Old River at Tracy Road	Generally increased with noticeable changes	Sometimes increased and sometimes decreased with minor-to-noticeable changes	Generally increased with noticeable changes	Generally increased with noticeable changes
Middle River at Howard Road	Generally increased with noticeable changes	Generally increased with noticeable changes, and occasionally decreased with minor changes	Generally increased with noticeable changes	Generally increased with noticeable changes
Clifton Court Forebay	Generally increased with noticeable changes	Sometimes increased and sometimes decreased with minor-to-noticeable changes	Generally increased with noticeable changes	Generally increased with noticeable changes
Notes: DO = dissolved oxygen, Org-N = organic nitrogen, Org-P = organic phosphorus ^a The results decreased with minor degrees in June ~ August 2001, July ~ September 2007, June ~ August 2008, and June ~ August 2009.				

Table 2-7 Summary of Findings Comparing Algae_Die_0.002 Scenario's Results with the Baseline

2.4 Next Steps and Potential Future Efforts to Improve Model Calibration

The DSM2 nutrients modeling sensitivity analysis intended to provide a general idea about which constituent reaction rates may be significant and how significant reaction rates may be if a manual calibration approach was used to calibrate the DSM2-GTM. Results of the example locations demonstrated how the model responded when changing certain constituent reaction rates. This chapter documents the preliminary findings to date. Because of the current scope, this analysis did not conduct a more thorough investigation on some model result anomalies. For the future analysis, potential steps that may be carried out include:

- **Testing other nutrient reaction rates.** This analysis is an on-going study and will continue to test the sensitivity of model results when there is a need to assess certain constituents' reaction rates.
- **Localizing constituents' reaction rate changes.** The current rate changes applied to the entire Delta system. It may be beneficial to change rates for certain regions in the Delta to assess the regional sensitivity.
- **Performing detailed results assessments.** Some unexpected results shown in the previous section demonstrated the challenges to assess model results, especially the algae and DO results. This may be because the results were post-processed in the format of daily average, which may be not comprehensive enough to consider the nutrients' natural effects. For example, the interactions (e.g., photosynthesis and respiration) between algae and DO during the day-night solar cycle was not fully captured and shown in terms of the daily average. A more completed analysis, such as by using the hourly results, may be needed to conduct a more thorough investigation. The saturated DO values will also be estimated to examine the effects of algae on supersaturation of DO.

As mentioned previously, the main purpose of this sensitivity analysis is to assist the DSM2-GTM calibration. In addition to the sensitivity analysis, other potential future efforts that may improve the model calibration include:

- Making meteorology data regionalized to account for differences in wind speed and other variables.
- Conducting surveys of sediment deposits along locations of concern to determine spatial variations in benthic/sediment oxygen demand and the nitrogen and phosphorus content in the sediments to improve calibration of the model.
- Subject to a consistent expansion of the database, augmenting future extensions in the model to add additional variables, such as zooplankton and benthic algae, which are likely to result in improvement in model performance.
- Including a dynamic interaction of sediments with simulated constituents in future extension of the model (Rajbhandari 2004).

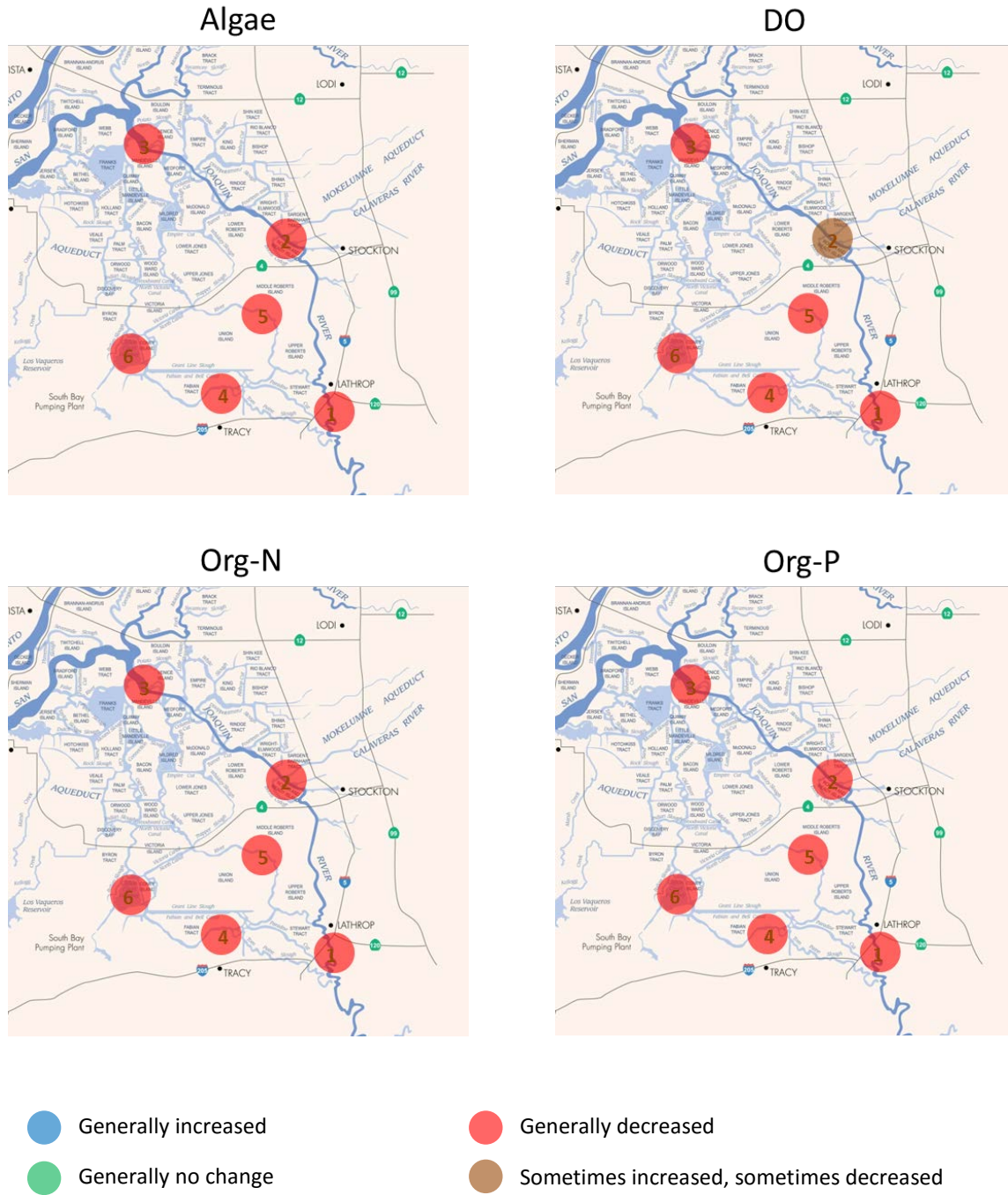


Figure 2-3 Qualitative Assessments on Model Results of Algae_Growth_1.0 Scenario Compared with the Baseline Scenario

Notes: DO = dissolved oxygen, Org-N = organic nitrogen, Org-P = organic phosphorus

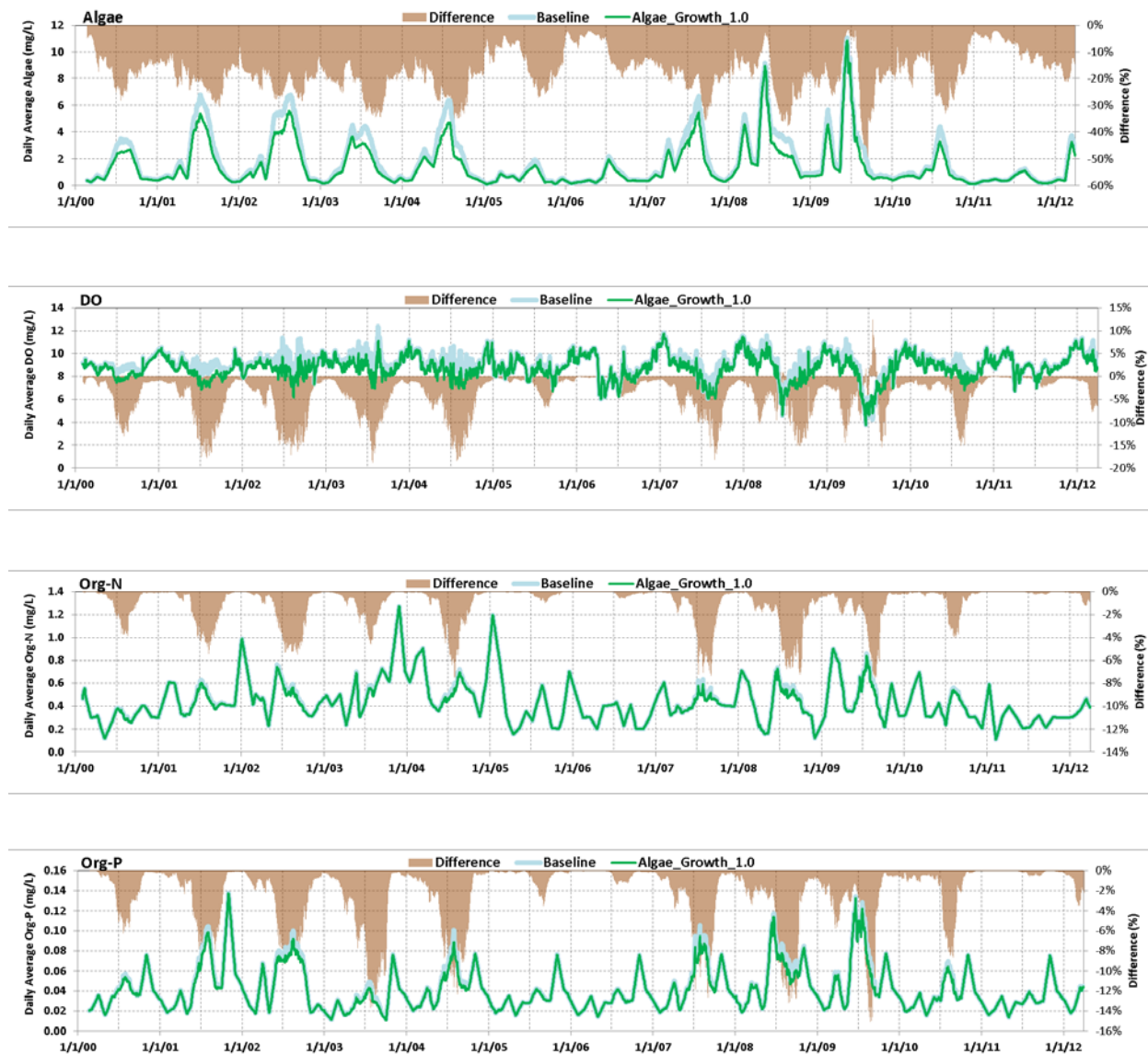
(1) San Joaquin River at Mossdale

Figure 2-4 Time-Series Results of Baseline and Algae_Growth_1.0 Scenarios at San Joaquin River at Mossdale

Notes: DO = dissolved oxygen, mg/L = milligrams per liter, Org-N = organic nitrogen, Org-P = organic phosphorus

(2) Rough and Ready Island

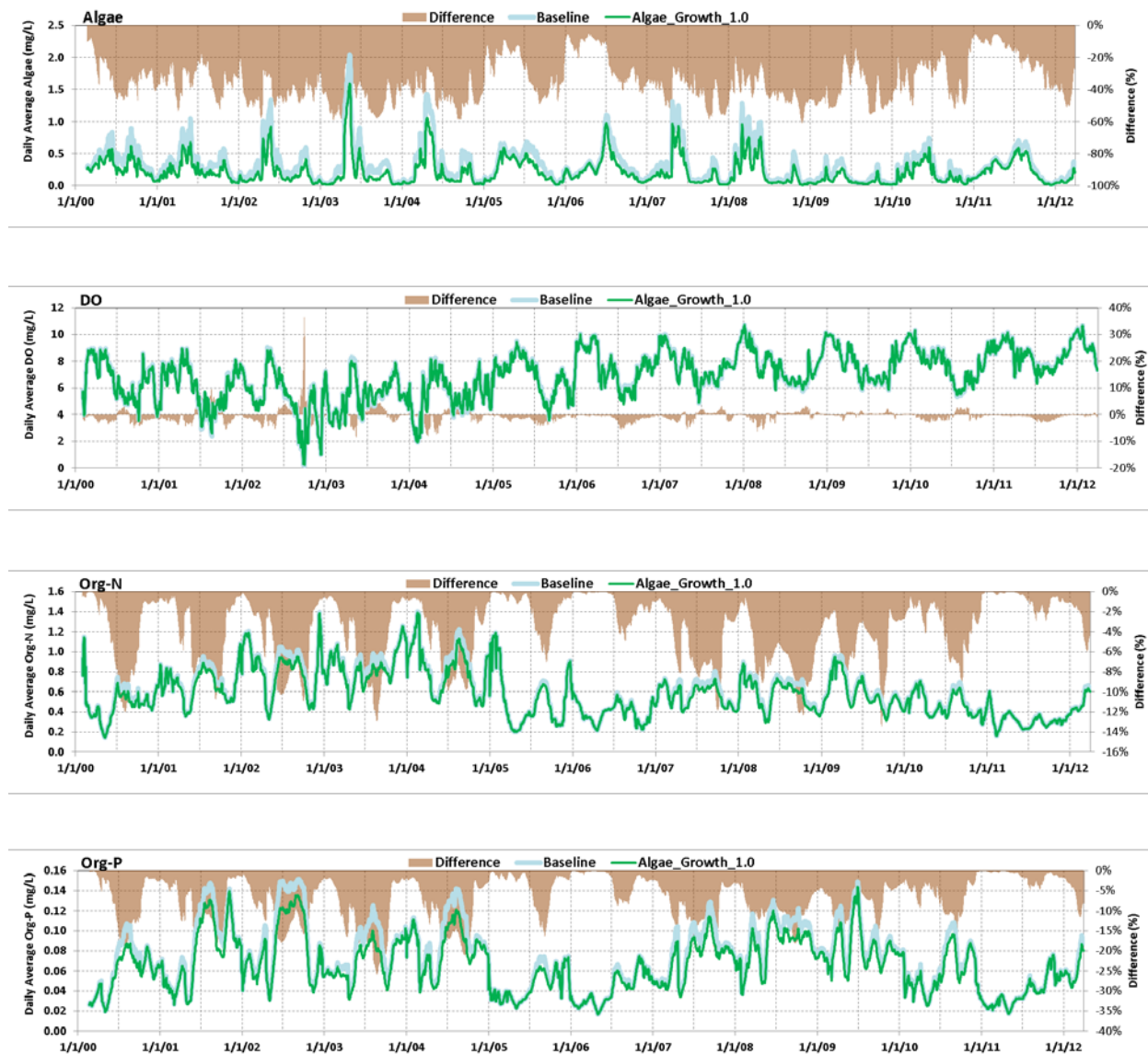


Figure 2-5 Time-Series Results of Baseline and Algae_Growth_1.0 Scenarios at Rough and Ready Island

Notes: DO = dissolved oxygen, mg/L = milligrams per liter, Org-N = organic nitrogen, Org-P = organic phosphorus

(3) San Joaquin River at Prisoners Point

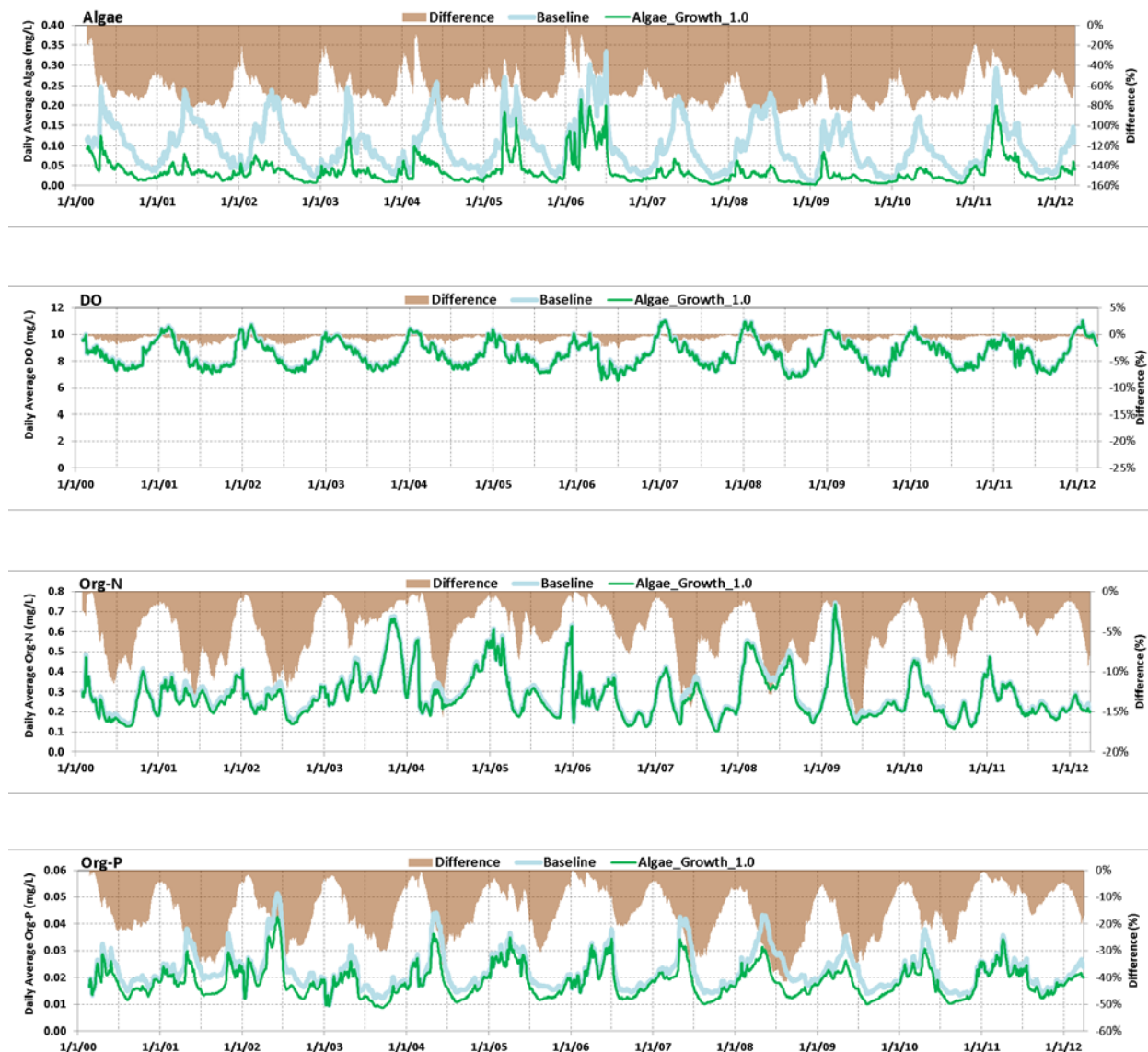


Figure 2-6 Time-Series Results of Baseline and Algae_Growth_1.0 Scenarios at San Joaquin River at Prisoners Point

Notes: DO = dissolved oxygen, mg/L = milligrams per liter, Org-N = organic nitrogen, Org-P = organic phosphorus

(4) Old River at Tracy Road

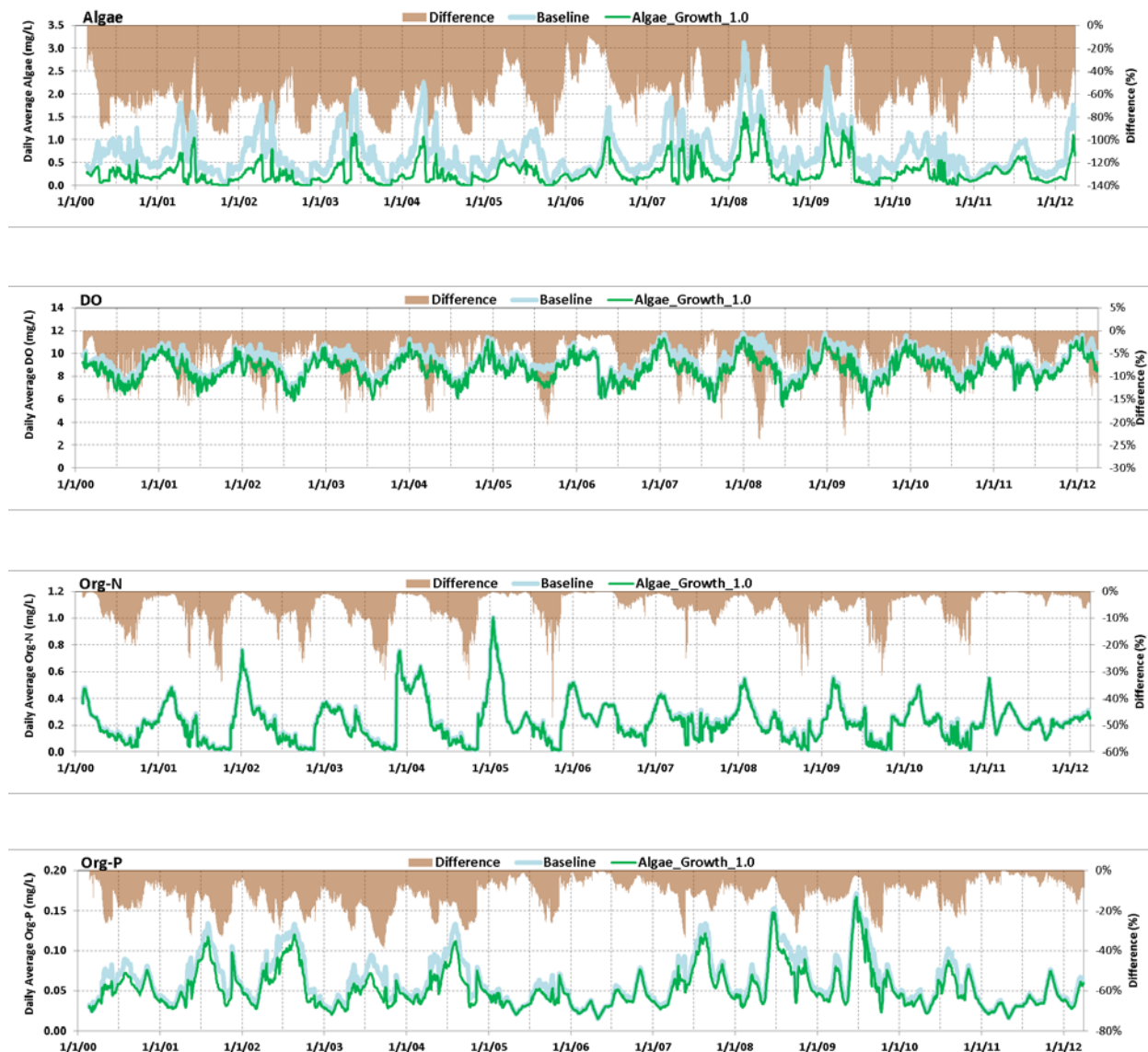


Figure 2-7 Time-Series Results of Baseline and Algae_Growth_1.0 Scenarios at Old River at Tracy Road

Notes: DO = dissolved oxygen, mg/L = milligrams per liter, Org-N = organic nitrogen, Org-P = organic phosphorus

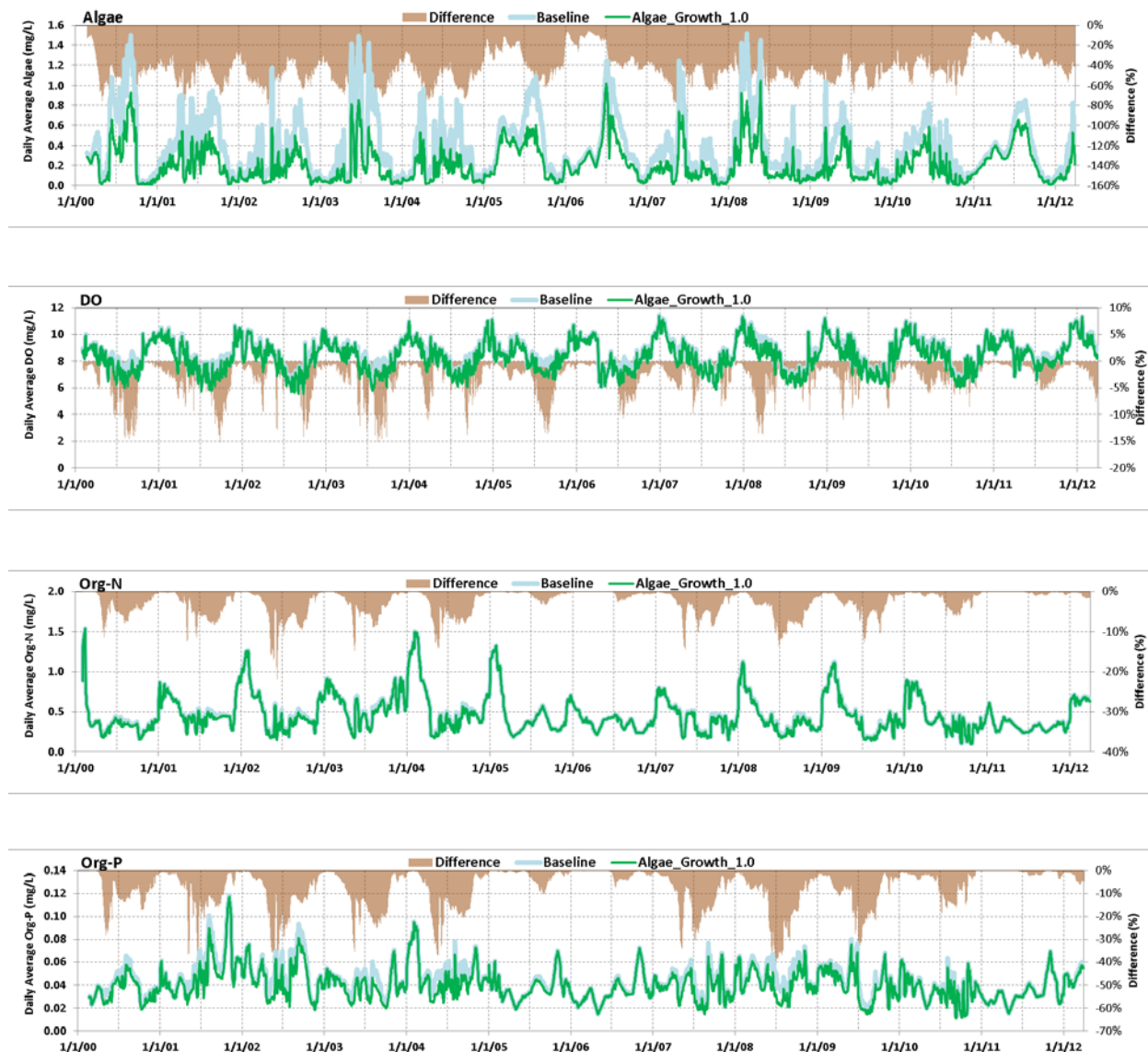
(5) Middle River at Howard Road

Figure 2-8 Time-Series Results of Baseline and Algae_Growth_1.0 Scenarios at Middle River at Howard Road

Notes: DO = dissolved oxygen, mg/L = milligrams per liter, Org-N = organic nitrogen, Org-P = organic phosphorus

(6) Clifton Court Forebay

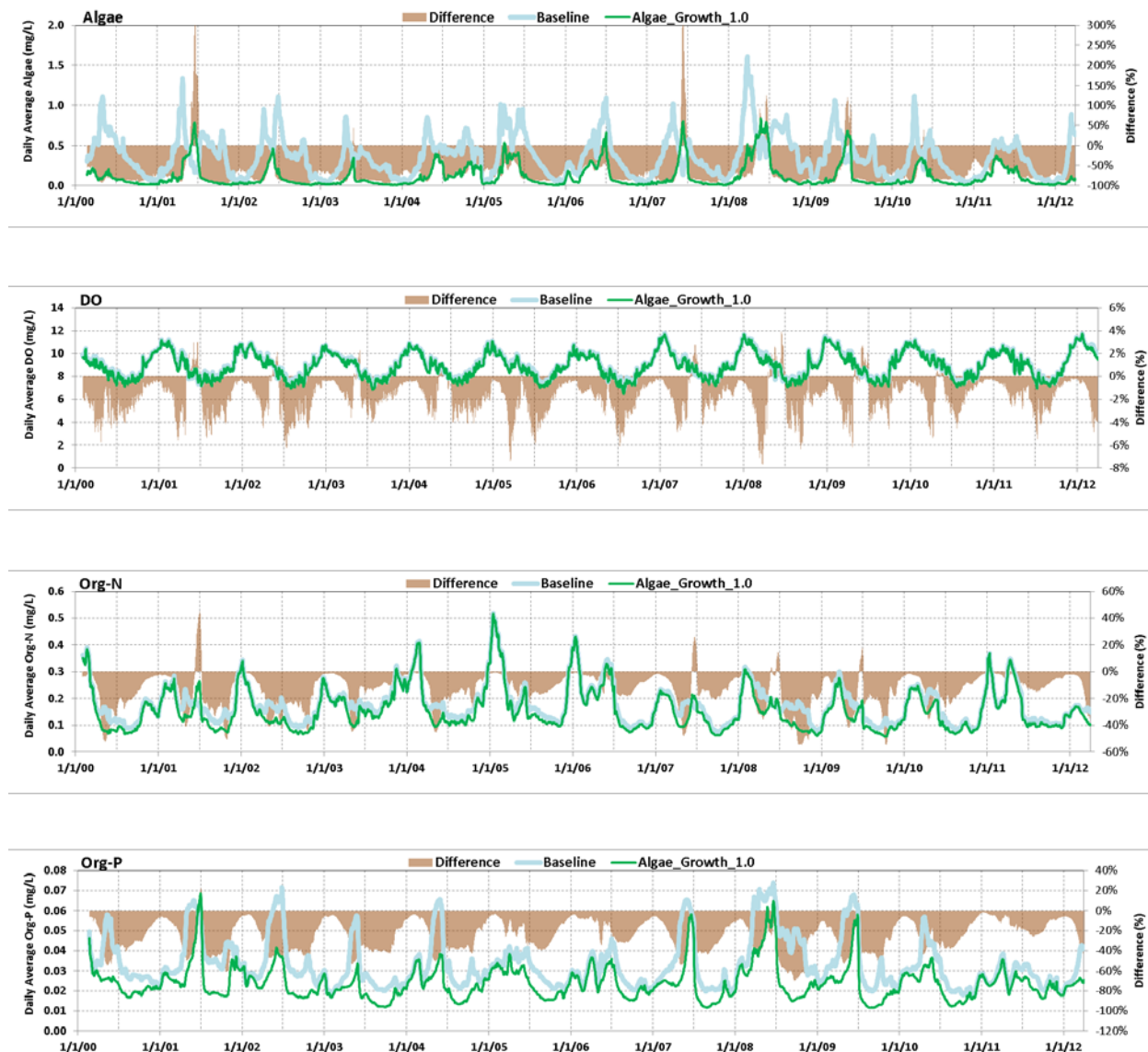


Figure 2-9 Time-Series Results of Baseline and Algae_Growth_1.0 Scenarios at Clifton Court Forebay

Notes: DO = dissolved oxygen, mg/L = milligrams per liter, Org-N = organic nitrogen, Org-P = organic phosphorus

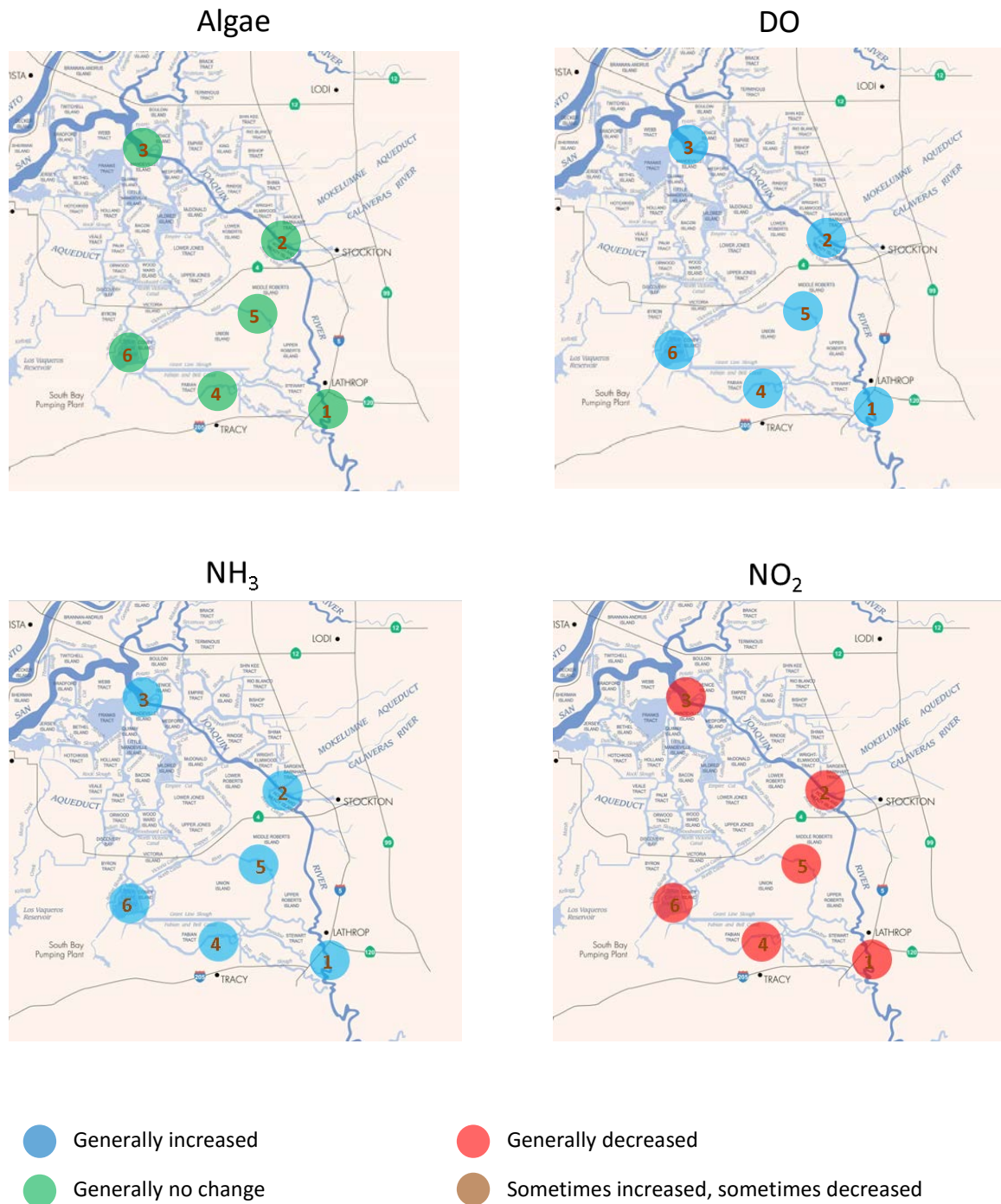


Figure 2-10 Qualitative Assessments on Model Results of NH₃_Decay_0.02 Scenario Compared with the Baseline Scenario

Notes: DO = dissolved oxygen, NH₃ = ammonia, NO₂ = nitrite

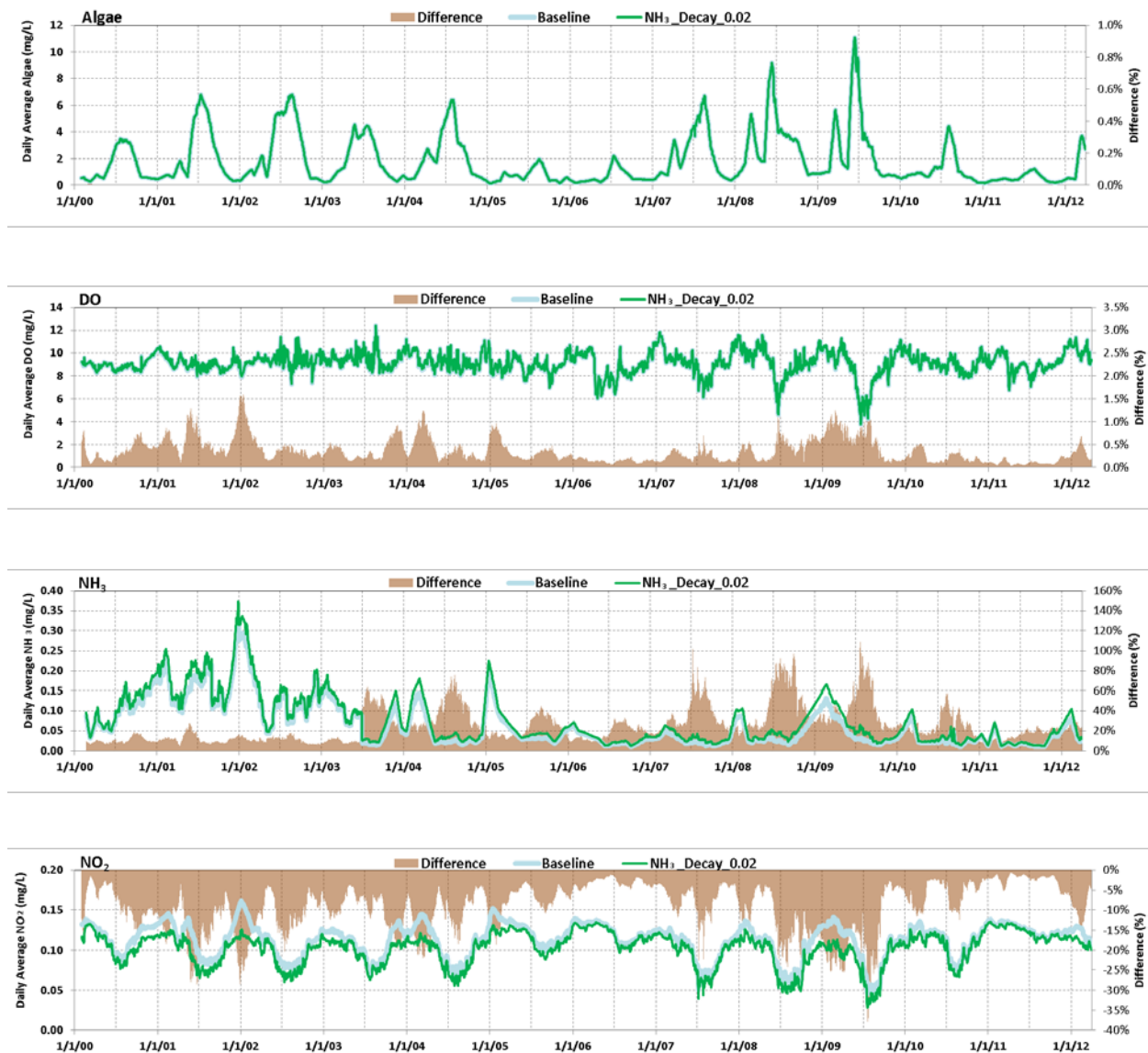
(1) San Joaquin River at Mossdale

Figure 2-11 Time-Series Results of Baseline and $\text{NH}_3\text{-Decay}_0.02$ Scenarios at San Joaquin River at Mossdale

Notes: DO = dissolved oxygen, mg/L = milligrams per liter, NH_3 = ammonia, NO_2 = nitrite

(2) Rough and Ready Island

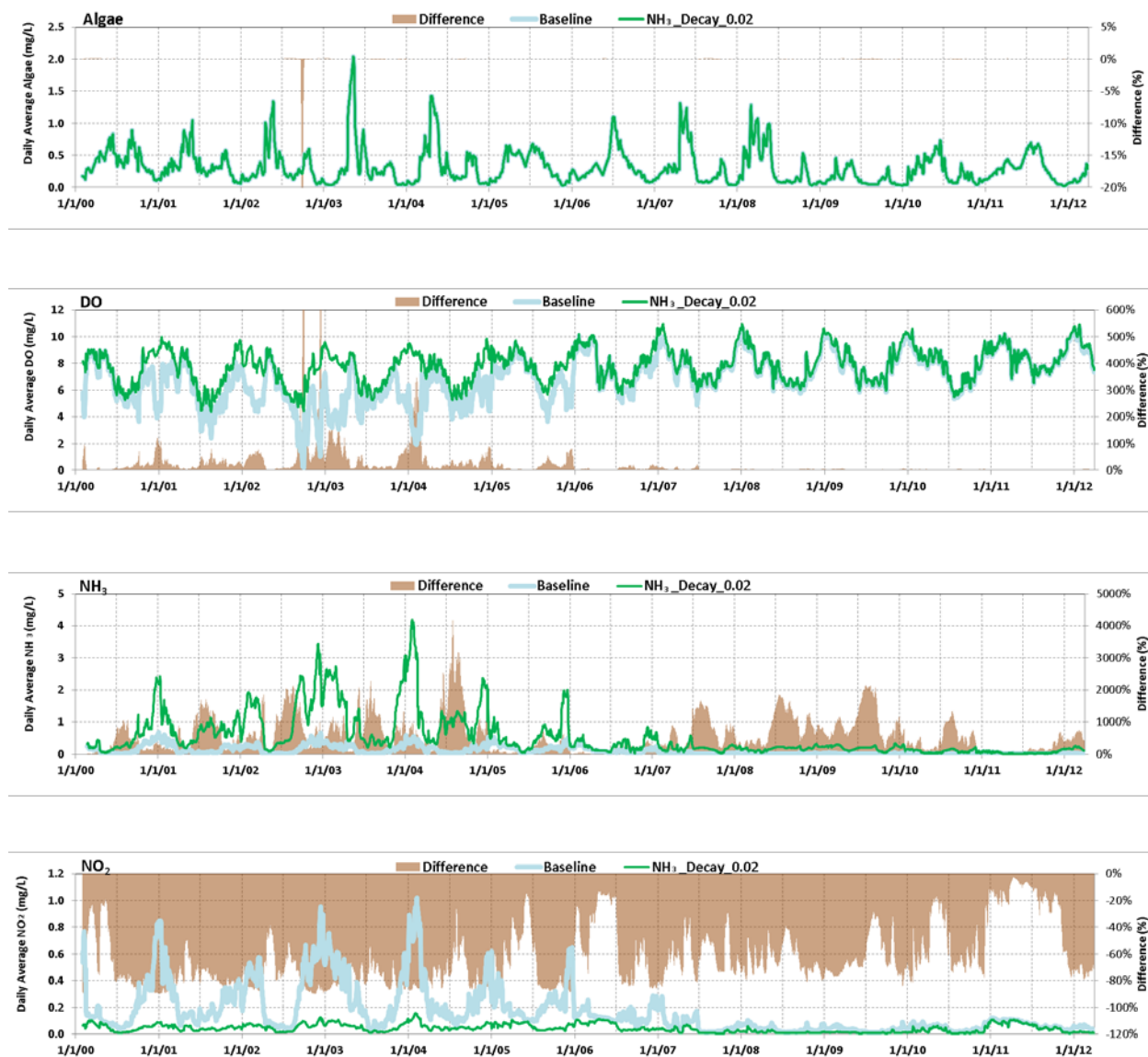


Figure 2-12 Time-Series Results of Baseline and $\text{NH}_3\text{-Decay}_0.02$ Scenarios at Rough and Ready Island

Notes: DO = dissolved oxygen, mg/L = milligrams per liter, NH_3 = ammonia, NO_2 = nitrite

(3) San Joaquin River at Prisoners Point

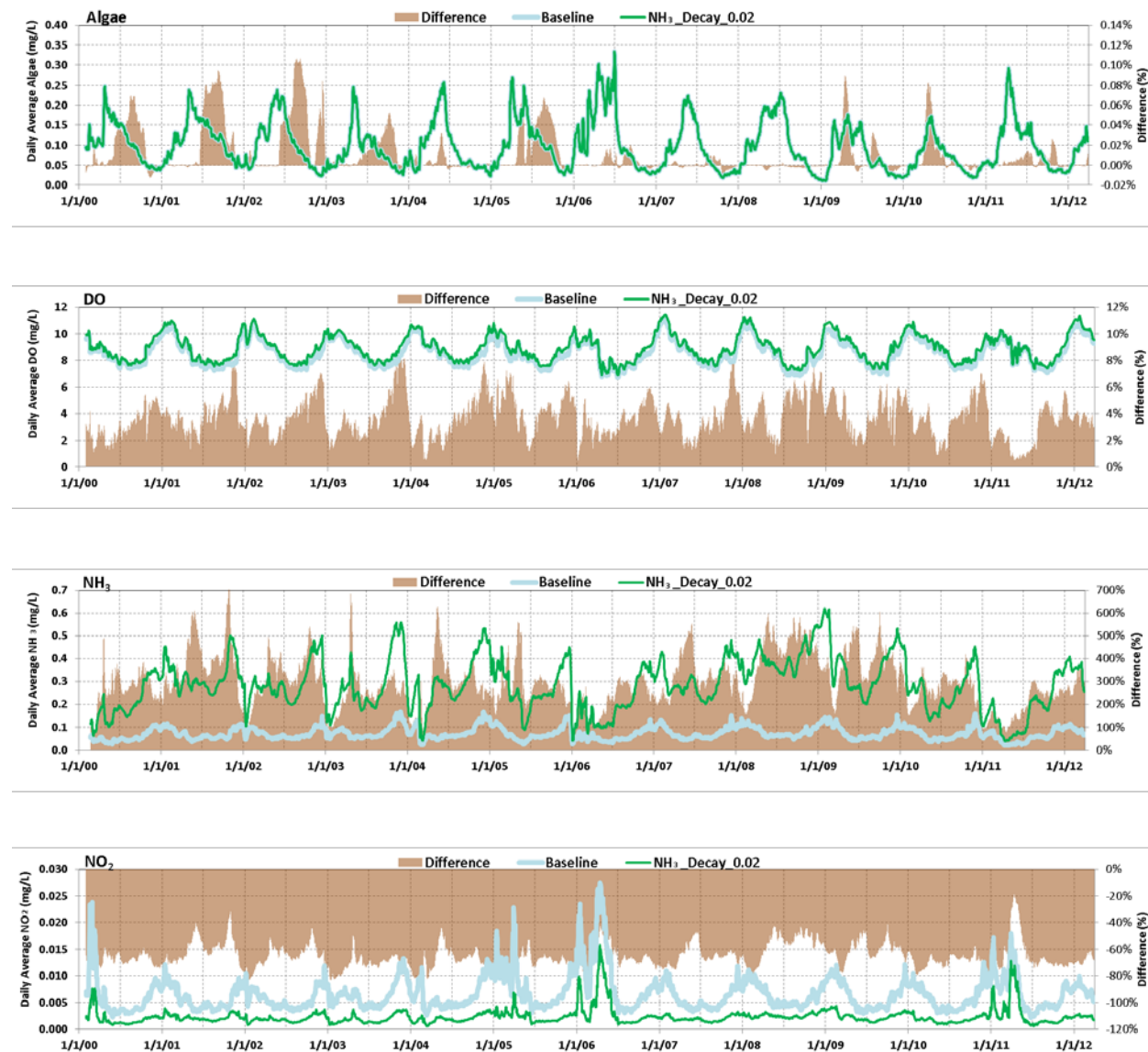


Figure 2-13 Time-Series Results of Baseline and $\text{NH}_3\text{-Decay}_0.02$ Scenarios at San Joaquin River at Prisoners Point

Notes: DO = dissolved oxygen, mg/L = milligrams per liter, NH_3 = ammonia, NO_2 = nitrite

(4) Old River at Tracy Road

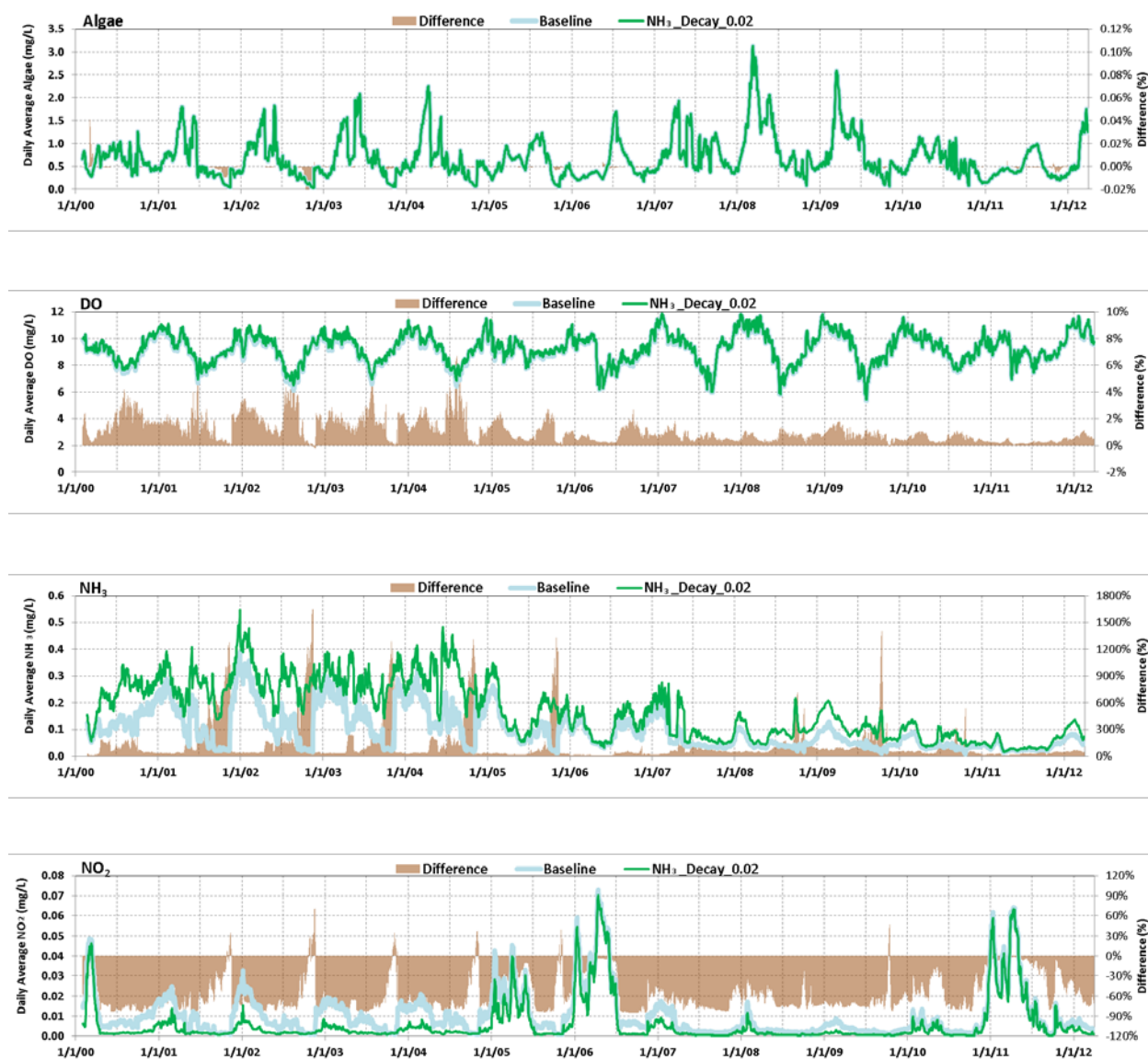


Figure 2-14 Time-Series Results of Baseline and NH₃_Decay_0.02 Scenarios at Old River at Tracy Road

Notes: DO = dissolved oxygen, mg/L = milligrams per liter, NH₃ = ammonia, NO₂ = nitrite

(5) Middle River at Howard Road

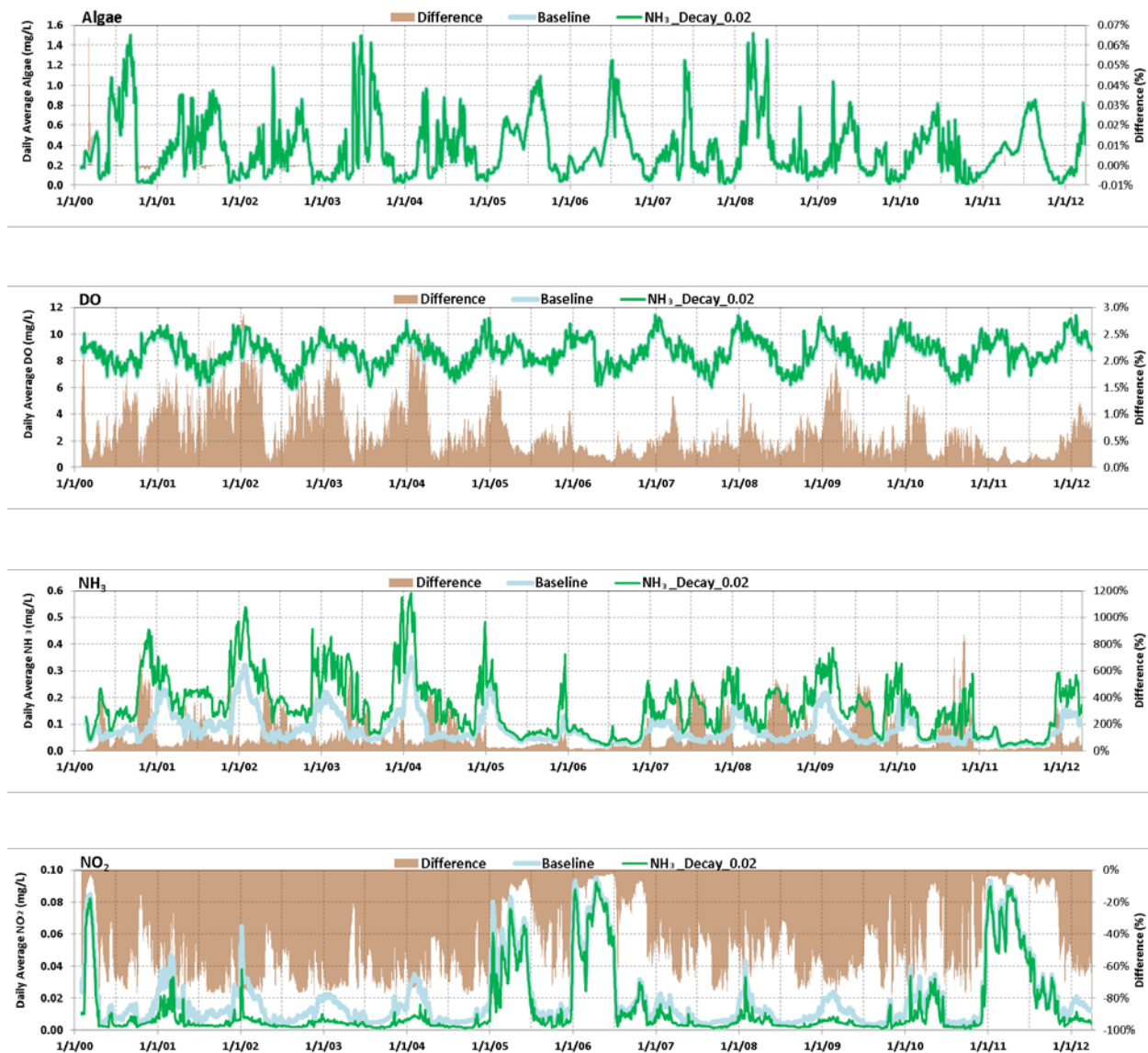


Figure 2-15 Time-Series Results of Baseline and $\text{NH}_3\text{-Decay}_0.02$ Scenarios at Middle River at Howard Road

Notes: DO = dissolved oxygen, mg/L = milligrams per liter, NH_3 = ammonia, NO_2 = nitrite

(6) Clifton Court Forebay

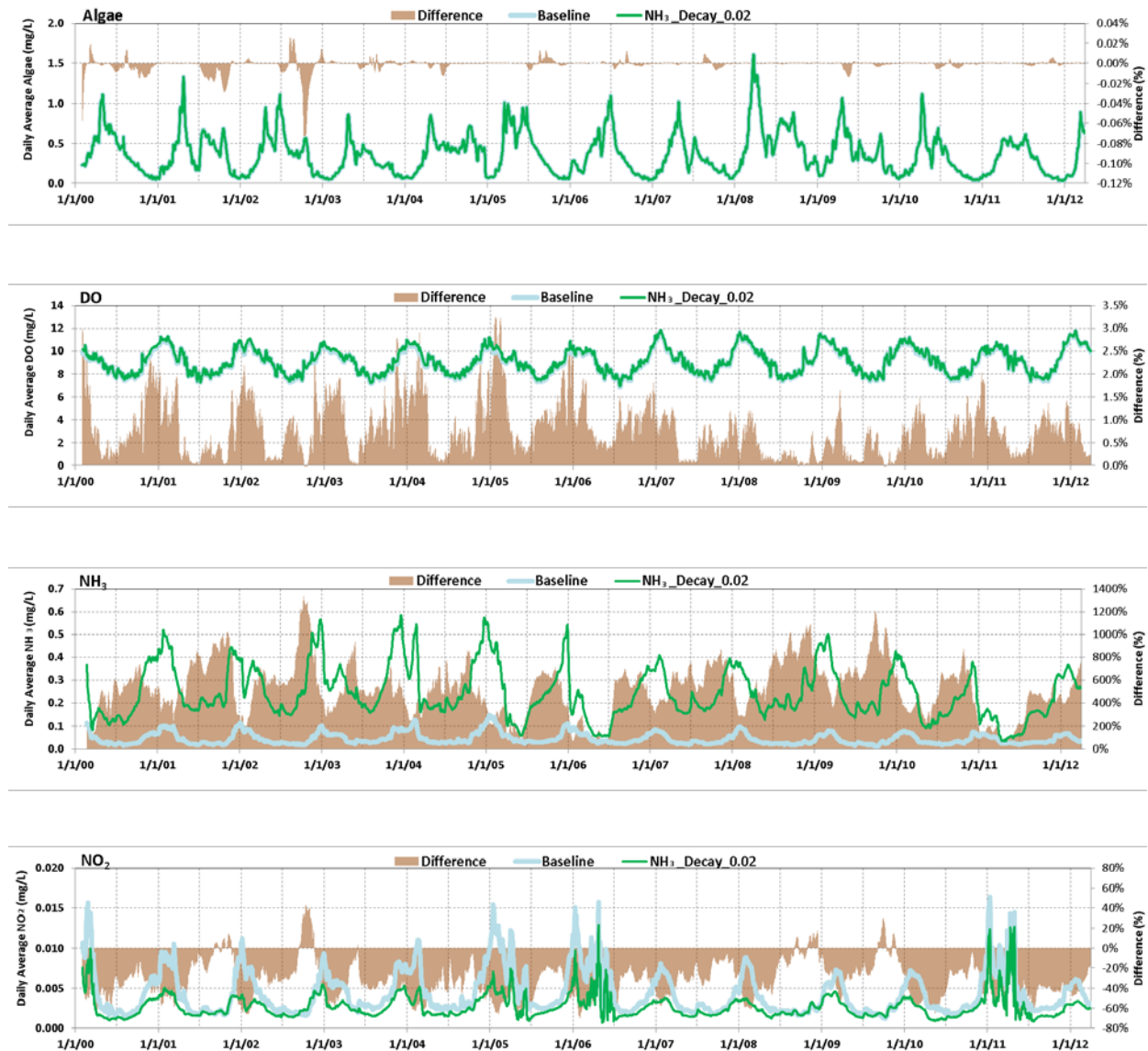


Figure 2-16 Time-Series Results of Baseline and NH₃_Decay_0.02 Scenarios at Clifton Court Forebay

Notes: DO = dissolved oxygen, mg/L = milligrams per liter, NH₃ = ammonia, NO₂ = nitrite

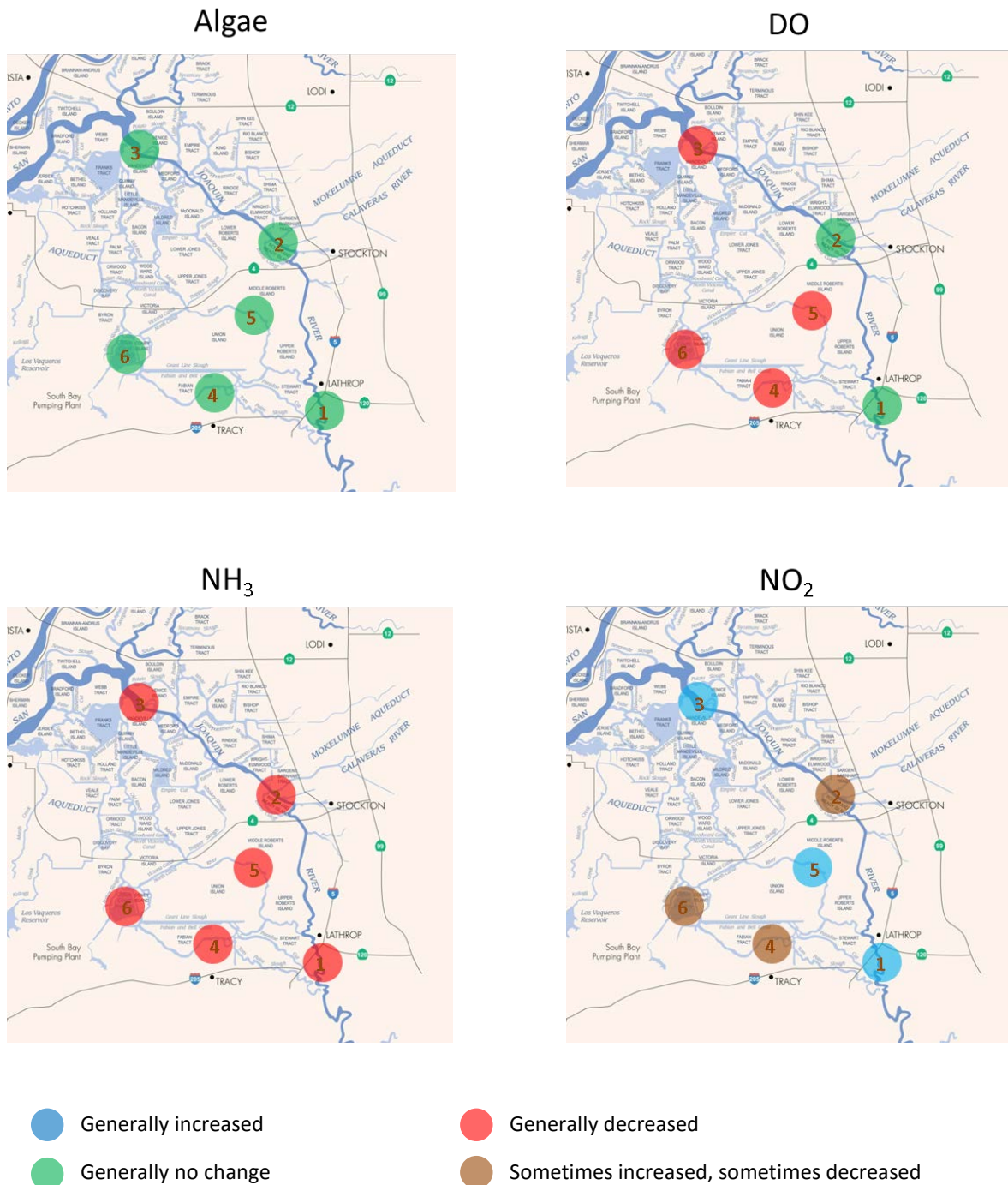


Figure 2-17 Qualitative Assessments on Model Results of NH₃_Decay_0.6 Scenario Compared with the Baseline Scenario

Notes: DO = dissolved oxygen, NH₃ = ammonia, NO₂ = nitrite

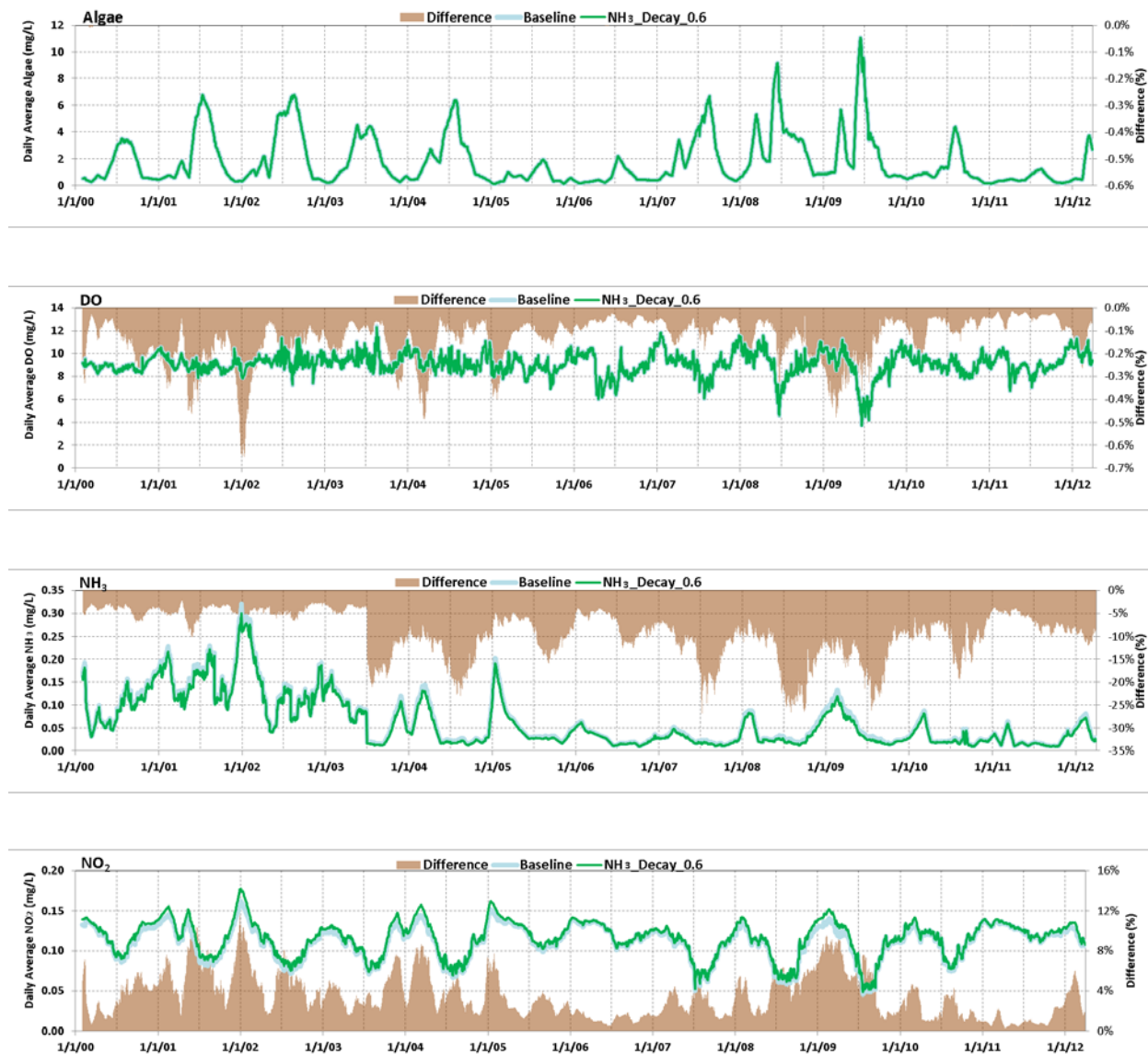
(1) San Joaquin River at Mossdale

Figure 2-18 Time-Series Results of Baseline and $\text{NH}_3\text{-Decay}_0.6$ Scenarios at San Joaquin River at Mossdale

Notes: DO = dissolved oxygen, mg/L = milligrams per liter, NH_3 = ammonia, NO_2 = nitrite

(2) Rough and Ready Island

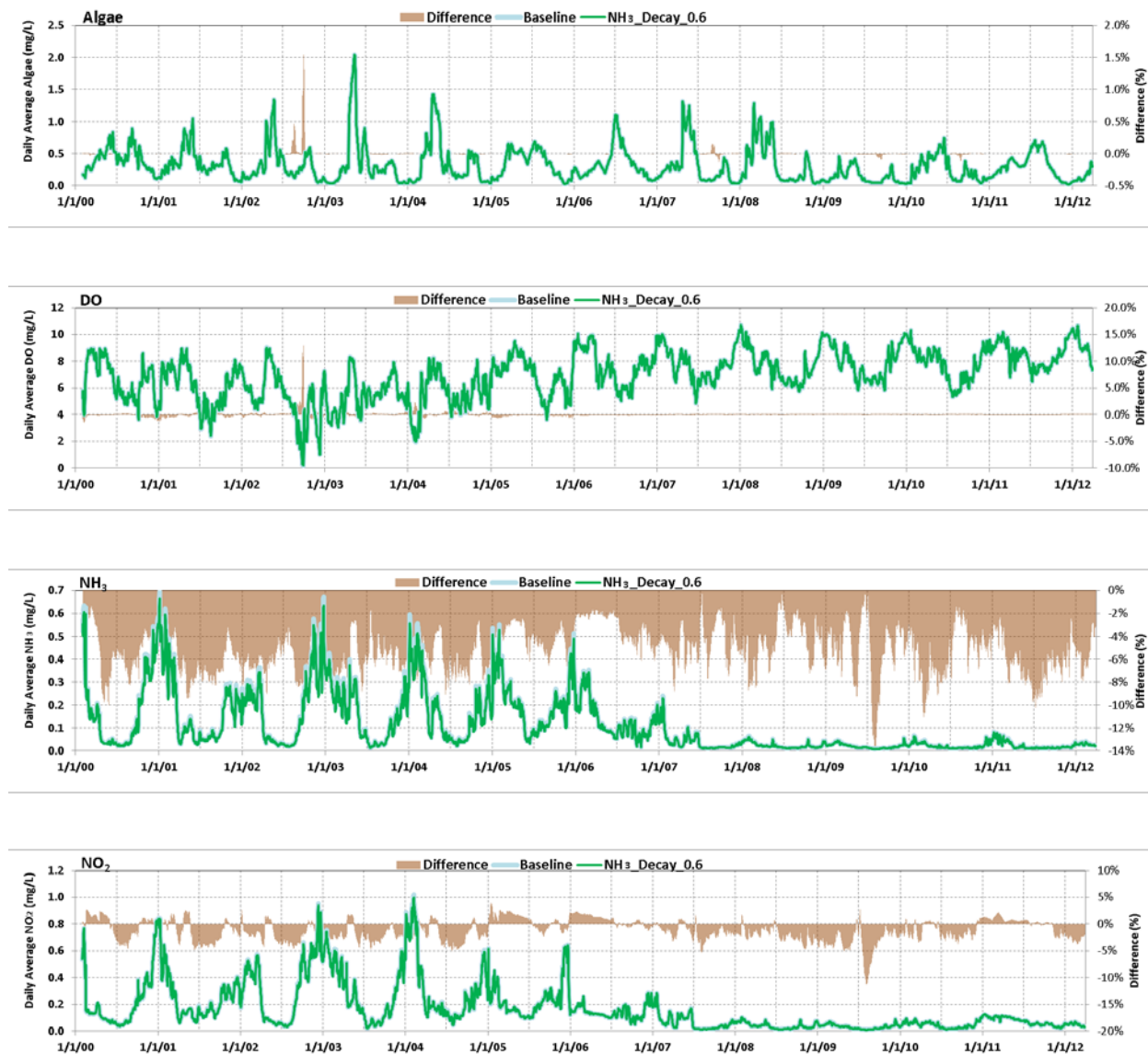
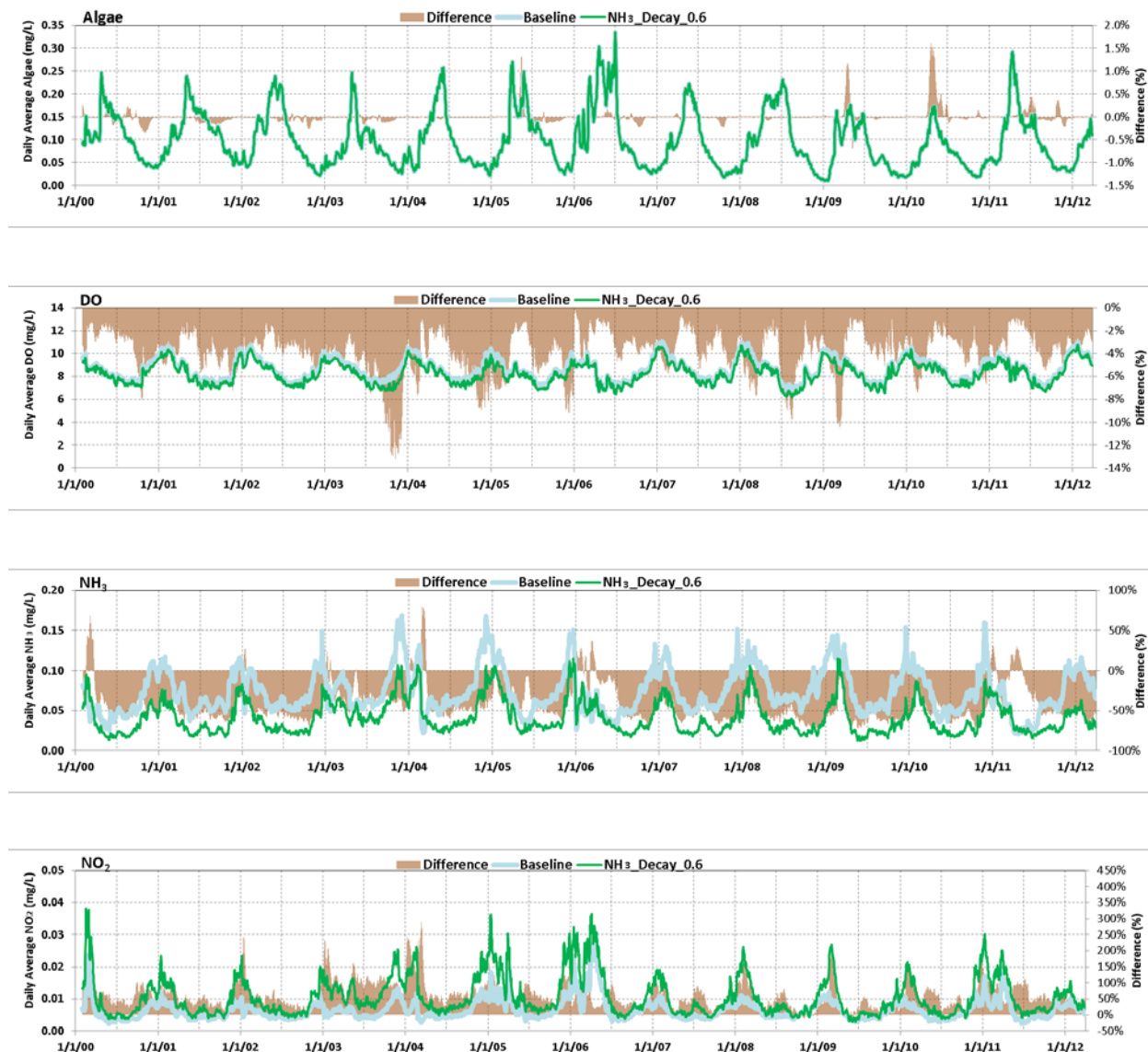


Figure 2-19 Time-Series Results of Baseline and $\text{NH}_3\text{-Decay}_0.6$ Scenarios at Rough and Ready Island

Notes: DO = dissolved oxygen, mg/L = milligrams per liter, NH_3 = ammonia, NO_2 = nitrite

(3) San Joaquin River at Prisoners Point



**Figure 2-20 Time-Series Results of Baseline and $\text{NH}_3\text{-Decay}_0.6$ Scenarios
at San Joaquin River at Prisoners Point**

Notes: DO = dissolved oxygen, mg/L = milligrams per liter, NH_3 = ammonia, NO_2 = nitrite

(4) Old River at Tracy Road

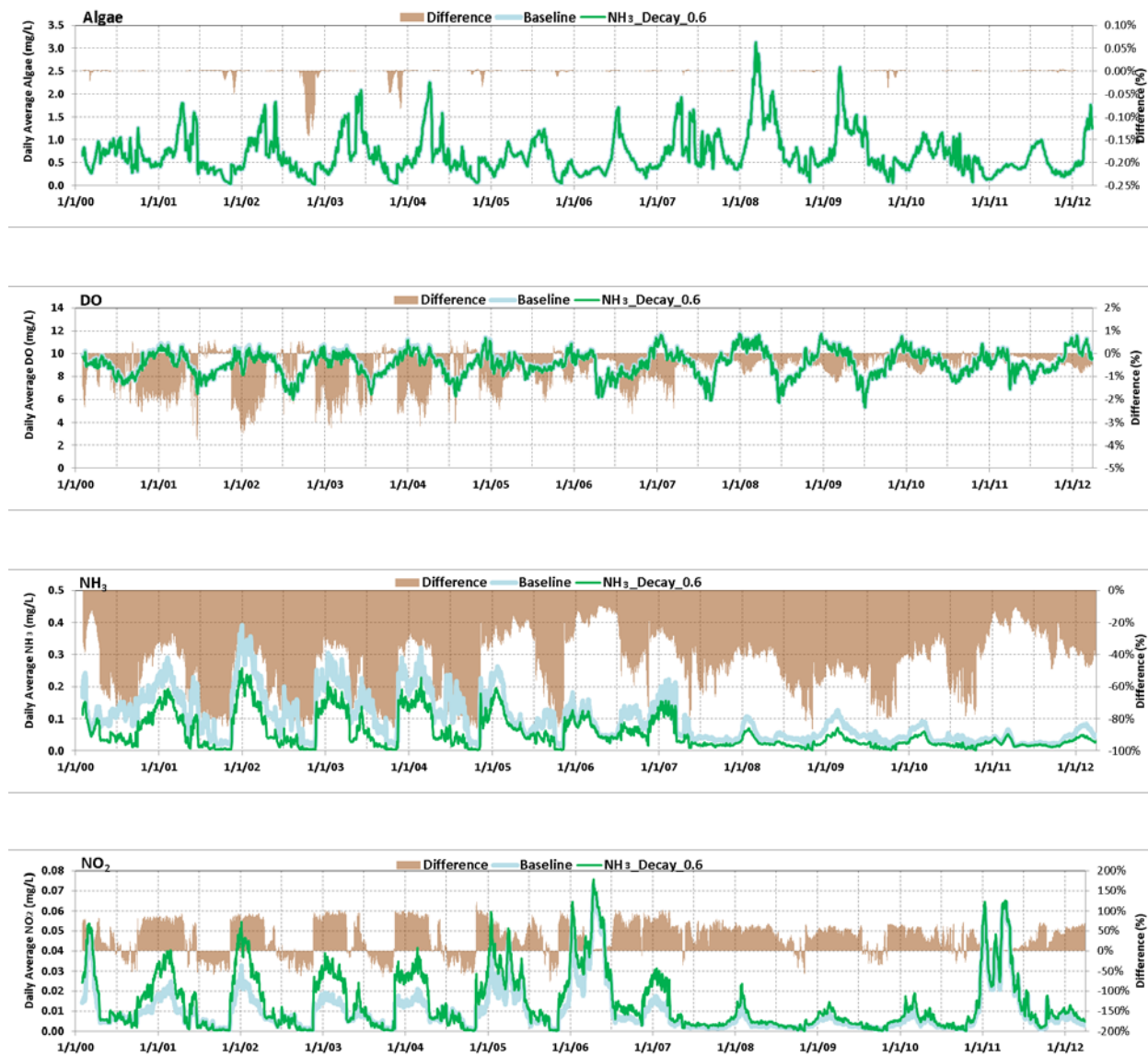
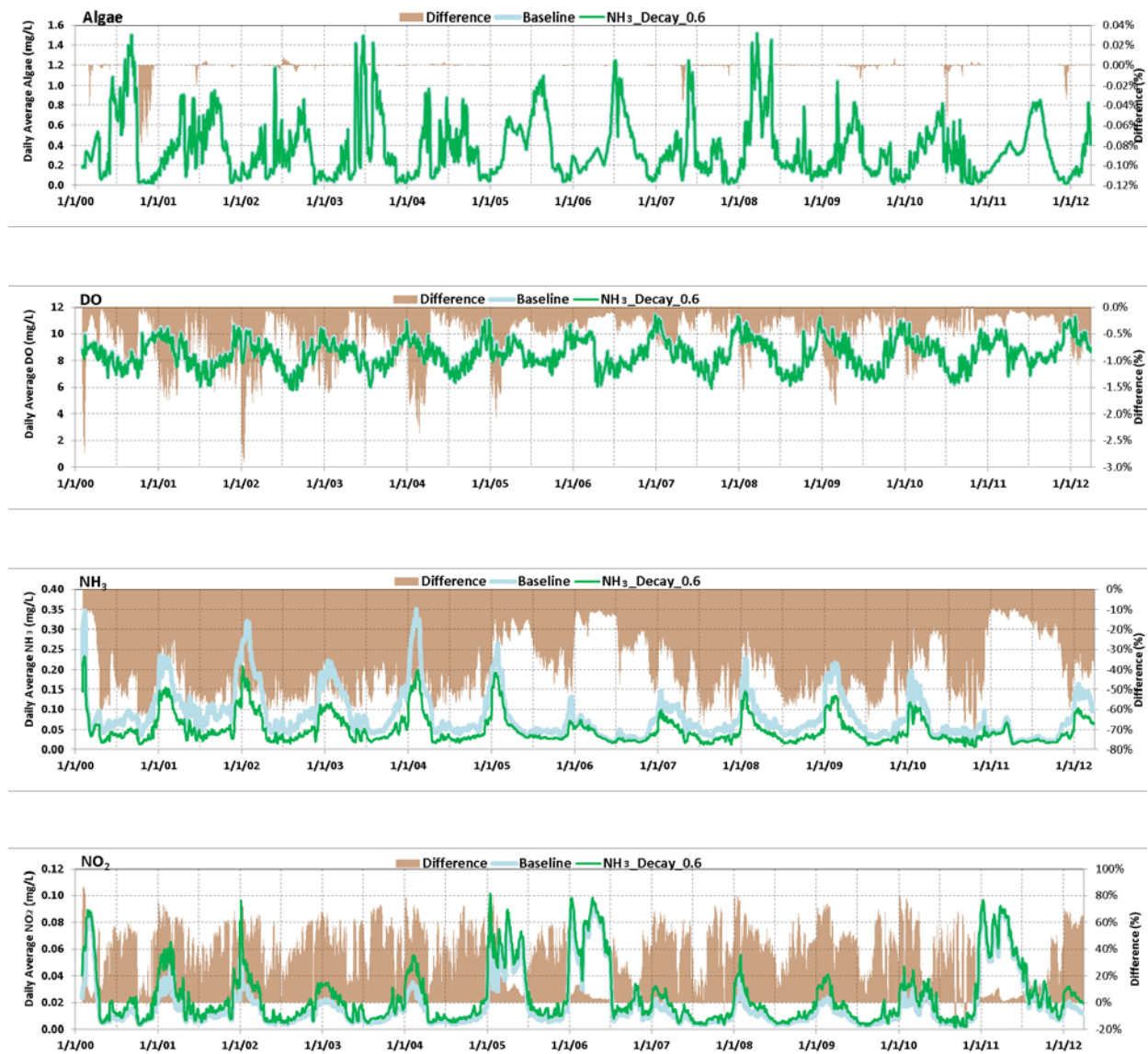


Figure 2-21 Time-Series Results of Baseline and $\text{NH}_3\text{-Decay}_0.6$ Scenarios at Old River at Tracy Road

Notes: DO = dissolved oxygen, mg/L = milligrams per liter, NH_3 = ammonia, NO_2 = nitrite

(5) Middle River at Howard Road



**Figure 2-22 Time-Series Results of Baseline and $\text{NH}_3\text{-Decay}_0.6$ Scenarios
at Middle River at Howard Road**

Notes: DO = dissolved oxygen, mg/L = milligrams per liter, NH_3 = ammonia, NO_2 = nitrite

(6) Clifton Court Forebay

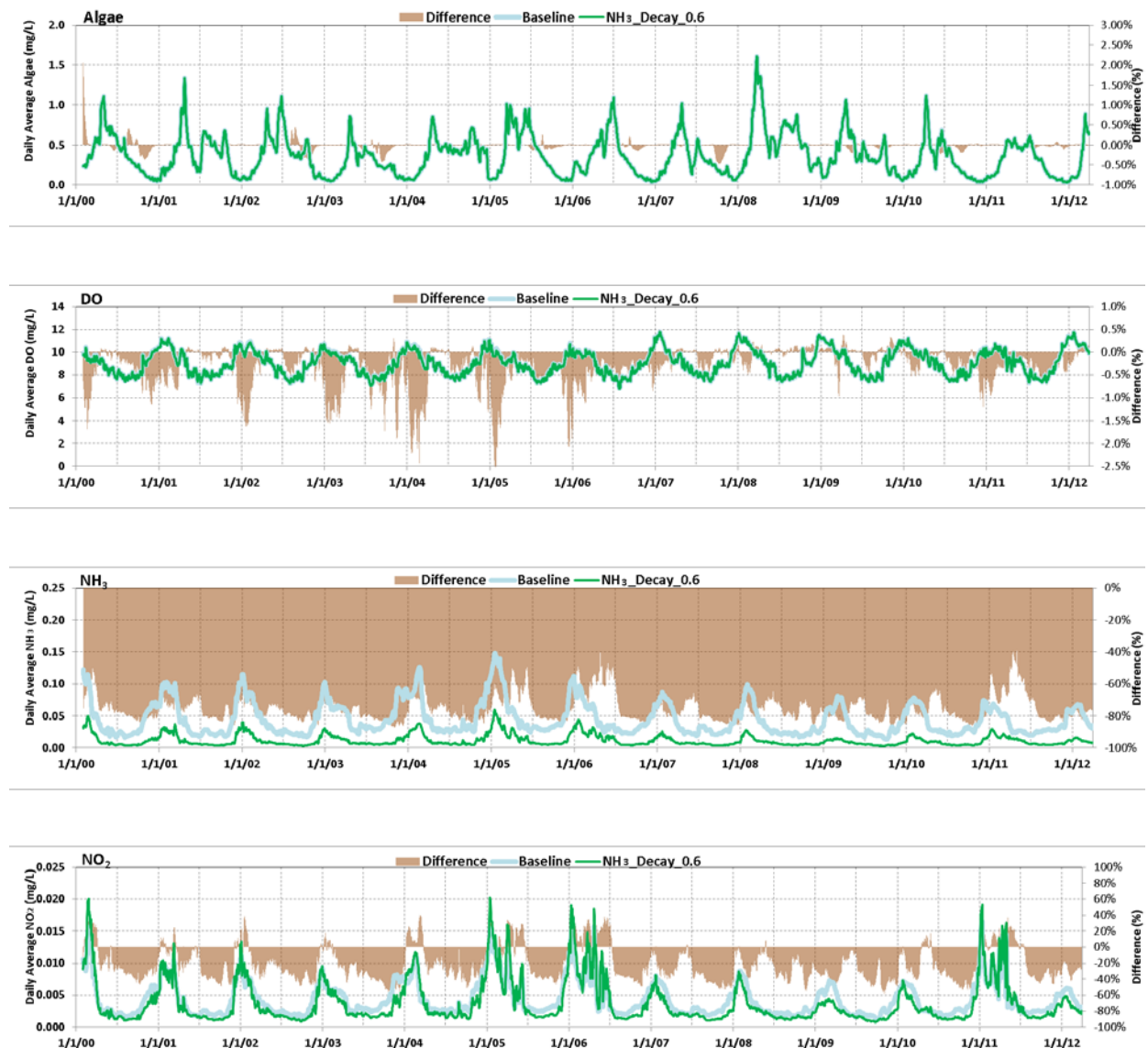


Figure 2-23 Time-Series Results of Baseline and $\text{NH}_3\text{-Decay}_0.6$ Scenarios at Clifton Court Forebay

Notes: DO = dissolved oxygen, mg/L = milligrams per liter, NH_3 = ammonia, NO_2 = nitrite

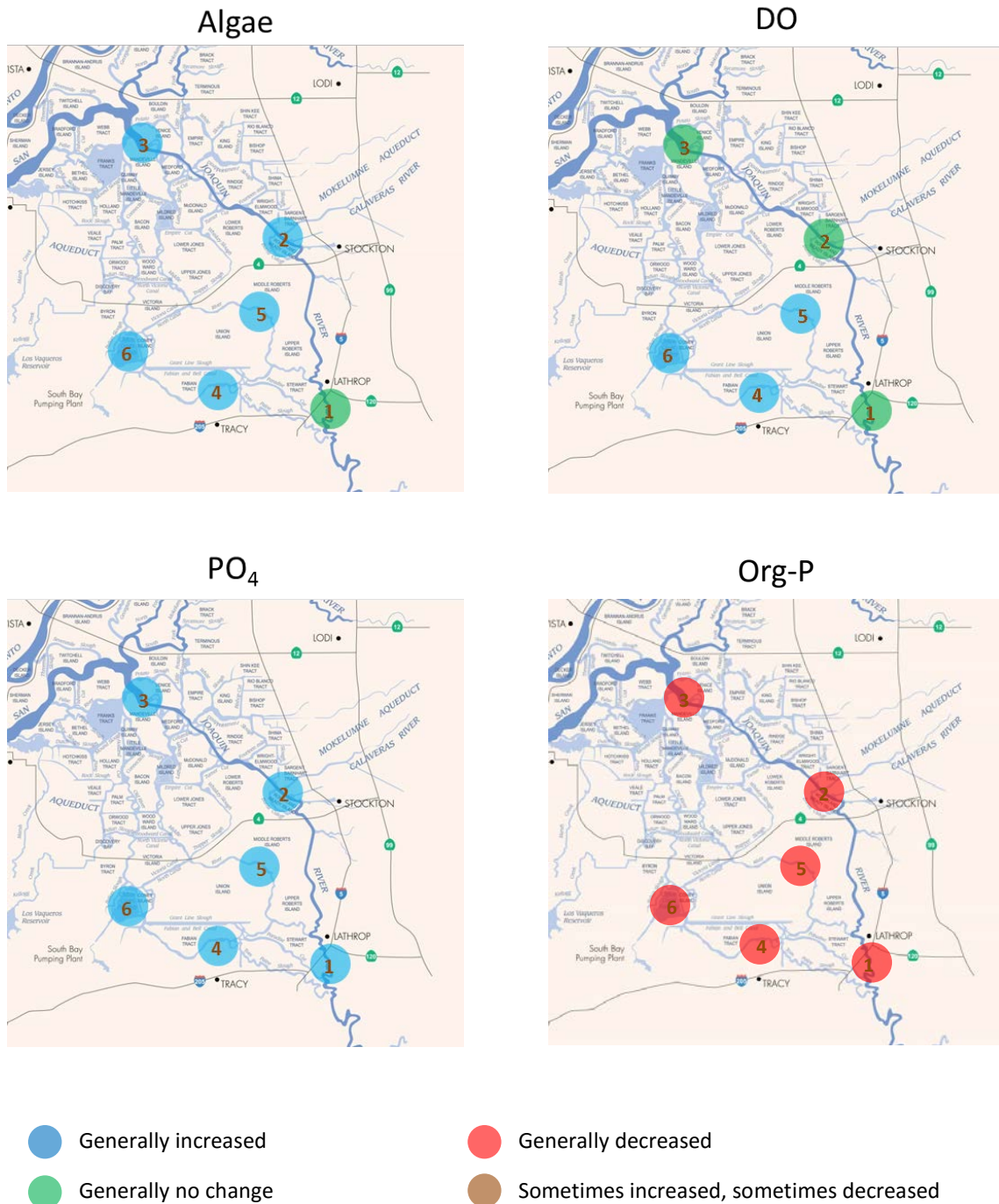


Figure 2-24 Qualitative Assessments on Model Results of Org-P_Decay_0.05 Scenario Compared with the Baseline Scenario

Notes: DO = dissolved oxygen, Org-P = organic phosphorus, PO₄ = ortho-phosphate, assumed to represent dissolved phosphorus

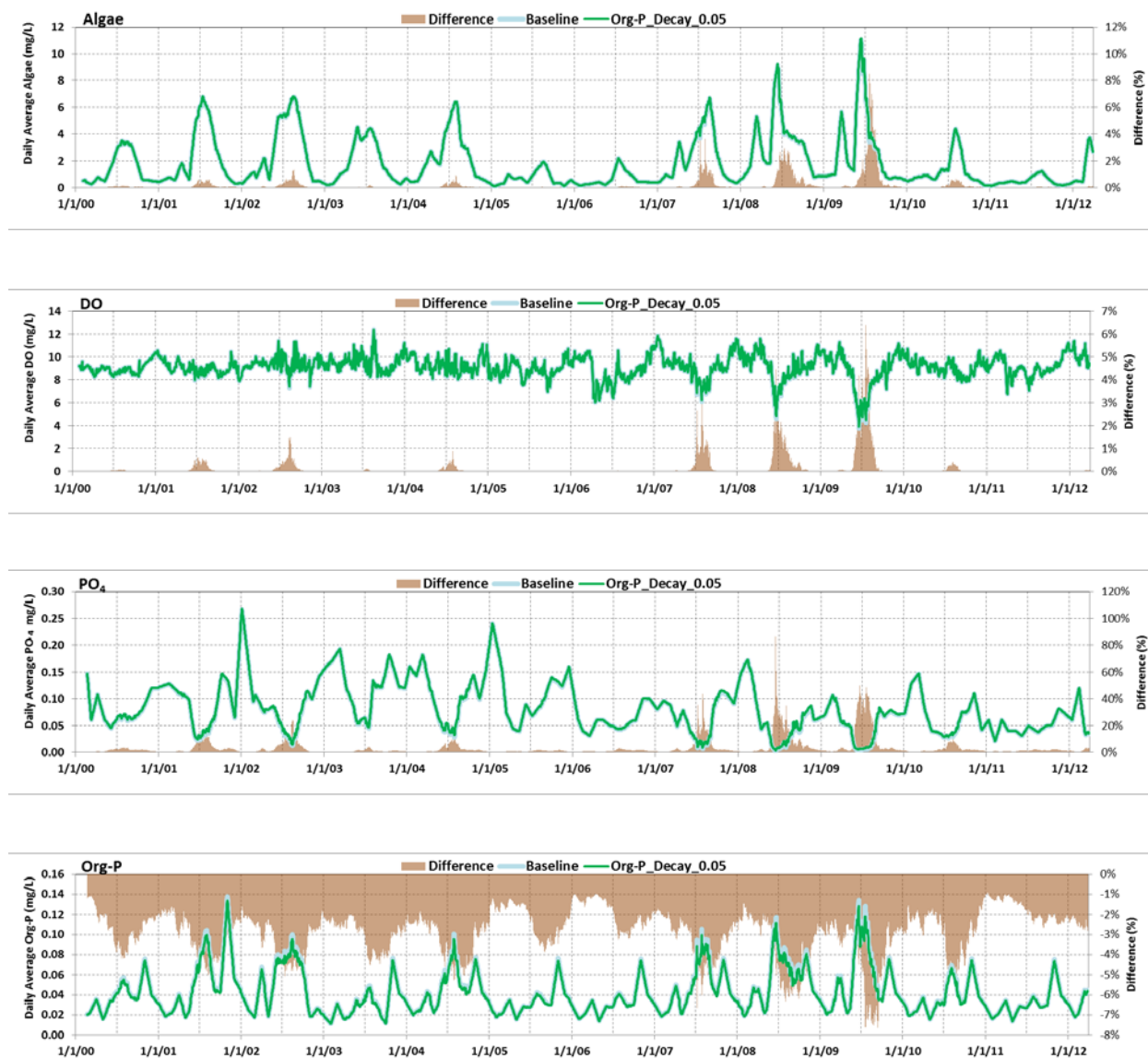
(1) San Joaquin River at Mossdale

Figure 2-25 Time-Series Results of Baseline and Org-P_Decay_0.05 Scenarios at San Joaquin River at Mossdale

Notes: DO = dissolved oxygen, mg/L = milligrams per liter, Org- P = organic phosphorus, PO₄ = ortho-phosphate, assumed to represent dissolved phosphorus

(2) Rough and Ready Island

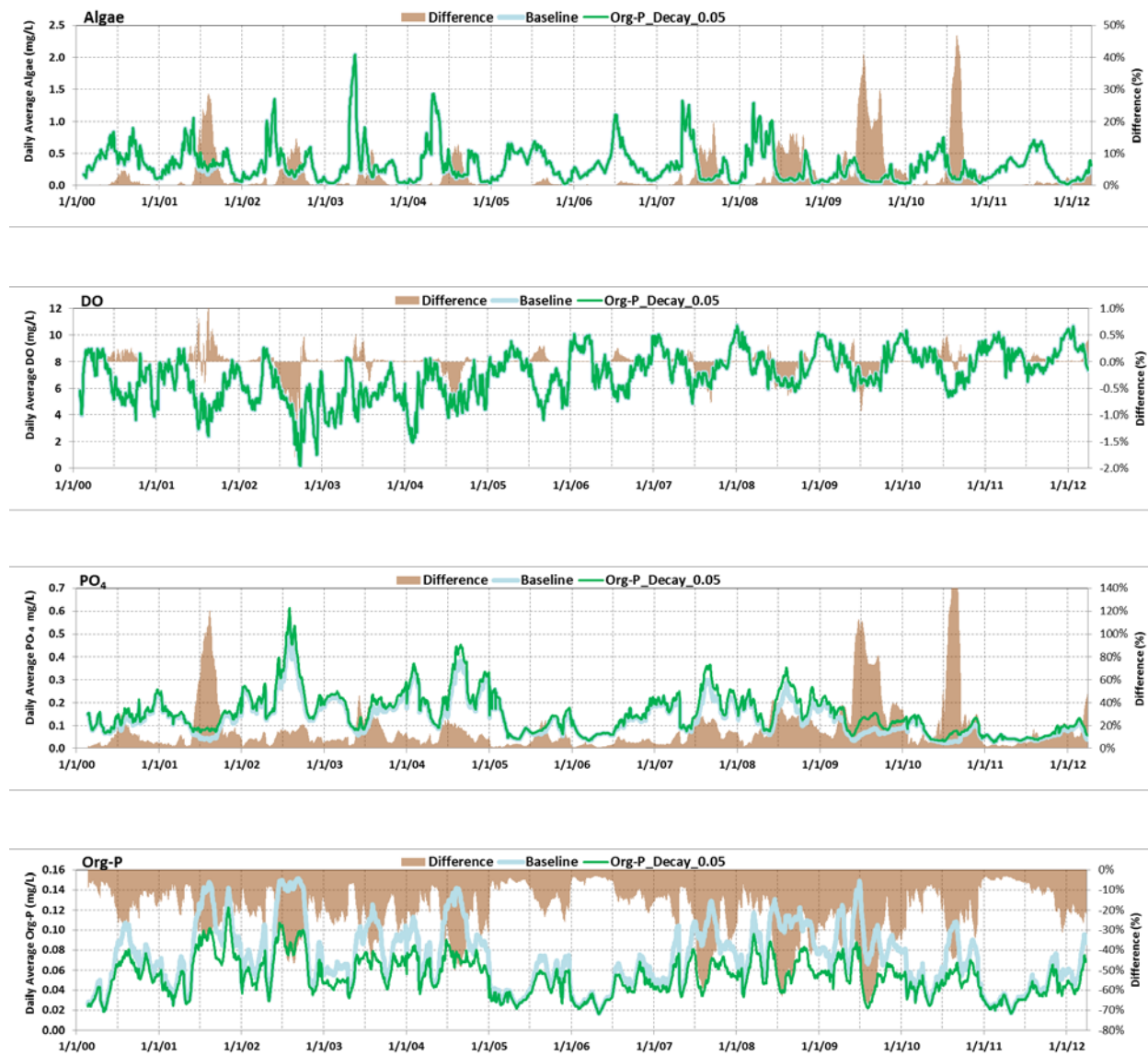


Figure 2-26 Time-Series Results of Baseline and Org-P_Decay_0.05 Scenarios at Rough and Ready Island

Notes: DO = dissolved oxygen, mg/L = milligrams per liter, Org- P = organic phosphorus, PO₄ = ortho-phosphate, assumed to represent dissolved phosphorus

(3) San Joaquin River at Prisoners Point

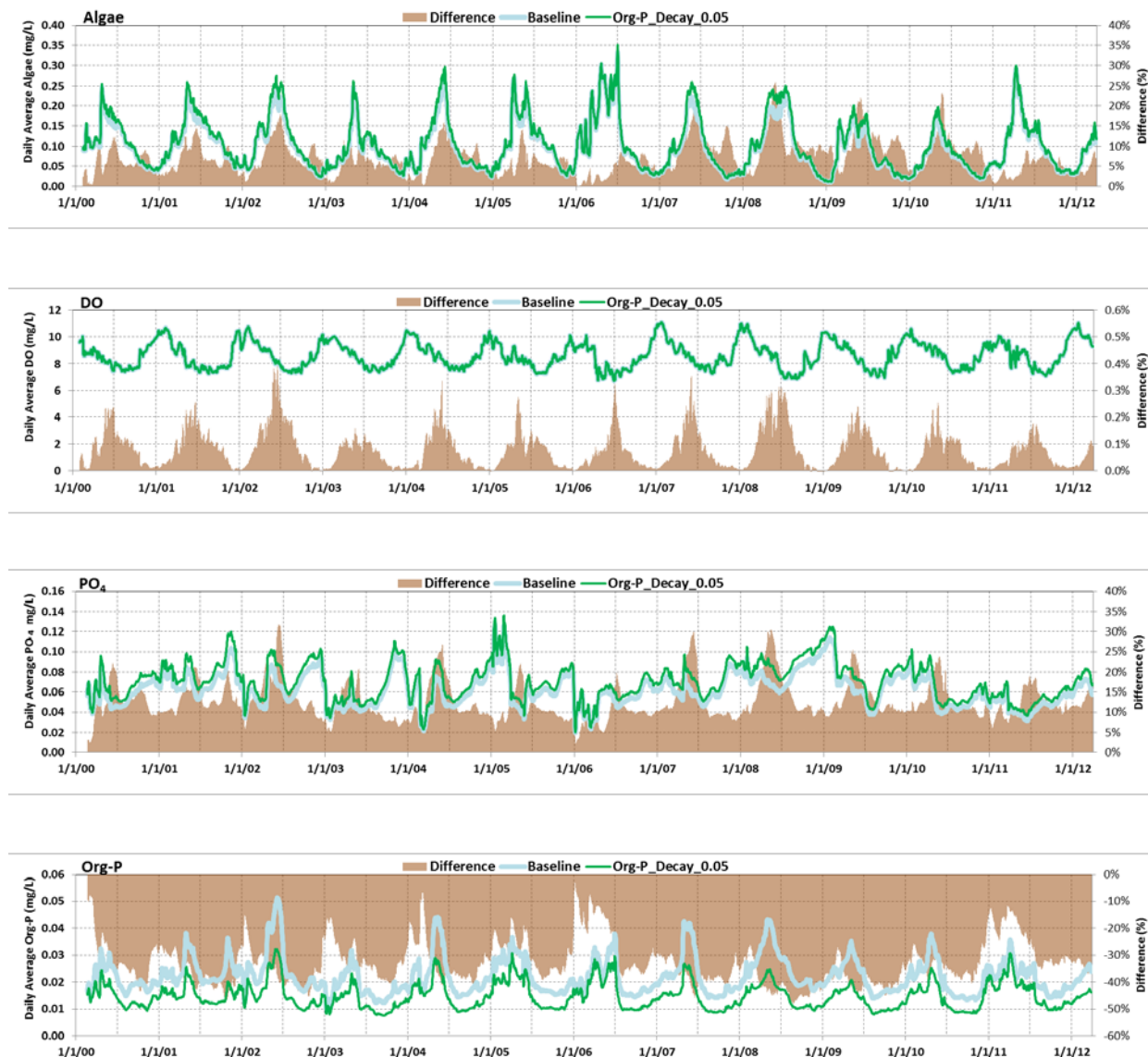


Figure 2-27 Time-Series Results of Baseline and Org-P_Decay_0.05 Scenarios at San Joaquin River at Prisoners Point

Notes: DO = dissolved oxygen, mg/L = milligrams per liter, Org- P = organic phosphorus, PO₄ = ortho-phosphate, assumed to represent dissolved phosphorus

(4) Old River at Tracy Road

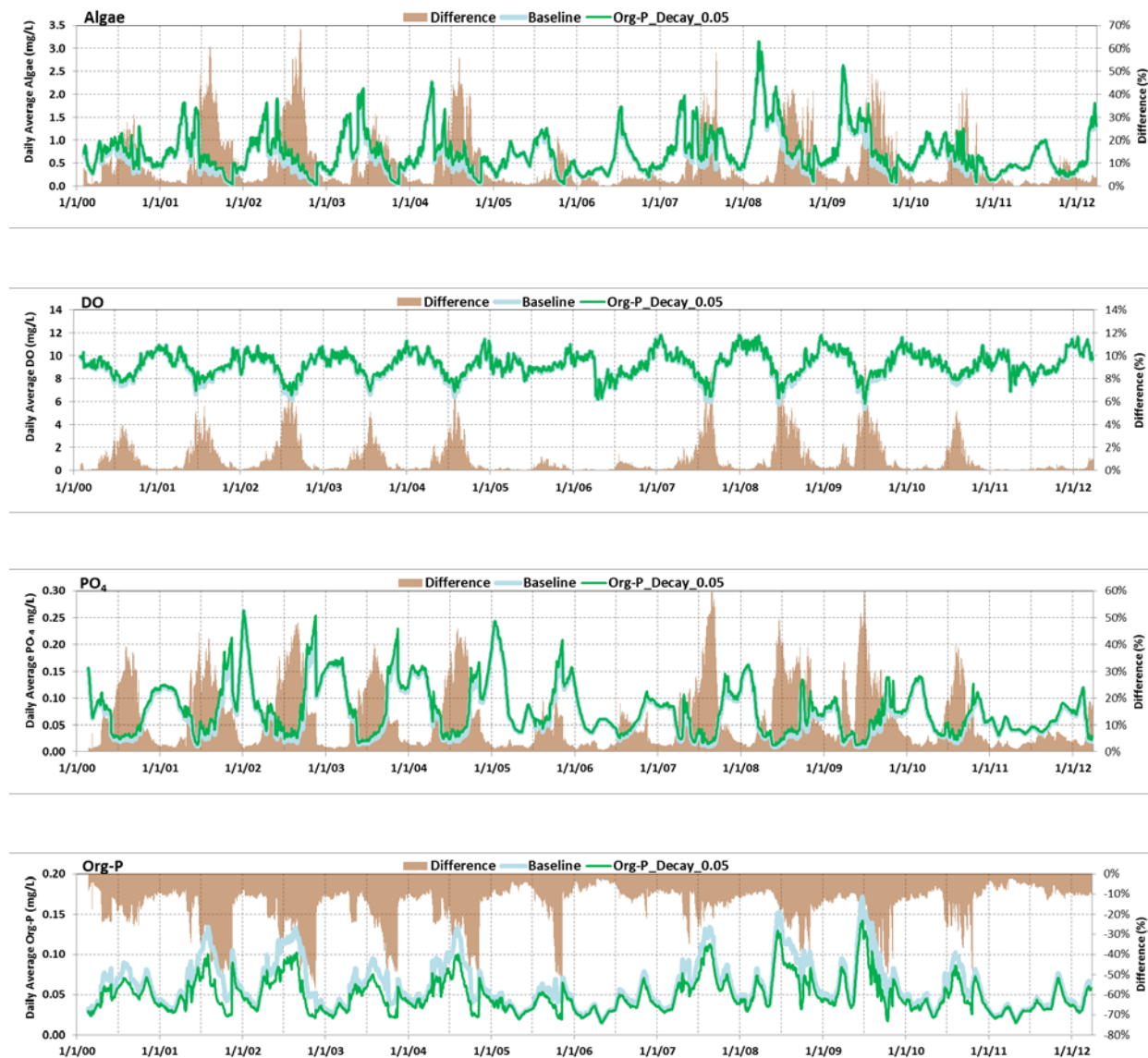


Figure 2-28 Time-Series Results of Baseline and Org-P_Decay_0.05 Scenarios at Old River at Tracy Road

Notes: DO = dissolved oxygen, mg/L = milligrams per liter, Org- P = organic phosphorus, PO₄ = ortho-phosphate, assumed to represent dissolved phosphorus

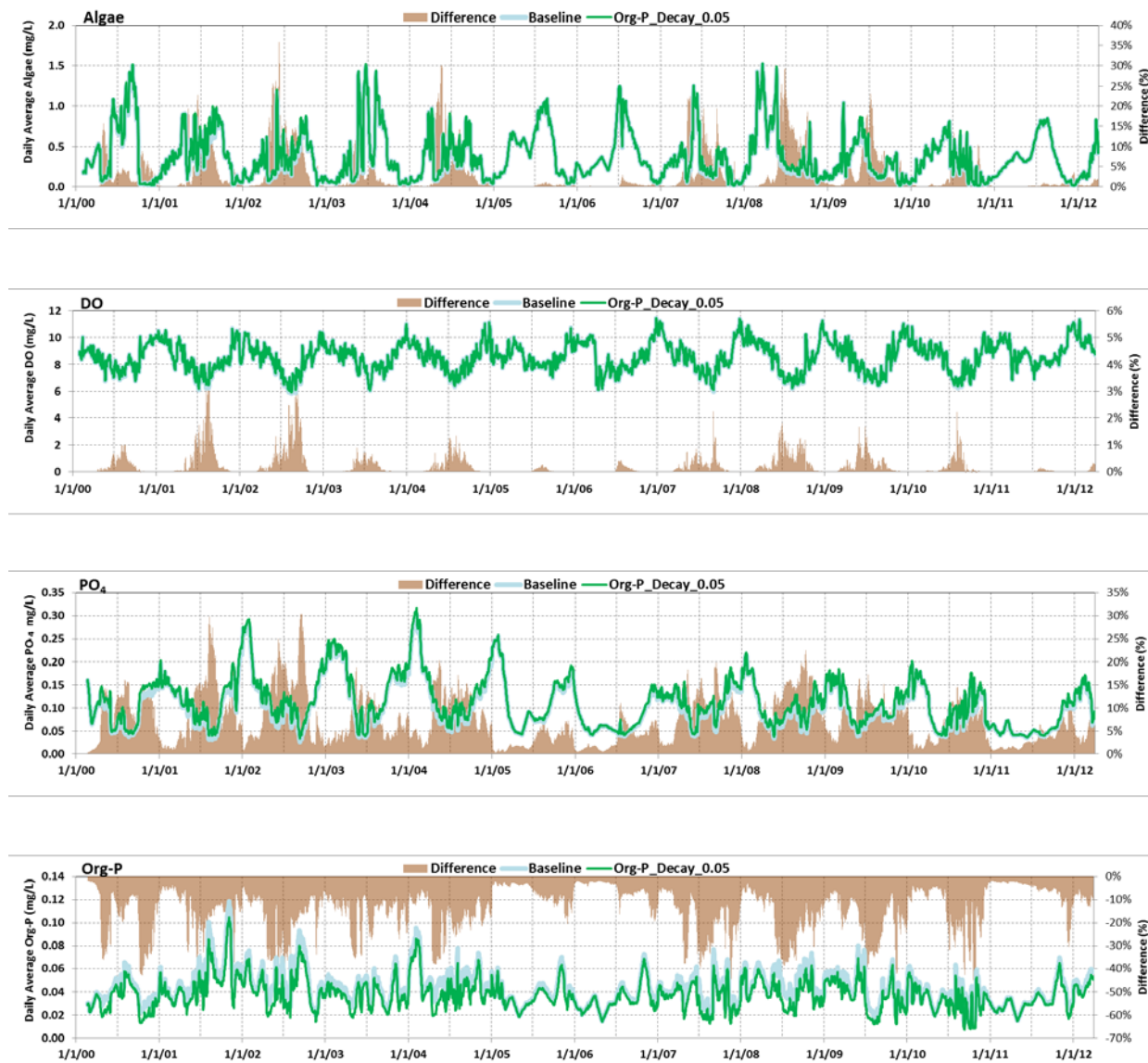
(5) Middle River at Howard Road

Figure 2-29 Time-Series Results of Baseline and Org-P_Decay_0.05 Scenarios at Middle River at Howard Road

Notes: DO = dissolved oxygen, mg/L = milligrams per liter, Org- P = organic phosphorus, PO₄ = ortho-phosphate, assumed to represent dissolved phosphorus

(6) Clifton Court Forebay

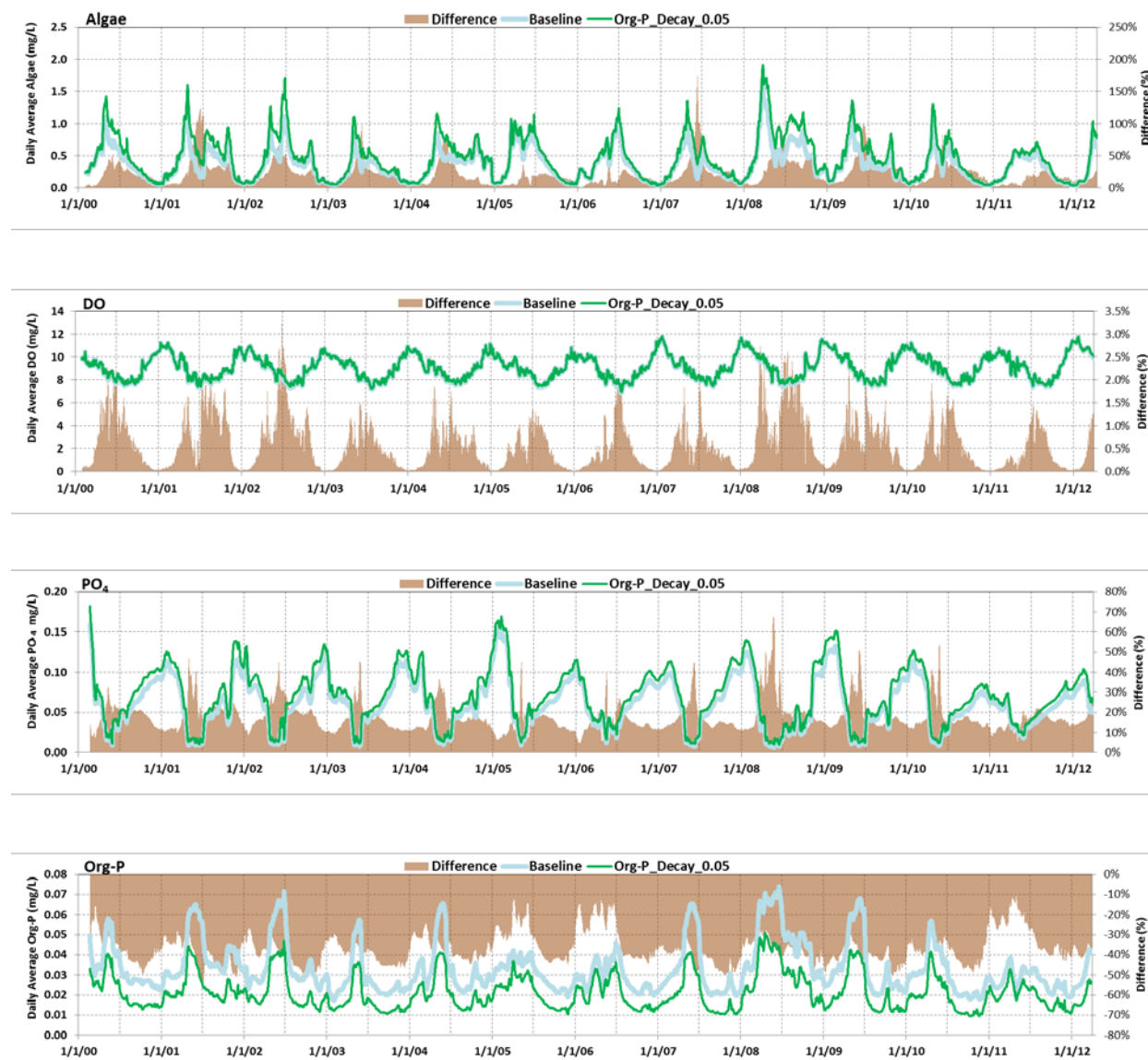


Figure 2-30 Time-Series Results of Baseline and Org-P_Decay_0.05 Scenarios at Clifton Court Forebay

Notes: DO = dissolved oxygen, mg/L = milligrams per liter, Org- P = organic phosphorus, PO₄ = ortho-phosphate, assumed to represent dissolved phosphorus

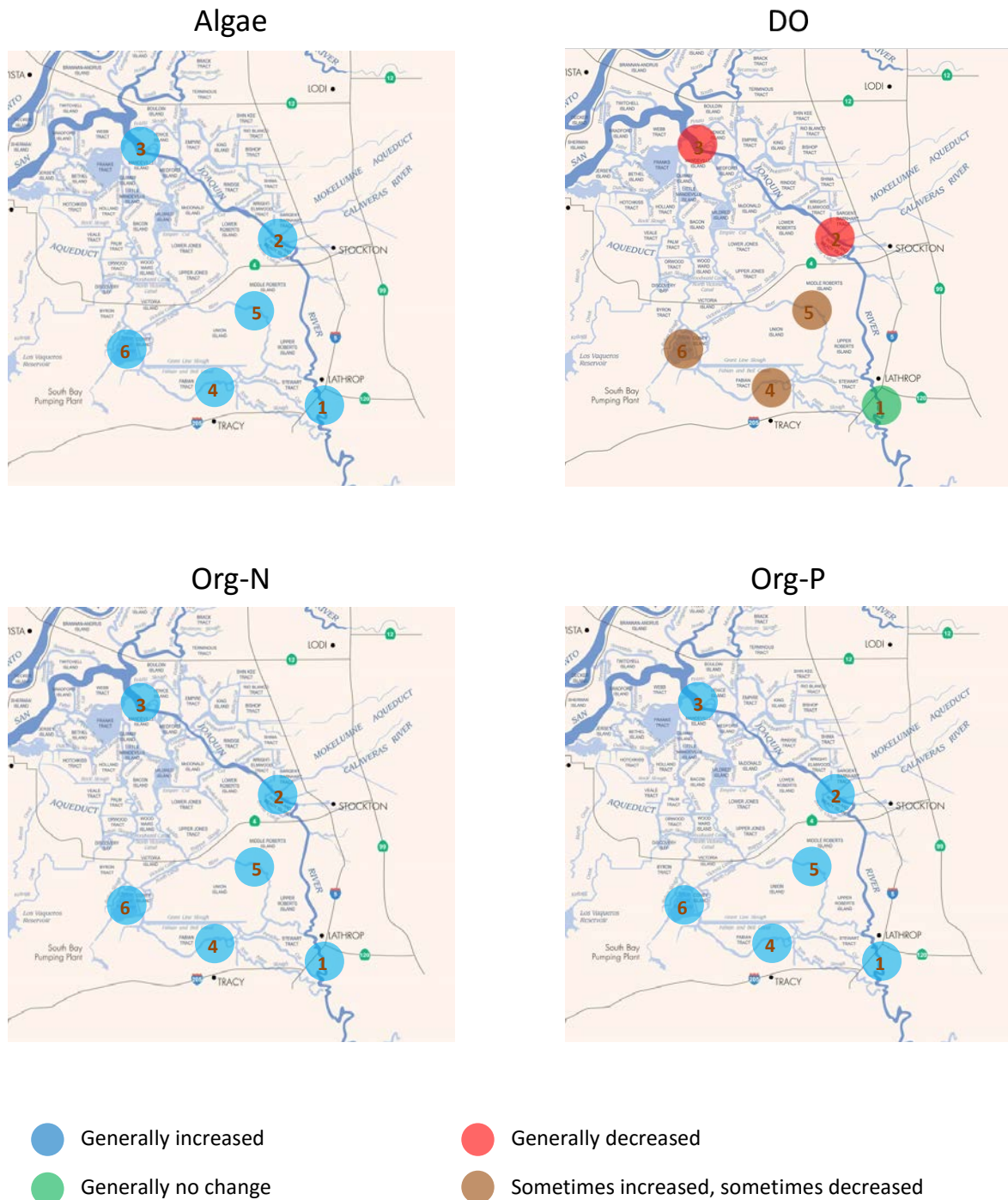


Figure 2-31 Qualitative Assessments on Model Results of Algae_Die_0.002 Scenario Compared with the Baseline Scenario

Notes: DO = dissolved oxygen, Org-N = organic nitrogen, Org-P = organic phosphorus

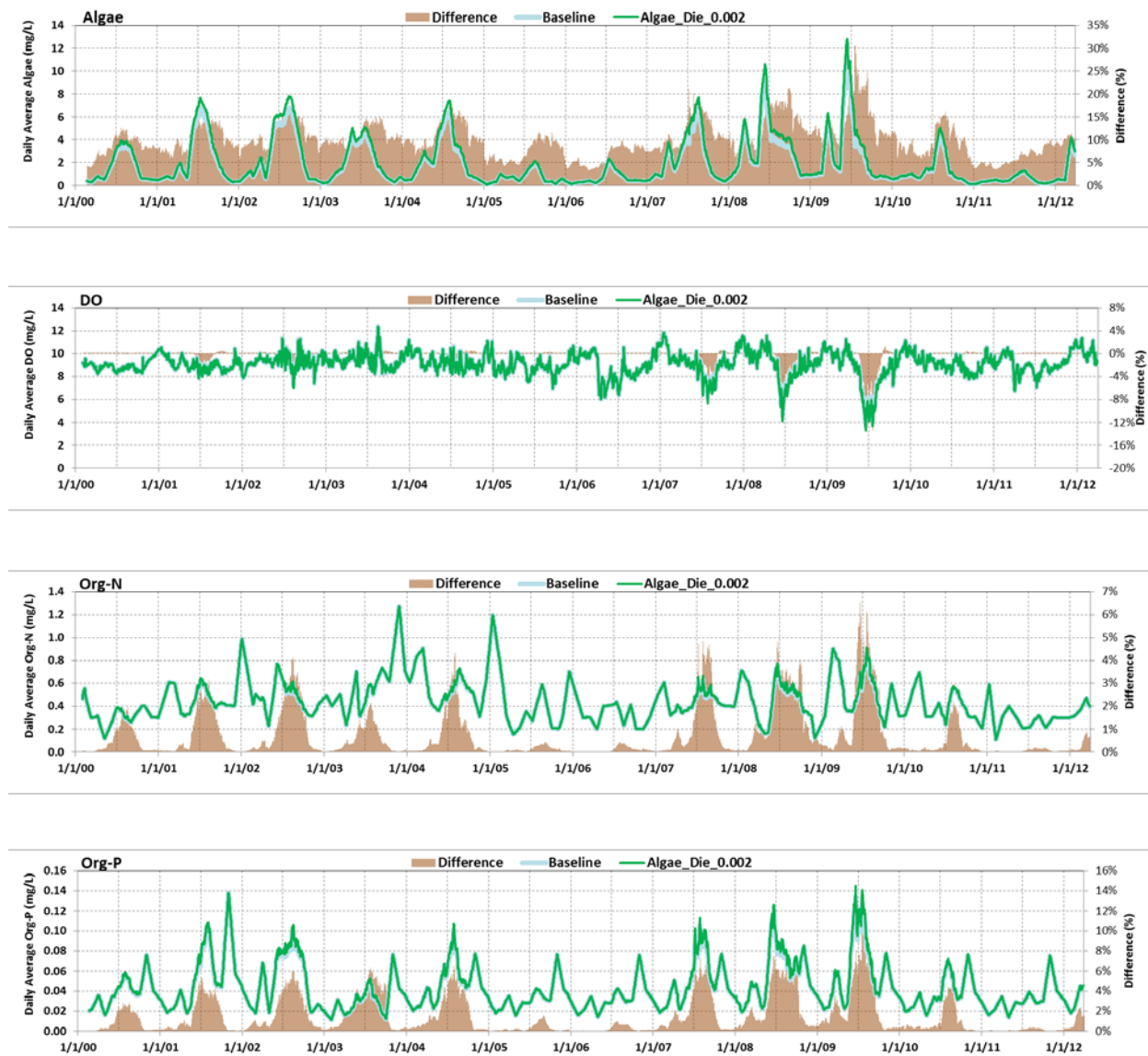
(1) San Joaquin River at Mossdale

Figure 2-32 Time-Series Results of Baseline and Algae_Die_0.002 Scenarios at San Joaquin River at Mossdale

Notes: DO = dissolved oxygen, mg/L = milligrams per liter, Org-N = organic nitrogen, Org-P = organic phosphorus

(2) Rough and Ready Island

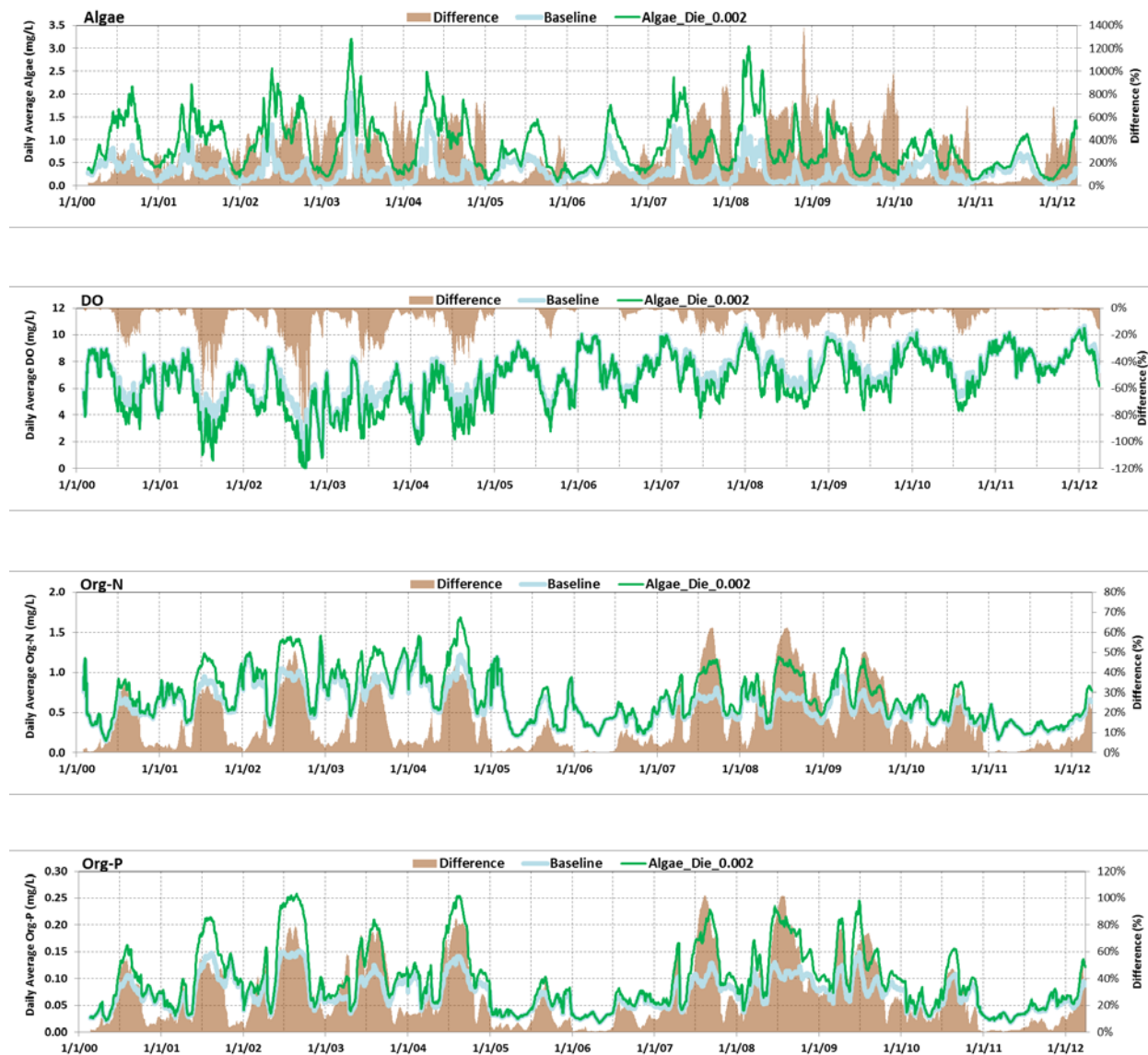


Figure 2-33 Time-Series Results of Baseline and Algae_Die_0.002 Scenarios at Rough and Ready Island

Notes: DO = dissolved oxygen, mg/L = milligrams per liter, Org-N = organic nitrogen, Org-P = organic phosphorus

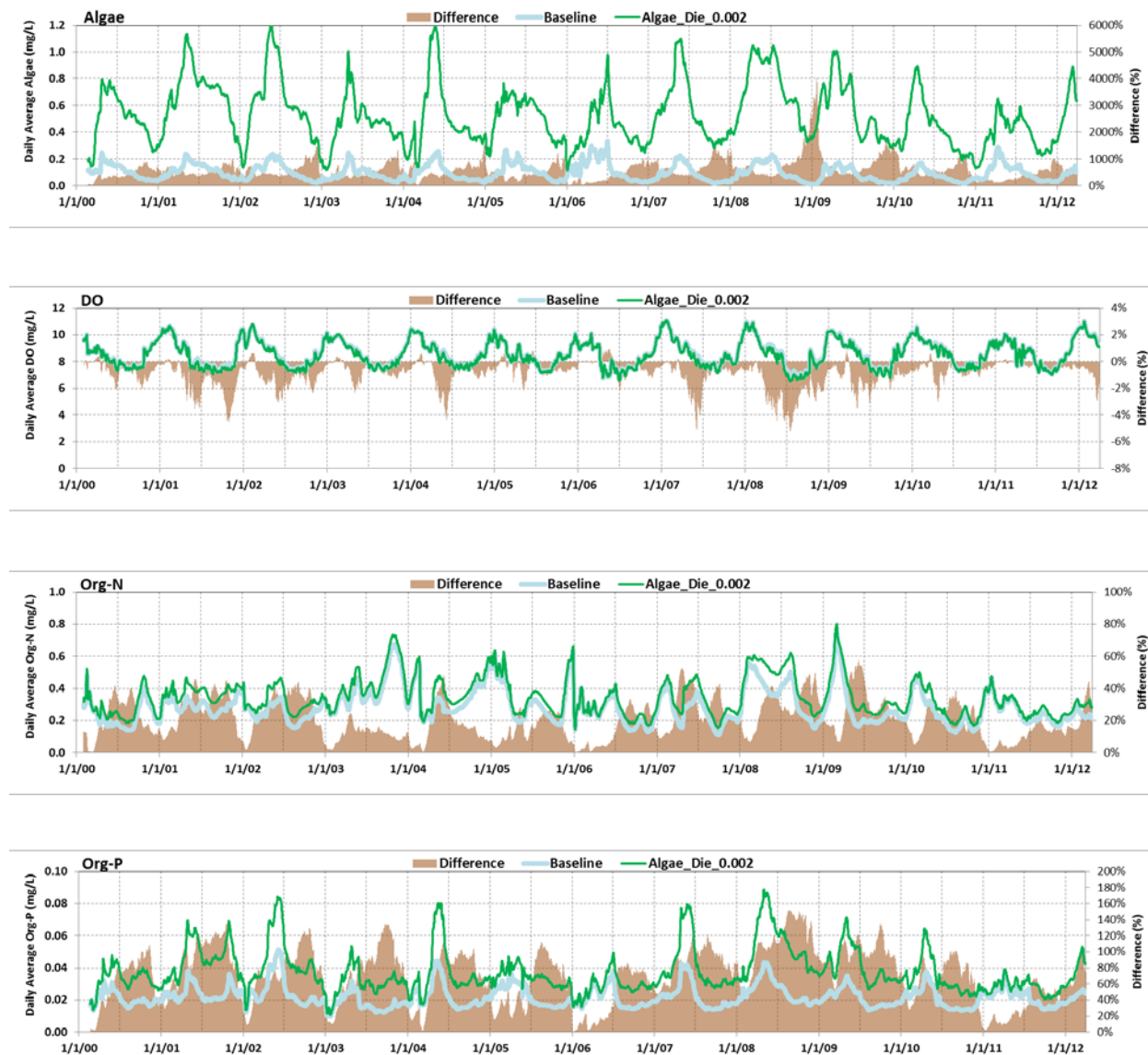
(3) San Joaquin River at Prisoners Point

Figure 2-34 Time-Series Results of Baseline and Algae_Die_0.002 Scenarios at San Joaquin River at Prisoners Point

Notes: DO = dissolved oxygen, mg/L = milligrams per liter, Org-N = organic nitrogen, Org-P = organic phosphorus

(4) Old River at Tracy Road

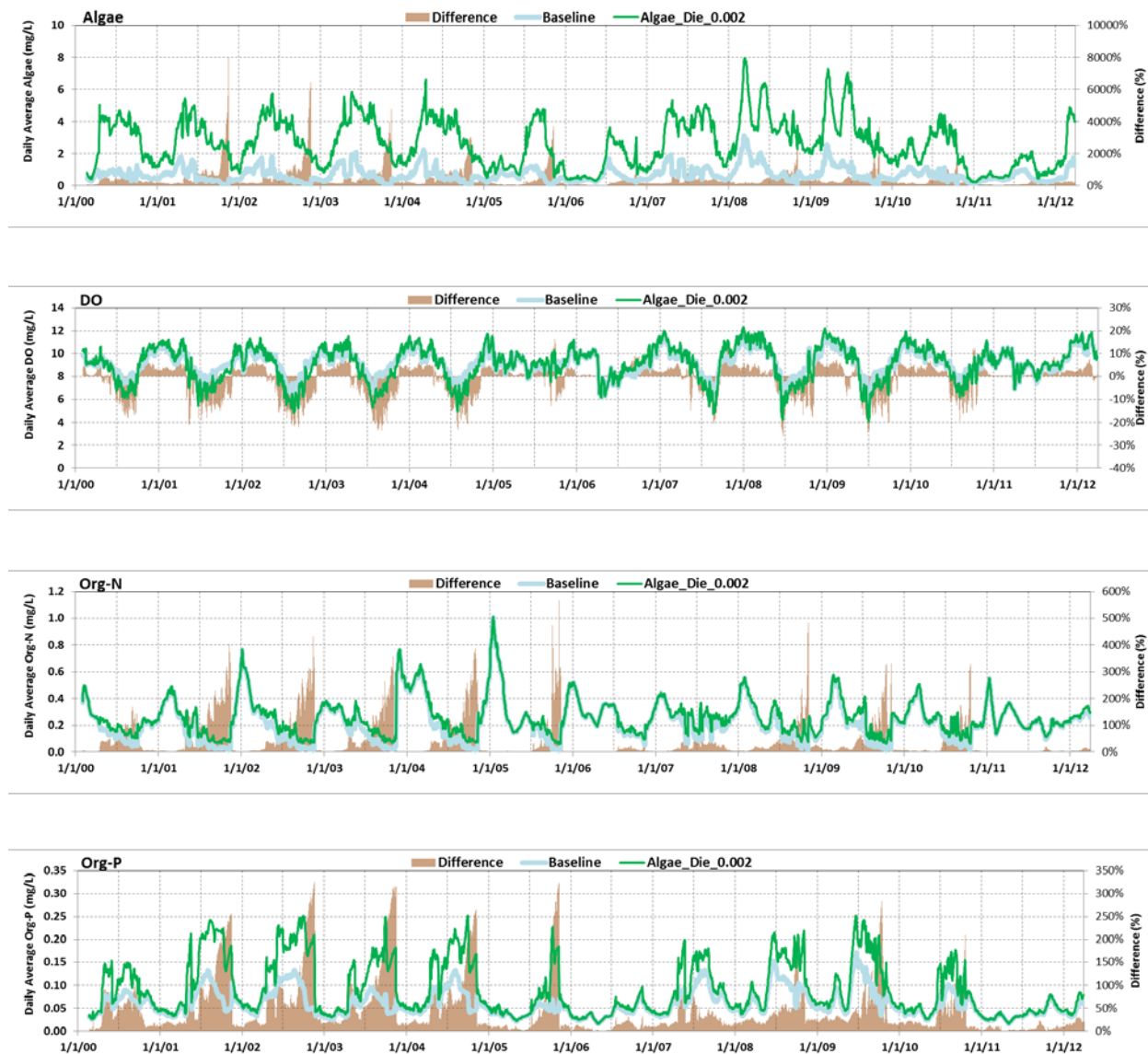


Figure 2-35 Time-Series Results of Baseline and Algae_Die_0.002 Scenarios at Old River at Tracy Road

Notes: DO = dissolved oxygen, mg/L = milligrams per liter, Org-N = organic nitrogen, Org-P = organic phosphorus

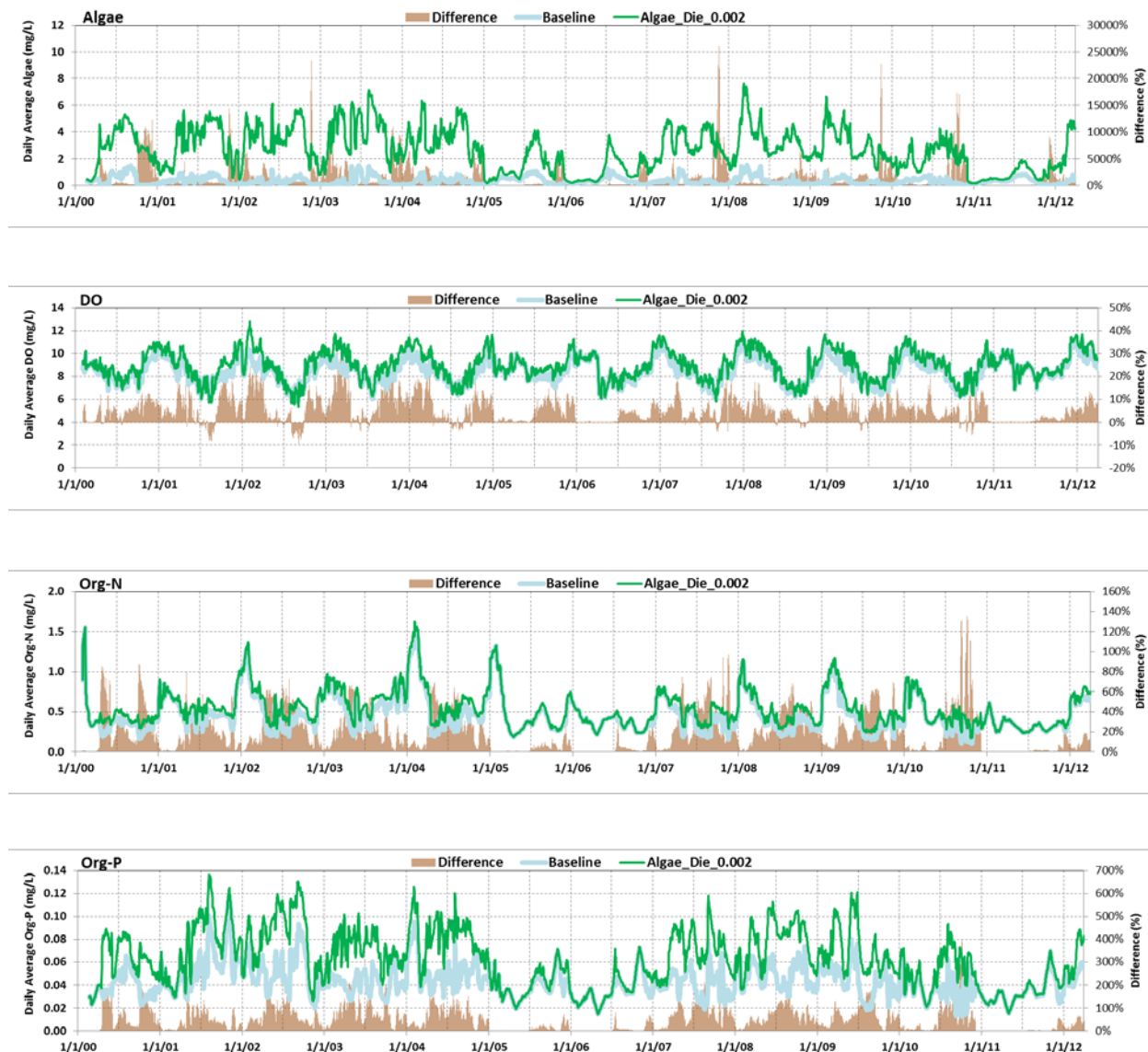
(5) Middle River at Howard Road

Figure 2-36 Time-Series Results of Baseline and Algae_Die_0.002 Scenarios at Middle River at Howard Road

Notes: DO = dissolved oxygen, mg/L = milligrams per liter, Org-N = organic nitrogen, Org-P = organic phosphorus

(6) Clifton Court Forebay

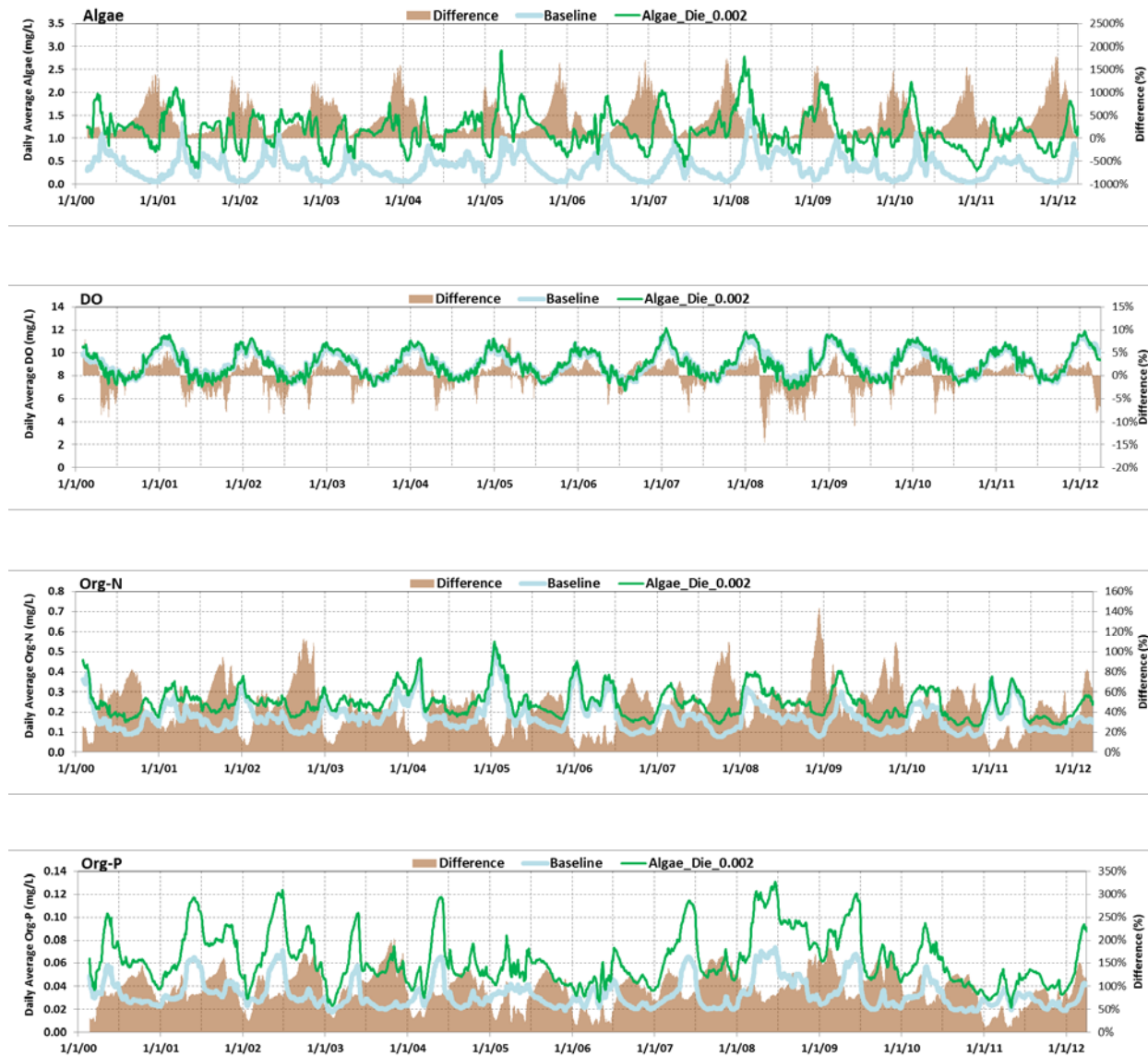


Figure 2-37 Time-Series Results of Baseline and Algae_Die_0.002 Scenarios at Clifton Court Forebay

Notes: DO = dissolved oxygen, mg/L = milligrams per liter, Org-N = organic nitrogen, Org-P = organic phosphorus

2.5 References Cited

- Chapra SC. 1997. *Surface Water-Quality Modeling*. New York (NY): McGraw-Hill. 835 pp.
- Guerin M. 2015. *Modeling the Fate and Transport of Nutrients Using DSM2: Calibration/Validation Report*. Davis (CA): Resource Management Associates. 237 pp. Viewed online at: <http://sfbaynutrients.sfei.org/sites/default/files/Appendix%206%20Updating%20DSM2%20nutrient%20calibration.pdf>.
- Hsu E, Ateljevich E, Sandhu P. 2014. "DSM2-GTM." In: *Methodology for Flow and Salinity Estimates in the Sacramento-San Joaquin Delta and Suisun Marsh*. 35th Annual Progress Report to the State Water Resources Control Board. Sacramento (CA): Bay-Delta Office. Delta Modeling Section. California Department of Water Resources. Chapter 4. 22 pp.
- Rajbhandari H. 1998. "DSM2-Qual." In: *Methodology for Flow and Salinity Estimates in the Sacramento-San Joaquin Delta and Suisun Marsh*. 19th Annual Progress Report to the State Water Resources Control Board. Sacramento (CA): Bay-Delta Office. Delta Modeling Section. California Department of Water Resources. Chapter 3. 17 pp.
- _____. 2004. "Model Assessment of Dissolved Oxygen and Flow Dynamics in the San Joaquin River Near Stockton, California." In: Spaulding ML, editor. *Proceedings of the 8th International Conference on Estuarine and Coastal Modeling, California*. November 3–5. Monterey, CA. Reston (VA): American Society of Civil Engineers. pp 236-255.

Methodology for Flow and Salinity Estimates in the Sacramento-San Joaquin Delta and Suisun Marsh

**38th Annual Progress Report
June 2017**

Chapter 3

Implementing DETAW in Modeling Hydrodynamics and Water Quality in the Sacramento-San Joaquin Delta

Authors: Lan Liang and Bob Suits
Delta Modeling Section
Bay-Delta Office
California Department of Water Resources



Contents

Chapter 3 Implementing DETAW in Modeling Hydrodynamics and Water Quality in the Sacramento-San Joaquin Delta	3-i
3 Implementing DETAW in Modeling Hydrodynamics and Water Quality in the Sacramento-San Joaquin Delta	3-1
3.1 INTRODUCTION	3-1
3.2 BACKGROUND.....	3-1
3.2.1 <i>Current DWR Models</i>	3-2
3.2.2 <i>DETAW v1.0</i>	3-3
3.3 DETAW v2.0: IMPLEMENTING DETAW IN THE MODELING OF DELTA HYDRODYNAMICS AND WATER QUALITY	3-5
3.3.1 <i>Rewriting DETAW v1.0.</i>	3-5
3.3.2 <i>Updating Seepage Rate Assumptions</i>	3-5
3.3.3 <i>Updating Crop Coefficients for Field Crops and Native Vegetation</i>	3-6
3.3.4 <i>Calibrating Crop Stress Coefficients</i>	3-6
3.3.5 <i>Estimating Net Channel Depletion for DETAW v2.0</i>	3-11
3.4 DATA INPUT FOR DETAW v2.0	3-12
3.4.1 <i>Land Use</i>	3-12
3.4.2 <i>Precipitation</i>	3-13
3.4.3 <i>Air Temperature</i>	3-14
3.5 DETAW v2.0 RESULTS AS COMPARED WITH DETAW v1.0, DICU, AND DAYFLOW	3-14
3.5.1 <i>Delta Net Channel Depletion</i>	3-14
3.5.2 <i>Net Delta Outflow</i>	3-15
3.5.3 <i>Simulation of Delta Electrical Conductivity with DSM2</i>	3-18
3.6 CONCLUSION.....	3-25
3.7 REFERENCES CITED	3-25
3.7.1 <i>Personal Communications</i>	3-26

Figures

Figure 3-1 Schematic Showing the Water Balance for a Delta Island	3-2
Figure 3-2 DETAW Consumptive Use Subareas.....	3-4
Figure 3-3 Variation in Grain Crop Coefficient (Kc) During A Year	3-7
Figure 3-4 The Total Delta Consumptive Use in 2007 by Four Models.....	3-9
Figure 3-5 Total Delta Consumptive Use in 2009 by Four Models	3-10

Figure 3-12 DSM2 Simulation of Historical EC under DICU and DETAW v2.0 Compared with Observed EC, 2000–2004.....	3-22
--	------

Tables

Table 3-1 Stress Coefficients and Adjusted Peak Crop Coefficients Generated from SEBAL Analysis.....	3-8
Table 3-2 Total Delta Consumptive Use from March through September 2007 (TAF) by DICU, DETAW v1.0, DETAW v2.0, and SEBAL.....	3-9
Table 3-3 The Total Delta Consumptive Use from March through September 2009	3-10
Table 3-4 DETAW v2.0 Crop Categories and Land-Use Identifiers	3-13

3 Implementing DETAW in Modeling Hydrodynamics and Water Quality in the Sacramento-San Joaquin Delta

3.1 Introduction

Numerical modeling of the hydrodynamics and water quality in the Sacramento-San Joaquin Delta (Delta) channels requires accounting for in-Delta net channel depletion, because of agricultural diversions including seasonal leaching, seepage from channels to Delta lowland islands, riparian and native vegetation evapotranspiration, and evaporation from free-water surfaces. The California Department of Water Resources (DWR) has recently developed a new model, the Delta Evapotranspiration of Applied Water Model (DETAW v2.0), which is a significant improvement over current methods for estimating Delta consumptive use and net channel depletion. This report presents the key aspects of DETAW v2.0 and its implementation in the detailed modeling of Delta conditions.

3.2 Background

Diversions of water to agricultural lands for irrigation are not metered and are difficult to measure, because the diversions are made through siphons, pumps, and floodgates operating under continuously fluctuating water levels in Delta channels. These diversions are withdrawn at more than 1,800 locations in the Delta. Some areas of the Delta, namely the Delta lowlands (areas of the Delta below the 5 feet mean sea-level contour), receive seepage from adjacent channels. This seepage to islands in the Delta lowlands contributes to net channel depletion, but it is not directly measurable. For these reasons, most estimates of Delta net channel depletion are based on estimates of crop-water demands (crop evapotranspiration [ET]) and the sources of water to meet these demands. The main sources consist of: applied water (I_A), soil moisture (SM) and precipitation (PPT). Within the Delta lowlands, seepage of water from adjacent Delta channels is also a source. Also common in the lowlands is the leaching of salts from the root zone through large irrigation applications. Typically, applied leach water (LW_A) is applied from October through December and drained (LW_D) from January through April. Excess water is also pumped from the Delta islands back into the Delta. This water consists of excess irrigation water (ID), drained leach water (LW_D), and surface runoff (RO) from precipitation.

Net channel depletion equals total diversions (DIV) plus total seepages (S) minus total drainages or return flows (RET). These relationships are defined by Equations 1 through 5 and graphically shown in Figure 3-1.

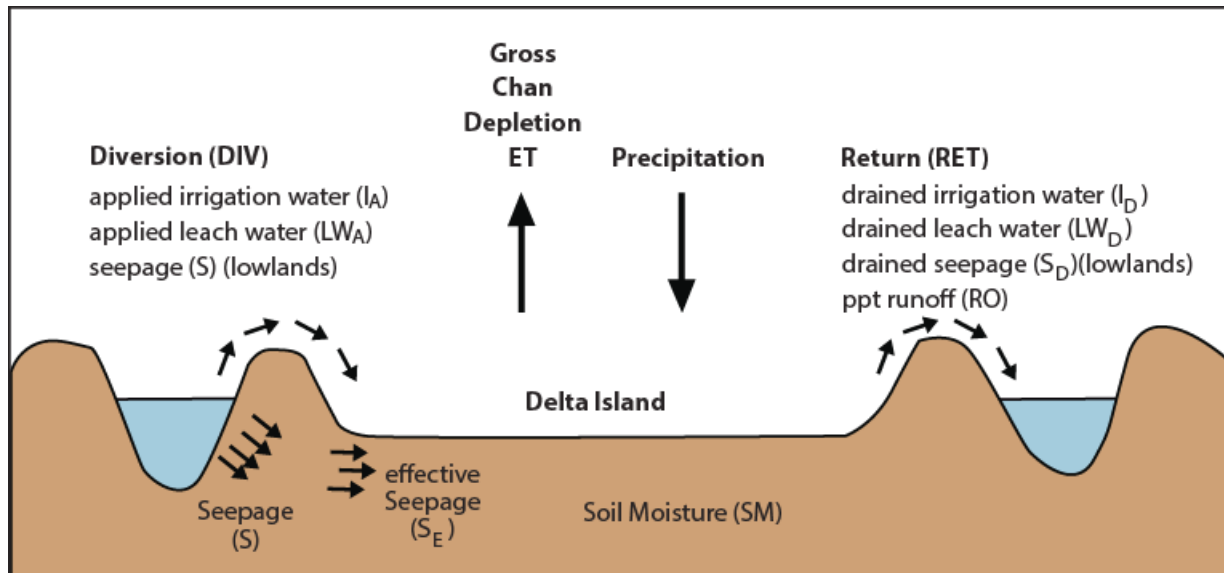


Figure 3-1 Schematic Showing the Water Balance for a Delta Island

Notes: Chan = channel, ET = evapotranspiration, ppt = precipitation

Where

$$\text{DIV} = I_A + LW_A. \quad (1)$$

$$\text{RET} = I_D + LW_D + RO + S_D. \quad (2)$$

$$S = S_E + S_D. \quad (3)$$

$$\text{Net channel depletion} = \text{DIV} - \text{RET} + S. \quad (4)$$

$$\text{Net channel depletion} = I_A - I_D + LW_A - LW_D - RO + S_E. \quad (5)$$

The models for estimating Delta net channel depletion vary in the degree in which key factors are simplified. These assumptions will affect any estimation of Delta outflow based, in part, on simulated net channel depletion. These models, discussed below, are DAYFLOW (a computer program designed to estimate daily average Delta outflow), the Consumptive Use (CU) Model and the Delta Island Consumptive Use (DICU) Model.

The current models estimating net channel depletion assume Delta channels are not hydraulically connected to groundwater. Accordingly, seepage is assumed to directly deplete adjacent channels and does not replenish ground water.

3.2.1 Current DWR Models

DWR currently uses three models to estimate Delta net channel depletion. These models, DAYFLOW, CU, and DICU base estimates of net channel depletion on estimates of Delta island consumptive use of water, which are, in turn, based upon crop acreage, crop-unit water demands, and some indicator of evapotranspiration potential. These models vary in the extent to which key factors are simplified. DAYFLOW is an accounting tool for determining historical Delta boundary hydrology. Monthly gross Delta depletions are based on land-use surveys that were completed in 1957, 1958, and 1961 and are repeated each year. This corresponds to the assumption that both Delta land use and factors, which determine monthly patterns of crop evapotranspiration, are constant for all years. Delta net channel

depletion is calculated by applying precipitation measured at Stockton Fire Station No. 4 to the entire Delta and then assuming that all of the precipitation is available to meet Delta consumptive-use demands. Implementing DAYFLOW in Delta modeling requires extensive assumptions of how Delta-wide net channel depletion is distributed among Delta islands.

DICU is the model currently used by DWR to generate Delta agricultural diversions and drainage needed for simulation of Delta hydrodynamics and water quality. DICU is based on DWR's earlier consumptive use model, CU, which provides the Delta uplands and lowlands net channel depletion used by DWR's water resources planning model, which is currently CALSIM II. DICU estimates, on a monthly basis, the water that enters, leaves, or is stored in each of 142 Delta subareas. Factors considered in tracking water are land use, plant-rooting depths, seepage, soil moisture, the irrigation season, ET, and precipitation. Land use is categorized according to 20 types, and acreage is based on historical surveys. DICU tracks subarea soil moisture and estimates the amount of water in the soil that is available to plants. Soil moisture limits in DICU are based on extensive DWR neutron probe measurements of Delta islands that occurred during the 1960s. Month-end minimum soil moisture levels are assumed to force an observed yearly pattern, which is Delta soil moisture being at near-capacity at the beginning of each irrigation season. The moisture in the soil is then mined before approaching the wilting point at the end of the irrigation season. Crop-root depths vary by crop and by whether an island is in the uplands or lowlands.

Delta ET, estimated by DICU, is based on pan evaporation and monthly unit ET by crop. Long-term ET values by crop and month are based on various studies that were done during the 1970s and 1980s. Pan evaporation is determined by measuring the evaporation in a standardized evaporation pan holding water at a given location. Long-term average pan evaporation by month is based on data from two sites in Davis during 1956–1984. Pan evaporation for any given historical month and year, since Water Year (WY) 1991, comes from reported pan evaporation from Manteca.

For subareas in Delta lowlands, the DICU model simulates the practice of applying water during winter months to leach salts from the root zone. Timing and volume of leach water are based on a 1981 DWR study. Monthly Delta-wide leach volumes and later drainage are proportionally distributed among subareas, based on subarea acreage.

Precipitation in each of the 142 subareas is determined by weighting the precipitation of five Delta stations by using a Thiessen polygon interpolation routine.

DICU has two significant limitations. The first is calculating Delta crop ET for the monthly averaged pan evaporation at one location, the long-term average crop ET, and pan evaporation. The calculated ET at a particular location is difficult to represent ET spatial variations in the Delta. The second limitation is DICU uses a monthly time step instead of a daily time step for precipitation.

The implementation of DICU in Delta modeling requires estimating the sources of water used to meet water demands and the drainage from Delta islands because of excess seepage, rainfall, and applied water.

3.2.2 DETAW v1.0

In 2006, DETAW v1.0 was developed by the University of California, Davis, to better estimate consumptive water demands within the Delta. (See Snyder 2006 for full documentation.)

DETAW v1.0 estimates consumptive water demands for 168 subareas within the Delta Service Area (Figure 3-2). As in DICU, daily precipitation for each subarea is estimated from seven precipitation gaging stations in and adjacent to the Delta and areal weighting factors calculated from Thiessen polygons.

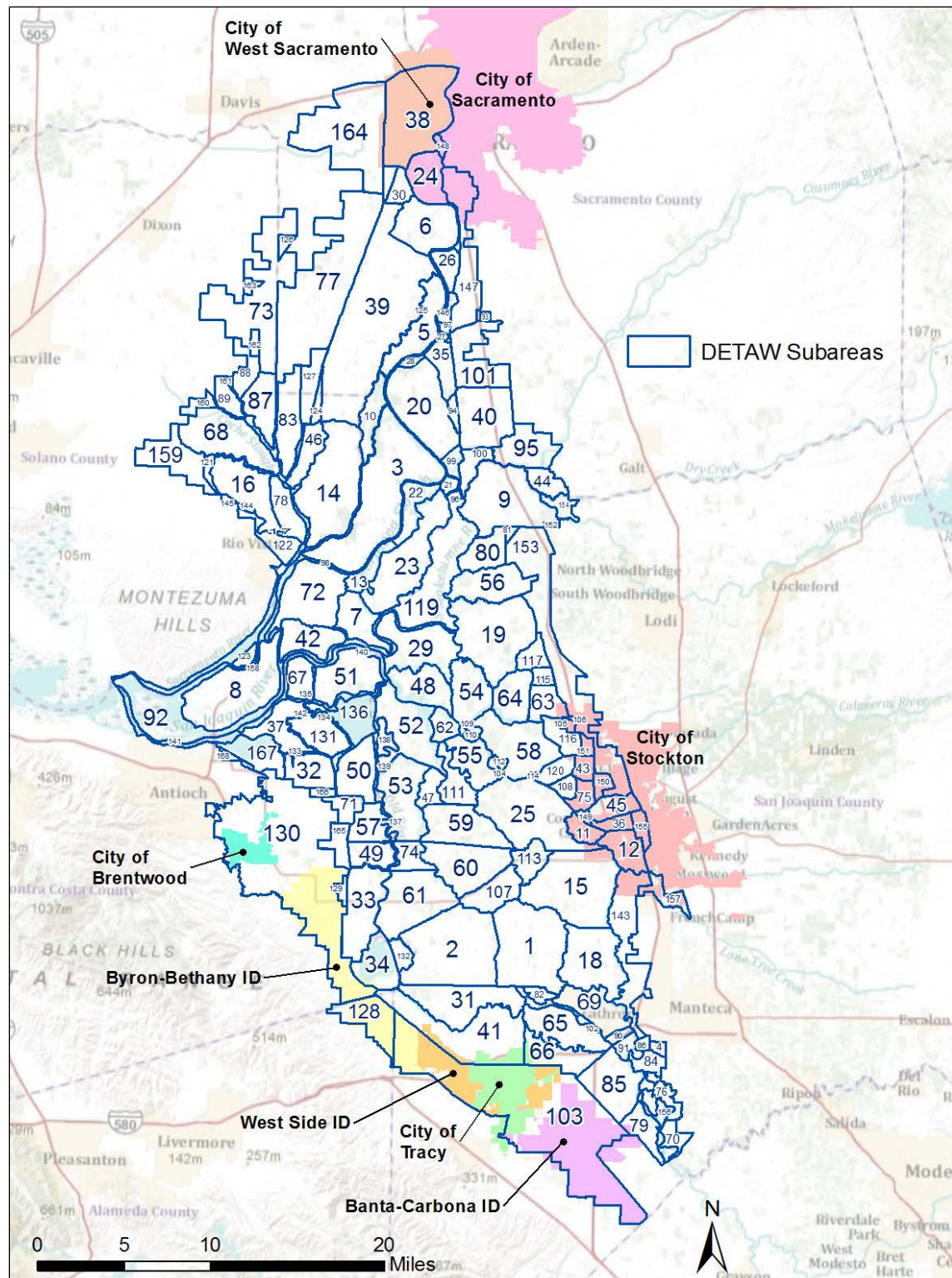


Figure 3-2 DETAW Consumptive Use Subareas

Notes: DETAW = Delta Evapotranspiration of Applied Water, ID = irrigation district

By using the Hargreaves Samani (HS) equation, the reference evapotranspiration (ETo) at the California Irrigation Management Information System (CIMIS) Lodi station was calculated; and by using the Penman-Monteith (PM) equation from nine CIMIS stations, including Lodi, isolines of correction factors to estimate Delta subareas ETo from the Lodi HS ETo were developed. Note that the PM equation uses more meteorological variables (mean temperature, wind speed, relative humidity, and solar radiation) than the HS equation, which uses minimum and maximum temperature and solar radiation. The Lodi CIMIS station is the only station that has the long-term daily temperature data to support the HS ETo simulation from 1922 to recent years. The previously mentioned nine CIMIS stations lack sufficient long-term climate data needed for PM equation, so their data were applied to determine the spatial correction factors of ETo.

Then geographic information system (GIS) contouring was used to estimate correction factors for each subarea within the Delta. In this way, DETAW v1.0 estimates daily Delta ETo, which varies spatially. Daily crop ET-unit rates are computed by using seasonal crop coefficient curves. Daily water balances are used to estimate daily ET of applied water by subarea. Irrigations (diversions from Delta adjacent channels) are triggered when island soil moisture content drops below a specified threshold after accounting for effective precipitation and seepage.

In contrast to DICU, DETAW v1.0 uses daily values of unit consumptive use and precipitation. Because of this daily time step, DETAW v1.0 can reproduce large, sporadic runoff events, both in terms of runoff volume and constituent response, which is not available in DICU. This can be important for modeling water quality in the south Delta, when relatively large spring storms generate significant island runoff to channels with lesser circulation.

3.3 DETAW v2.0: Implementing DETAW in the Modeling of Delta Hydrodynamics and Water Quality

In order to use DETAW-based information in Delta modeling, additional development has been required. This consists of rewriting the program in Python script; updating seepage assumptions; calibrating crop coefficients based on satellite image-based estimates of consumptive use; estimating actual net channel depletion by estimating island diversions, seepages, and drainages; and assigning island diversions, seepages, and returns to model nodes. These activities are presented below. Together, the measures define a new version of DETAW, which is DETAW v2.0.

3.3.1 Rewriting DETAW v1.0

DETAW v1.0, written in C++ language, was rewritten in Python script in order to make some minor changes to some algorithms, provide more control over input and output, increase efficiency of calculations and storage of interim results, and enable easier future development of code necessary for full implementation of model results. DETAW v1.0 generates separate Comma Separated Values(CSV) output files, including the daily output file, the monthly output file, and the yearly output file for each Delta subarea and each crop category. This results in enormous output for long simulations. In order to reduce the time to run DETAW, the program interface was modified and output was shifted to two Data Storage System (DSS) files, one for daily values and one for monthly values, and each contained data for all 168 subareas and 15 land-use categories.

3.3.2 Updating Seepage Rate Assumptions

Both DICU and DETAW v1.0 assume that seepage available for plants in Delta lowlands is 0.3 inches per foot of crop-rooting depth per month. This value was determined from studies conducted to calibrate soil moisture storage by adjusting the seepage (California Department of Water Resources 1995). But under this seepage rate, the estimated amount of seepage to native and riparian vegetation falls far

below their water requirements. Since these two crop categories do not receive any applied water, seepage is the major water source besides precipitation. DETAW v2.0 assumes that the seepage rate for these two crops increases to 1.8 inches per ft of crop-rooting depth per month, which intends on balancing the water requirements.

3.3.3 Updating Crop Coefficients for Field Crops and Native Vegetation

Crop coefficients are needed as a way to properly adjust the ET_o to more realistically represent actual Delta crop ET. Referring to Anderson et al. (2009), Richard L. Snyder and Morteza N. Orang in 2012 suggested changing the crop coefficients of field and native vegetation. This suggestion was based on lower crop production in the Sacramento-San Joaquin Delta as compared with crop production in the Sacramento Valley. The crop coefficient for field crops was lowered from 1.04 (critical and dry years) and 1.02 (noncritical/dry years) to 0.9. The crop coefficient for native vegetation in DETAW v2.0 was raised from 0.3 to 0.5.

3.3.4 Calibrating Crop Stress Coefficients

The total Delta consumptive use calculated by DETAW v1.0 is approximately 60 percent higher than that calculated by DICU. Such higher consumptive-use estimates will result in much higher net channel depletion estimates and this raises a concern whether all the crop coefficients in DETAW v1.0 were appropriate for the Delta environment. The crop coefficients in DETAW v1.0, based on the Doorenbos and Pruitt (1977) method, were developed to simulate the potential crop ET (ET_c) under the ideal conditions. With consideration of the effect of local conditions and agricultural practices, it is better to adjust the potential ET_c to the actual ET_c, which the hydrodynamic and water quality models need to simulate the historical condition.

In DETAW v1.0, the crop coefficients of each crop category in every year are separated into four growth stages: initial, rapid, mid-season, and late season (Figure 3-3). During the off-season and initial growth stage with less than 10 percent canopy ground cover, the crop coefficient mainly reflects bare soil evaporation. During the mid-season growth stage, the peak crop coefficient of the actual ET_c in DETAW v2.0 (K_c) is reached when the canopy ground cover is above 70–80 percent, which is a time when the interception of radiation by the foliage increases and transpiration, rather than soil evaporation, dominates ET_c. During the rapid-growth period and late-season, crop coefficient is assumed to linearly change between the crop coefficient in the initial growth period and peak crop coefficient. Two sets of crop coefficients are used in DETAW v1.0; one set is used for critical and dry years and one set is used for wetter years.

Potential ET_c is calculated as the product of the ET_o and the crop coefficient for each crop category. Crop coefficient values were determined under standard field conditions without crop stress. The actual ET_c, to some extent, will be lower than the potential ET_c calculated by DETAW v1.0. The actual ET_c is calculated by the product of the potential ET_c and a stress coefficient (K_s) for each crop category. K_c and the actual ET_c are defined below.

$$K_c = K_{co} * K_s \quad (6)$$

$$ET_c = K_s * ET_{co} = K_c * ET_o \quad (7)$$

Where

K_c is the crop coefficient of the actual ET_c in DETAW v2.0,

K_{co} is the original crop coefficient in DETAW v1.0 to calculate the potential ET_c,

K_s is the stress coefficient,

ET_c is the actual ET_c DETAW v2.0 generates,

ET_{co} is the potential ET_c DETAW v1.0 generates, and

ET_o is the reference ET.

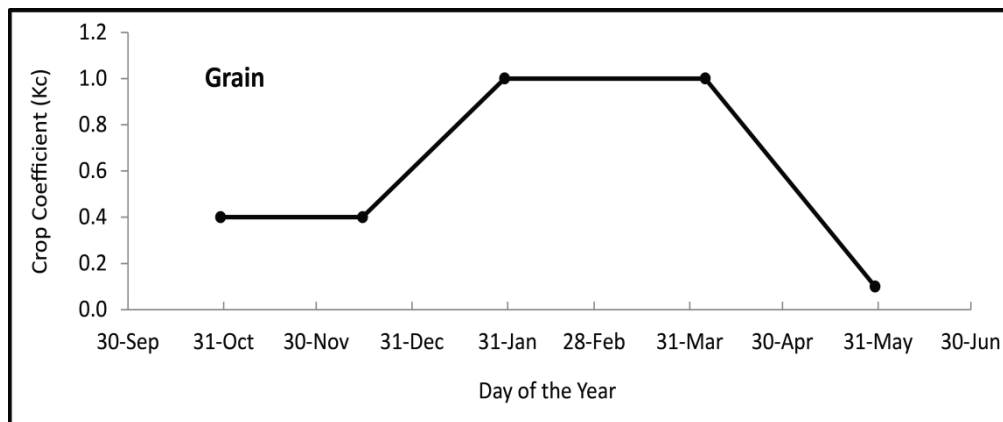


Figure 3-3 Variation in Grain Crop Coefficient (K_c) During A Year

The stress coefficient accounts for factors such as water temperature, air temperature, wind, salinity, soil saturation-reduced root-zone oxygen O₂, and low soil-moisture-induced wilt. Once the stress coefficient is determined, the actual ET_c can be estimated.

Anderson et al (pers. comm. 2010) studied the energy balance and crop coefficient of rice, weeds, and bare soil on Twitchell Island. They found that rice production in the Delta is lower than that in the Sacramento Valley, which is a phenomenon they attributed to the Delta's lower water and air temperatures, compared with those in the Sacramento Valley. But developing Delta stress coefficients for the 15 crop categories, based on field studies, is not possible at this time because of a lack of data. Instead, an approach based on the Surface Energy Balance Algorithm for Land (SEBAL)-based Delta consumptive-use estimates was used.

SEBAL computes a land-surface energy balance and actual ET_c, based on satellite images and weather data. The ET_c in SEBAL equals the "residual" energy flux found by subtracting the soil heat flux and sensible heat flux from the net radiation at the surface. SEBAL has been tested and applied successfully since the 1990s. Bastiaanssen (1998) reports that SEBAL's estimates of consumptive use are within approximately 90 percent of estimates based on field-water models, depending on the scale of study and other factors. When used alongside land use by crop type, SEBAL can provide estimates of monthly net Delta-wide consumptive use and ET_c per crop category.

SEBAL was used to estimate ET_c from March through September, 2007 in order to calibrate crop stress coefficients and from March through September, 2009 in order to validate them. Satellite images for other months, when crop coefficients are lower, are generally obstructed by cloud cover to be of use. Stress coefficients are applied to only peak crop coefficient for each crop category. Crop coefficients during the initial and the late-season stages are unaffected by stress coefficients. Table 3-1 presents the stress coefficients and potential and actual crop coefficients as calibrated for DETAW's 15 crop categories. The stress coefficient of each crop category equals the 2007 SEBAL Delta ET_c divided by

DETAW v1.0-generated Delta ETc. Not all DETAW v1.0-generated ETc values were adjusted through stress coefficients after incorporating SEBAL results. Some did not need an adjustment. As mentioned before, crop coefficient values for native vegetation and urban were determined from field observation and are already indicated as actual ETc. For some crop categories, the total Delta ETc produced by SEBAL and DETAW v1.0 were significantly different, reflecting issues beyond the difference between potential and actual crop coefficients.

Crop Categories	Original potential crop coefficients in DETAW v1.0		Adjusted crop coefficient based on field studies Kco	Calibrated coefficients based on 2004 SEBAL Study	
	Critical, dry years	Non-critical/dry years		Stress coefficient	Updated crop coefficient
	Kco	Kco		Ks	Kc
Alfalfa	1	1	--	0.77	0.77
Dry grain	0.9	0.9	--	1.00	0.9
Field	1.04	1.02	0.9	1.00	0.9
Grain	1.1	1.1	--	1.00	1.1
Native vegetation	0.3	0.3	0.5	1.00	0.5
Orchard	1.05	1.04	--	0.71	0.75
Pasture	0.95	0.95	--	0.79	0.75
Rice	1.05	1.05	--	0.76	0.8
Riparian vegetation	1	0.97	--	0.85	0.85
Sugar beets	1.15	1.15	--	0.70	0.8
Tomato	1.1	1.1	--	0.64	0.7
Truck	1.01	1	--	0.59	0.6
Urban	0.35	0.35	--	1.00	0.35
Vineyard	0.8	0.8	--	0.56	0.45
Water	1.1	1.1	--	1.00	1.1

Table 3-1 Stress Coefficients and Adjusted Peak Crop Coefficients Generated from SEBAL Analysis

Notes: DETAW = Delta Evapotranspiration of Applied Water Model, Kc = crop coefficient of the actual ETc in DETAW v2.0, Kco = original crop coefficient in DETAW v1.0 to calculate the potential ETc, Ks = stress coefficient, SEBAL = Surface Energy Balance Algorithm for Land

Table 3-2 and Figure 3-4 show the estimates of total Delta consumptive use in 2007 from SEBAL, DETAW v1.0, and DETAW v2.0 with calibrated crop stress coefficients. The total Delta consumptive use (DCU) from March through September, 2007 calibrated by using DETAW v2.0, is within 2 percent of that by SEBAL. But the total DCU of these two models in June, 2007 differs by 94 thousand acre-feet (TAF), which is approximately 30 percent of the DCU. Generally, the yearly highest consumptive use occurs in July, which indicates SEBAL's DCU in June is suspect. Monthly ETc by SEBAL is based on two or three satellite images each month, and the samples from June, 2007 possibly caught non-representative conditions at the beginning or the end of the month. The total DCU during several months should be more meaningful. Davids Engineering produced the 2007 actual ETc estimates by using SEBAL. After a meeting with Davids Engineering in 2012, DETAW v1.0 and v2.0 developers agreed on considering

cumulative values to calibrate stress coefficients for DETAW v2.0 based on SEBAL. Bastiaanssen(1998) also reported that the accuracy of SEBAL depended on the areal and time scales. For these reasons, stress coefficients were calibrated based on the summation of ET_C values during March through September, 2007.

Month	DICU	DETAW v1.0	DETAW v2.0	SEBAL
March	89	167	163	123
April	143	221	210	134
May	174	254	223	229
June	243	316	274	368
July	256	358	312	296
August	193	331	292	285
September	102	216	193	209
Total	1,200	1,862	1,667	1,644
Rate to DICU	100%	155%	139%	137%

**Table 3-2 Total Delta Consumptive Use from March through September 2007 (TAF)
by DICU, DETAW v1.0, DETAW v2.0, and SEBAL**

Notes: DETAW = Delta Evapotranspiration of Applied Water Model, DICU = Delta Island Consumptive Use Model, SEBAL = Surface Energy Balance Algorithm for Land

Numbers are in thousand acre-feet (TAF).

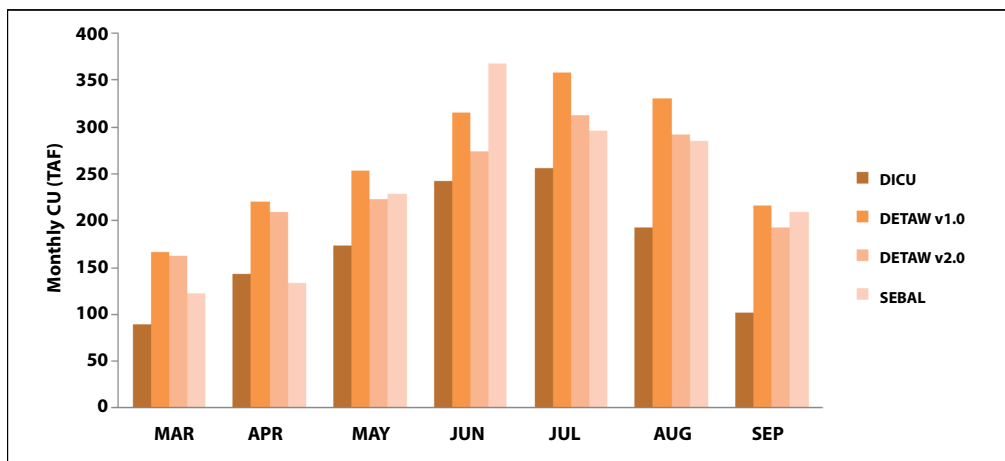


Figure 3-4 The Total Delta Consumptive Use in 2007 by Four Models

Notes: CU = consumptive use, DETAW = Delta Evapotranspiration of Applied Water Model, DICU = Delta Island Consumptive Use Model, SEBAL = Surface Energy Balance Algorithm for Land, TAF = thousand acre-feet

By using the calibrated set of stress coefficients, DETAW v2.0 was validated by comparing ETc to SEBAL-generated ETc for 2009. Table 3-3 and Figure 3-5 show a 3 percent difference in ETc between the two models from March through September 2009, which is a similar amount to that in the 2007 calibration. Moreover, the ETc of each month in 2009, calibrated by DETAW v2.0 and SEBAL, matches the SEBAL monthly consumptive use better than in the 2007 calibration. Compared with the consumptive use difference between DETAW v2.0 and SEBAL in June 2007, the difference for each month in 2009 seems much slighter. DETAW v2.0 simulates the trend and magnitude of the actual ETc for the Delta as a whole reasonably well.

Month	DICU	DETAW v1.0	DETAW v2.0	SEBAL
March	101	158	154	167
April	115	205	191	185
May	156	277	245	263
June	220	314	272	266
July	264	366	315	292
August	186	321	280	264
September	107	245	218	211
Total	1,149	1,886	1,675	1,648
Rate to DICU	100%	164%	146%	143%

Table 3-3 The Total Delta Consumptive Use from March through September 2009

Notes: DICU = Delta Island Consumptive Use Model, DETAW = Delta Evapotranspiration of Applied Water Model, SEBAL = Surface Energy Balance Algorithm for Land

Numbers are in thousand acre-feet (TAF).

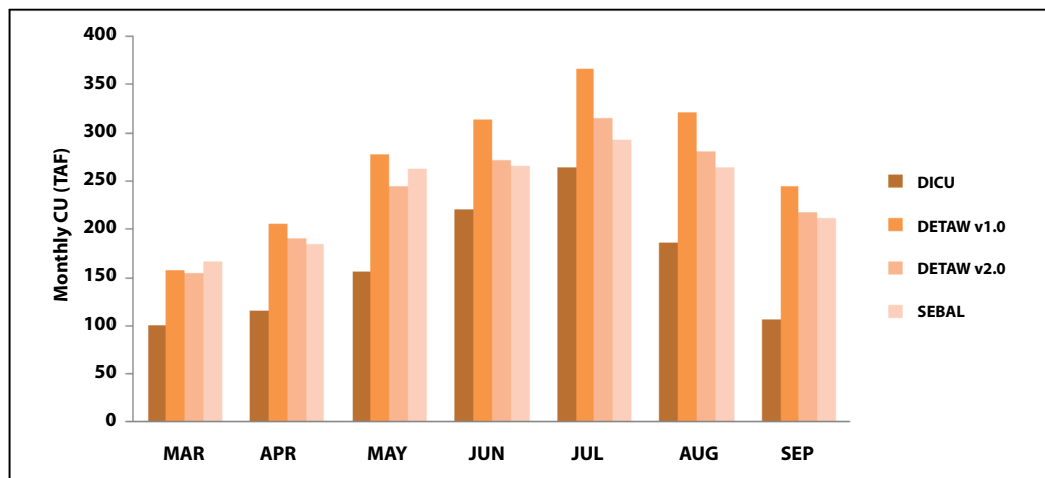


Figure 3-5 Total Delta Consumptive Use in 2009 by Four Models

Notes: CU = consumptive use, DICU = Delta Island Consumptive Use Model, DETAW = Delta Evapotranspiration of Applied Water Model, SEBAL = Surface Energy Balance Algorithm for Land
TAF = thousand acre-feet

3.3.5 Estimating Net Channel Depletion for DETAW v2.0

DETAW v1.0 only considers water demands and supplies in tracking the ground surface-water balance (i.e., the root-zone water balance — the water balance on the top layer of the ground). But some activities related to Delta islands, while not directly satisfying crop water needs, affect the water transfer between channels and Delta islands and influence the river hydrodynamics, water quality, and salinity intrusion in the Delta. These factors include excess applied water associated with irrigation efficiency, island runoff, drained seepage, and diversion and drainage of leach water. Although these water activities do not affect the ground surface-water balance, they need to be accounted for in modeling Delta conditions. The methodology used in DICU has been mostly adopted to do this for DETAW v2.0.

An important component missing in the current modeling of Delta conditions is the role of groundwater as a source for recharging soil moisture and as a sink for deep percolation. Field studies within Delta lowlands are needed to help understand this complex issue. Work is currently underway in the DWR Delta Modeling Support Branch to enable better modeling of subsurface water in the Delta. Future work is expected to generate similar consumptive-use estimates to those estimated by DETAW v2.0, but net channel-depletion estimates could significantly change at times to better reflect the understanding of how subsurface water is involved with the hydrology of the Delta.

Figure 3-1 shows the components of net channel depletion and Equations 1–5 present how net channel depletion is conceptually calculated. Crop consumptive use is the driving force behind estimating applied irrigation water, but several key components of net channel depletion have to be assumed. These components are seepage rate and proportion that is drained for lowlands, soil-moisture limits and crop-rooting depths, precipitation spatial distribution and timing of runoff and proportion that is lost to deep percolation, timing and amount of leaching diversions and drainages, and irrigation efficiency. Together, these assumptions, along with estimated consumptive use, determine the timing and amount of water diverted to Delta islands through applied water and seepage and the water that is drained to adjacent Delta channels.

For a given DETAW v2.0 subarea, once the amount of applied irrigation water is estimated, total diversion from channels and total drainage can be calculated and the resulting net channel depletion is known. The sequence of calculations includes:

1. Finding the amount of crop water needs on subarea (consumptive use).
2. Finding the amount of current day seepage available to meet water demand.
3. Finding the amount of precipitation available to meet water demand.
4. Finding the amount of soil moisture contributing to water demand.
5. Finding the amount of applied irrigation water needed.
6. Finding the total amount of irrigation water diverted from channels.
7. Finding the total amount of water drained to channels.

The actual calculations are shown in Equations 8–11.

$$\text{DIV} = I_{AN} / \eta + LW_A \quad (8)$$

$$\text{RET} = RO + (1 - \eta) * I_{AN} / \eta + LW_D + S_D \quad (9)$$

$$S = S_E + S_D \text{ (lowlands)} \quad (10)$$

$$RO = (1 - DP) * (PPT - PPT_E) \quad (11)$$

Where

DIV is the total diversion;

LW_A is the applied leach water;

S is the total seepages;

S_E is the effective seepage;

S_D is the drained seepage;

RET is the return flows;

RO is the surface runoff;

I_{AN} is the amount of irrigated applied water needed by crops as calculated by DETAW v2.0,

PPT is the precipitation,

PPT_E is the effective precipitation, the amount that is used to replenish the soil moisture,

DP is the deep percolation rate, assumed to be 0.25. This is a new term in DETAW v2.0, and

η is the irrigation efficiency factor and is assumed to be 0.7 for the majority of islands.

DETAW v2.0 adopts the same practice as in DAYFLOW of distributing precipitation during four days, starting on the first day of rainfall. It adopts the same drained seepage rates as are used in DICU (California Department of Water Resources 1995) and assigns the same amount as DICU of leach-applied water and leach-drained water.

After the irrigation, drainage, and seepage of each subarea in the Delta are estimated, DETAW v2.0 then inherits the same Delta Simulation Model 2 (DSM2) node allocation factors as in DICU in order to distribute the subarea values into DSM2 node values.

3.4 Data Input for DETAW v2.0

Input data to DETAW v2.0 includes land use, plant-rooting depths, seepage rates, soil-moisture limits, irrigation season, precipitation, DSM2 node allocation factors for diversions and drainages, lowlands leaching volumes and monthly schedule, and irrigation efficiency. Most input structures were borrowed from those used in DETAW v1.0 and DICU; some were modified for DETAW v2.0. These inputs are the annual land use for 168 subareas, the daily precipitation at seven stations, specified in section 3.4.2, on the periphery of the Delta, and daily maximum and minimum temperature at Lodi.

3.4.1 Land Use

DETAW v2.0 will be used for both historical and projected simulations of Delta hydrodynamic and water quality conditions. Projections use two sets of land use; one set is used for the wet and normal years and the other set is used for dry and critical dry years. These are based on past Delta land surveys done in 1976 and the 1980s. Historical simulations are based as much as possible on actual land-use surveys. As in DETAW v1.0, DETAW v2.0 also depicts the Delta as having 168 subareas. Acreage of each subarea is assigned as much as 15 crop categories and land-use identifiers (Table 3-4).

Land-use data for the 15 land-use categories by subarea for Water Years 1922–2003 were developed for DETAW v1.0 by the DWR Bay-Delta Office Modeling Support Branch. In 2007, crop acreages for each of the 168 subareas were developed based on land surveys placed in GIS format. Land use from 2004 through 2007 was assumed to be the same as that based on the 2007 survey. Land use in 2008 was estimated by averaging the data from 2007 and 2009. From 2009 through 2015, DETAW v2.0 land-use

	Crop Category	Land-Use Identifier
1	Urban	UR
2	Pasture	PA
3	Alfalfa	AL
4	Field crops	FI
5	Sugar beets	SB
6	Grain	GR
7	Rice	RI
8	Trucks	TR
9	Tomatoes	TO
10	Orchards	OR
11	Vineyards	VI
12	Riparian vegetation	RV
13	Native vegetation	NV
14	Non-irrigated grain	DGR
15	Water surfaces	WS

Table 3-4 DETAW v2.0 Crop Categories and Land-Use Identifiers

Note: DETAW = Delta Evapotranspiration of Applied Water Model

acreage was based on data from United States Department of Agriculture, National Agricultural Statistics Service.

3.4.2 Precipitation

Precipitation data is retrieved from the California weather database maintained by the Statewide Integrated Pest Management Program at University of California (UC IPM). This database includes data from CIMIS and the National Climatic Data Center (NCDC), which is part of the National Oceanic and Atmospheric Administration (NOAA). Generally, DETAW uses NOAA data. If national climate data is not available, CIMIS data is substituted.

The precipitation data comes from seven NOAA cooperative observer stations: Brentwood, Davis, Galt, Lodi, Rio Vista, Stockton, and Tracy. Currently, NOAA only provides the precipitation data at the Davis, Lodi, Stockton, and Tracy stations. Data for recent years are missing at the other three stations. Correlations to other stations for DETAW v1.0 were developed to estimate precipitation at Brentwood, Galt, and Rio Vista. These are listed in Equations 12, 13, and 14.

$$\text{PPT at Brentwood} = 1.37 * (\text{PPT at Tracy}) \quad (12)$$

$$\text{PPT at Galt} = 1.01 * \text{PPT at Lodi} \quad (13)$$

$$\text{PPT at Rio Vista} = 0.98 * \text{PPT at Davis} \quad (14)$$

3.4.3 Air Temperature

The air temperature data is downloaded from UC IPM. The daily air temperature at Lodi is the required temperature input for DETAW v2.0. UC IPM collects temperature from two Lodi stations, LODI.C from NCDC and LODI_WEST.A from CIMIS. DETAW v2.0 gives priority to LODI.C as the source since all the precipitation data in DETAW v2.0 comes from NCDC. Data from LODI_WEST.A are used in case of missing data or errors.

3.5 DETAW v2.0 Results as Compared with DETAW v1.0, DICU, and DAYFLOW

DETAW v2.0 has been applied for historical Water Years 1975–2010 in order to compare results with those computed by DICU and DAYFLOW. From the perspective of modeling Delta water quality, simulated net channel depletion, which incorporate assumptions of the sources of water to meet Delta consumptive use demands, are directly related to estimated Delta outflow and accompanying salinity intrusion. And so, average monthly Delta-wide net channel depletion, distribution of monthly Delta-wide net channel depletion, and distribution of monthly Delta outflow are presented from the three models.

3.5.1 Delta Net Channel Depletion

DETAW v2.0 generates the applied water, drainage, and seepage of each subarea and then assigns flows to DSM2 nodes. The net channel depletion reflects the water transfer between channels and islands and can be found through combining applied water, drainage, and seepage (Equation 15).

$$\text{Net channel depletion} = \text{applied water} + \text{seepage} - \text{drainage} \quad (15)$$

Delta-wide net channel depletion can be found by adding all the net channel depletion assigned to DSM2 nodes. Since DICU estimates the monthly irrigation, drainage, and seepage of DSM2 nodes, the monthly Delta net channel depletion can be calculated by using the same method as DETAW v2.0.

DAYFLOW provides estimates of net channel depletion, which equals the gross channel depletion plus miscellaneous water transfers minus Delta precipitation runoff. The same daily gross channel depletion is used for all water years. Miscellaneous water transfers are those diversions or transfers other than gross channel depletion, precipitation, and exports.

The averages of the monthly Delta net channel depletion for WYs 1975–2010 by DAYFLOW, DICU, and DETAW v2.0 are shown in Figure 3-6. The years are chosen because DSM2 historical simulation is available for these years. The monthly Delta net channel depletion calculated by DETAW v2.0 is generally several hundred cubic feet per second (cfs) higher than that by the other two models for most months, except the winter months. Delta net channel depletion calculated by DETAW v2.0 is based on

the SEBAL-calibrated crop ET. If the original crop ET calculated by DETAW v1.0 is applied, the net Delta net channel depletion would be increased by another several hundred cfs. The relatively large difference between DETAW v2.0 and DAYFLOW calculations exist during February–May, while that difference between DETAW v2.0 and DICU calculations exists for almost all the irrigation season, March–September.

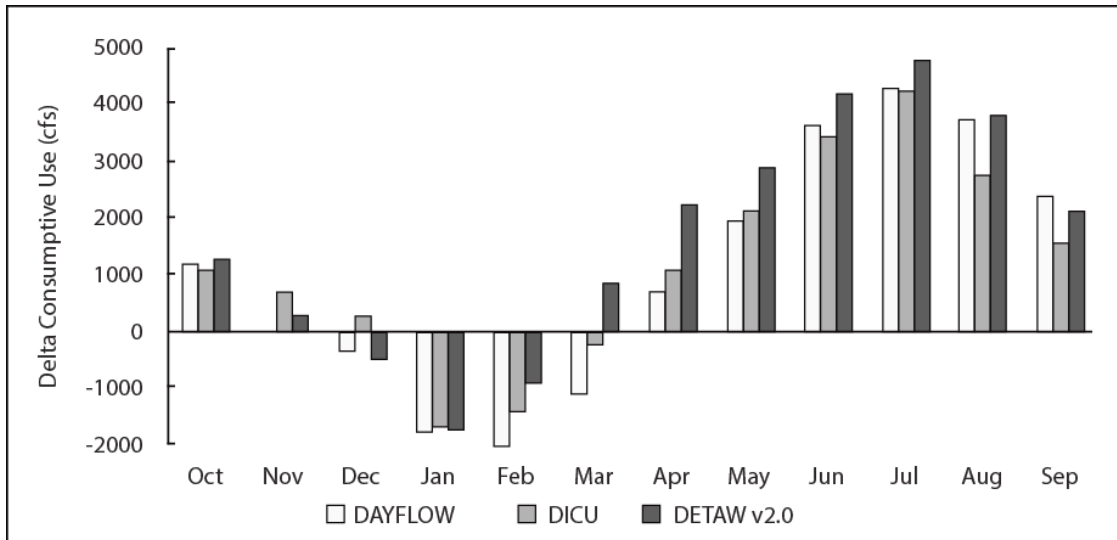


Figure 3-6 Average Delta Net Channel Depletion for WYs 1975–2010 as Modeled by DAYFLOW, DICU, and DETAW v2.0

Notes: cfs = cubic feet per second, DAYFLOW = program designed to estimate daily average Delta outflow, DICU = Delta Island Consumptive Use Model, DETAW = Delta Evapotranspiration of Applied Water Year, WY = water year

Figure 3-7 presents distributions of monthly net channel depletion for the same period through box-and-whisker plots. During the winter and spring months, the monthly Delta net channel depletion can vary widely because of the variability in precipitation. During the summer and fall, Delta net channel depletion is fairly consistent because of the relatively consistent ETc. DETAW v2.0 generally generates higher Delta net channel depletion than the other two models. Figure 3-7 shows that the variation in each month of DETAW v2.0 is similar to that of DAYFLOW, especially in November, December, May, and June.

3.5.2 Net Delta Outflow

Net Delta Outflow (NDO) is computed by using Equation 16.

$$\text{NDO} = \text{Delta inflows} - \text{Delta exports} - \text{Delta net channel depletion} \quad (16)$$

Delta inflows and exports from DAYFLOW have been assumed in order to compare calculated NDO from DAYFLOW, DICU, and DETAW v2.0. The differences in NDO between any two models of DICU and DETAW v2.0 and DAYFLOW are the same as the differences in Delta net channel depletion. Since DETAW v2.0 estimates summer net channel depletion to be several hundred cfs higher than for DAYFLOW and DICU, NDO under DETAW v2.0 is lower by the same amount compared with the NDO under DAYFLOW and DICU.

Figure 3-8 shows the distribution of monthly Delta outflows for WYs 1975–2010 falling below 25,000 cfs. The magnitude and duration of lower Delta outflow indicate the potential for significant yearly salinity

intrusion into the Delta in late summer and fall. Figure 3-9 shows the average Delta outflow during July–October for WYs October, 1975–September, 2010. These months usually have the lowest average Delta outflow during any year. Average outflow under DETAW v2.0 is lower than both DAYFLOW- and DICU-assumed net channel depletion, particularly in July and August.

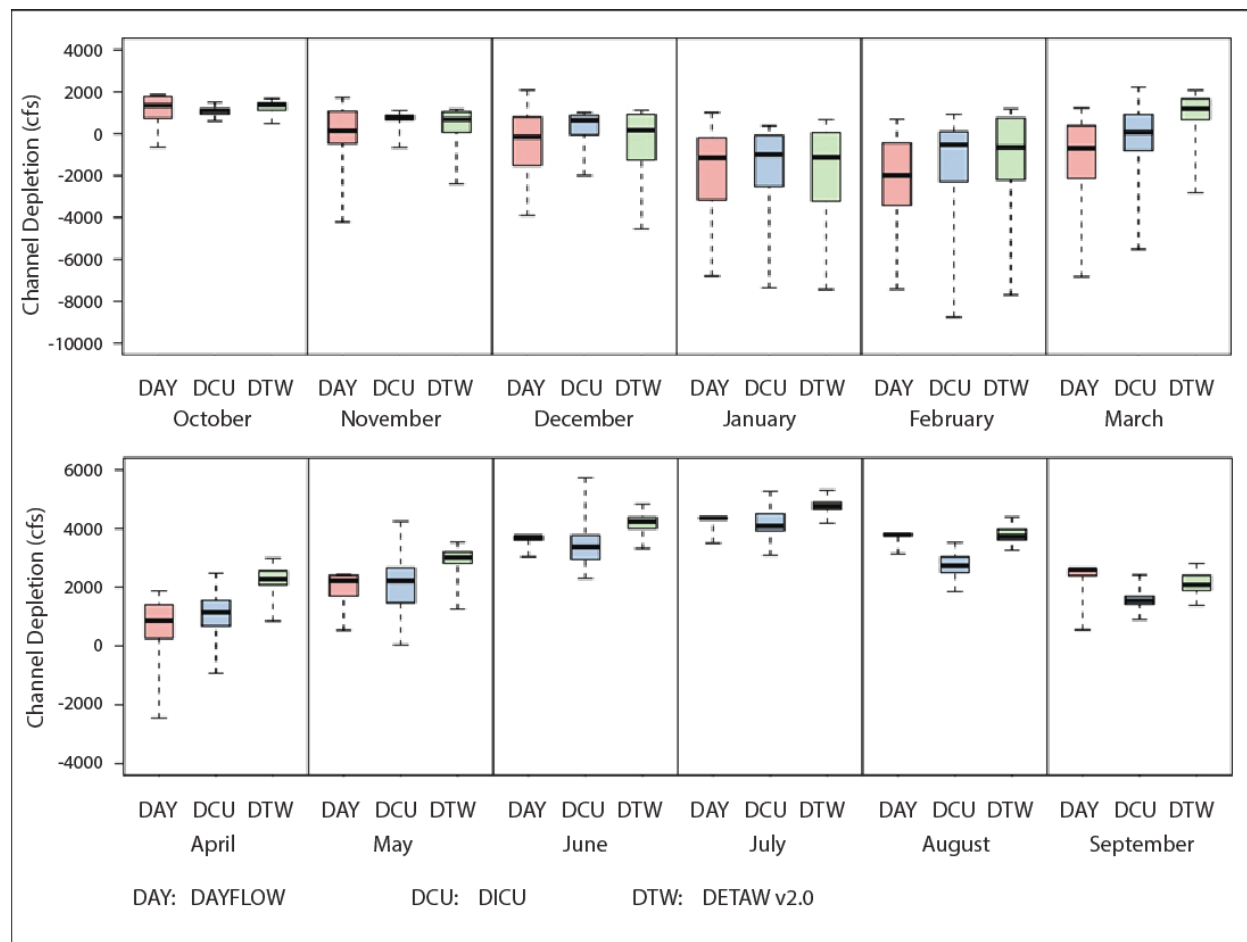


Figure 3-7 The Distribution of Monthly Delta Net Channel Depletion for WYs 1975–2010

Notes: cfs = cubic feet per second, DAYFLOW = program designed to estimate daily average Delta outflow, DETAW = Delta Evapotranspiration of Applied Water Model, DICU = Delta Island Consumptive Use Model, WY = water year

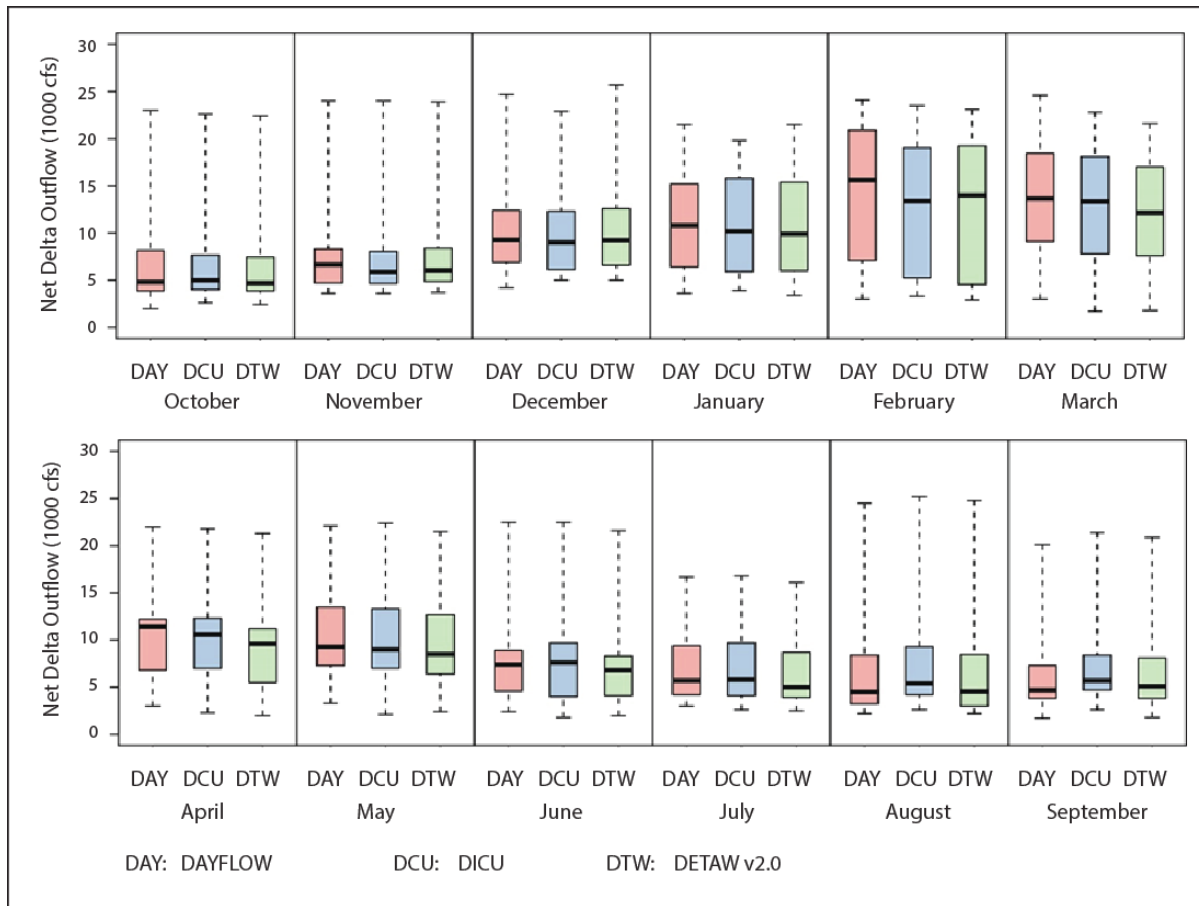


Figure 3-8 Distribution of Monthly Delta Outflows of Less Than 2,500 cfs for WYs 1975–2010

Notes: cfs = cubic feet per second, DAYFLOW = program designed to estimate daily average Delta outflow, DETAQ = Delta Evapotranspiration of Applied Water Model, DICU = Delta Island Consumptive Use Model, WY = water year

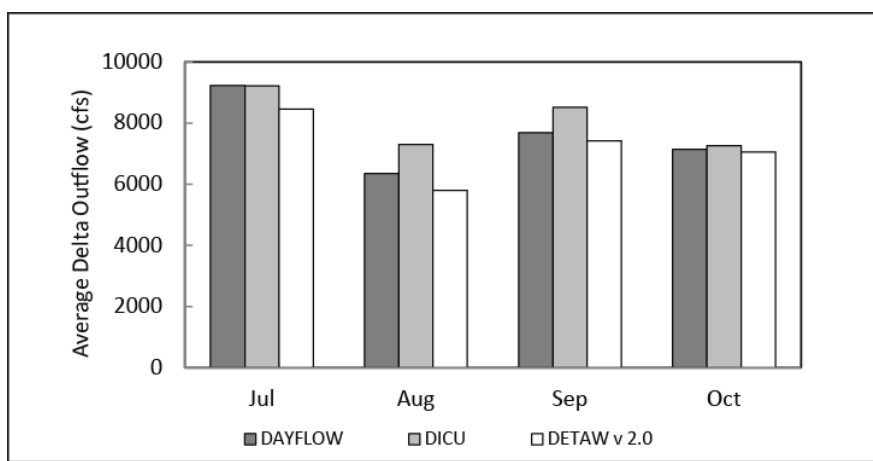


Figure 3-9 Monthly Average Delta Outflow During July–October, WYs 1975–2010

Notes: cfs = cubic feet per second, DAYFLOW = program designed to estimate daily average Delta outflow, DETAQ = Delta Evapotranspiration of Applied Water Model, DICU = Delta Island Consumptive Use Model, WY = water year

3.5.3 Simulation of Delta Electrical Conductivity with DSM2

Estimates of Delta consumptive use, net channel depletion, and island drainage affect simulated Delta salinity in two ways. First, as indicated above, estimates of Delta net channel depletion directly affect estimates of Delta outflow. Current understanding of historical Delta outflow is based partly on the consumptive use reported by DAYFLOW. State Water Resources Control Board Decision D-1641 relies on the Net Delta Outflow Index as determined by DAYFLOW, which includes net Delta consumptive use as part of its calculations. Observed electrical conductivity (EC) in the Carquinez Strait at Martinez (DSM2's downstream boundary) is understood to be related to DAYFLOW-based Delta outflow estimates. Yet, the water quality module of the current version of DSM2 was calibrated based on DICU-derived net channel depletion. Computing DSM2 historical simulations under different net channel depletion estimates (i.e., DICU and DETAW v2.0) will result in different salinity intrusion scenarios. This will affect modeled EC in the west and central Delta and up Old River toward project export locations.

In addition, in areas of relatively low circulation, such as the south Delta when temporary barriers are installed, simulated island diversions and drainage — the magnitude of total applied water and the amount, timing, and water quality of drainage — can strongly affect simulated water quality in local channels.

DSM2 simulations with DICU-based net channel depletion show a pattern of somewhat overestimating EC in the summer and underestimating EC in the winter. A DWR report (Thein and Nader-Tehrani 2006) about a DSM2-DICU simulation of historical 1975–1989 conditions found that large discrepancies between observed and DSM2-simulated EC occurred during the summer of very dry years when the estimated net Delta outflow was particularly low. Overall, the calibration of DICU-based DSM2 resulted in the latest released version of DSM2, which performs well in most years.

The accuracy of localized modeling of the water quality impacts, because of nearby diversions and drainage, is limited to the extent that relevant information is known. Hundreds of pumps are located in the Delta that irrigate and drain the islands. Actual pumping rates are unknown. Unmeasurable seepage is continual all along channel banks. A fairly extensive drainage water quality sampling study was conducted by DWR's Municipal Water Quality Investigations section in the 1990s, but the variation found in the data, both spatially and temporally, prevented insightful interpretation; instead, data were averaged to generate a table of monthly agricultural drainage EC for each of three Delta regions (Jung and Associates 2000). These values repeat for all years.

In order to show how DETAW v2.0 affects simulated EC, historical Delta conditions of 1990–2009 were simulated by using net channel depletion and island drainage based on DICU and DETAW v2.0. Delta inflows and exports and the EC boundary at Martinez were identical in the two simulations, but because net channel depletions differed, Delta outflow also differed. The current version of DSM2's water quality module was calibrated and verified by using DICU-generated net channel depletion. Accordingly, DICU-based DSM2 simulations are expected to match observed EC better than DETAW-based calculations, with respect to salt intrusion from the west Delta boundary.

As shown in Figures 3-10–3-13, Delta outflow by using DETAW v2.0 can be 1,000 cfs less than by using DICU during the time of year when EC is highest, which is late summer and fall. This reduction can cause significant additional salinity intrusion in the DSM2 simulation and lead to significant overestimation of EC. This happened in 1992, 1994, 2001, 2002, 2008, and 2009. However, at other times, large decreases in Delta outflow, caused by using DETAW v2.0 instead of DICU, results in little change in EC at Antioch, Jersey Point, and Emmaton. Figure 3-14 shows the sensitivity of salinity to Delta outflow at Antioch, Jersey Point, and Emmaton, as indicated by DSM2 simulations. At monthly average Delta outflows of less than approximately 6,000 cfs, salinity sharply increases for even small decreases in outflow. This can

be inferred that DETAW v2.0-based net channel depletion and also Delta outflow in DSM2 simulations of historical conditions increases the incidents of low outflow and higher EC at all three locations. That is, DSM2 simulations of Delta conditions under DETAW v2.0 result in an increase in the occasions when simulated EC in the west Delta is highly sensitive to outflow.

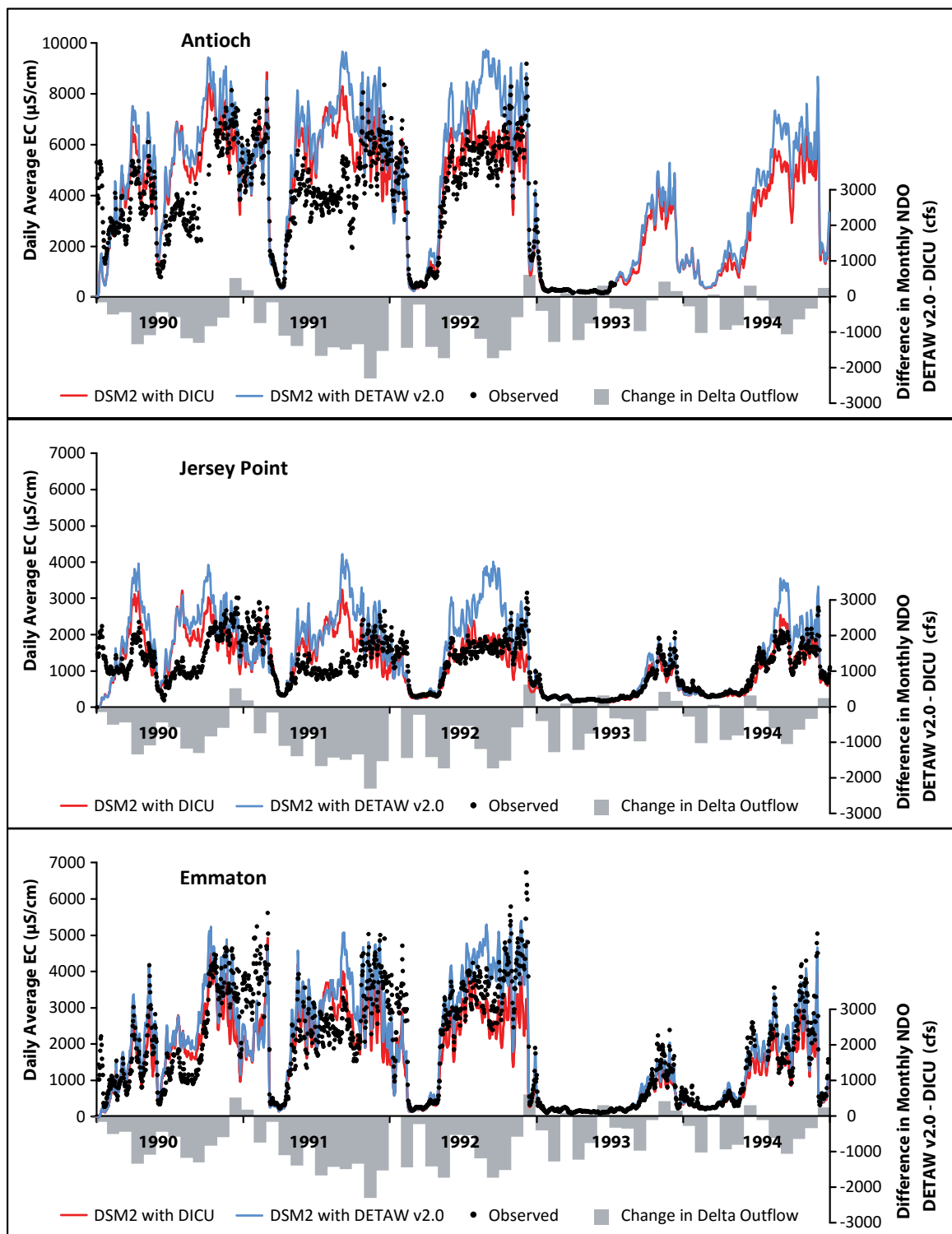


Figure 3-10 DSM2 Simulation of Historical EC under DICU and DETAW v2.0 Compared with Observed EC, 1990–1994

Notes: $\mu\text{S}/\text{cm}$ = microSiemens per centimeter, cfs = cubic feet per second, DETAW = Delta Evapotranspiration of Applied Water Model, DICU = Delta Island Consumptive Use Model, DSM2 = Delta Simulation Model 2, EC = electrical conductivity, NDO = Net Delta Outflow

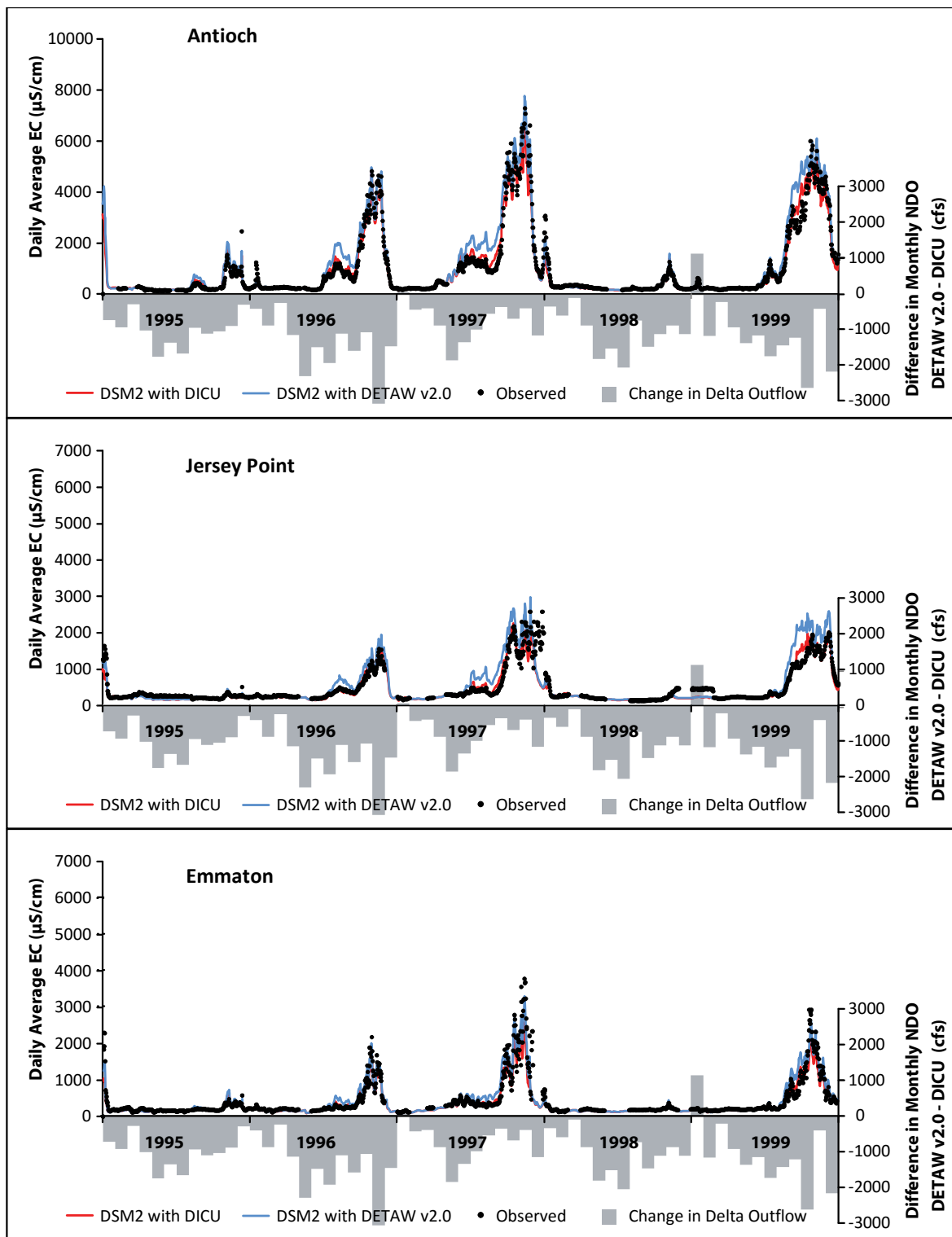


Figure 3-11 DSM2 Simulation of Historical EC under DICU and DETAW v2.0 Compared with Observed EC, 1995–1999

Notes: $\mu\text{S}/\text{cm}$ = microSiemens per centimeter, cfs = cubic feet per second, DETAW = Delta Evapotranspiration of Applied Water Model, DICU = Delta Island Consumptive Use Model, DSM2 = Delta Simulation Model 2, EC = electrical conductivity, NDO = Net Delta Outflow

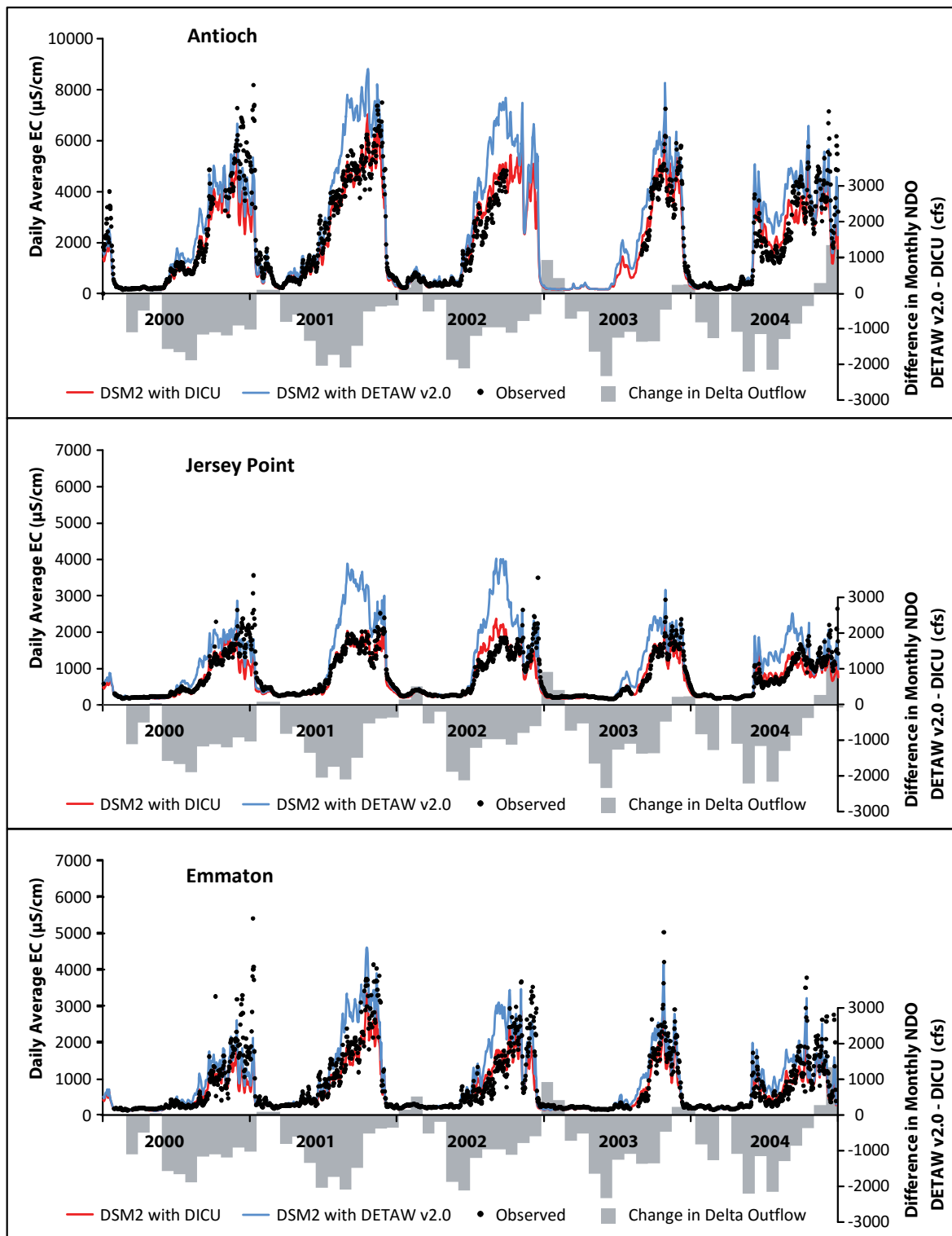


Figure 3-62 DSM2 Simulation of Historical EC under DICU and DETAW v2.0 Compared with Observed EC, 2000–2004

Notes: $\mu\text{S}/\text{cm}$ = microSiemens per centimeter, cfs = cubic feet per second, DETAW = Delta Evapotranspiration of Applied Water Model, DICU = Delta Island Consumptive Use Model, DSM2 = Delta Simulation Model 2, EC = electrical conductivity, NDO = Net Delta Outflow

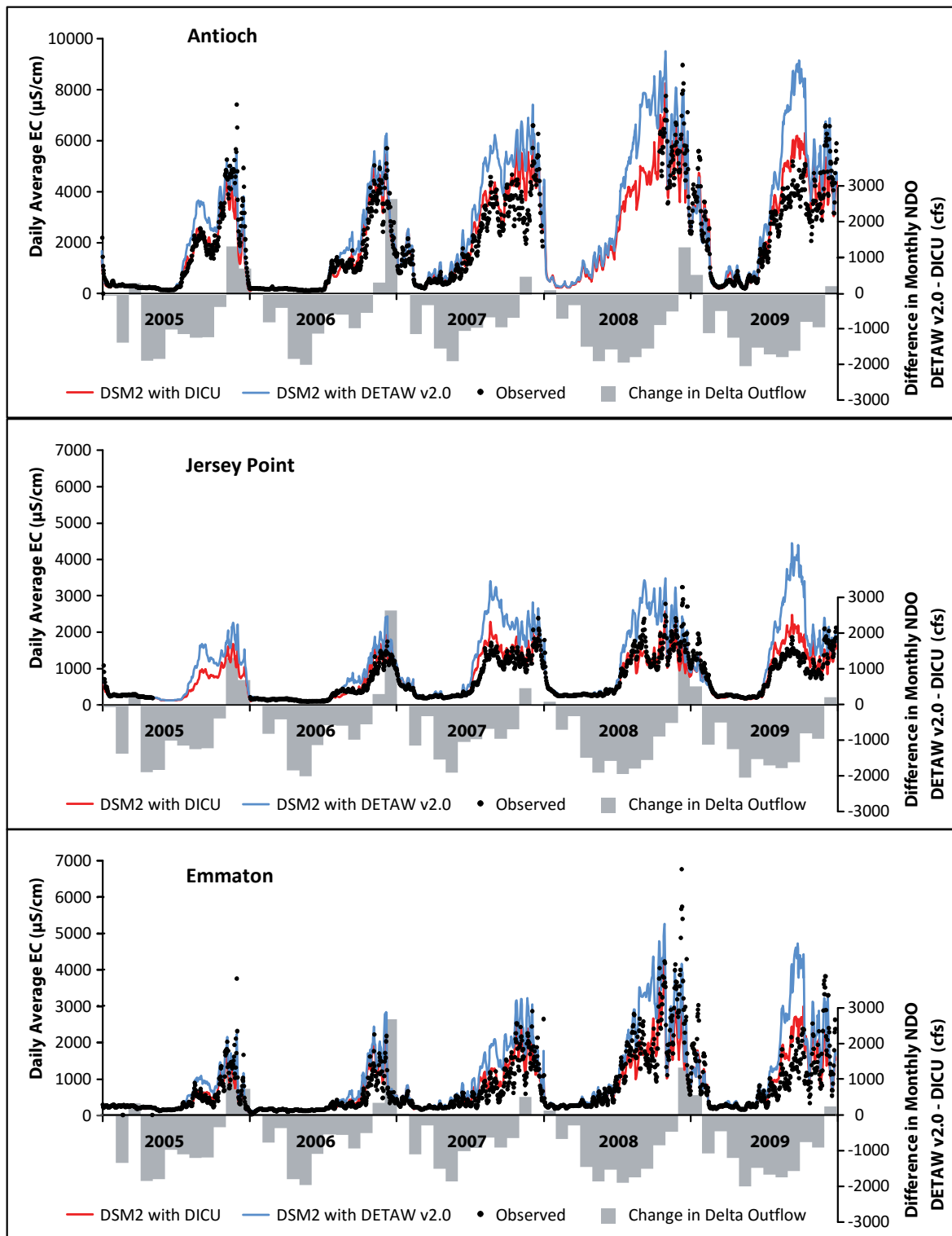


Figure 3-13 DSM2 Simulation of Historical EC under DICU and DETAW v2.0 Compared with Observed EC, 2004–2009

Notes: $\mu\text{S}/\text{cm}$ = microSiemens per centimeter, cfs = cubic feet per second, DETAW = Delta Evapotranspiration of Applied Water Model, DICU = Delta Island Consumptive Use Model, DSM2 = Delta Simulation Model 2, EC = electrical conductivity, NDO = Net Delta Outflow

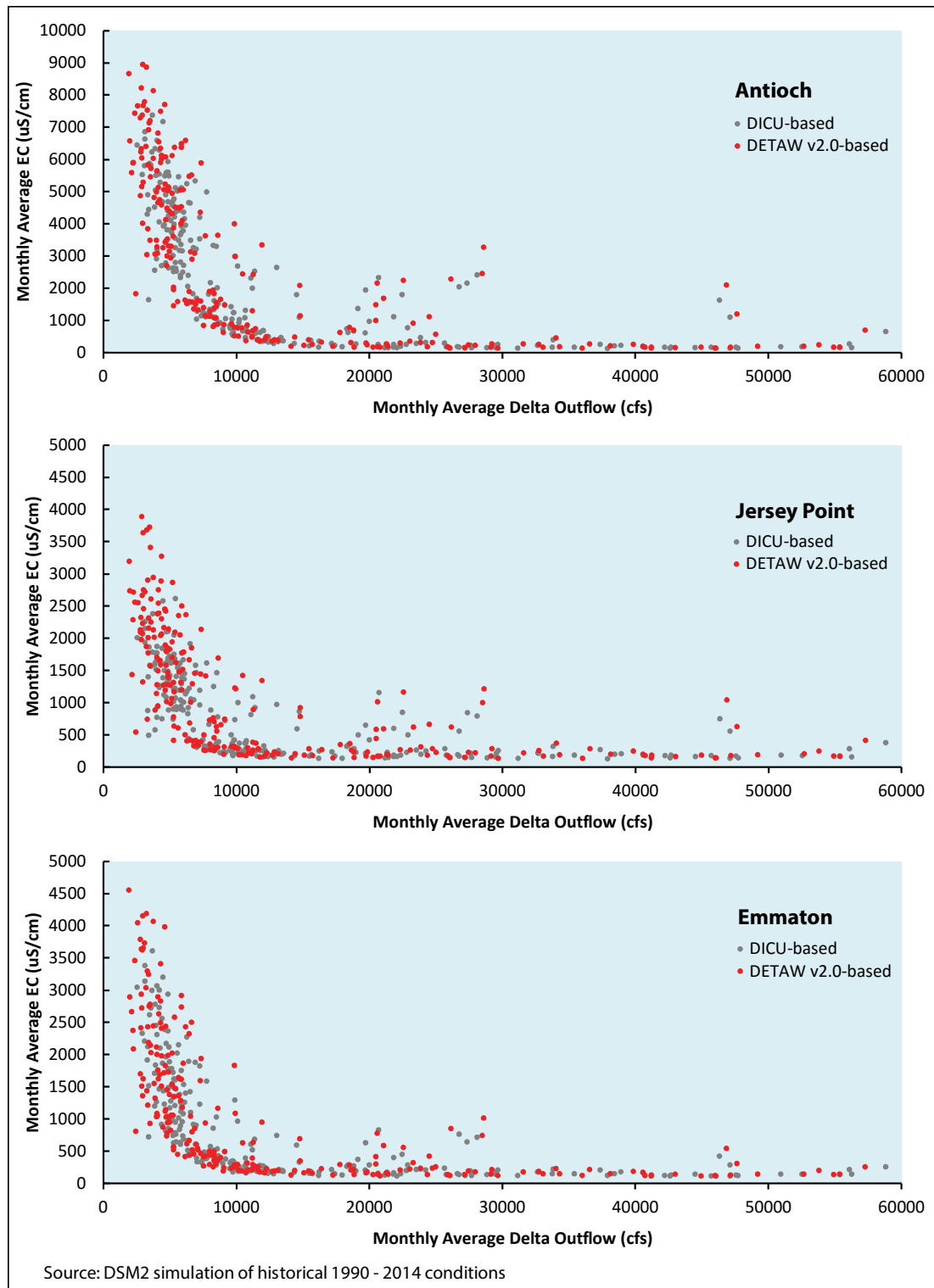


Figure 3-14 DSM2-Simulated EC and Delta Outflow under DICU and DETAW v2.0 for Historical 1990–2014 Conditions

Notes: $\mu\text{S}/\text{cm}$ = microSiemens per centimeter, cfs = cubic feet per second, DETAW = Delta Evapotranspiration of Applied Water Model, DICU = Delta Island Consumptive Use Model, DSM2 = Delta Simulation Model 2, EC = electrical conductivity

3.6 Conclusion

DETAW v2.0 code has been developed to link a ground surface-water balance model to DSM2 and other surface-water models. A method for employing crop-consumed water (consumptive use) in estimating the amount of water transferred between Delta islands and channels has been built and a preliminary model output has been analyzed. The analysis concludes that a recalibration of QUAL, the water quality module of DSM2, and DETAW v2.0 are required.

Many factors need to be considered in a DETAW v2.0 calibration, because net channel depletion is determined by crop ET, leach water, seepage, applied water, irrigation efficiency, and so on. Since the Delta crop ET has been calibrated with SEBAL data, the crop-consumed water should be reliable enough for further application.

A challenge to calibrating the net channel depletion model is the unmeasurable or unknown agricultural activities, which do not relate to the water to satisfy crop ET, but affect the movement of water from channels to islands and from islands back into channels.

The processes of leaching, seepage, irrigation efficiencies, and deep percolation vary spatially and temporally. Investigations are needed to determine how to represent these dynamic processes in the model and how to calibrate the parameters. For example, deep percolation in this model has been simplified as part of precipitation that does not supply the crop ET. It might be more reasonable to consider it in the calculation of the root-zone water balance.

Some of the unknowns have not been included in the model, such as island drainage required, because of subsidence in the lowlands. On some islands, groundwater levels can be above the ground surface and farmers need to continuously drain water to maintain the groundwater levels that are deep enough for crops to grow.

Since many unknowns exist in DETAW v2.0, it is difficult to calibrate the model, itself. As pointed out above, simulated EC can be very sensitive to Delta outflow and accordingly net channel depletion. EC could be taken as an indicator to simultaneously calibrate both DETAW v2.0 and DSM2.

For example, both DETAW v2.0 and DSM2 could be calibrated to observed EC in the west Delta. Delta surface water is a comprehensive system. The internal water movement in the system includes the water balance in root zones, the water transfer between root zones and channels, and the hydrodynamics and the transport of salinity or other substances in channels. If all the components can be simulated reasonably well for a long period, the major movement of water in the system should be captured by DETAW v2.0 and DSM2. The Sacramento-San Joaquin River confluence area is the key region where Delta outflow and salinity intrusion are highly correlated. If EC in this region is simulated rationally, the estimated total Delta net channel depletion should be meaningful.

Once DETAW v2.0 and DSM2 at the confluence area have been calibrated, calibrating DSM2 upstream of the confluence area is the next step. This seems more complicated and might include both calibrating DSM2 for the whole Delta and modifying the assumptions of the distribution and water quality of island drainages.

3.7 References Cited

Anderson, FE, Detto M, Verfaille J, Baldocchi D, Snyder RL. 2009. "Variations in the surface energy balance for rice grown in the Sacramento-San Joaquin Delta and the Sacramento Valley." Poster sent to Lan Liang.

Bastiaanssen WGM et al. 1998. "A remote sensing surface energy balance algorithm for land (SEBAL) 2. validation." Journal of Hydrology. pp. 213-229. [Journal article].

California Department of Water Resources. 1995. *Estimation of Delta island diversion and return flows*. Sacramento (CA): Division of Planning. 144 pp. Viewed online at:
http://www.calwater.ca.gov/Admin_Record/C-032892.pdf.

Doorenbos J. and Pruitt WO. 1977. *Guidelines for predicting crop water requirements*. Rome (IT): Food and Agriculture Organization of the United Nations. Irrigation and Drainage Paper 24. 154 pp. Viewed online at: <http://www.fao.org/3/a-f2430e.pdf>.

Marvin Jung and Associates, Inc. 2000. *Revision of representative Delta island return flow quality for DSM2 and DICU model runs*. Sacramento (CA): Report prepared for the California Department of Water Resources. Division of Planning and Local Assistance. 191 pp. Viewed online at:
http://baydeltaoffice.water.ca.gov/modeling/deltamodeling/models/dicu/DICU_Dec2000.pdf.

Myint T and Nader-Tehrani P. 2006. "Chapter 9: DSM2 Simulation of Historical Delta Conditions over the 1975-1990 Period." In: *Methodology for Flow and Salinity Estimates in the Sacramento-San Joaquin Delta and Suisun Marsh. 27th Annual Progress Report to the State Water Resources Control Board*. Sacramento(CA): California Department of Water Resources. Bay-Delta Office.

Snyder RL et al. 2006. *Final report, Delta evapotranspiration of applied water (DETAW) Version 1.0*. California Department of Water Resources. Department of Land, Air, and Water Resources. University of California, Davis.

3.7.1 Personal Communications

Anderson FE. 2010 — email correspondence between Anderson FE and Liang L, California Department of Water Resources — comments about energy balance and crop coefficient of rice, weeds, and bare soil on Twitchell Island.

Methodology for Flow and Salinity Estimates in the Sacramento-San Joaquin Delta and Suisun Marsh

**38th Annual Progress Report
June 2017**

Chapter 4 Clifton Court Forebay Transit Time Modeling Analysis

Authors: Qiang Shu, Eli Ateljevich
Bay-Delta Office
Delta Modeling Section
Department of Water Resources



Contents

Contents

4. Clifton Court Forebay Transit Time Modeling Analysis.....	4-1
4.1 INTRODUCTION.....	4-1
4.1.1 Site Characterization	4-1
4.2 MODEL DESCRIPTION.....	4-7
4.2.1 Hydrodynamics	4-7
4.2.2 Radial Gate Parameterization.....	4-8
4.2.2.1 Evaporation	4-8
4.2.3 Particle Tracking	4-8
4.2.4 Mesh and Time Discretization	4-9
4.3 INPUT DATA SOURCES.....	4-11
4.3.1 Banks Pumping Plant Flow.....	4-11
4.3.2 Radial Gate Operations	4-11
4.3.3 Bathymetry.....	4-11
4.3.4 Wind.....	4-11
4.4 CALIBRATION AND VALIDATION	4-13
4.5 TRANSIT TIME AND VELOCITY ANALYSIS	4-21
4.5.1 Dredge and Fill Alternatives.....	4-21
4.5.2 Methods.....	4-21
4.5.3 Key Results	4-24
4.5.3.1 Patterns and Variations in Particle Trajectories	4-24
4.5.4 Transit Time.....	4-27
4.6 DISCUSSION.....	4-30
4.7 REFERENCES CITED.....	4-33
4.7.1 Personal Communications.....	4-34

Figures

Figure 4-1 Location and Aerial View of Clifton Court Gates	4-2
Figure 4-2 Bathymetric Map of Clifton Court Forebay	4-3
Figure 4-3 Priority Schedules Describing the Eligible Periods for Opening Clifton Court Radial Gates	4-4
Figure 4-4 Skinner Delta Fish Protection Facility	4-6
Figure 4-5 Horizontal Mesh.....	4-10
Figure 4-6 U.S. Geological Survey Sampling Locations for Upward-looking ADCPs and Drifters	4-14
Figure 4-7 Sketch of Upward-Looking ADCP Beam and Sampling Bins	4-14
Figure 4-8 Boundary Flows and Wind (top) and Comparisons with Observed Velocity at Site CCFWE	4-15

Figure 4-9 Boundary Flows and Wind (top) and Comparisons with Observed Velocity at Site CCFNE	4-16
Figure 4-10 Boundary Flows and Wind (top) and Comparisons with Observed Velocity at Site CCFSC....	4-17
Figure 4-11 Boundary Flows and Wind (top) and Comparisons with Observed Velocity at Site CCFCS....	4-18
Figure 4-12 Boundary Flows and Wind (top) and Comparisons with Observed Velocity at Site CCFNO ...	4-19
Figure 4-13 Boundary Flows and Wind (top) and Comparisons with Observed Velocity at site CCFCN....	4-20
Figure 4-14 Base Case and Dredging and Filling Options Explored in This Report.....	4-22
Figure 4-15 Radial Gate Flow, Banks Intake Flow, and Wind Conditions for 2012 (top), 2016 (middle), and 2017 (bottom).....	4-23
Figure 4-16 Particle Trajectories and Velocity Gradients in Low Flow Under Three Bathymetry Options..	4-25
Figure 4-17 Particle Trajectories and Velocity Gradients in High Flow Under Three Bathymetry Options .	4-26
Figure 4-18 Retention Curves for Base and Filling Options, Low-Flow (2016) Case	4-28
Figure 4-19 Retention Curves for Base and Dredge + Fill Options, Low-Flow (2016) Case..	4-Error! Bookmark not defined.
Figure 4-19 Retention Curves for Base and Dredge + Fill Options, Low-Flow (2016) Case.....	4-28
Figure 4-20 Retention Curves for Base and Dredge + Fill Options, High-Flow (2012) Case.....	4-29
Figure 4-21 Retention Curves for Base Bathymetry in Low-medium Flow (2016), Medium-High Flow (2012), and Extreme High Flow (2017)	4-29

4. Clifton Court Forebay Transit Time Modeling Analysis

4.1 Introduction

This chapter is excerpted from Shu and Ateljevich (2017), referred to from this point on as the “Report,” and summarizes 3D hydrodynamic modeling performed by the California Department of Water Resources’ (DWR’s) Bay-Delta Office (BDO) to assess flow patterns and transit time in the Clifton Court Forebay (Forebay). The motivation for this work comes from the National Marine Fisheries Service 2009 Biological Opinion, Action IV.4.2 (National Marine Fisheries Service 2011), which prescribes limits on pre-screen losses of salmonids and steelhead in the Forebay and obliges DWR to study methods to reduce this loss. The Report focuses on model development that has been completed and a study based on this model of how transit time across the Forebay responds to various filling and dredging actions. The premise underlying this investigation is that fish will benefit from faster transit, which reduces their exposure to predators.

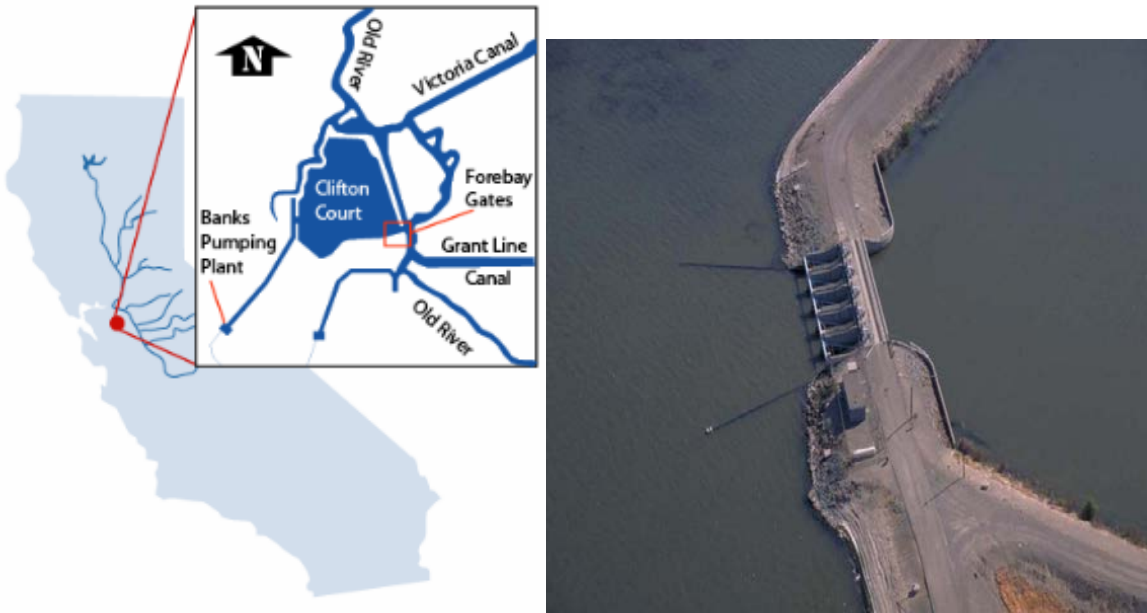
The Report characterizes the site, model formulation, and validation on field data. It supports the following findings:

1. Filling scour areas near the Clifton Court radial gates reduces transit time and enhances the benefits of dredging options.
2. Some dredging actions reduce transit time significantly when combined with filling of scour areas.
3. Transit time is more sensitive to flow operations than bathymetry.
4. The transit time interventions that are most effective and straightforward to model operate by shortening primary particle trajectories in the first few 2–5 days after entry.

The Report does not address engineering and design concerns or the morphological stability of the proposed bathymetry alterations.

4.1.1 Site Characterization

Clifton Court Forebay was completed in 1969. Located in the southern portion of the Sacramento-San Joaquin Delta (Delta) (Figure 4-1), the Forebay is a regulating reservoir that serves as a buffer between diversions from the Delta and State Water Project (SWP) pumping at the Harvey O. Banks Pumping Plant (Banks Pumping Plant). The Forebay affords DWR operators flexibility in meeting daily allocations, preserving sufficient water levels for south Delta agricultural diversions, and scheduling pumping around diurnal fluctuations in electricity prices. With an area of 2,200 acres (97.5 million square feet [sq ft]), an average depth of 7 feet (ft), and a typical water-level range of several ft, the Forebay has only enough storage volume to fulfill this flow-regulation role on a short-term basis. For example, the full volume of the Forebay at a 2.3 ft, North American Vertical Datum of 1988 (NAVD88) water level, is equivalent to 8,000 cubic feet per second (cfs) for one day. We will use this estimate throughout this document when



Source: Adapted from Wilde 2006

Figure 4-1 Location and Aerial View of Clifton Court Gates

estimating mean (volumetric) residence times at other operational levels, for instance two days at 4,000 cfs.

Figure 4-2 identifies some of the bathymetric features and facilities referred to in this chapter. Much of the Forebay is 4.0–6.5 ft deep under typical operating conditions. The deepest area in the Forebay is the scour hole just beyond the apron of the inlet radial gates, which reaches a depth of 64 ft. A ring of sediment lies behind the scour hole that is mostly less than 3 ft deep, shallower in some places. This shoal is one of the factors that limit conveyance through the Forebay. An internal channel or finger cuts through the sediment toward the north. The location of this internal channel is not static. Comparisons of bathymetry from 2004 and 2016 suggest that the scour hole has deepened and the internal channels have migrated. A repeat survey by DWR’s North Central Regional Office (NCRO) anticipated for 2017 should lend some insight as to how fast these changes occur following a shift from low flows to very high flows.

Flow into the Forebay enters from a gate inlet channel off Old River/West Canal. Discharge is controlled by five identical but independently operable radial gates. The gates are 20 ft wide, with a sill elevation of -13.2 ft NAVD88 (-15.5 ft National Geodetic Vertical Datum of 1929 [NGVD29]). Flow through the structure normally varies between a few hundred cfs and approximately 16,000 cfs; there was possibly greater flow in January, 2017. In principle, operators seek to limit flows to 12,000 cfs to prevent scour in the inlet channel leading to the gates, but the ceiling is informal and the DWR Delta Field Division (DFD) estimates the flow by means of a legacy rating curve from a technical memorandum by Hills (1988) with limited accuracy (Ateljevich et al. 2015).

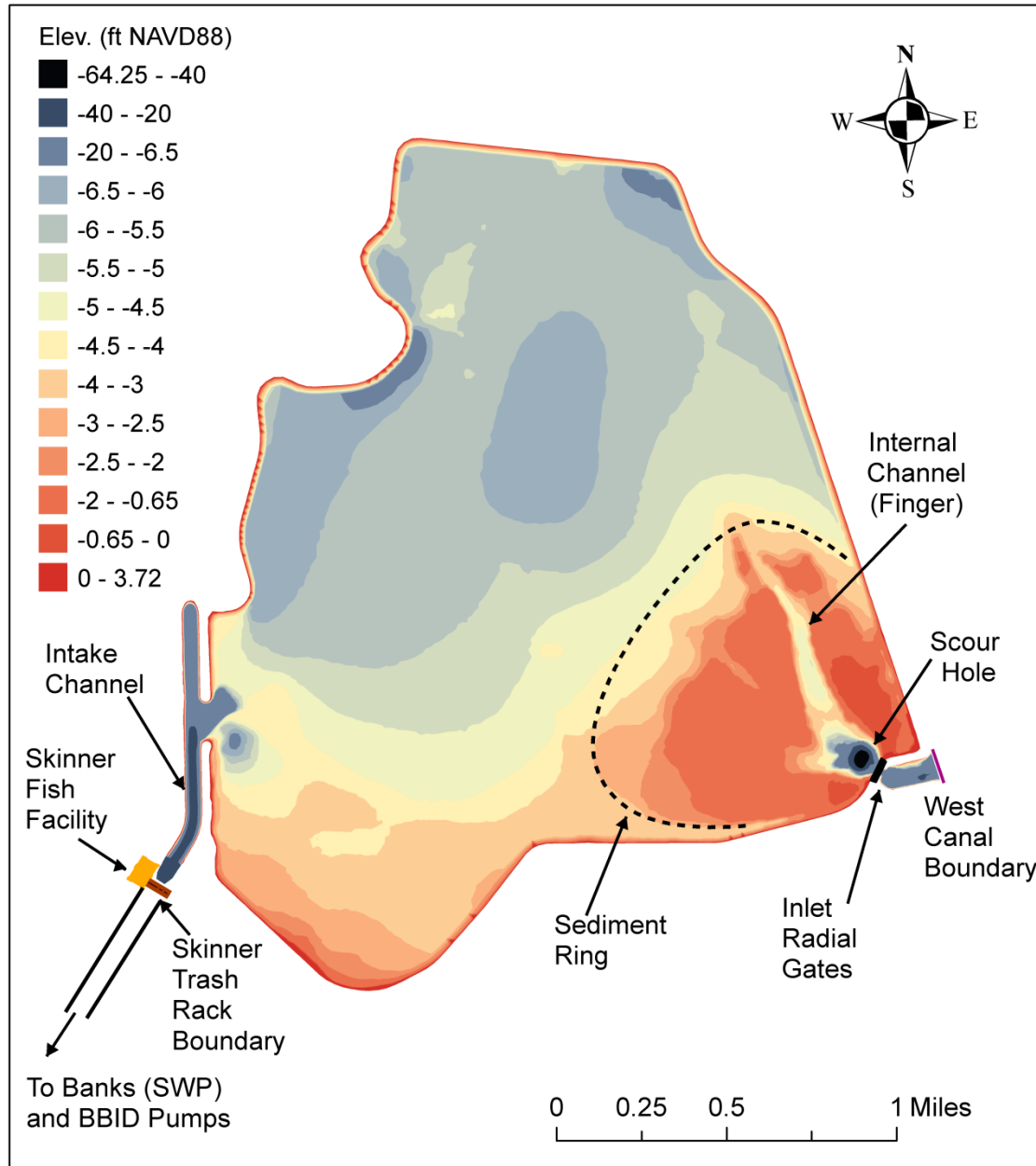


Figure 4-2 Bathymetric Map of Clifton Court Forebay

Notes: Banks = Harvey O. Banks Pumping Plant, BBID = Byron Bethany Irrigation District, Elev. = elevation, ft NAVD88 = feet in North American Vertical Datum of 1988, SWP = State Water Project

Radial gate flows are manipulated to satisfy multiple objectives. Operators seek to reduce the effect of Clifton Court operations on south Delta water levels, meet SWP allocations from the Delta, and limit entrainment of federal Endangered Species Act- and California Endangered Species Act- protected species. Preliminary gate schedules are developed in advance by the DWR Operation and Maintenance Division (DWR O&M) based on tide tables. These requests specify when the gates are eligible to be open according to the Priority System, which is a set of tidal rules developed to reduce impacts on south Delta diverters. The most common schedule is the one labeled as Priority 3 in Figure 4-3. The gates may be

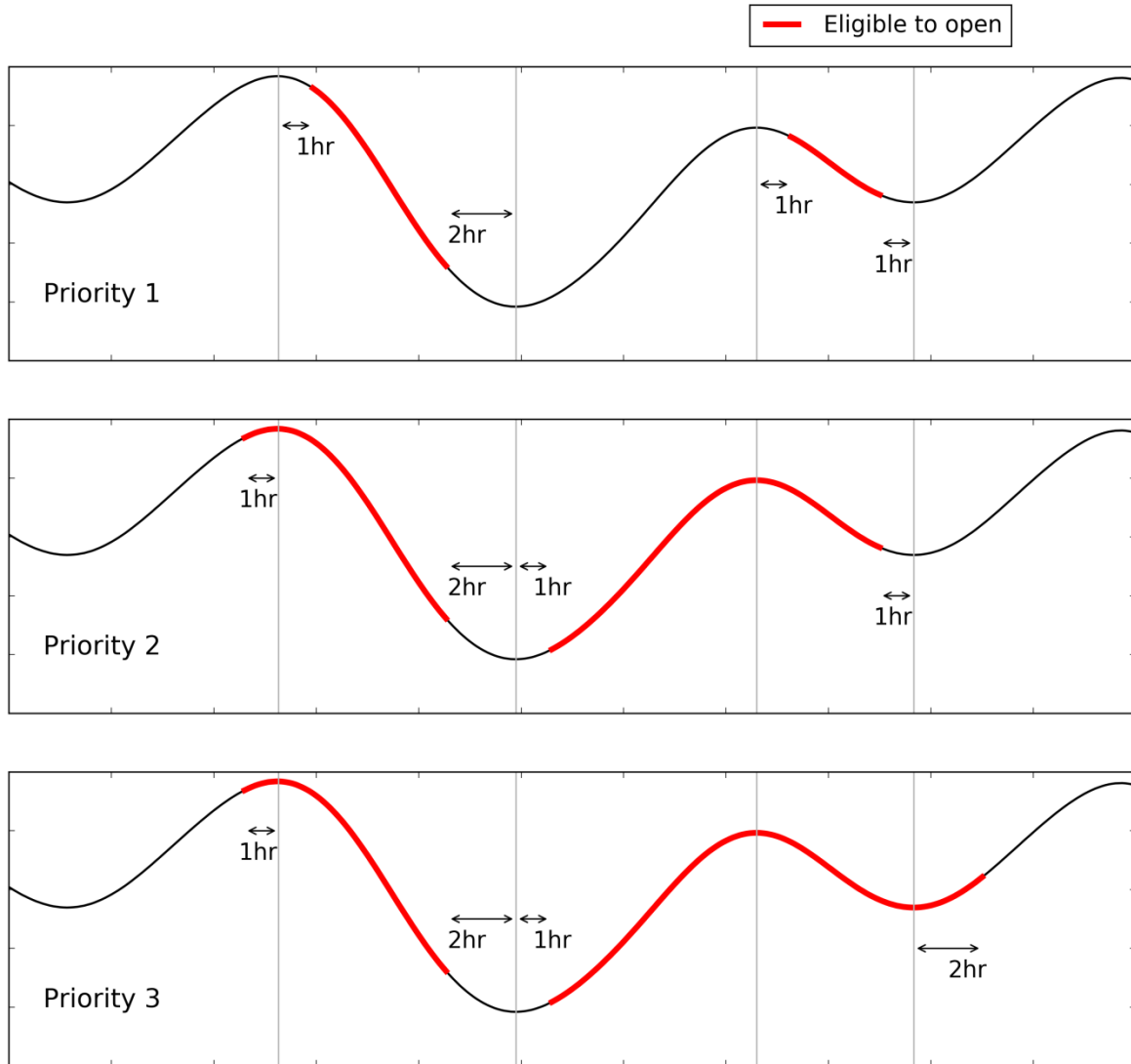


Figure 4-3 Priority Schedules Describing the Eligible Periods for Opening Clifton Court Radial Gates

opened one hour after lower-low tide, closed two hours after higher-low tide, opened one hour before higher-high tide, and closed two hours before the next lower-low tide. The Priority 1 and Priority 2 schedules are used in circumstances, such as drought, when allocations are low. Special schedules are also employed in weak neap tides when it is difficult to fulfill the day's allotment, although the methods used to prepare them appear to have varied over time.

Priority 3 schedules are also subject to change because of operational considerations. These include revised predictions of water levels, allotment changes, and maintenance. Also, the Priority Schedules only delineate periods when radial gates are *potentially* open. The schedule is interpreted by DFD whose staff has some discretion in how to set gate heights and fulfill inflow-target volumes. Once daily allocations are met, the gates are closed, regardless of whether there is remaining eligible time on the schedule. It is also possible for inflows to fall short of the allocation for the day, in which case DFD may

change gate heights or the Joint Operations Center may reschedule gate openings to make up for unused allocation on the following day.

The Clifton Court radial gates can be operated close to being fully open, which means approximately 15–18 ft above the sill, or be partially opened to as little as a few feet above the sill. Operating with the radial gates fully open was apparently a more prevalent operation early in the history of the Forebay, although data from the last 10 years suggest this type of operation is still used with some frequency when water supply demands are adequate, and fish triggers do not constrain operations. In recent years, a *sipping* strategy has been adopted, in which the radial gates are opened to a much smaller height for a longer period, attempting to take in water over the full eligible opening period at a lower rate. Sipping is the predominant gate operation in recent years during the January–June period of greatest fishery concern.

Across the Forebay from the radial gates, water flows out an intake canal to the Banks Pumping Plant. Banks Pumping Plant has a capacity of 10,300 cfs and lifts water 244 ft from the Delta to the California Aqueduct. The daily export volume is dictated by project demands, agreements, and regulatory constraints; but the hour-by-hour scheduling of pumping is planned around available water in the Forebay, the price of electricity, and maintenance of the facilities.

As a guiding goal, DFD likes to leave water levels at approximately 1.8 ft NAVD88 (-0.5 ft NGVD29) at midnight. This rule is apparently adjusted for challenging tidal circumstances or large-flow allocations. The balance between exports and gate allocations is achievable on a daily average basis during spring tides, but this is more difficult to achieve during neap tides when the head difference across the gates is small.

The main fish protection facilities are in the intake channel. Before water is pumped, it traverses the John E. Skinner Delta Fish Protective Facility (SDFPF) (Figure 4-4). The SDFPF was designed to protect fish from entrainment into the California Aqueduct by diverting them into holding tanks where they can be salvaged and safely returned to the western Delta. Water is drawn to the SDFPF from the Forebay via the intake canal and past a floating trash boom. The trash boom is designed to intercept floating debris and guide it to a trash conveyor on shore. Water and fish then flow through a trash rack, which is equipped with a trash rake, to a series of louvers arranged in a V pattern shown in Figure 4-4. Fish are behaviorally guided via the louvers and directed to holding tanks for salvage. More complete descriptions of the facility, its efficiency, and sampling challenges can be found in Castillo et al. (2012). Details of the facility are not included in our model domain, which terminates at the trash rack.

Byron Bethany Irrigation District (BBID) diverts a small additional volume from a location along the SWP intake downstream of the fish protection facilities at 37° 48' 51.81" north latitude and 121° 36' 20.71" west longitude. Operators also strive to prevent water levels in the Forebay from dropping below approximately 0.3 ft NAVD88 (-2.0 ft NGVD29) because of potential cavitation issues at the BBID's diversion point. Low water levels also can potentially limit conveyance in the main Forebay during high-flow or low-exterior water levels. Such conditions were not the focus of our study, but the presented dredging operations would be expected to benefit conveyance capacity through Clifton Court.

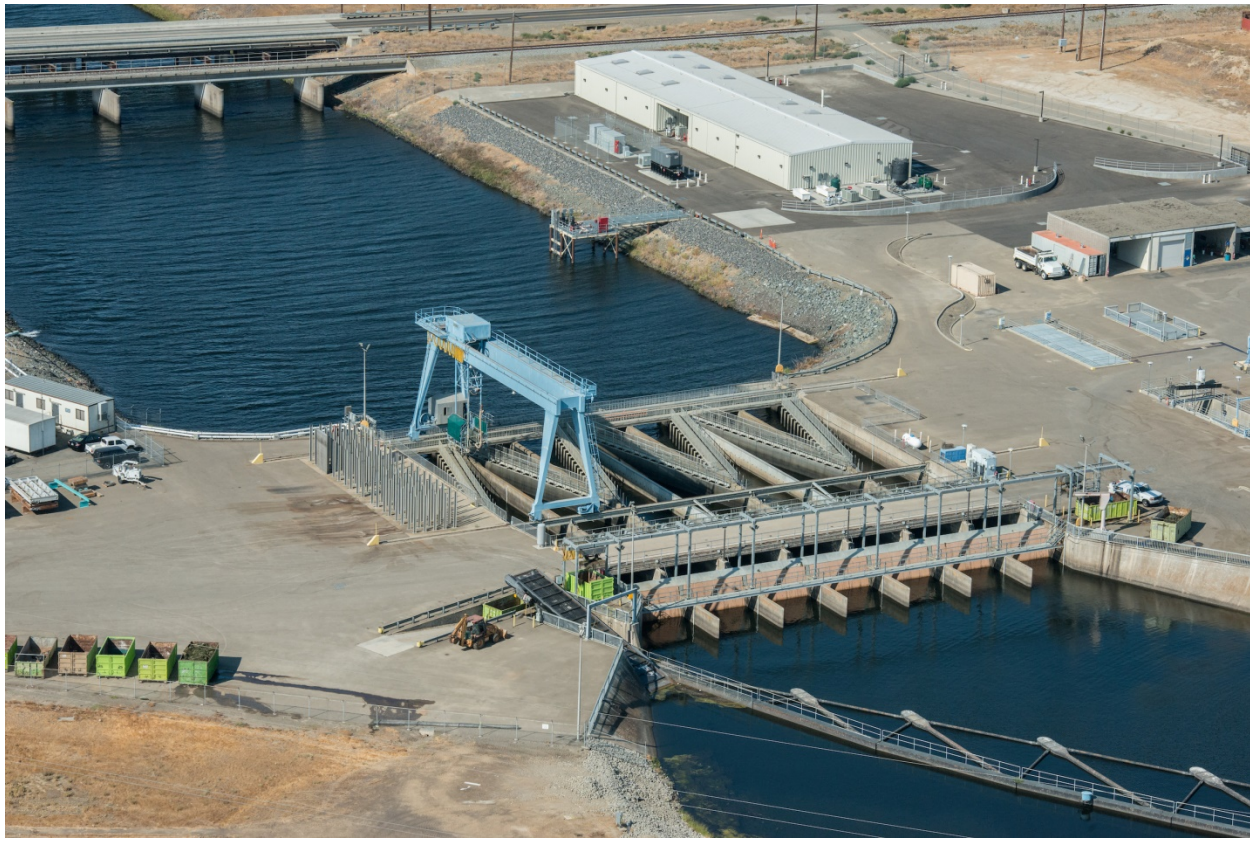


Figure 4-4 Skinner Delta Fish Protection Facility

4.2 Model Description

4.2.1 Hydrodynamics

The model used for this analysis is the 3D SCHISM (Zhang and Baptista 2008; Zhang et al. 2015; 2016). Although this is the same computational code used in the Bay-Delta SCHISM project (Ateljevich et al. 2013), the domain in this case is restricted to the Forebay intake channel up to the SDFPF trash rack.

As used here, SCHISM solves the 3D hydrostatic Reynolds-averaged shallow water equations, including mass conservation and horizontal momentum conservation. For this project, we have dropped terms involving baroclinic pressure (salt and temperature gradients are small). Density terms in the turbulence closure were also neglected. We experimented with horizontal viscosity, although the results here are presented without it, which is the most common practice among 3D models in the estuary. The elimination of horizontal viscosity is justified on the assumption that a well-resolved horizontal grid and modest amount of numerical diffusion are sufficient to model horizontal mixing.

Boundary conditions for the water column are given by wind stresses at the free surface and shear at the bed. For wind, the boundary condition is

$$\nu \frac{\partial u}{\partial z} = \tau_w, \text{ at } z = \eta \quad (1)$$

using the wind stress (τ_w) formulation from Pond and Pickard (1983). The boundary condition at the bed ($z = -h$) is

$$\nu \frac{\partial u}{\partial z} = \tau_b, \text{ at } z = -h \quad (2)$$

with bottom stress (τ_b) derived from a quadratic formulation based on the velocity (\mathbf{u}_b) evaluated at the top of the bottom computational cell and is

$$\tau_b = C_D |\mathbf{u}_b| \mathbf{u}_b \quad (3)$$

The drag coefficient (C_D) of roughness is calculated dynamically from a roughness parameter ($z_0=0.8$ millimeters) by using standard boundary layer assumptions as described in Zhang and Baptista (2008).

The turbulent eddy viscosity (ν) is generated by using an independent set of turbulence closure equations, specifically the k- ϵ 2.5 equation closure with a background eddy viscosity of $0.0096 \text{ ft}^2/\text{s}$. As described previously, only terms related to barotropic characteristics of the mean flow were included in the closure calculations, such as production of turbulence by shear. We dropped terms associated with density stratification that play little role in Clifton Court dynamics. The closure is implemented in SCHISM using the Generic Length Scale approach of Umlauf and Burchard (2003). Relative to turbulence, the closure used in the stratified part of the Bay-Delta estuary (k- ω , for instance), the choice of the k- ϵ closure and the use of non-trivial background viscosity can be regarded as diffusive choices. Our parameter choices are intended to dissipate eddies that form during abrupt gate openings and propagate forth in the upper water column. The results seem to tally well with the 2008–2009 field

measurements, which were mostly taken during periods of light or medium wind. In windy conditions, pronounced layered flow does develop in both the model and field data.

4.2.2 Radial Gate Parameterization

We included the Forebay radial gates directly within the model, which is the domain that extends upstream of the gates to the junction with West Canal. This approach is somewhat more complex than just terminating the domain at the gates and imposing a flow. For our work, the approach has two compensating advantages. First, it is more extensible should the model need to be nested within the greater Bay-Delta. Second, the approach has a stabilizing effect on water levels during longer simulations in the presence of episodic data discrepancies between inflows and outflows.

No matter how the boundary on the gate side is approached, a reasonable rating formula is required to produce flows from water levels and radial gate heights. Daily average flows are inverted from Banks Pumping Plant tallies and midnight storage changes, but these are too coarse in time to use in a study of velocity. Finer time-step gate-flow estimates are also calculated by DWR, based on the antiquated Hills Equation. These take gate heights, interior, and exterior water levels as inputs, which are available at finer time scales, particularly after 2012. For this study, we incorporated the rating equation for the gates developed by Ateljevich et al. (2015). Further details may be found in that work or the Report. As a consequence of our approach, some of our gate flows in this chapter have considerably higher peak values than those plotted by MacWilliams and Gross (2013). In fact, our estimates are similar in magnitude to those of the most accurate methods reported in that work, called the “scaled gate equation.” But the authors used a different technique for the bulk of their analysis, disaggregating daily volume over the gate opening period with a flat line. This simplification results in peak flows, as much as 50 percent lower. One other notable thing about the MacWilliams and Gross (2013) approach is that the scaling they apply algebraically constrains water levels to match historical water-level changes on a daily basis. This is an advantage in historical modeling, as far as water levels are concerned, but it is harder to extend to hypothetical operations, such as our brief gate-export lagging experiment in section 4.5.4, “Transit Time.”

4.2.2.1 Evaporation

We did not include evaporation. Assuming a typical Central Valley summer evaporation rate of 0.75 ft/month, we expected evaporation in the Forebay to reach 20 cfs during July–August, but to be as low as 3–4 cfs during January–March when fishery concerns are highest. Either rate is small compared with other boundary uncertainties. Also, evaporation occurs diffusely over the whole surface and consequently has a particularly small effect on momentum and currents.

4.2.3 Particle Tracking

We modeled transit by using streamlines of neutrally buoyant particles introduced randomly in the top 3.3 ft (1 meter [m]) of the water column within the wingwalls downstream of the radial gates. For purposes of this study, the equations of motion for each particle are accordingly advection with flow.

$$\frac{dx_i}{dt} = \mathbf{u}(\mathbf{x}_i, t) \quad (4)$$

where \mathbf{x}_i is the position of the i 'th particle. This formulation omits the random-walk component because of eddy diffusivity that provides a linkage with the transport equation for dissolved species. Particles are injected randomly in the upper part of the water column, but afterwards vertical migration is slower than that of a particle subject to turbulent mixing. This amounts to an implicit stabilizing “behavior,” particularly in the vertical direction; particles do not jump vertically from one contrasting horizontal flow structure to another. This is more of an important assumption in windy flow, where the top and bottom of the water column can have very different velocity patterns. In flows driven by gates and exports, vertical structure in the flow is limited to mild shear and the impact of the assumption is smaller.

4.2.4 Mesh and Time Discretization

The horizontal mesh is shown in Figure 4-5. The mesh is mostly triangular, but contains quadratic elements near the radial gates and pump intakes. The mesh is unstructured, with flexible resolution to conform to terrain features. Overall, there are 25,716 horizontal elements in the model. Typical length scales are 5 m near the radial gates, 10 m near the pump intakes, and 20–30 m in the mid-Forebay.

The vertical mesh in the present model uses an S-grid (Song and Haidvogel 1994) with eight levels. An S-grid is a terrain-conforming vertical grid with linear (triangles) or bilinear (quadrilaterals) representation of bathymetric and spatial features. For most of the domain and under typical reservoir heights, these yield a vertical resolution of approximately 0.8 ft (0.25 m) in the body of the Forebay. In deeper regions, eight levels represents a vertical resolution of 3.3 ft (1 m) or coarser in places like the scour hole. In these less-resolved areas, the mesh is somewhat clustered near the surface, so that region remains relatively resolved.

The time step for the hydrodynamic model is 60 seconds, which we found was the coarsest time step that smoothly integrates transitions at abrupt gate openings without creating spurious currents. Hydrodynamic information for particle tracking is saved at intervals of 120s, or every other hydrodynamic time step. The particle tracking model reports at this nominal time step of 120s, but the integration scheme uses a subdivided time step, typically 12s.

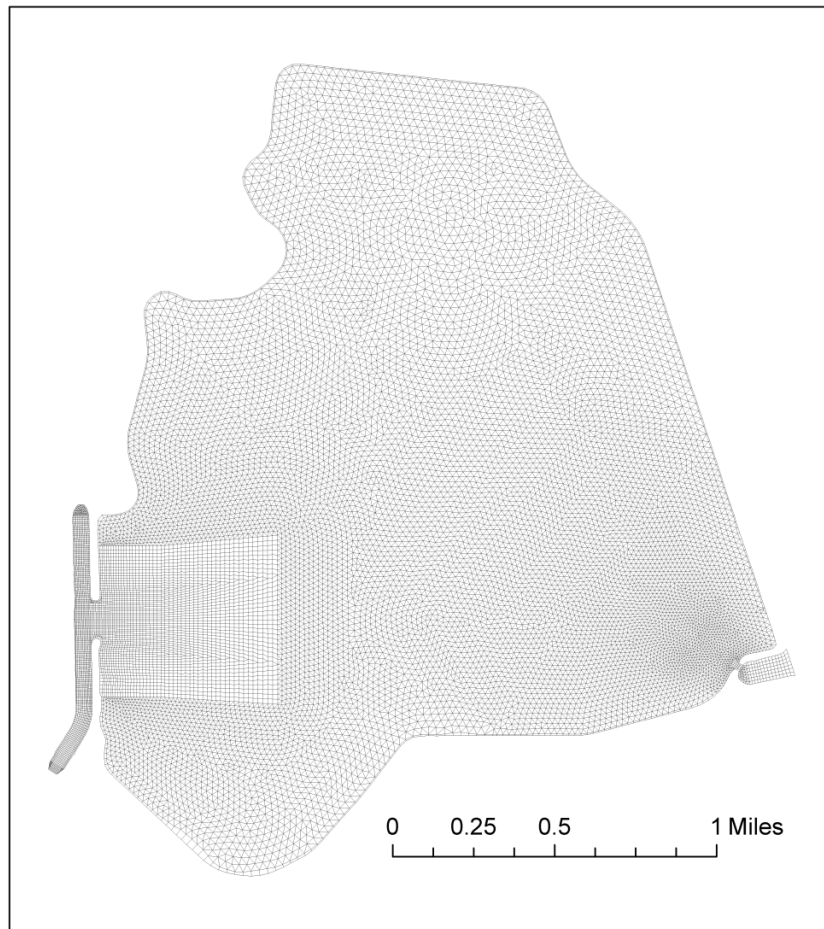


Figure 4-5 Horizontal Mesh

4.3 Input Data Sources

The major time-series data requirements for our model are Banks Pumping Plant pumping flows and Clifton Court radial gate heights and wind, all required at an hourly or better time step. Additionally, the model requires bathymetric elevations.

Below we list where we acquired data for the various years that we simulated and the reliability and caveats we believed to be associated with those sources. One that applies generally involves time stamps of historical data. DWR operational databases return data time stamped with Daylight Savings Time. We preferred to model in Pacific Standard Time and attempt to align data to Pacific Standard Time (PST), but have found in some cases there are ambiguities that arise over the shifting of older records. Similar comments apply to other sources of data, with California Data Exchange Center (CDEC) serving data with time stamps that are not rigorous. The DWR NCRO and U.S. Geological Survey (USGS) distribute data time stamped in PST.

4.3.1 Banks Pumping Plant Flow

Instantaneous flow at the pumps is not observed directly. This is a matter of some confusion and lore. Flow measurement equipment has been installed in the past, but the instruments have not been maintained. Instead, DFD infers instantaneous flows by logging which pumping units are operating and summing their individually rated capacities. The start- and stop-times upon which flow estimates are made have been stored with very fine temporal resolution as part of the internal DWR Systems Applications and Products (SAP) data logging system since 2006 (SAP report titled *Unit Status Log Exclude Report 2*). Earlier historical records are available from the Interagency Ecological Program and other sources, but these were not utilized in this study. Daily averaged exports constructed from spreadsheets using similar methods and formulas are reported in public databases, such as CDEC. BBID diversions are taken from the CDEC station BBI, which is a daily average. As the total volume is low, no site-specific processing is performed on this data.

4.3.2 Radial Gate Operations

We modeled the Clifton Court radial gates explicitly by using a radial gate-rating formula. This calculation requires gate heights, interior water levels, and exterior water levels. Interior water levels are taken from the hydrodynamic model's dynamic state. Radial gate heights and exterior gage heights must be supplied as input data.

Historical gate heights, going back to approximately 2011, are available from the DWR Control Systems Branch (CSB) Information Server at a very high time resolution (< = 10 min), which captures the gradual opening and closing of the gate.

For exterior water levels, we used historical gauge heights from the DWR NCRO station Old River at Clifton Court Ferry (B95340). These differ slightly from the upstream water levels recorded by DWR O&M. We chose the NCRO station because we felt more confident about the datum.

4.3.3 Bathymetry

The main bathymetry survey used in the study was done in January, 2016 by NCRO in connection with this project. The survey is multi-beam and very dense around the scour hole, but single beam with adaptive resolution in the sediment and finger areas beyond, where the shallows make multi-beam collection less practical because it has limited extent at close range. At times, we will discuss an earlier collection in 2004 also conducted by NCRO using single-beam soundings. This collection was less resolved in the scour-hole area, because it has no multi-beam component. Farther afield in the sediment deposition area, it followed a more gridded sampling approach, which is less adaptive to bathymetric features but is generally more resolved.

The two collections reveal different morphological states of the Forebay, particularly in the scour and depositional areas near the gate. In 2004, the scour hole was shallower and channelization through the perimeter sediment ring was less developed. By 2016, the scour hole had deepened and a prominent subchannel through the sediment had developed in the north. Neither survey is detailed enough to make detailed quantitative comparisons.

4.3.4 Wind

In this modeling application, we made the simplification that wind is uniform over the full domain. Because of data gaps, we made use of three local stations: Clifton Court Gates (CDEC code CLC), Banks Pumping Plant (CDEC code HBP), and Rough and Ready Island (CDEC code RRI) near Stockton. The CLC station is the only one of these stations situated within the modeling domain, and we attempted to make it our standard. But, CLC and HBP were new and only beginning to be archived during the 2008–2009 validation period, with regular CDEC coverage beginning respectively in July, 2008 and October, 2009. The authors received an unarchived copy of wind data from MacWilliams (pers, comm, Jul 13, 2016) that extends the Clifton Court Radial Gate wind record to most of summer 2008 that appears to originate from data loggers at CLC.

CLC was also subject to erratic values in January, 2017 during our very-high-flow particle analysis. Specific details about imputing missing data are available in Shu and Ateljevich (2017). We found the wind field to be complex, taking on directionally and seasonally mixed characteristics of wind at HBP and RRI.

4.4 Calibration and Validation

In this section, we compare model results to observed data, including Forebay water levels, gate flow, vertical velocity, and drifter tracks. The comparison is mostly a calibration result, rather than validation, because we had access to the data during model development, and the study used model comparisons to make a small number of parameter and algorithmic choices (roughness, background eddy viscosity and turbulence closure). We utilized several data sources. Significantly, in 2008–2009, the USGS conducted a series of field studies in the Forebay, including drifter releases in June, 2008, and velocity measurements, by using upward-looking ADCPs between September, 2008, and January, 2009. We also validated flow in the intake channel against USGS transects. For brevity, only the velocity component is described here. Water level validation, intake flows and particle trajectories may all be found in the Report. The water levels and intake flows corroborate the gate rating of Ateljevich (2015).

Between fall 2008 and spring 2009, the USGS established upward-looking ADCPs at the locations noted in Figure 4-6. The instruments were deployed during two periods — the first period was 09/19/2008–01/13/2009 and the second period was 01/13/2009–04/14/2009. The configuration of the instruments and data within the water column is sketched in Figure 4-7. Each ADCP is anchored to the bed, with the observation cones extending upward. Velocities cannot be observed over a blanking distance of 1.65 ft (0.50 m). Above that, the observations were arranged in one, two, or three 1.65 ft (0.50 m) cells, allowing a limited glimpse of vertical velocity structure. The region immediately below the surface is not normally reported because of errors caused by reflection and sidelobe interference and, given the shallowness of the Forebay, only one station had more than two good bins. In the field data, velocities are averaged over the vertical cell extents. In the model, which is smoother in velocity, we extracted cell mid-points.

Figure 4-8–Figure 4-13 show modeled compared with observed results at the six locations for both components of velocity. The plots are marked with the direction (u is eastward, v is northward) as well as an ADCP bin (1 or 2). Only two bins were used per station, and just one was used in CCFCN.

The model reproduces the full range of velocities near the pumps (station CCFWE). It also performs well on velocities midway between the gates and pumps, particularly at station CCFSC. On the eastern edge of the Forebay (CCFNE), the most significant velocities are also captured well, although there are stations (e.g., CCFNO) where velocities are seemingly small compared with background fluctuations.

The two largest discrepancies involve the upper velocity bins at stations CCFSC and CCFCN, and in each of these cases, only one component of velocity and one bin are affected. In the case of CCFSC, large easing (u) velocities are present in the upper bin of the observations, but are not in the model. At station CCFCN, large northing (v) velocities develop in the upper bin of the model, but not in the observations. In both cases, the issue is a far-field effect of gate or pumping operations (wind is weak) and in both locations bathymetry is part of the issue. Swapping 2004 bathymetry for 2016 bathymetry does not fix the problem completely, but it does change the component of velocity that is problematic.

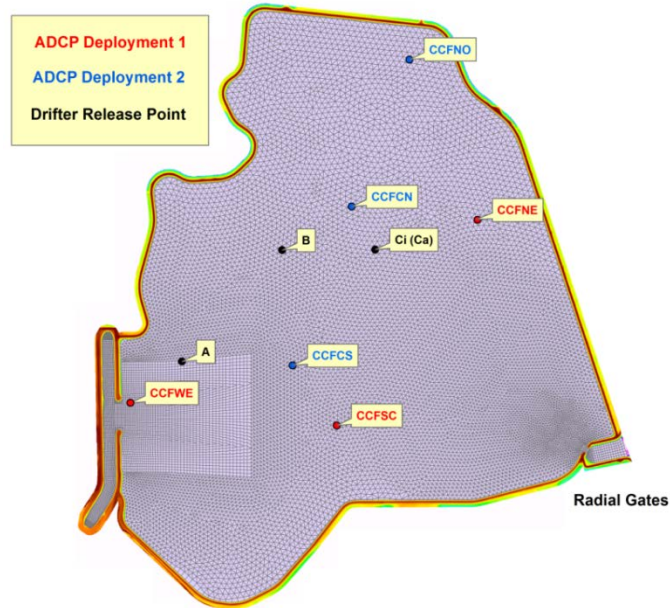


Figure 4-6 U.S. Geological Survey Sampling Locations for Upward-looking ADCPs and Drifters

Notes: ADCP = acoustic Doppler current profiler, CCFCN, CCFNE, CCFCS, and CCFWE = USGS codes for ADCP locations in Clifton Court Forebay, A, B = drifter release points.

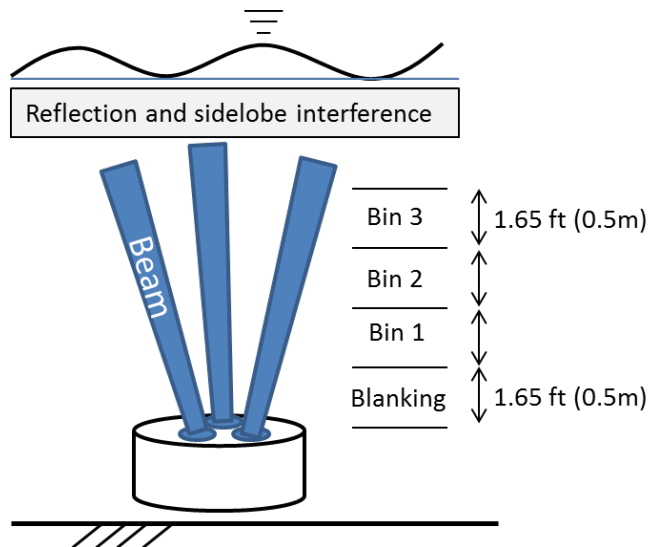


Figure 4-7 Sketch of Upward-Looking ADCP Beam and Sampling Bins

Notes: ADCP = acoustic Doppler current profiler, ft = feet, m = meter

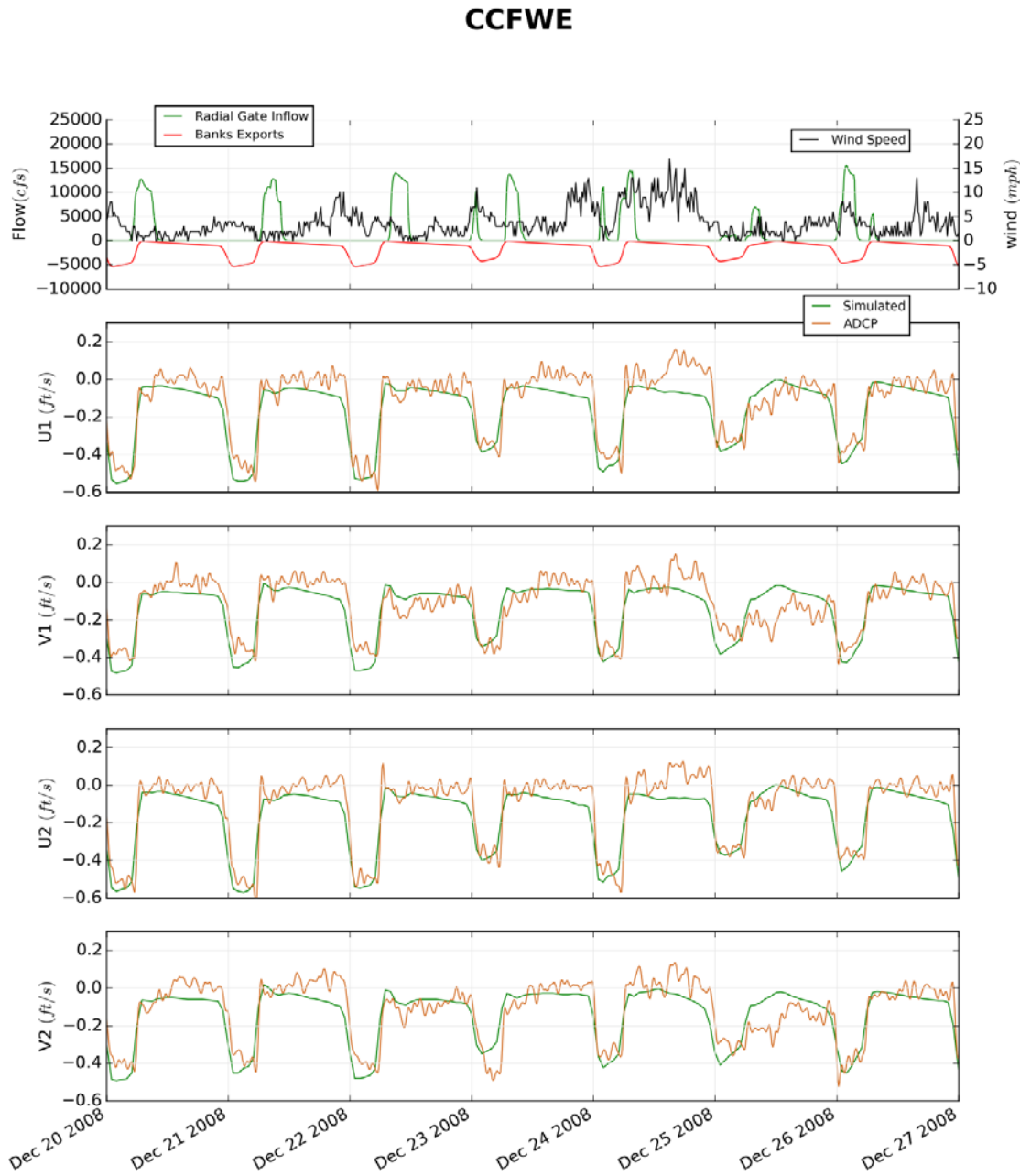


Figure 4-8 Boundary Flows and Wind (top) and Comparisons with Observed Velocity at Site CCFWE

Notes: ADCP = acoustic Doppler current profiler, cfs = cubic feet per second, ft/s = feet per second, CCFWE = USGS code name for location in Clifton Court Forebay,

mph = miles per hour

The U (easting) and V (northing) part of the axis label indicate direction, and the V1 and U1 (lower charts) and V2 and U2 (mid and upper charts) indicate the vertical position of the ADCP bin.

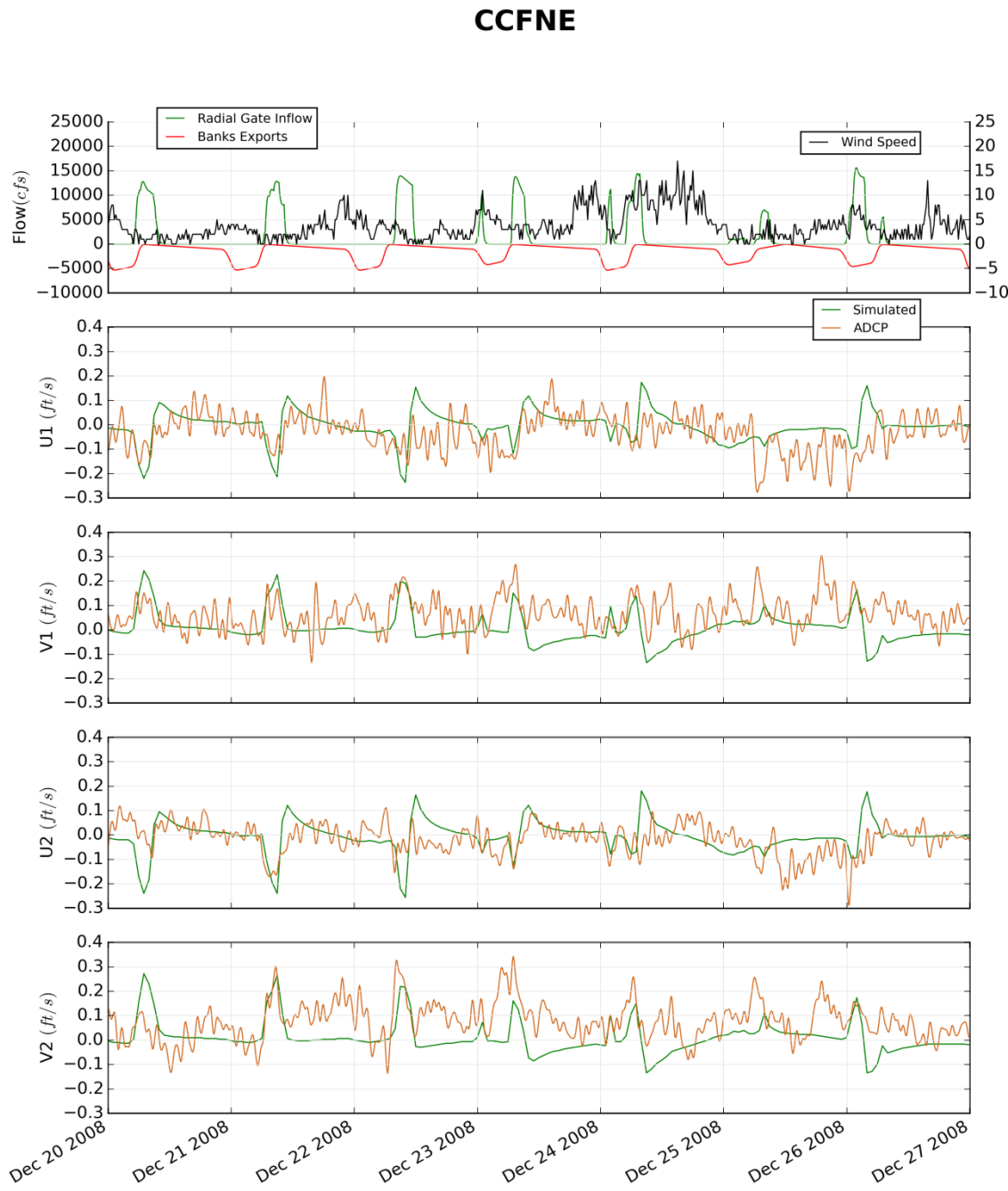


Figure 4-9 Boundary Flows and Wind (top) and Comparisons with Observed Velocity at Site CCFNE

Notes: ADCP = acoustic Doppler current profiler, CCFNE = USGS code for station in Clifton Court Forebay, cfs = cubic feet per second, ft/s = feet per second, mph = miles per hour

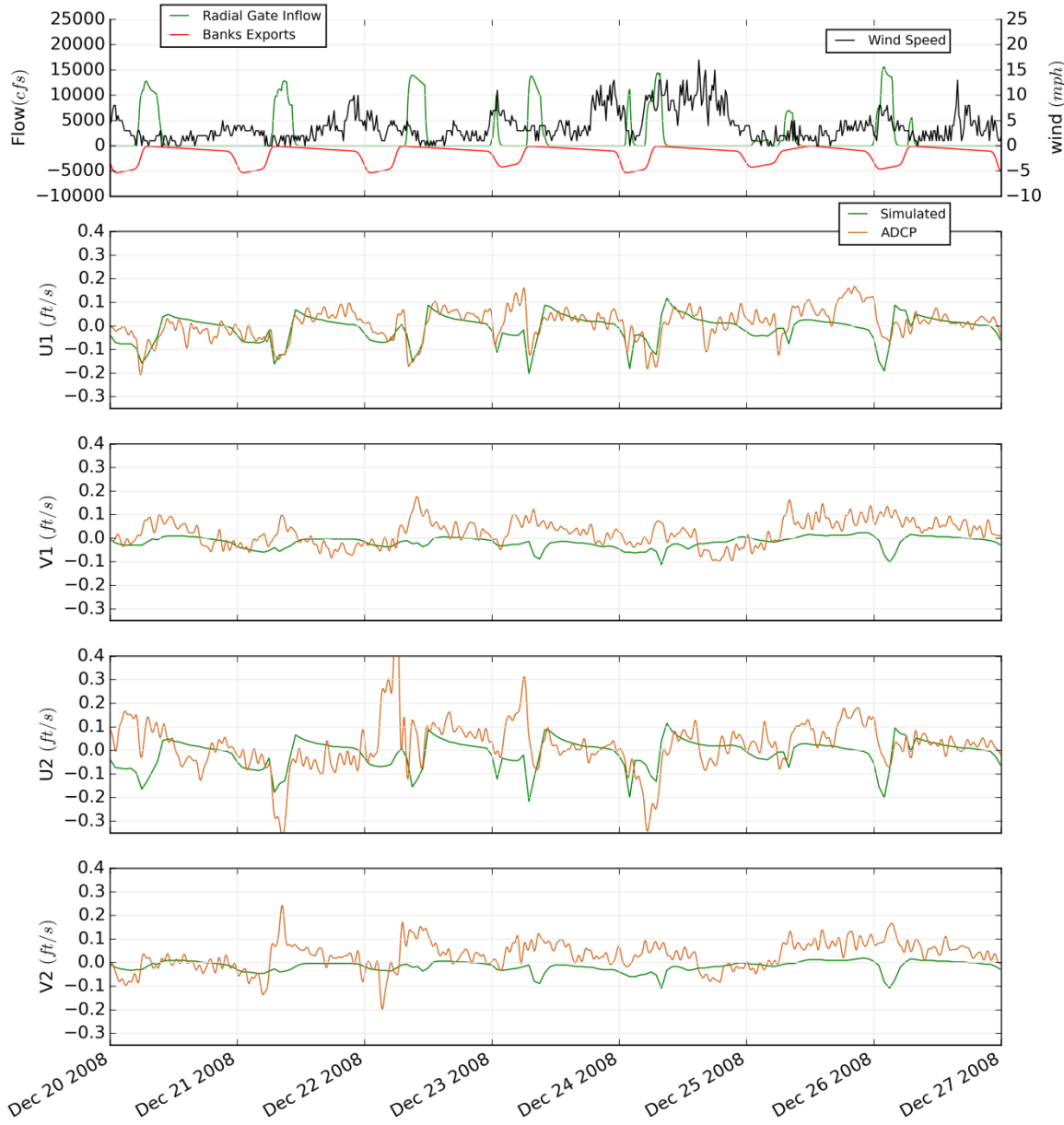
CCFSC

Figure 4-10 Boundary Flows and Wind (top) and Comparisons with Observed Velocity at Site CCFSC

Notes: ADCP = acoustic Doppler current profiler, CCFSC = USGS code for a station in Clifton Court Forebay, cfs = cubic feet per second, ft/s = feet per second, mph = miles per hour
The u (easting) and V (northing) part of the axis label indicate direction and the V1 and U1 (lower charts) and V2 and U2 (mid and upper charts) indicate the vertical position of the ADCP bin.

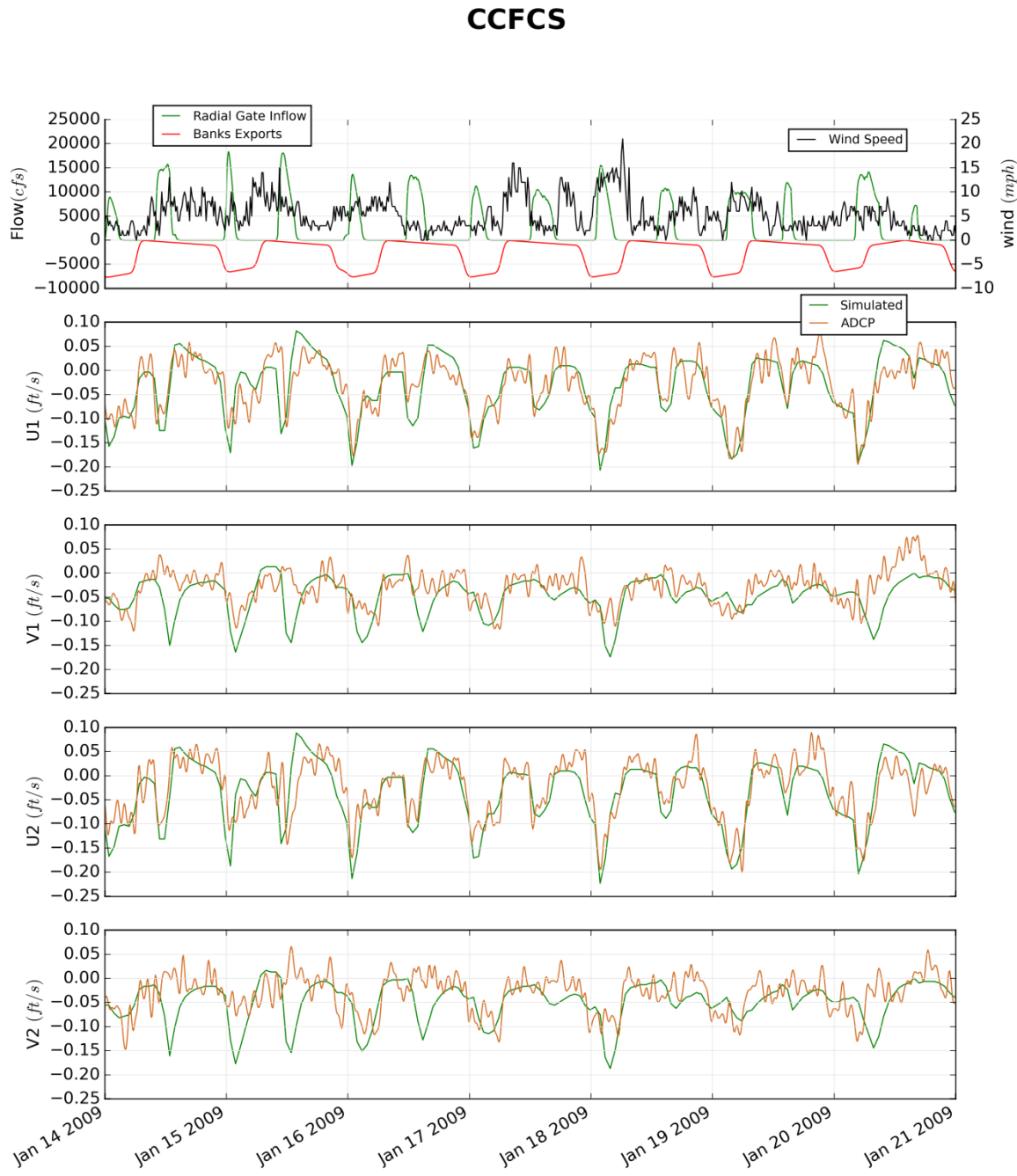


Figure 4-11 Boundary Flows and Wind (top) and Comparisons with Observed Velocity at Site CCFCS

Notes: ADCP = acoustic Doppler current profiler, CCFSC = USGS code for a station in Clifton Court Forebay, cfs = cubic feet per second, ft/s = feet per second, mph = miles per hour

The u (easting) and V (northing) part of the axis label indicate direction and the the V1 and U1 (lower charts) and V2 and U2 (mid and upper charts) indicate the vertical position of the ADCP bin.

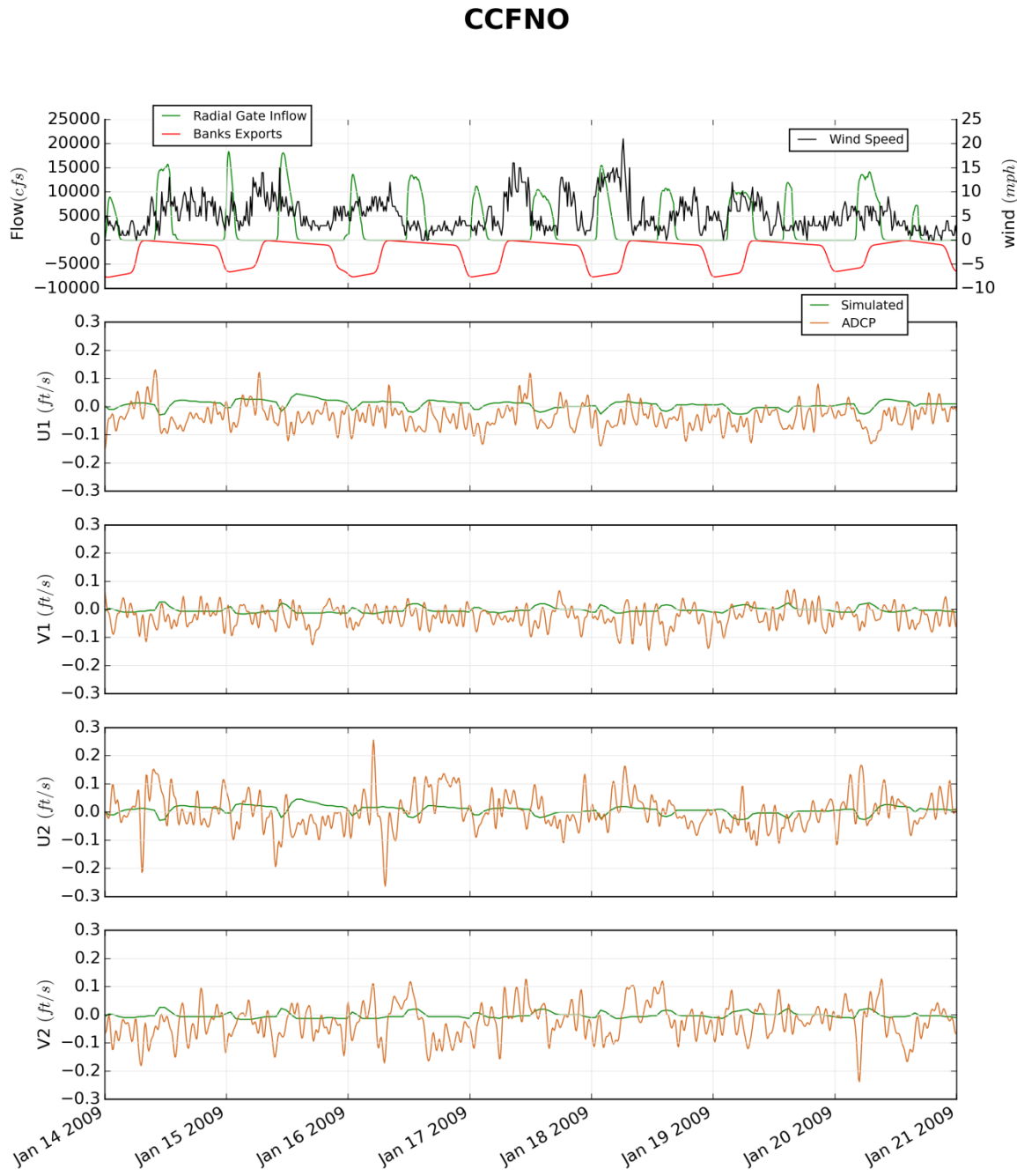


Figure 4-12 Boundary Flows and Wind (top) and Comparisons with Observed Velocity at Site CCFNO

Notes: ADCP = acoustic Doppler current profiler, CCFNO = USGS code for a station in Clifton Court Forebay, cfs = cubic feet per second, ft/s = feet per second, mph = miles per hour
The u (easting) and V (northing) part of the axis label indicate direction and the V1 and U1 (lower charts) and V2 and U2 (mid and upper charts) indicate the vertical position of the ADCP bin.

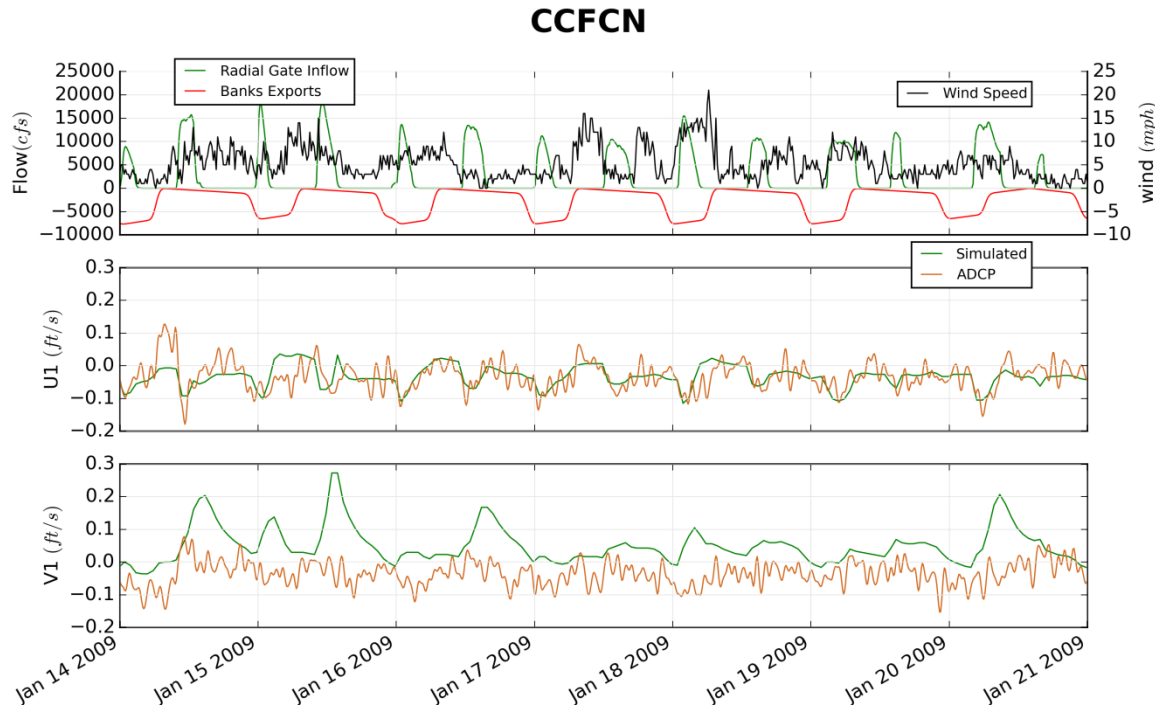


Figure 4-13 Boundary Flows and Wind (top) and Comparisons with Observed Velocity at site CCFCN

Notes: ADCP = acoustic Doppler current profiler, CCFCN = USGS code for a station in Clifton Court Forebay, cfs = cubic feet per second, ft/s = feet per second, mph = miles per hour

The u (easting) and V (northing) part of the axis label indicate direction and the V1 and U1 (lower charts) and V2 and U2 (mid and upper charts) indicate the vertical position of the ADCP bin — in this case there is only one bin.

4.5 Transit Time and Velocity Analysis

4.5.1 Dredge and Fill Alternatives

We experimented with a number of dredging and filling alternatives to examine their effect on transit time. The alternatives are permutations of the following components, many of which are illustrated in Figure 4-14.

Base. The base is established by the 2016 bathymetry survey.

Fill scour hole. This option involves filling the scour hole immediately beyond the radial gates to -4 ft (-1.22 m) NAVD88 or -6.56 ft (-2. m) NAVD88 in combination with certain dredging options, as described below. In 2016, the scour hole was surveyed as being 63 ft deep. Filling the scour hole was deemed beneficial for predator habitat reduction, and we included filling the scour hole for any dredging option marked “filled.”

Fill finger channel. This option involves filling the northern subchannel through the sediment ring to 0.656 ft (-0.2 m) NAVD88. There were two motives for filling this channel. First, it reinforces a more northward velocity path that sends particles to the northwest side of the Forebay where they tend to linger. Second, the feature resembles dredging, and we preferred to focus on other dredging alternatives in isolation. The finger channel is filled for any option marked “filled,” except for the curved dredge and near gate dredge, which overlap and effectively overwrite the bathymetry of the finger channel.

Dredge straight channel. This option involves dredging a straight path from the gates to the pumps at -6.56 ft NAVD88. Two variants were attempted, one 325 ft (100 m) wide and the other 1,000 ft (300 m) wide. Scour hole is filled to -6.56 ft NAVD88 for options marked “filled.”

Dredge curved channel. This option dredges an arc path from the gates to the pumps. The pattern was inspired by streamlines in moderate flow. Although this option seemed promising in early work over a limited set of operations and winds, ultimately it turned out to yield fewer benefits.

Dredge sediment near gate. In this option, the sediment ring near the gate is dredged to -4 ft NAVD88. The scour hole is also filled to -4 ft NAVD88, if marked “filled.”

Dredge southern sediment near gate. The southern half of the sediment ring near the gate is dredged to -4 ft NAVD88. The scour hole is filled to -4 ft NAVD88 for options marked “filled. The quantity of materials moved for this option is lower than those moved for the 1,000 ft-wide straight channel.

4.5.2 Methods

For the analysis of bathymetry changes, we compared the distributions of transit times resulting from particle releases over a variety of operational and tidal conditions. After developing flow fields for each weeks, we made two releases of 7,500 particles, each for a duration of approximately two weeks. The first began April 26, 2016, and represented a period of low-medium-gate/pumping flows (1,175 cfs daily

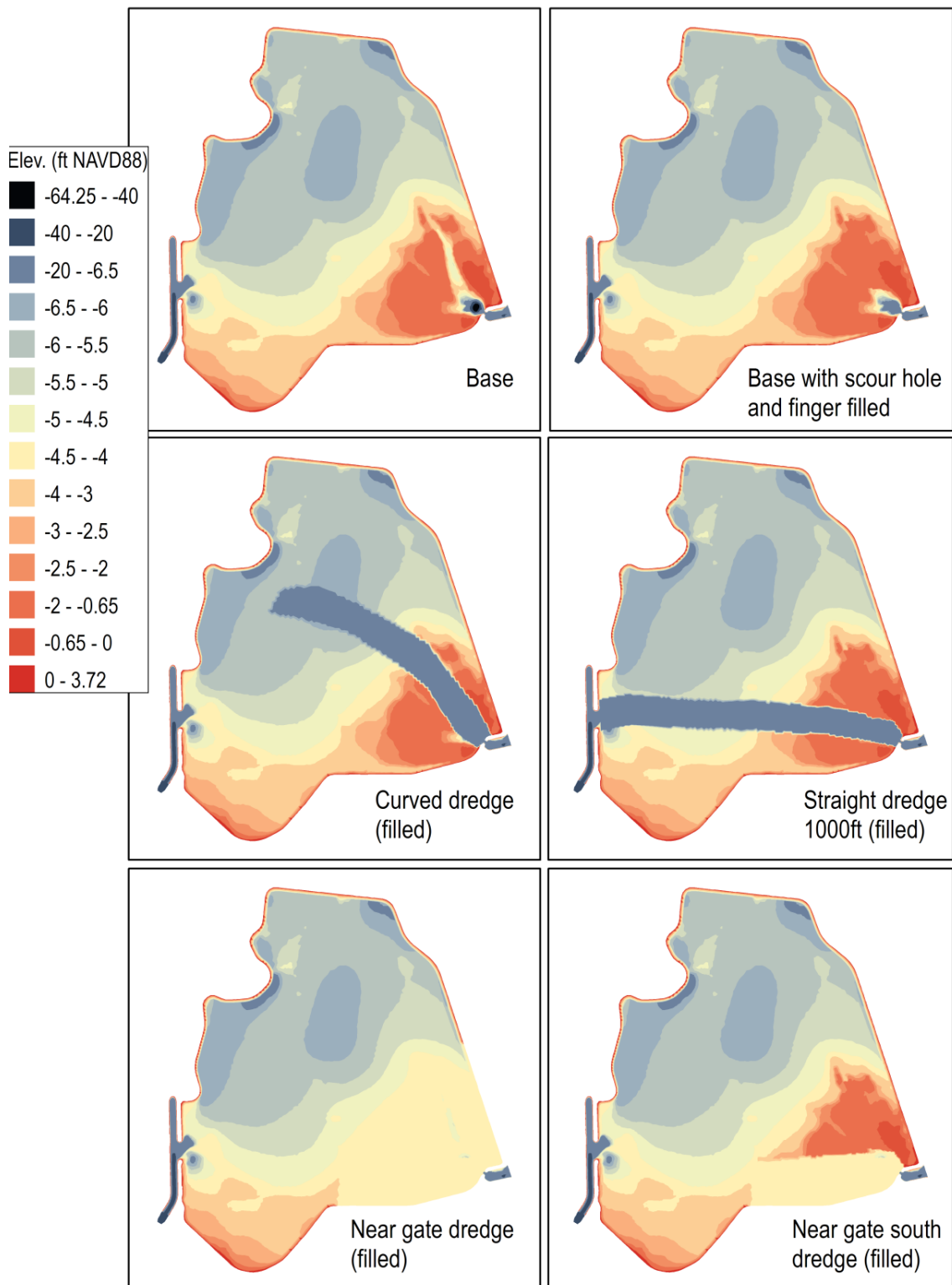


Figure 4-14 Base Case and Dredging and Filling Options Explored in This Report

Notes: Elev. = elevation, ft NAVD88 = feet in North American Vertical Datum of 1988

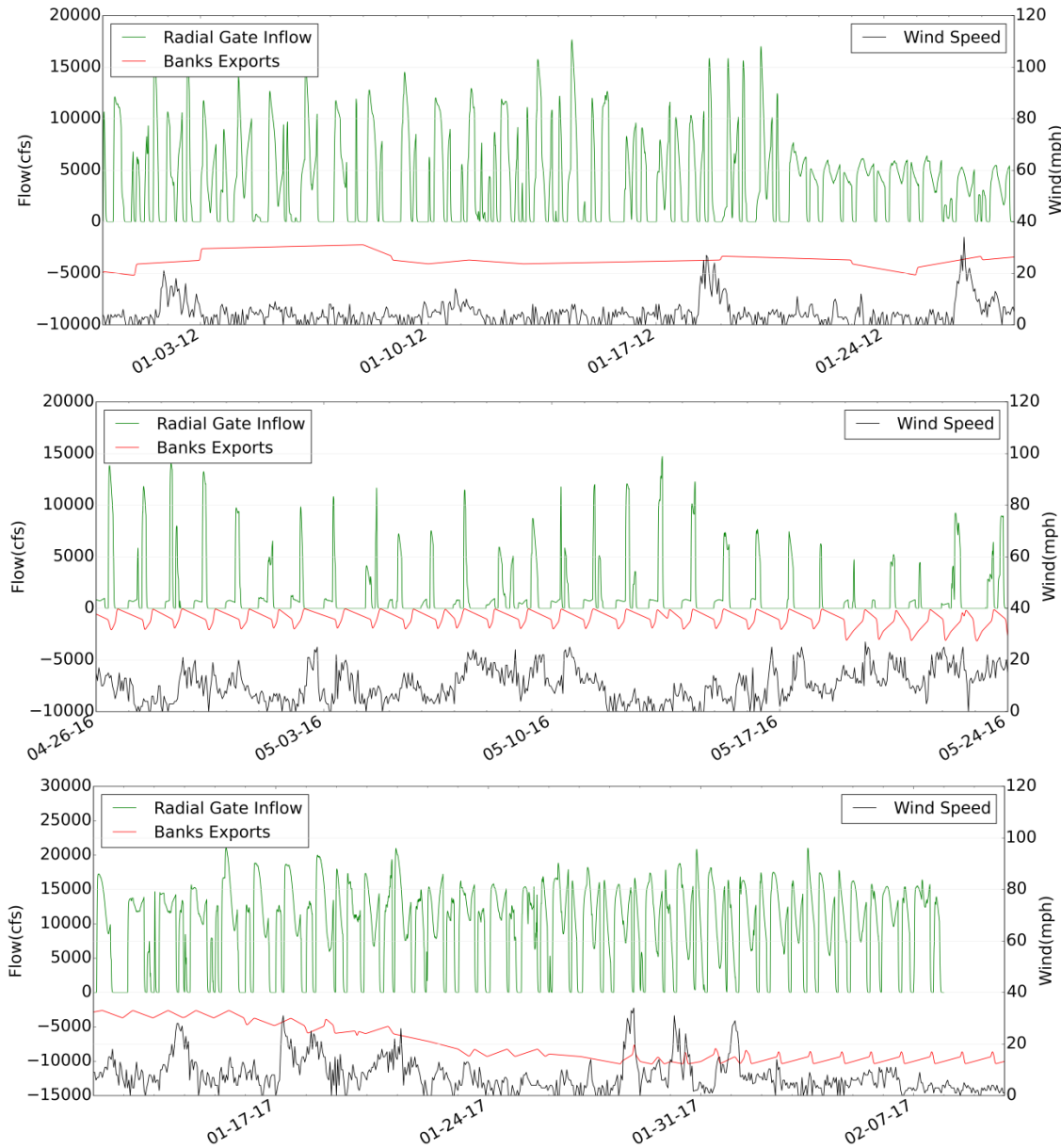


Figure 4-15 Radial Gate Flow, Banks Intake Flow, and Wind Conditions for 2012 (top), 2016 (middle), and 2017 (bottom)

Notes: Banks = Harvey O. Banks Pumping Plant, cfs = cubic feet per second, mph = miles per hour

average exports) and moderate wind. The second began December 31, 2011, and represented a period of relatively high-gate/pumping flows (3,800 cfs of exports). We also present a few results for January 13, 2007 under flood conditions (9,700 cfs of exports), which are interesting as a bracketing case, but are seldom relevant for the traditional January–June fish protection season. Banks Pumping Plant pumping, gate flows and wind conditions for these periods are shown in Figure 4-15. Note that as flows get larger, Banks Pumping Plant pumping transitions from a pulse flow pattern (based on electricity prices) to a constant flow (based more on maintenance considerations).

During each of the release periods, particles were introduced randomly using a distribution proportional to flow. Spatially, each particle released was random (uniform) and was situated between the wingwalls' interior of the radial gate. After introduction, particles were observed until 14 days after the introduction of the last particle, for a total of 28 days of simulation. We recorded particle paths, velocity results, as well as summaries of entry and exit details for each particle. Particle trajectories were scrutinized for all the bathymetry and flow options. A selection of trajectories is plotted in section 4.5.3.1, "Patterns and Variations in Particle Trajectories" and is paired with velocity gradient spatial plots to give a sense of the manner and extent to which dredging and filling can manipulate particle streamlines.

4.5.3 Key Results

4.5.3.1 Patterns and Variations in Particle Trajectories

The Forebay experiences several flow patterns depending on operations at the gates, export pumping, and wind. Generally speaking, the stronger the forcing by flow, the simpler the current structure is and the more bendable the main trajectories are under dredging alternatives. Figure 4-16 shows particle paths and velocity gradients resulting from inflow on April 27, 2016 for the base case, which is a case where the scour and finger hole are filled, and a case with these fill actions plus the 1,000 ft straight dredging alternative. Panels (a), (c), and (e) show particle trajectories and panels (b), (d), and (f) show the respective velocity gradients.

The filling option accelerates particles through the scour region, causing particle trajectories that move far over the gate opening, but also mix more vigorously. It also slightly accentuates a tunnel-like path through the scour and deposition that may be exploitable by predators. The option that adds a straight channel not only accelerates the particles, but bends streamlines more towards the gate. This option reduces transit time mostly in low flows, but it also produces the strongest velocity gradients.

Figure 4-17 shows analogous trajectories and gradients in the 2012 high-flow case. In this case, many of the particles traverse the Forebay within a day of when they enter the gates. Others make it most of the way, leaving them clustered within the zone of influence of the pumps the next day. The 1,000 ft (300 m) dredge reduces transit time initially, conspicuously guiding particles towards the pumps.

Figure 4-16 and Figure 4-17 are representative of the trends, but streamlines vary considerably based on recent flow and wind conditions, particularly at the beginning and ending of a gate operation, when particles can take routes that are much less direct. Particles that do not make it to exports when a day's operations conclude are subject to chaotic mixing by eddies or wind that persist through inertia. Even in light wind, particles do not remain clustered for long. If they are retained in the Forebay for longer than approximately the mean residence time (or approximately four days, whichever is shorter) they will start to become randomly distributed.

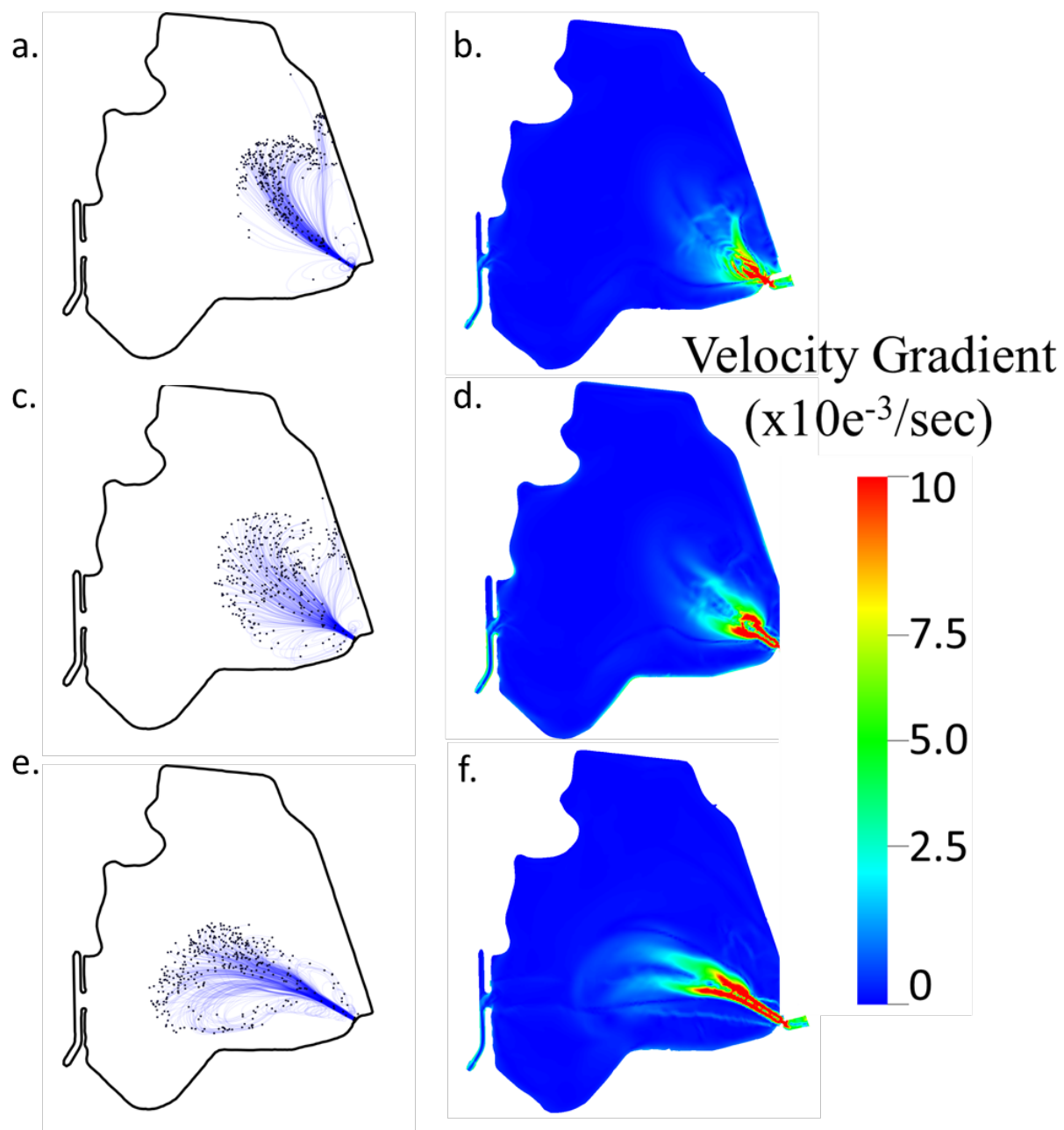


**Figure 4-16 Particle Trajectories and Velocity Gradients in Low Flow
Under Three Bathymetry Options**

Notes: (a) = particle trajectory for the base bathymetry under a 2016 low-flow allotment, (b) = maximum velocity gradient over the same gate opening as in (a) for base bathymetry, (c-d) = particle trajectories and velocity gradients with scour hole and finger hole filled, (e-f) = particle trajectories and velocity gradients for case with these fill actions plus a 1,000 ft (300 m) -wide straight channel from gates to export intake

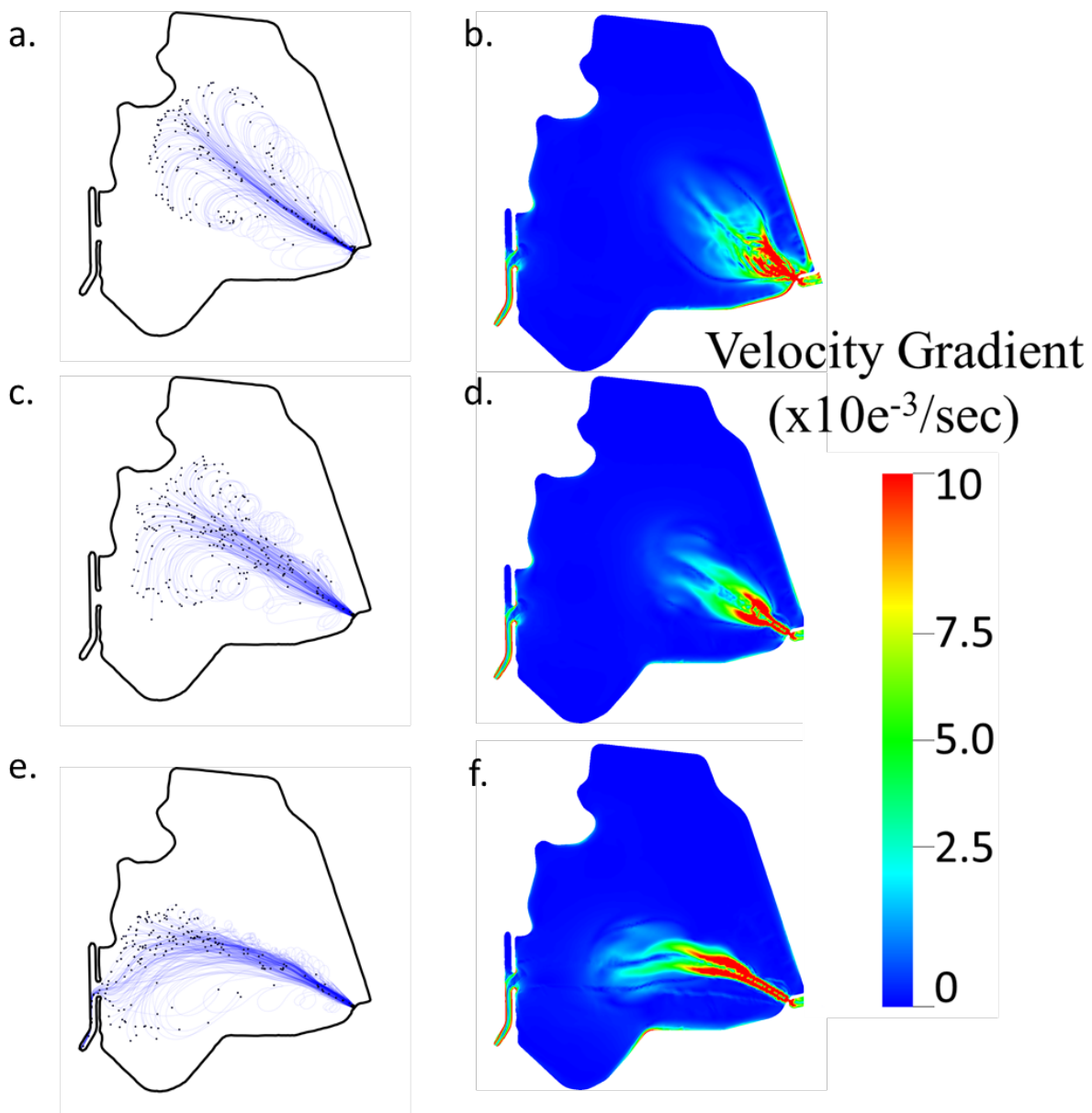


Figure 4-17 Particle Trajectories and Velocity Gradients in High Flow Under Three Bathymetry Options

Notes: (a) = particle trajectory for the base bathymetry under a 2012 high-flow allotment, (b) = maximum velocity gradient during the same gate opening as (a) for base bathymetry, (c-d) = particle trajectories and velocity gradients with scour hole and finger hole filled, (e-f) = particle trajectories and velocity gradients for case with these fill actions plus a 1,000 ft (300 m)-wide straight channel from gates to export intake

4.5.4 Transit Time

The transit time of particles from Clifton Court gates to the Banks Pumping Plant intake can be summarized in retention curves that are the analog of Kaplan-Meier survival plots. Figure 4-18 shows plots of retention curves for the base case and filling options for the 2016 low-flow case. Filling the scour hole leads to improve transit time, in particular early transit, and filling the finger channel has an insignificant effect. The 2012 high-flow case is omitted here, but is included in the Report. The larger flow makes a big difference in reducing transit time relative to bathymetry. The gains by filling the scour hole are modest, because the extra velocity that helps usher particles across the scour region also generates chaotic mixing as shown in the particle trajectory images from Figure 4-16 and Figure 4-17. Filling the scour hole is an important option, even with modest gains, for two reasons. First, it is motivated by other goals, such as reduction of predator habitat, in which case we only have to establish lack of harm in terms of transit time. Second, the option is compatible with or even synergistic with dredging options.

Retention curves for the options including dredging are shown in Figure 4-19 and Figure 4-20 . When combined with filling of the scour hole and finger channel, the 1000 ft straight channel and full dredging of the sediment ring both achieve a substantial reduction in transit time in the 2016 low flow case relative to filling alone. The other projects do not achieve big marginal benefits compared to filling. In the 2012 high flow case, all the dredging options increased transit within the first two days. After two days, there are few particles left in the system, so results are probably less reliable – assuming the results are still valid, they indicate a slight worsening of transit time.

Flow plays a deciding role in transit time under any bathymetry option. To underscore this point, Figure 4-21 compares retention time with the base bathymetry among three years with very different flows: 2016 (daily average exports 1,175 cfs), 2012 (3,800 cfs), and 2017 (9,700 cfs). Gate flows are generally similar on a daily averaged basis. The mean volumetric residence time of these samples ranges from more than seven days in 2016 to less than one day in 2017. Cross-hatching in the 2017 plot indicates estimates that are influenced by censorship; particles in 2017 exit the system early and sample sizes going out 10 days or so are very small. Such cross-hatching would appear in the other plots as well, but the censorship starts more than 14 days into the experiment and is caused by the termination of particle tracking. The dominance of flow holds for any bathymetry option.

With flow being so important to transit, it seems natural to ask whether relative timing of gate and export flows is equally important. We examine this but concluded that shifts in relative timing were not very important.

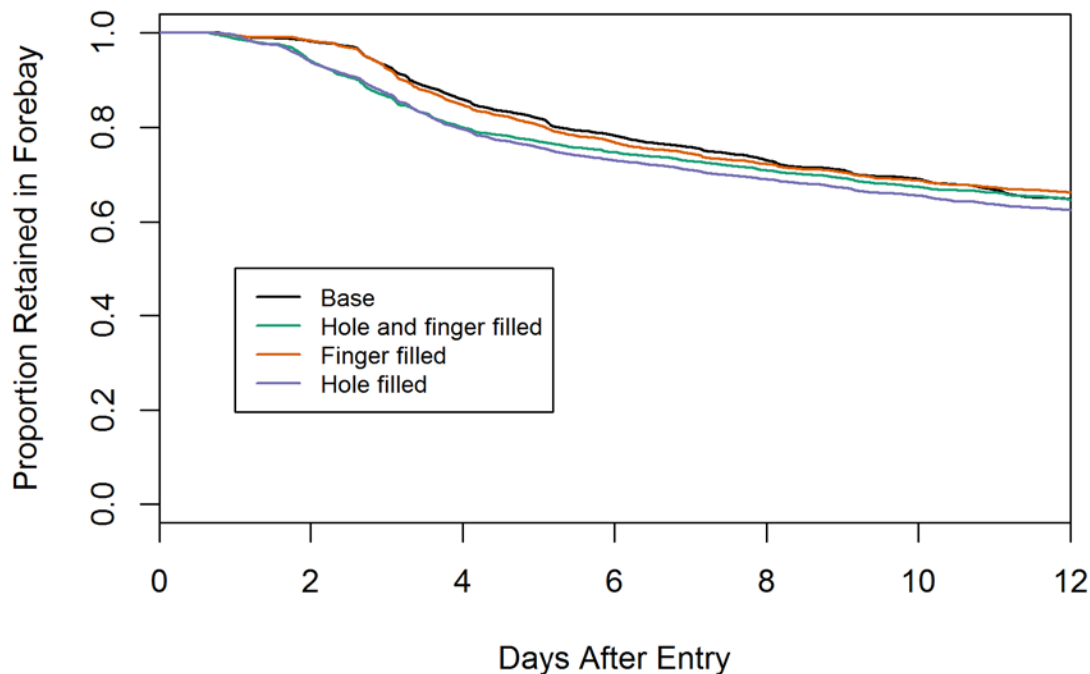


Figure 4-18 Retention Curves for Base and Filling Options, Low-Flow (2016) Case

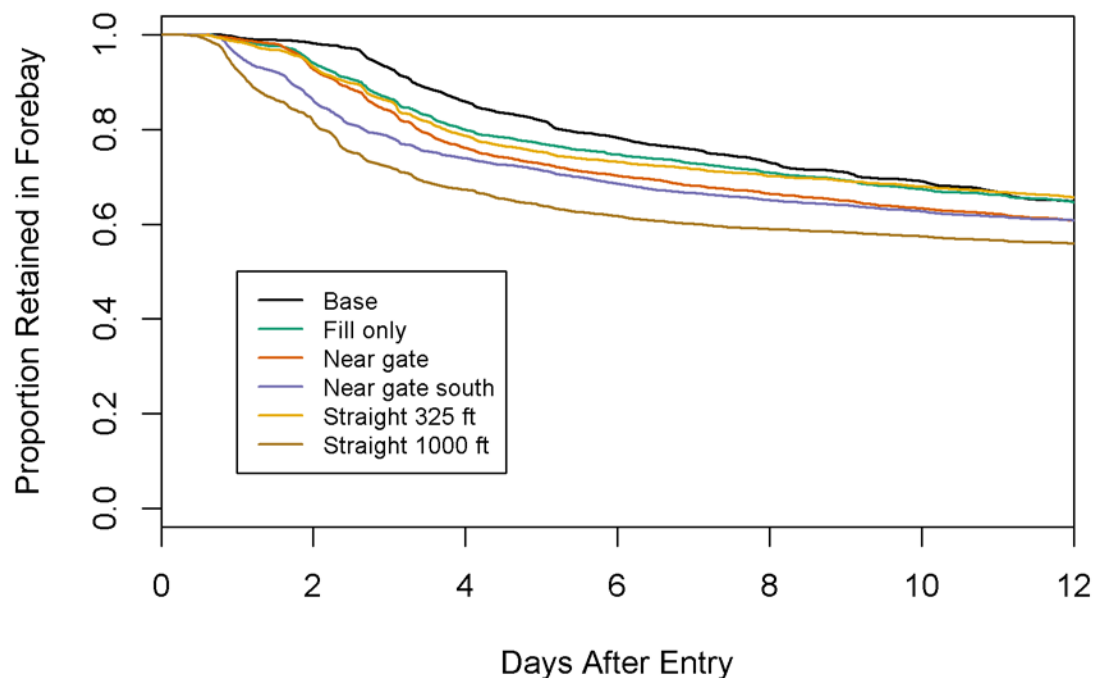


Figure 4-19 Retention Curves for Base and Dredge + Fill Options, Low-Flow (2016) Case

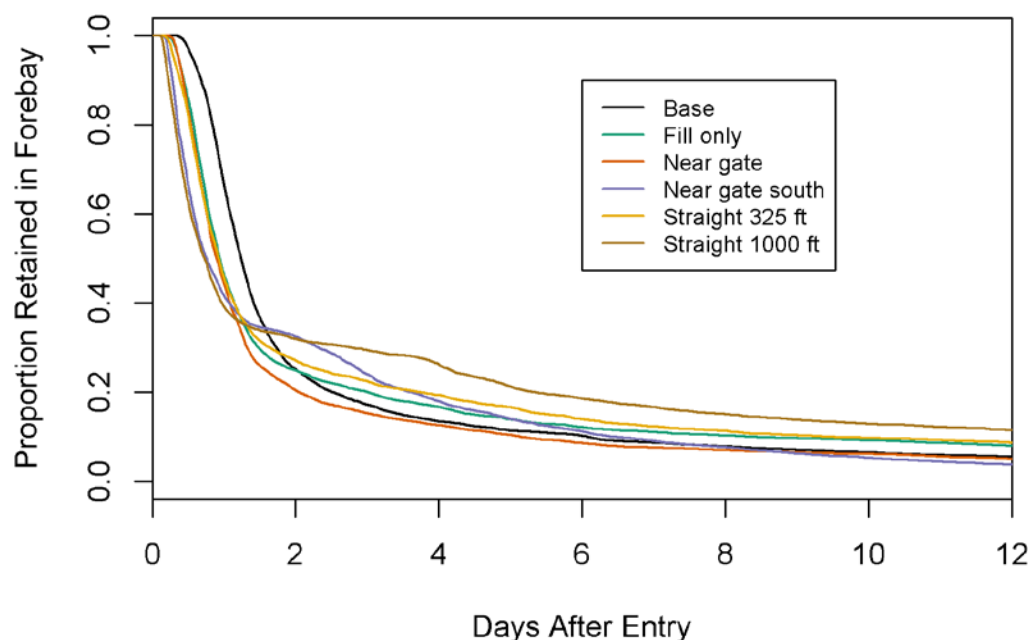


Figure 4-20 Retention Curves for Base and Dredge + Fill Options, High-Flow (2012) Case

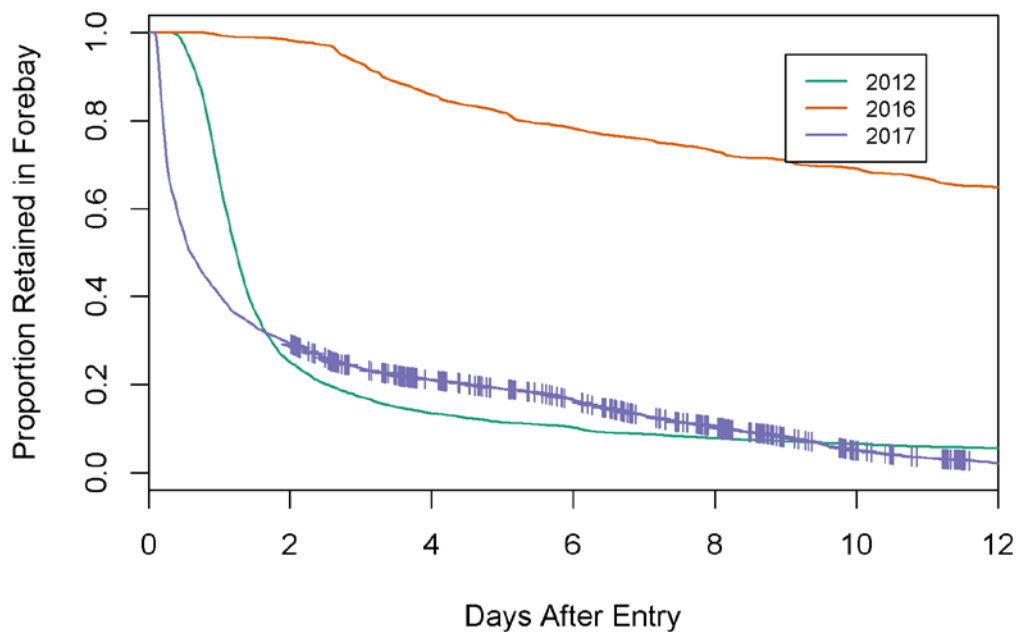


Figure 4-21 Retention Curves for Base Bathymetry in Low-medium Flow (2016), Medium-High Flow (2012), and Extreme High Flow (2017)

Note: Cross-hatching indicates points that are developed with censored data.

4.6 Discussion

In this study, we developed a transit time model of the Forebay and validated the model in terms of observed water levels, velocities, and particle trajectories. The model successfully reproduces observed velocities at a number of stations in the Forebay, particularly those that are forced by gate and pumping operations. Our velocity results in high wind are consistent with prior modeling, but there is limited field data to corroborate the complex exchange flows that develop under these conditions.

Our particle tracking results suggest that trajectories are influenced in a predictable way by gate and pump flows, with higher flows leading to faster transit. These boundary flows move particles across the Forebay in a velocity pattern with a simple vertical structure. Eddies and wind-generated velocities create more complex velocities that disperse the particles. It is likely that the most effective methods for reducing transit time will be those that focus on primary flows and coax particles across the Forebay soon after entry. These are the actions that produce velocities that are large enough to remain relevant after biological behavior is factored in. They are also the most dependable to model.

By far, the most important variables determining transit time under Reynolds-averaged flow are gate and export flows, which tend to vary together on a daily averaged basis under current policy. When gate and export flows are low (1,175 cfs daily average), volumetric residence time is fairly long (eight days in our example), and only a modest fraction of particles entering the gates makes it across the Forebay to be salvaged within 72 hours. Particles advance in advective pulses as operations alternate on and off, and at lower flows it can take several days to cross the Forebay. At the same time, the particles are dispersed by secondary or wind-driven currents. In strong gate and pumping flows (4,000 cfs), volumetric residence time is short (two days), many particles are entrained within a day, and a majority of particles reach the pumps within 72 hours. Particles that are entrained are swept along by larger velocities, which may be important where biological behavior is involved. Particles that are not salvaged are dispersed chaotically by eddies into regions where entrainment rates are lower.

Of the bathymetry manipulations we tested, filling the scour hole seems like a promising step. This filling accomplishes some of what is possible in terms of transit time reduction. Filling the scour hole is associated with other biological and logistical advantages and is compatible with the various dredging options, enhancing their benefits. Possible disadvantages that might arise from this action are higher local velocities and more-pronounced velocity gradients. In a biological setting, alleys of high-velocity water might be attractive to predators, in which case the reduction in transit time would be offset by higher hazard rates. Additionally, of course, the sediment dynamics in this area are complex, and maintaining the scour hole in its filled state and a dredged channel in its deeper state would be an engineering challenge. The other filling option we looked at, filling the finger channel through the sediment ring beyond the scour hole, had only a minor effect.

Of the dredging options, the ones that seemed most beneficial were the 1,000 ft (300 m) wide dredged straight channel and the dredging of the sediment ring that lies beyond the scour hole. These options achieve a substantial improvement in early salvage relative to the base bathymetry, particularly in the low-flow 2016 hydrology. Both are large-scale proposals, and their scaled-down variants do not achieve nearly as much. Neither option is as effective if the scour hole is not filled. Also, in high flow, the straight

channel conspicuously prolongs transit time after about two days. This may not be important given that transit time is, in any event, still quite low.

In the Report, we comment on enhancements to the model and further study from the point of view of transit time and survival analysis.

4.7 References Cited

- Ateljevich E, Nam K, Zhang Y, Wang R, Shu Q. 2014. "Bay-Delta SELFE calibration overview." In: *Methodology for Flow and Salinity Estimates in the Sacramento-San Joaquin Delta and Suisun Marsh. 35th Annual Progress Report to the State Water Resources Control Board*. Chapter 7. Sacramento (CA): Bay-Delta Office. Delta Modeling Section. California Department of Water Resources.
- Ateljevich E, Tu M-Y, Le, K. 2015. "Calculation Clifton Court Forebay inflow and re-rating the forebay gates." In: *Methodology for Flow and Salinity Estimates in the Sacramento-San Joaquin Delta and Suisun Marsh. 36th Annual Progress Report to the State Water Resources Control Board*. Chapter 6. Sacramento (CA): Delta Modeling Section. California Department of Water Resources.
- Castillo G, Morinaka J, Lindberg J, Fujimura R, Baskerville-Bridges B, Hobbs J, Tigan G, Ellison L. 2012. "Pre-screen loss and fish facility efficiency for delta smelt at the south Delta's State Water Project, California." *San Francisco Estuary and Watershed Science*. 10(4). Viewed online at: <http://escholarship.org/uc/item/28m595k4>. [Journal article].
- Hills E. 1988. *New Flow Equations for Clifton Court Gates*. State Water Project Division of Operations and Maintenance. California Department of Water Resources. [Technical Memorandum].
- MacWilliams ML and Gross E. 2013. "Hydrodynamic simulation of circulation and residence time in Clifton Court Forebay." *San Francisco Estuary and Watershed Science*. 11(2). Viewed online at: <http://escholarship.org/uc/item/4q82g2bz>. [Journal article].
- National Marine Fisheries Service. 2009. *Final Biological Opinion and Conference Opinion of the Proposed Long-term Operations of the Central Valley Project and State Water Project*. U.S. Department of Commerce. National Marine Fisheries Service. Viewed online at: http://www.westcoast.fisheries.noaa.gov/publications/Central_Valley/Water%20Operations/Operations,%20Criteria%20and%20Plan/nmfs_biological_and_conference_opinion_on_the_long-term_operations_of_the_cvp_and_swp.pdf. Accessed: June 4, 2009.
- . 2011. *2009 RPA with 2011 Amendments*. U.S. Department of Commerce National Marine Fisheries Service. Viewed online at: http://www.westcoast.fisheries.noaa.gov/publications/Central_Valley/Water%20Operations/Operations,%20Criteria%20and%20Plan/040711_ocap_opinion_2011_amendments.pdf. Accessed: April 7, 2011.
- Pond S and Pickard GL. 1983. *Introductory Dynamical Oceanography*. Second edition. Oxford (UK): Butterworth-Heinemann Ltd. 349 pp.
- Shu Q and Ateljevich E. 2017 *Clifton Court Forebay Transit Time Modeling Analysis*. Sacramento (CA): Bay-Delta Office. Delta Modeling Section. California Department of Water Resources.
- Song Y and Haidvogel DB. 1994. "A semi-implicit ocean circulation model using a generalized topography-following coordinate." *Journal of Computational Physics*. 115(1). pp. 228-244. [Journal article].

Umlauf L and Burchard H. 2003. "A generic length-scale equation for geophysical turbulence models." *Journal of Marine Research*. 61(2)6. pp. 235–265.

Wilde J. 2006. "Priority 3 Clifton Court Forebay Operations for Extended Planning Studies." In: *Methodology for Flow and Salinity Estimates in the Sacramento-San Joaquin Delta and Suisun Marsh. 27th Annual Progress Report to the State Water Resources Control Board*. Chapter 8. Sacramento (CA): Delta Modeling Section. California Department of Water Resources.

Zhang Y and Baptista AM. 2008. "SELFE: A semi-implicit Eulerian-Lagrangian finite-element model for cross-scale ocean circulation." *Ocean Modelling*. 21(3-4). pp. 71-96. [Journal article].

Zhang Y, Ateljevich E, Yu HS, Wu CH, Yu J. 2015. "A new vertical coordinate system for a 3D unstructured-grid model." *Ocean Modelling*. 85. pp. 16-31. [Journal article].

Zhang Y, Ye F, Stanev EV, Grashorn S. 2016. "Seamless cross-scale modeling with SCHISM. Ocean Modelling." 102. pp. 64-81. [Journal article].

4.7.1 Personal Communications

MacWilliams ML, Partner at Anchor QEA, San Francisco (CA). Jul. 13, 2016 — email correspondence with Ateljevich, E, California Department of Water Resources Delta Modeling Section, Sacramento (CA) — transmitting wind data from prior Clifton Court study